HUMAN RIBOSOME BIOGENESIS AND THE REGULATION OF THE TUMOUR SUPPRESSOR p53

Andria Pelava

Submitted for Doctor of Philosophy

Final submission: December 2016

Institute of Cell and Molecular Biosciences

Faculty of Medical Sciences

Newcastle University

Abstract

Ribosome production is an energetically expensive and, therefore, highly regulated process. Defects in ribosome biogenesis lead to genetic diseases called Ribosomopathies, such as Dyskeratosis Congenita (DC), and mutations in ribosomal proteins and ribosome biogenesis factors are linked to multiple types of cancer. During ribosome biogenesis, the ribosomal RNAs (rRNAs) are processed and modified, and defects in ribosome biogenesis lead to the activation of p53. This project aimed to investigate the functions of Dyskerin, mutated in X-linked DC, in human ribosome biogenesis and p53 regulation, and to explore the link between ribosome production and p53 homeostasis.

Dyskerin is an rRNA pseudouridine synthase and required for telomere maintenance. There is some debate as to whether DC is the result of telomere maintenance or ribosome biogenesis defects. It is shown here that human Dyskerin is required for the production of both LSU and SSU, and knockdown of Dyskerin leads to p53 activation via inhibition of MDM2 via the 5S RNP, an LSU assembly intermediate which accumulates after ribosome biogenesis defects. My data indicate that p53 activation, due to defects in ribosome biogenesis, may contribute to the clinical symptoms seen in patients suffering with DC.

In addition, it is shown that defects in early or late stages of SSU or LSU biogenesis, result in activation of p53 via the 5S RNP-MDM2 pathway, and that p53 is induced in less than 12 hours after ribosome biogenesis defects. SSU defects do not cause any obvious defects in LSU production, but they result in inhibition of export of the pre-LSU in the cytoplasm, suggesting that p53 activation after SSU defects is probably due to defects in pre-LSU export. Finally, there are evidence that RPS27a or RPL40, two ribosomal proteins produced as ubiquitin-fusion precursors in the cell, might be novel regulators of the 5S RNP-MDM2 pathway.

In conclusion, this work shows the importance of ribosome biogenesis in the regulation of p53 for the development of Ribosomopathies and cancer.

Declaration

I certify that the work presented here is my own, unless when acknowledged. No part of this work has been previously submitted for other qualifications at any university.

Acknowledgements

I would like to thank my supervisor, Dr Nick Watkins, for all his help and support throughout my PhD, a character-building process from which I have learnt a lot as a scientist and as a person. I would also like to thank Dr Claudia Schneider for her advice and help over the past few years, and everyone in the Watkins/Schneider lab for putting up with me! Special thanks to Dr Loren Gibson for her help during experimental procedures and her support since the beginning. Thank you to Dr Katherine Sloan and Dr Christopher Hoyland for their precious help at the beginning of my PhD, to Dr Neil Perkins for providing some of the human cell lines used and to my panel assessors, Dr Elizabeth Veal and Dr Viktor Korolchuk, for their help and advice during my PhD.

Furthermore, I would like to thank my friends Dr Claire Whitworth and Kerrie Brusby for the coffee breaks during stressful days, Ellouise for her valuable advice and inspiration, and Charis for all her support from far away. A huge thank you to Rozi and Miriam for their understanding and constant support throughout, and to all of my Capoeira family, especially to Will, Patrick, Rob and Glenn. Special thanks to Jimi, who has supported me like a second father while I was away from home. I would like to thank my “kouklitsa” Eleni; you have been my rock since the beginning and I could not have done this without you. Last but not least, I would like to thank my sister, Christia, my brother, Stylianos and my parents, Nikos and Eftychia, for being the best parents I could have asked for. I could not have done any of this without your support and your love. Thank you for everything you have taught me and for being there no matter what.

This work was funded by the BBSRC-DTP and the Diamond-Blackfan Anaemia Foundation, U.K.

BBSRC bioscience for the future

Help Find a Cure for Diamond Blackfan Anemia

.

Table of Contents

List of Figures

List of Tables

List of Abbreviations

µg	micro-gram
µl	micro-litre
µM	micro-molar
A	Alanine
A. melanoleuca	*Ailuropoda melanoleuca*
ActD	Actinomycin D
Asn	Asparagine
ATP	Adenosine triphosphate
B. taurus	*Bos taurus*
cDNA	complementary DNA
CHH	Cartilage-Hair Hypoplasia
CMV	Cytomegalovirus
CSL4	Exosome complex component
C-terminal	Carboxy-terminal
CTP	Cytidine triphosphate
D	Aspartic acid
D. danglia	*Danio danglia*
DAPI	4’,6-Diamidino-2-Phenylindole, Dihychloride
DBA	Diamond-Blackfan Anaemia
DC	Dyskeratosis Congenita
DMEM	Dulbecco’s Modified Eagle Medium
DNA	Deoxyribonucleic acid
dNTP	Deoxy-nucleoside triphosphate
DTT	Dithiothreitol
E.coli	*Escherichia coli*
ECL	Enhanced chemiluminescence
EDTA	Ethylenediaminetetraacetic acid
EtBr	Ethidium Bromide
ETS	External Transcribed Spacer
FCS/FBS	Fetal Bovine Serum
FRT	Flippase recognition target
G. gallus	*Gallus gallus*
G1	Gap 1

G2	Gap2
Gly	Glycine
GTP	Guanosine 5’-triphosphate
H. sapiens	*Homo sapiens*
HCl	Hydrochloric acid
HEPES	4-(2-hydroxyethyl)-1-piperazineethanesulfonic acid
HRP	Horseradish peroxidase
IF	Immunofluorescence
Ile	Isoleucine
ITS	Internal Transcribed Spacer
kb	kilo base
KCl	Potassium Chloride
kDa	kilo Dalton
L. major	*Leishmania major*
LSU	Large ribosomal subunit
M	molar
M. musculus	*Mus musculus*
MDM2	Mouse double minute 2
$MgCl_2$	Magnesium Chloride
ml	Millilitre
mM	Milli-molar
mTOR	mammalian target of rapamycin
mTORC	mammalian target of rapamycin complex
$Na_3C_6H_5O_7$	Trisodium citrate
NaCl	Sodium Chloride
NaOH	Sodium Hydroxide
$NaPO_4$	Sodium Phosphate
NLS	Nuclear Localization Signal
N-terminal	Amino-terminal
ORF	open reading frame
P. furiosus	*Pyrococcus furiosus*
P. pygmaeus	*Pongo pygmaeus*
P. troglodytes	*Pan troglodytes*
pA	Polyadenylation
PAGE	Polyacrylamide gel

PBS	Phosphate Buffer Saline
PCR	Polymerase Chain Reaction
Phe	Phenylanine
PIPES	Piperazine-N,N′-bis(2-ethanesulfonic acid)
Pol	Polymerase
pre-rRNA	precursor ribosomal RNA
R. rattus	*Rattus rattus*
RNA	Ribonucleic acid
RNAi	RNA interference
RNP	Ribonucleoprotein particle
RP	Ribosomal Protein
rRNA	Ribosomal RNA
RT	Reverse Transcription
S. cerevisiae	*Saccharomyces cerevisiae*
S. pombe	*Saccharomyces pombe*
S.cerevisiae	*Saccharomyces cerevisiae*
SDS	Shwachman-Diamond syndrome
SDS	Sodium Dodecyl Sulphate
siRNA	Small-interfering RNA
snoRNA	Small nucleolar RNA
snRNA	Small nuclear RNA
S-phase	Synthesis phase
SSC	Saline sodium citrate
SSU	Small ribosomal subunit
TBE	Tris-Boric Acid EDTA
TC	Treacher Collins
TERC	Telomerase RNA component
TERT	Telomerase reverse transcriptase
tet	tetracycline
Thr	Threonine
TTP	Thymidine triphosphate
U.V.	Ultraviolet light
Ub	Ubiquitin
X. leavis	*Xenopus leavis*
Ψ	Pseudouridylation

1. Chapter One. Introduction

1.1. The eukaryotic ribosome

Ribosomes are ribonucleoproteins complexes consisting of protein and RNA components, essential for protein synthesis. Eukaryotic ribosomes consist of two subunits: the large (LSU or 60S) and the small (SSU or 40S) ribosomal subunit. The LSU contains the peptidyl-transferase centre where the catalysis of the peptide bond formation occurs for the synthesis of the nascent polypeptide chain. The SSU has a decoding function, where the complementarity of the tRNA with the mRNA is inspected (Gamalinda and Woolford, 2015). Ribosomes are structurally well-conserved across all organisms, even though the prokaryotic ribosomes (70S) are smaller than the eukaryotic ones (80S) (Moore and Steitz, 2002).

In eukaryotes, the LSU (60S) consists of the 28S (25S in yeast), 5.8S and 5S ribosomal (r)RNAs, as defined by their sedimentation co-efficient, and 46 ribosomal proteins. In contrast, the SSU (40S) contains the 18S rRNA and approximately 33 ribosomal proteins (Gamalinda and Woolford, 2015). The 28S, 18S and 5.8S rRNAs are transcribed in the nucleolus by RNA polymerase (pol) I as a single 47S transcript, which is subsequently processed and modified for the production of the mature rRNAs. The 5S rRNA is transcribed in the nucleoplasm by RNA polymerase III (Granneman and Baserga, 2004, Orsolic et al., 2015).

1.2. Ribosome Biogenesis

In mammals, there are approximately 10 million ribosomes in each cell (Kenmochi et al., 1998) and ribosome production is a major energy-consuming process, and, therefore, very tightly regulated. In yeast, approximately 60% of the cellular energy is predicted to be consumed by ribosome biogenesis (Warner, 1999). More than 200 proteins were shown to be involved in rRNA processing and maturation, which takes place in different compartments in the cell (Henras et al., 2008), including the nucleolus, nucleus and cytoplasm (Kressler et al., 2010). Ribosome production was found to be up-regulated during cell growth (Sulic et al., 2005), and down-regulated during cell proliferation and differentiation (Warner, 1999). Not surprisingly, ribosome

biogenesis was found to play a key role in cancer, since it is up-regulated during tumourigenesis (Ruggero and Pandolfi, 2003).

1.2.1. The nucleolus

The first steps of ribosome biogenesis take place in a distinct nuclear compartment, called the nucleolus (Boisvert et al., 2007). The 28S, 18S and 5.8S rRNAs are transcribed from ribosomal DNA (rDNA) repeats in a telomere-to-centromere fashion (Worton et al., 1988, McStay and Grummt, 2008), which cluster in the nuclear organizer regions (NORs) within the nucleolus (Henderson et al., 1972). These genes are found on the short arms of the acrocentric chromosomes 13, 14, 15, 21 and 22 in humans (Kenmochi et al., 1998), so that they are separated from genes transcribed by RNA polymerases II and III (Henderson et al., 1972). The NORs are highly conserved, since the 5'-end of the rDNA clusters as well as the non-rDNA repeats around it are conserved in all 5 pairs of chromosomes.

The nucleolus is formed around rRNA-transcribing genes and it is organized in three distinct compartments, as identified by Electon-Microscopy (EM): the fibrillarin centre (FC), the dense fibrillarin component (DFC) and the granular component (GC) (Figure 1.1) (Haaf et al., 1991, Haaf and Schmid, 1991, Smirnov et al., 2016). It was shown that the pre-rRNAs grow on the rDNA as small fibrils, which create a structure of approximately 4.5-6μm in length (Cheutin et al., 2002). Transcription of the 47S precursor rRNA by RNA polymerase I takes place at the border between the FC and DFC, whereas processing of the pre-rRNAs takes place in DFC (Cheutin et al., 2002). Indeed, RNA polymerase I is found in high levels in the FC region in the nucleolus (Boisvert et al., 2007). The first cleavage steps of the 47S rRNA are believed to take place in the DFC compartment (Derenzini et al., 1990), whereas later steps of the rRNA precursor processing take place in the GC compartment (Gerbi and Borovjagin, 1997), where most ribosomal proteins are found (Boisvert et al., 2007).

The nucleolus has been linked to cancer for the past few years. Silver-staining of NORs (Ag-NOR staining) has shown that the nucleolar structure changes in tumour cells, since it is usually increased in size and numbers, leading to an up-regulation of ribosome biogenesis (Orsolic et al., 2015).

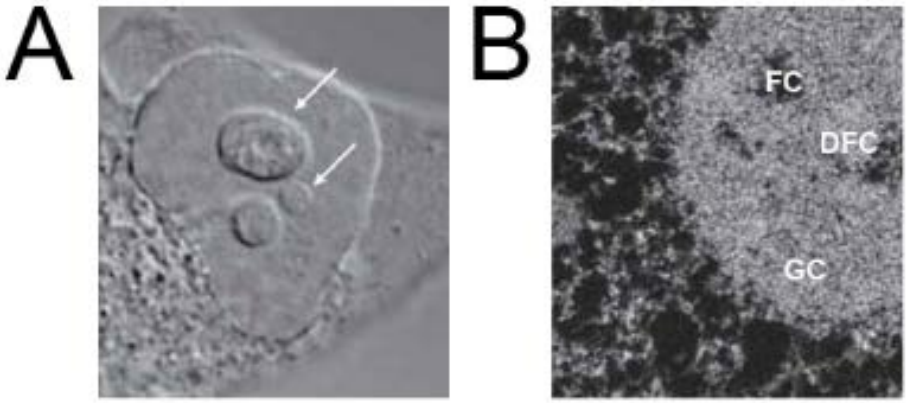

Figure 1.1. Structure of the nucleolus revealed by electron microscopy. (A) The nucleoli shown in the nucleus of a HeLa cell, as indicated by the arrows, by differential interfering contrast (DIC). **(B)** Nitrogen-enriched image showing the fibrillarin centre (FC), dense fibrillarin component (DFC) and granular component (GC). (From: (Boisvert et al., 2007)).

1.2.2. rRNA transcription

The 28S (25S in yeast), 18S and 5.8S rRNAs are transcribed as a single transcript (47S, 35S in yeast) by RNA polymerase I in the nucleolus (Woolford and Baserga, 2013). In yeast, there is a promoter region upstream of the rDNA gene and a terminator sequence downstream of the gene. In humans, the upstream region of the rRNA gene contains a promoter and an upstream control element, whereas several termination sequences are found at the 3' end of the rDNA genes (Russell and Zomerdijk, 2005). The upstream control element in humans is bound by the upstream binding factor (UBF), which then recruits the human selectivity factor (SL1 complex) to the promoter region (Russell and Zomerdijk, 2005). The SL1 complex consists of the TATA-box-binding protein (TBP) and three TBP-associated factors (Grummt, 1999). Binding of the SL1 recruits the RNA polymerase I to the promoter region, forming the pre-initiation complex, consisting of UBF, SL1 and RNA polymerase I, which leads to promoter opening (Russell and Zomerdijk, 2005). The RNA polymerase I is then able to move across the gene so that transcription is initiated, but the UBF and SL1 complex remain bound to the promoter region so that multiple RNA polymerase I units can be recruited to the promoter for a number of transcription rounds (Panov et al., 2001). The clearance of the promoter region by RNA polymerase I shift appears to be the rate-limiting step for the transcription of the rRNAs (Panov et al., 2001). Finally, RNA polymerase I halts when it reaches the TTF-1 factor, which is bound at the termination sequences, and it gets released by the PTRF factor, which is associated with TTF-1 at

the termination sequence (Jansa and Grummt, 1999). The 47S rRNA precursor produced is processed co-transcriptionally for the formation of the mature 28S, 5.8S and 18S rRNAs (Russell and Zomerdijk, 2005).

The 5S rRNA is transcribed in the nucleoplasm by RNA polymerase III (Paule and White, 2000), which is found at multiple sites in the nucleus (Pombo et al., 1999). The 5S rDNA gene clusters, found on human chromosome 1, contain a 5' flanking region, which is necessary for its transcription by RNA polymerase III (Sorensen and Frederiksen, 1991). In lower eukaryotes, this region contains internal elements, including the A-box at the 5', the intermediate element (IE) and the C-box at the 3' (Cloix et al., 2003). This class of promoter regions was found in *X. leavis* (Pieler et al., 1987), *D. melanogaster (Sharp and Garcia, 1988)* and *S. cerevisiae* (Lee et al., 1995), which are bound by the RNA polymerase III and three transcription factors: TFIIIA, which is specific to 5S rRNA (Pelham and Brown, 1980), TFIIIB, TFIIIC (Cloix et al., 2003). In humans and other higher eukaryotes, such as mice, an additional element, called the D-box is found upstream of the 5S rDNA gene, which is required for the efficient transcription of the 5S rRNA (Hallenberg and Frederiksen, 2001). TFIIIA binds the C-box at the 5' region of the 5S rDNA, which then recruits TFIIIC. TFIIIA and TFIIIC binding position TFIIIB at the promoter region, so that RNA polymerase III is assembled at the promoter (Ishiguro et al., 2002). Once transcription is initiated, TFIIIC is released but TFIIIB remains bound on the promoter region for multiple rounds of initiation (Kassavetis et al., 1998, Kumar et al., 1998).

1.2.3. rRNA processing

Most of our knowledge on the rRNA processing pathway and the factors involved are known from yeast, where the primary 35S rRNA transcript is processed both co-transcriptionally and post-transcriptionally. Removal of 5' ETS occurs by the co-transcriptional cleavage at sites A0, A1 and A2, which occurs simultaneously (Figure 1.2). The mechanisms and enzymes responsible for cleavage at sites A0 and A1 are yet to be determined, but there is evidence for the requirement of the SSU processome complex (Phipps et al., 2011, Osheim et al., 2004), U3 (Dragon et al., 2002), U14 (Henras et al., 2015) and snR30/U17 snoRNAs (Fayet-Lebaron et al., 2009, Tollervey, 1987), and a number of ribosomal proteins (O'Donohue et al., 2010) (Figure 1.2). It was originally thought that the endonuclease Rcl1p is involved in cleavage at site A2

(Horn et al., 2011), whereas recent evidence suggest that this is not the case and the endonuclease Utp24 was shown to be essential for this (Figure 1.2) (Wells et al., 2016). Separation of the LSU and SSU precursors occurs after cleavage at A2 site of the ITS1 (internal transcribed spacer 1) (Kressler et al., 1999), resulting in the formation of the 20S SSU and the 27S LSU rRNA precursors (Figure 1.2) (Henras et al., 2015). Cleavage at site A3 involved the MRP RNase (Lygerou et al., 1996), and the RNA-binding protein Rrp5p (Venema and Tollervey, 1996) and Nop4p protein (Berges et al., 1994, Sun and Woolford, 1994) were shown to be important (Figure 1.2).

The 20S SSU rRNA precursor is exported to the cytoplasm, where it is further cleaved at site D for the production of the mature 18S rRNA (Figure 1.2). This cleavage step is dependent upon the action of Nob1p endonuclease (Pertschy et al., 2009) and Dim1 dimethylase (Kressler et al., 1999). The 27S LSU rRNA precursor is processed for the production of the mature 5.8S and 25S rRNAs (Figure 1.2). The 5' end of the 5.8S rRNA is processed by the exonuclease Rat1p (Kressler et al., 1999) and the rRNA processing protein Rrp17p (Petfalski et al., 1998, Oeffinger et al., 2009). Separation of the 5.8S and the 25S rRNA precursors occurs after cleavage at site C2 (Figure 1.2), but the factors involved in this are still unknown (Venema and Tollervey, 1995). Las1 endonuclease was shown to be involved in this cleavage step (Gasse et al., 2015) and other factors and ribosomal proteins, such as RPL35 (Babiano and de la Cruz, 2010) are also important. Maturation of the 5.8S rRNA takes place after 3' exonucleolytic processing (Figure 1.3) involving the exosome component RNA helicase Mtr4p (Jia et al., 2012) and the exonuclease Rrp6p (Briggs et al., 1998) in the nucleus, whereas the final 3' processing by Ngl2p (Faber et al., 2006) occurs in the cytoplasm (Thomson and Tollervey, 2010). The exonuclease Rat1p and its cofactor Rai1p were also found to be involved in the 5' end processing of the 5.8S rRNA (Fang et al., 2005). Maturation of the pre-25S rRNA LSU precursor occurs by exonucleolytic cleavage of the 5' end (Figure 1.2) by Rat1p in the nucleus (El Hage et al., 2008), which is then exported to the cytoplasm (Geerlings et al., 2000), where it is further processed for the production of the mature 5.8S rRNA (Thomson and Tollervey, 2010).

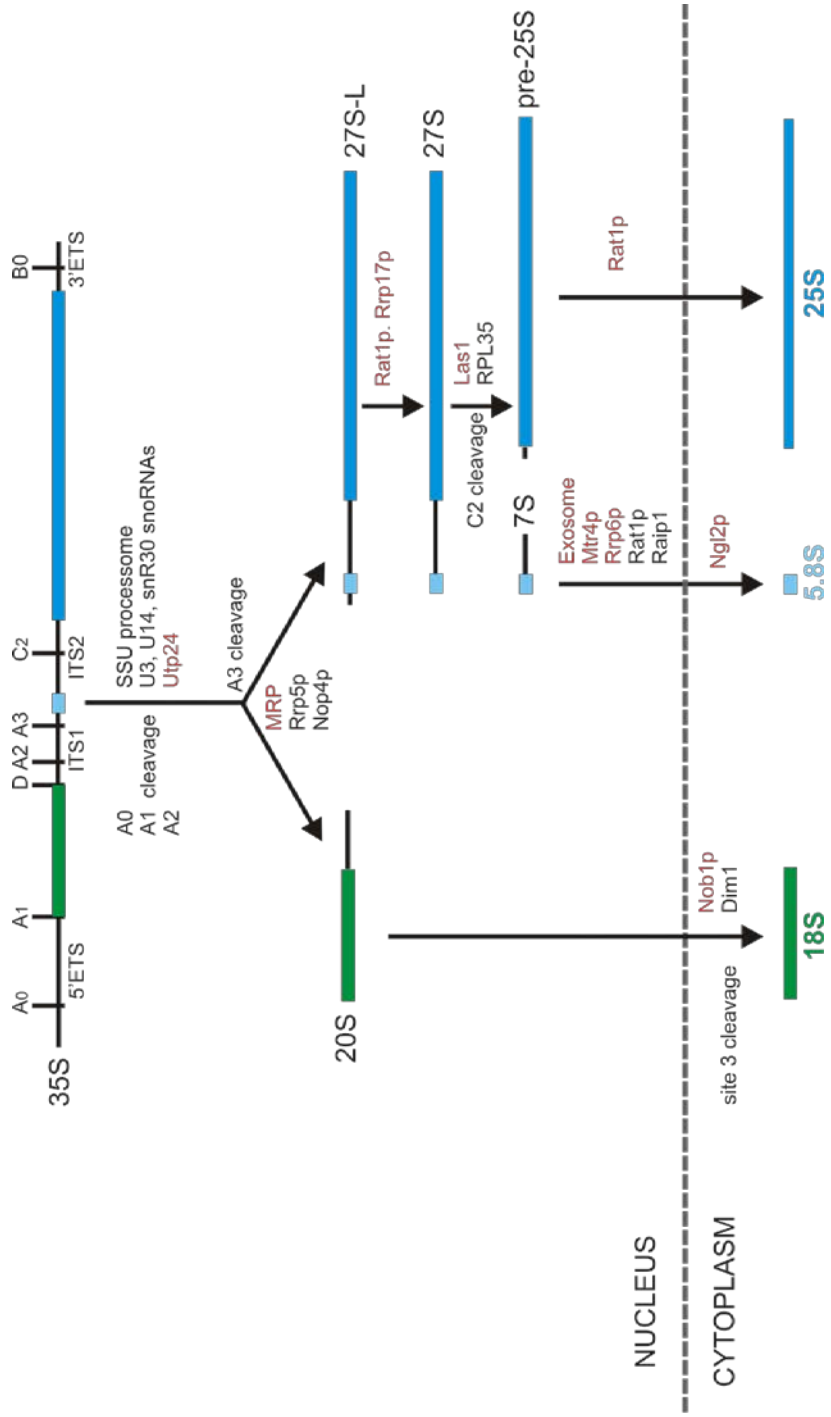

Figure 1.2. Schematic representation of the rRNA processing pathway in yeast. processing pathway in humans. The small ribosomal subunit (SSU) precursor and mature rRNAs are shown in green and the large ribosomal subunit (LSU) rRNAs are shown in blue. The cleavage sites are indicated at the top. The enzymes and factors essential for each cleavage step are shown in red and the important ones in black. The nucleus and the cytoplasm are clearly indicated (Adapted from: (Henras et al., 2015)).

In humans, the rRNA processing pathway is somewhat conserved, involving more than 200 proteins (Henras et al., 2008). As opposed to yeast, most of the processing at 5' ETS in humans occurs after ITS1 cleavage. An additional cleavage site A' is found at the human 5' ETS forming the 45S rRNA precursor, which is dependent on the UTP-

A complex. The exonuclease XRN2 and the surveillance factor MTR4 are also important for this cleavage step (Figure 1.3) (Sloan et al., 2014). It was originally thought that the U3 snoRNA was also important for this cleavage step (Enright et al., 1996), but it was recently shown that this is not the case (Sloan et al., 2014). Interestingly, the A' cleavage step in humans can be bypassed either in the absence of XRN2 or naturally in the cells (Sloan et al., 2014).

As opposed to yeast, there are two processing pathways in humans for the separation of the large and small subunit rRNA precursors and the processing of the LSU and SSU rRNA precursors (Sloan et al., 2013c, Rouquette et al., 2005, Mullineux and Lafontaine, 2012). The major pathway involves a single cleavage at site 2 of ITS1 by which leads to the production of 32S and 30S precursors of 28S and 18S respectively (Figure 1.3). The nuclease involved in this cleavage step is still unknown and the RNA binding protein RRP5 was shown to be important for this (Sloan et al., 2013c). The nucleolar protein NOL12, the ribosome biogenesis protein BOP1 and, in lesser extent, the RNA-binding protein RBM28, but not MRP RNase, are also involved in this cleavage event, which is comparable to A3 cleavage in yeast (Figure 1.3) (Sloan et al., 2013c). Processing of the 30S SSU rRNA precursor towards site 2a involves a number of proteins, including the RRP6 exonuclease, and the MTR4 helicase (TRAMP complex component), which is required for full RRP6 activity (Sloan et al., 2013c). Moreover the exosome, the ribosomal protein RPS19 and the ribosome biogenesis proteins ENP1 and RCL1 are required for the production of the 18SE SSU rRNA precursor (Figure 1.3) (Sloan et al., 2013b). The mature 18S rRNA is produced by cleavage at site 3, presumably by NOB1 endonuclease, in the cytoplasm (Figure 1.3) (Henras et al., 2015).

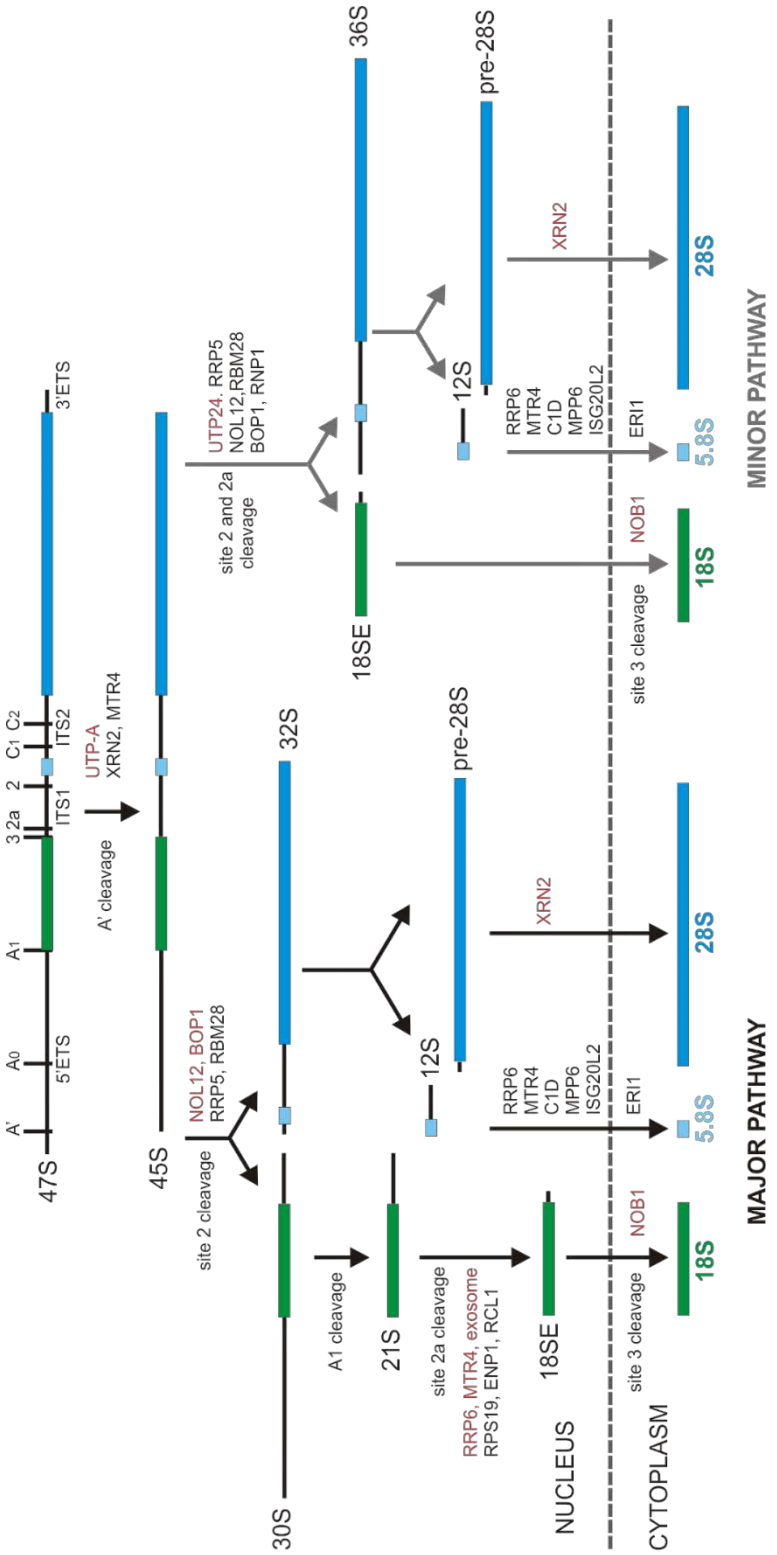

Figure 1.3. Schematic representation of the rRNA processing pathway in humans. The small ribosomal subunit (SSU) precursor and mature rRNAs are shown in green and the large ribosomal subunit (LSU) rRNAs are shown in blue. The cleavage sites are indicated at the top. The major pathway is indicated in black and the minor pathway is indicated in grey. The enzymes and factors essential for each cleavage step are shown in red and the factors important, but not essential, for the cleavages are shown in black. The nucleus and the cytoplasm are clearly indicated(Adapted from: (Sloan et al., 2013c)).

Processing of the 32S LSU rRNA precursor is less well-understood. Processing towards the 5' end of 5.8S takes place by XRN2 exonuclease and other nucleases are likely to be involved (Figure 1.3) (Sloan et al., 2013c). Cleavage at site 4 results in the separation of the 12S rRNA precursor and the 28S precursor (Figure 1.3), but the factors involved in this step are still unknown. Presumably Las1 endonuclease might be involved in this cleavage step, similarly to yeast (Gasse et al., 2015). Processing of the 5' end of the 12S rRNA precursor involves the exosome component RRP6 (Preti et al., 2013), the exosome associated-factors MTR4, C1D (Schilders et al., 2007) and MPP6 (Tafforeau et al., 2013), and the exonuclease ISG20L2 in the nucleus (Coute et al., 2008), and the exonuclease ERI1 (Ansel et al., 2008) in the cytoplasm, for the formation of the mature 5.8S rRNA. Processing of the pre-28S rRNA involves the exonuclease XRN2 in the nucleus (Wang and Pestov, 2011), and the mature 28S rRNA is then exported to the cytoplasm (Figure 1.3).

The minor pathway for rRNA processing compensates if the major pathway is blocked (Figure 1.3) (Sloan et al., 2013c). It has been recently shown that UTP24 endonuclease is required for site 2 cleavage (Wells et al., 2016) and cleavage at site 2a is dependent upon RRP5 (Sloan et al., 2013c). The ribosomal proteins NOL12, RBM28, BOP1 and RNP1 were also shown to be involved in the minor pathway (Sloan et al., 2013c). In this case, the 36S precursor of the 28S rRNA is produced rather than the 32S, and the 18SE precursor of the 18S is produced rather than the 30S (Figure 1.3). Further cleavage events take place as described above until the mature 18S, 28S and 5.8S are produced (Sloan et al., 2013c).

The ribosomal proteins play an important role in the rRNA processing pathway (Henras et al., 2015). Some ribosomal proteins have been found to be required for rRNA processing, indicating another function in ribosomal proteins. For example, RPL26 (Gazda et al., 2012) is necessary for SSU and LSU rRNA processing in humans. Furthermore, the association of the ribosomal proteins with the pre-rRNAs is important for the proper folding of the mature and stable ribosomal subunits in both prokaryotes (Chen and Williamson, 2013) and eukaryotes (Ferreira-Cerca et al., 2007, Ohmayer et al., 2013). Finally, the involvement of ribosomal proteins in several cleavage steps during rRNA processing is evident from depletion experiments mainly showing the requirement of almost half of the ribosomal proteins for processing of the 5' ETS site

in yeast (Ferreira-Cerca et al., 2005, Ferreira-Cerca et al., 2007) and humans (O'Donohue et al., 2010), as well as other processing steps (Henras et al., 2015).

1.2.4. Ribosomal protein production

The genes encoding for ribosomal proteins are transcribed by RNA polymerase II and they have been found in the majority of chromosomes in humans, including the sex chromosomes X and Y (Kenmochi et al., 1998). This is in contrast to bacteria where the genes encoding for ribosomal proteins are organized in operons found under the control of a single promoter (Nomura et al., 1984). Most of the ribosomal proteins are encoded in 5' TOP mRNAs, which have a Terminal OligoPyrimidine (TOP) tract at their 5' end. These mRNAs were discovered because they escaped rapamycin inhibition (Levy et al., 1991) and the mTOR pathway plays an important role in the translation of 5' TOP mRNAs in response to external stimuli and ribosome biogenesis defects (Gentilella et al., 2015).

A number of proteins associate with mTOR, forming the mTOR complex 1 (mTORC1), including Raptor (Hara et al., 2002), PRAS40 (Oshiro et al., 2007), Rheb-GTPase, RAG (Groenewoud and Zwartkruis, 2013) and GβL (Kim et al., 2003). mTORC1 is important for cell growth and metabolism, and, therefore, controlled by various intracellular and extracellular stimuli, including growth factors, energy status and oxygen levels (Laplante and Sabatini, 2009b). mTORC1 is involved in a number of downstream pathways and plays an important role in transcription and translation (Hay and Sonenberg, 2004). mTORC1 is involved in regulating mRNA translation initiation and elongation, and pyrimidine biosynthesis, leading to activation of translation initiation (Plas and Thomas, 2009). Finally, mTORC1 promotes ribosome biogenesis by activation of rDNA transcription in the nucleolus and nucleoplasm. Interestingly, phosphorylation of the ribosomal protein S6, which is a part of the small ribosomal subunit (SSU), and activation of LARP1 (La ribonucleoprotein domain family, member 1), a translational activator of 5' TOP mRNAs, is induced by mTORC1 (Gentilella et al., 2015). Taken together, activation of mTORC1 can affect ribosome biogenesis by regulation of both ribosomal protein and rRNA levels (Pende et al., 2004).

Interestingly, there are two ribosomal proteins, RPS27a and RPL40, which are transcribed as ubiquitin-fusion ribosomal proteins (Kimura and Tanaka, 2010). Further

details on this pathway are discussed later on. Most of the ribosomal proteins are translated in the cytoplasm and transferred back in the nucleus, and, subsequently, to the nucleolus, where ribosome biogenesis takes place (Zemp and Kutay, 2007), whereas some of them bind the ribosomal complexes in the cytoplasm, such as RPL10 (West et al., 2005). Ribosomal proteins produced in excess are unstable outside the ribosome and rapidly degraded by the proteasome (Lam et al., 2007).

1.2.5. The 5S RNP

The 5S RNP consists of the ribosomal proteins RPL5, RPL11 and the 5S rRNA, which is the smallest RNA in the ribosome. The 5S rRNA is transcribed in the nucleoplasm and contains 2-3 nucleotides on its 3' site, which are cleaved for the production of the mature 5S rRNA in both yeast (van Hoof et al., 2000) and in humans (Sloan et al., 2013c). In particular, the 3' processing of 5S rRNA in humans is dependent on RPL5 binding (Sloan et al., 2013a). In yeast, Rex1p, Rex2p and Rex3p exonucleases are essential for the 3' processing of the 5S rRNA precursor (van Hoof et al., 2000). Unlike the 28S, 18S and 5.8S, the nucleotides of the 5S rRNA are not usually modified (Ciganda and Williams, 2011), and defective or excess 5S rRNA produced is polyadenylated and targeted for degradation by the exosome (Kuai et al., 2004).

The secondary structure of the 5S rRNA is highly conserved amongst bacteria and eukaryotes, which consists of five helices, two hairpin loops, two internal loops and an internal hinge region (Szymanski et al., 2002). In lower organisms, such as *X. leavis*, the 5S rRNA is bound by the transcription factor TFIIIA, forming the 7S RNP (Layat et al., 2013, Sloan et al., 2013a). In humans, after transcription, the 5S rRNA is bound by the ribosomal protein RPL5, forming a pre-5S RNP complex, which is important for 5S rRNA stabilisation and for its localization in the nucleus. Furthermore, the levels of the 5S rRNA are dependent on the levels of RPL5 (Deshmukh et al., 1993, Sloan et al., 2013a), since the unbound 5S rRNA is highly unstable and gets degraded very rapidly. The 5S rRNA-RPL5 complex enters in the nucleolus where it is bound by the ribosomal protein RPL11, forming the mature 5S RNP (Sloan et al., 2013a), which is then integrated in the ribosome.

1.2.6. Recruitment of the 5S RNP in the large ribosomal subunit

The 5S RNP gets integrated in the LSU in the nucleolus. The 5S rRNA is located in the central protuberance of the LSU. Interestingly, the 5S rRNA does not interact with any of the tRNAs in either the P or A site of the ribosome, and neither with any other factors during mRNA translation. However, its localization is important for connecting the tRNAs, elongation factors and peptidyl-transferase centre factors together (Dinman, 2005). Notably, mitochondria do not encode for a 5S rRNA and other factors are involved in the stabilisation of translation factors in the ribosome. It was, however, found that the 5S rRNA is imported from the nucleoplasm in the mitochondria (Magalhaes et al., 1998), but its functions during mitochondrial mRNA translation are still unknown.

In yeast, the integration of the 5S RNP in the LSU is dependent upon the ribosome biogenesis factors Rrs1 and Rpf2p (Zhang et al., 2007). Using the yeast two-hybrid system, it was found that Rpf2p interact with RPL5 and RPL11 (Miyoshi et al., 2002, Morita et al., 2002). Furthermore, the structure of the Rrs1-Rpf2p complex was solved in the fungus *Aspergillus nidulans*, where it was shown that the Rrs1-Rpf2p complex interacts with the 5S rRNA-RPL5 complex, along with the ribosome biogenesis factor Rsa4, and that only Rpf2p interacts directly with the 5S rRNA, but not Rrs1 (Kharde et al., 2015). Similarly, in yeast, the Rrs1-Rpf2p complex contacts Rpl5, Rsa4 and the 25S rRNA, which is important for the integration of the 5S RNP in LSU (Madru et al., 2015). Furthermore, Symportin 1 (Syo1) also aids the recruitment of RPL5 and RPL11 to the 5S rRNA in yeast (Calvino et al., 2015). RPL11 docks on helix 84 and the 5S rRNA interacts with Rpf2p, found in a complex with Rrs1, so that it is stabilised in the ribosome. These interactions result in the fixing of the 5S RNP in the pre-LSU complexes so that it does not rotate from the central protuberance in the mature LSU (Kharde et al., 2015).

In humans, RRS1 and BXDC1 are the analogues of the Rrs1 and Rpf2p respectively. However, no interactions with the free 5S RNP were found after pull-down experiments (Sloan et al., 2013a). It was recently shown that RRS1 or BXDC1 knockdowns resulted in a reduction of RPL5 in the nucleolus, but only BXDC1 knockdown resulted in an altered RPL11 localization in the nucleolus. Furthermore, knockdowns of either RRS1 or BXDC1 resulted in the accumulation of RPL5 and RPL11 in the nucleoplasm (Sloan

et al., 2013a). PICT1, a ribosome biogenesis factor, and RPL11 were shown to be required for the integration of the 5S RNP in the ribosome. Knockdowns of either PICT1 or RPL11 resulted in a reduced incorporation of the 5S rRNA in the ribosome, whereas knockdowns of either RRS1 or BXDC1 had very little effect on the 5S rRNA ribosomal incorporation. Finally, knockdowns of PICT1, RPL11 or RRS1 resulted in a decreased LSU production, but only PICT1 and RPL11 knockdowns affected the 5S RNP recruitment to the ribosomal complexes (Sloan et al., 2013a). The exact functions of RRS1 and BXDC1 in humans are still unclear, whereas PICT1 is essential for the recruitment of the 5S RNP in the LSU (Sloan et al., 2013a).

1.2.7. Small and large ribosomal subunit assembly and proofreading

The majority of the ribosome assembly process takes place in the nucleus, with the first steps of ribosome biogenesis occurring in the nucleolus, and only the last maturation steps occurring in the cytoplasm. This ensures that no premature translation occurs in the cytoplasm before the ribosomes are formed correctly and efficiently (Zemp and Kutay, 2007). Furthermore, the binding of some ribosomal proteins on immature rRNAs is prevented by the association of ribosome biogenesis factors on the rRNA. For example, in yeast, Enp1 and Ltv1 ribosome biogenesis factors prevent the binding of ribosomal protein RPS10 on the 18S rRNA, and PNO1 prevents binding of RPS26 (Strunk et al., 2011). Surprisingly, these proteins do not show any sequence similarity to the SSU ribosomal proteins. Mrt4, another ribosome biogenesis factor, prevents binding of ribosomal protein P0 to 25S rRNA in yeast, by sequence homology. More specifically, Mrt4 is required for binding of P0 when the 25S rRNA is found at the right conformation, and P0 binding to the 25S rRNA triggers the release of Mtr4 (Rodriguez-Mateos et al., 2009).

Thirdly, it was shown in yeast that the mature LSU is required for the last processing stages for the maturation of SSU in the cytoplasm (Lebaron et al., 2012, Lamanna and Karbstein, 2011). The mature 60S subunit is important for GTP hydrolysis of Fun12, the yeast homologue of the translation initation factor eIF5B. This is important for the binding of Nob1 endonuclease on the pre-SSU complexes, which cleaves the 20S rRNA, resulting in the production of the mature 18S rRNA. Blocking the binding of Fun12 to the LSU rRNA resulted in the inhibition of 20S rRNA cleavage (Lebaron et al., 2012).

In addition, the joining of the pre-60S and pre-40S subunits is blocked by ribosome biogenesis factors, until the mature complexes are formed. For example, Nmd3 adaptor protein, which is required for nuclear export of the pre-60S complex (Sengupta et al., 2010) or Rei1 ribosome biogenesis factor, which is important for the maturation of the 60S complexes (Greber et al., 2016), prevent premature joining of the two subunits in yeast. Moreover, Tsr1 ribosome biogenesis factor fits in the 60S binding area of the pre-40S, blocking the association of the premature 60S (McCaughan et al., 2016). Furthermore, Tif6p ribosome biogenesis factor binds to the 60S subunit surface in yeast, preventing 40S joining (Klinge et al., 2011). Release of Tif6p requires GTP hydrolysis, which is dependent on the GTPase Efl1p (Senger et al., 2001), with the aid of the guanine nucleotide exchange factor Sdo1 (Menne et al., 2007). The human homologue of Tif6p, eIF6, prevents joining of the human pre-60S and pre-40S complexes. The GTP hydrolysis-dependent release of eIF6 in humans is triggered by SBDS and EFL1 ribosome biogenesis factors (Finch et al., 2011). Finally, premature translation of cytoplasmic mRNAs is prevented by RIO2, TSR1 and NMD3 ribosome biogenesis factors in humans (Karbstein, 2013).

1.2.8. Nuclear export

The pre-60S and pre-40S complexes are exported from the nucleus to the cytoplasm via the nuclear pores by exportins. Exportin Crm1 (or XPO1) is necessary for the export of both pre-LSU and pre-SSU particles. Exportin 5 (Exp5) is also involved in the nuclear export of the pre-LSU, apart from Crm1 (Wild et al., 2010). Both Crm1 and Exp5 have a Ran GTP-dependent mechanism, where the nuclear export of the premature ribosomal subunits is catalysed by the hydrolysis of Ran-GTP to Ran-GDP (Johnson et al., 2002).

The nuclear export of the pre-60S complexes is mainly dependent on Crm1, which binds to a nuclear export sequence (NES), consisting of a short leucine-rich motif (Hutten and Kehlenbach, 2007). However, no such signal is found on the pre-60S particles. For this reason, another protein, NMD3 (Nmd3p in yeast), is required for pre-60S export (Sengupta et al., 2010). Nmd3p binds to the mature pre-60S subunit, which acts as an adaptor for Crm1 recruitment (Zemp and Kutay, 2007). Interestingly, Nmd3p does not bind to immature or misfolded pre-60S particles, providing an additional proofreading mechanism (Johnson et al., 2002). Another ribosome biogenesis protein,

called Arx1, also acts as an adaptor protein in yeast, like Nmd3p (Hung et al., 2008). Other proteins are also thought to be involved in the pre-60S export, but their exact roles are still unclear. For example, Rrp12p is a protein containing HEAT repeats, which are associated with nuclear export of other proteins and complexes (Schafer et al., 2003). It was proposed that Rrp12p is involved in nuclear export in yeast, since it was found to be bound on the pre-ribosomal complexes and depletion of Rrp12p resulted in nuclear export impairment (Oeffinger et al., 2004). Furthermore, Mtr2p, a protein involved in mRNA nuclear export, is thought to be involved in the nuclear export of pre-60S, since it was detected in these complexes (Nissan et al., 2002).

Crm1 is the main exportin involved in the nuclear export of the pre-40S complexes as well. As with pre-60S, pre-40S particles also require protein adaptors, since no NES sequence was detected. However, Nmd3p was not found to be involved in pre-40S export. Instead, other proteins have been found to act as adaptors in yeast. Rio2p, a protein involved in the late maturation steps of SSU biogenesis (Vanrobays et al., 2003), was predicted to act as a nuclear adaptor for pre-40S export (Zemp and Kutay, 2007, Zemp et al., 2009), as it accumulated in the nucleus after Crm1 inhibition (Schafer et al., 2003). Furthermore, Dim2p and Ltv1p are two other potential protein adaptors found for pre-40S (Zemp and Kutay, 2007). Ltv1p is likely to facilitate the pre-40S nuclear export, but it is non-essential for this (Seiser et al., 2006). Rrp12p is thought to be a potential adaptor protein for export of both subunits, since it was found to be associated with pre-40S and pre-60S complexes (Oeffinger et al., 2004). In humans, the main adaptor protein for pre-40S export is RIO2, since deletion of RIO2 resulted in block of the final maturation and export of pre-40S because of recycling of trans-acting factors (Zemp et al., 2009), and TSR1 is also required (Carron et al., 2011). Furthermore, late-binding ribosomal proteins, such as RPS15, RPS18, RPS5 and RPS28, were also found to be involved in pre-40S nuclear export (Ferreira-Cerca et al., 2005).

1.3. Ubiquitin-ribosomal protein genes

1.3.1. The importance of ubiquitin in the cell

Ubiquitin (Ub) is a highly conserved, 76 amino acid-long peptide and highly abundant (Kimura and Tanaka, 2010), as it makes up 0.1-5% of all cellular protein (Ryu et al., 2007). Ubiquitination is a reversible post-translational modification, which is essential for various cellular processes. The ubiquitin molecule is added on the substrate by E3 ubiquitin ligases, where an isopeptide bond is formed between a lysine residue on the ubiquitin and a glycine residue on the protein (Pickart, 2001), which is cleaved by a group of proteases called de-ubiquitinases (Reyes-Turcu et al., 2009). Ubiquitin homeostasis is a tightly regulated process and it is estimated that mammals contain approximately 600 E3 ubiquitin ligases and 100 de-ubiquitinases (Li et al., 2008).

The attachment of ubiquitin to other ubiquitin molecules or the protein substrate is dependent on ATP hydrolysis (Kimura and Tanaka, 2010). Firstly, the C-terminus of the ubiquitin molecule is activated by a formation of a Ub-adenylate intermediate, which then interacts with a cysteine residue of the E1 ubiquitin-activating enzyme forming a thiol-ester bond (Figure 1.4) (Pickart and Eddins, 2004). The ubiquitin is then transferred to a cysteine residue on the E2 ubiquitin-conjugating enzyme (Figure 1.4). Finally, the ubiquitin is attached to a specific lysine on the protein substrate by the facilitation of an E3 ubiquitin-ligase enzyme (Figure 1.4) (Pickart and Eddins, 2004). This takes place by binding of the E3 ligase to the ubiquitination signal on the substrate, followed by the ligation of the ubiquitin (Pickart, 2001). Interestingly, there is a huge number of the E3 ligases conferring substrate specificity (Hershko and Ciechanover, 1998). Most E3 ligases contain a HECT (E6-AP carboxyl terminus) domain or a RING (really interesting new gene) domain (Pickart, 2001).

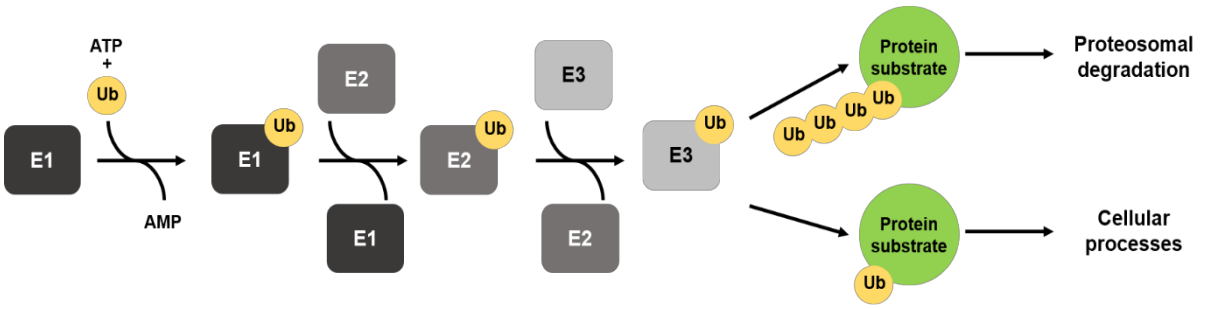

Figure 1.4. Schematic representation of the ubiquitin transfer process. The ubiquitin molecule is indicated in yellow and the protein substrate is indicated in green. The E1 ubiquitin-activating enzyme is shown in dark grey, the E2 ubiquitin-conjugating enzyme in grey and the E3 ubiquitin-ligase in light grey. ATP hydrolysis is indicated by the release of AMP (Adapted from (Ardley and Robinson, 2005)).

Mono-ubiquitination, the addition of one ubiquitin molecule on the protein substrate, is important for processes such as endocytosis and membrane trafficking (Ikeda and Dikic, 2008). For example, some transmembrane proteins are internalized in the cell after mono-ubiquitination (Miranda and Sorkin, 2007), such as some G-protein couple receptors (Tanowitz and Von Zastrow, 2002, Shenoy et al., 2001). Furthermore, mono-ubiquitination has been found to be important in DNA damage repair pathways. For instance, lysine 63 on histone H2AX is ubiquitinated when DNA damage occurs, which is then recognized by DNA damage repair enzymes resulting in homologous-recombination repair (Ikura et al., 2007). Moreover, ubiquitination of histones also affects gene regulation, since the chromatin structure is altered aiding in enhanced DNA transcription (Hammond-Martel et al., 2012). Finally, mono-ubiquitination was found to be important for cell-cycle regulation, by ubiquitination of cyclins, the cell cycle regulators (Teixeira and Reed, 2013), and apoptosis, by ubiquitination of the caspases involved in programmed cell death (Mukhopadhyay and Riezman, 2007, Huang et al., 2000).

On the other hand, poly-ubiquitination, the addition of multiple ubiquitin molecules on the substrate, is mainly involved in targeting the protein substrate for proteosomal degradation (Li and Ye, 2008). There are seven lysines on ubiquitin, where a poly-ubiquitin chain is presumed to be formed by interaction with other ubiquitin molecules (Komander and Rape, 2012). The most well-studied is lysine 48 (K48), where poly-ubiquitin chains are formed, consisting of at least four ubiquitins, leading to proteosomal degradation of the protein substrate (Hicke, 2001), which is important in

various cellular processes. Proteosomal degradation of a number of transcription factors or transcriptional activators leads to inhibition of gene transcription under certain physiological conditions (Lipford et al., 2005). Furthermore, proteins that are anomalously folded or damaged are targeted for proteosomal degradation (Lecker et al., 2006). For example, in cystic fibrosis, the mutant transmembrane protein CFTR is degraded and does not reach the cell membrane (Ward et al., 1995). Finally, poly-ubiquitination is important for apoptosis, since the IAP protein family, which inhibits pro-apoptotic proteins (Deveraux and Reed, 1999), is targeted for proteosomal degradation leading to the activation of the apoptotic pathway (Lee and Peter, 2003).

De-ubiquitinases are responsible for the cleavage of the peptide bond formed between ubiquitins or between the ubiquitin and the substrate, and they can be either cysteine proteases or zinc metalloproteases (Nijman et al., 2005). There are five classes of de-ubiquitinases: the ubiquitin C-terminal hydrolases (UCHs), the ubiquitin-specific proteases (USPs), the ovarian tumour proteases (OTUs) and the Josephins, which are cysteine proteases, and the JAB1/MPN/MOV34 (JAMMs), which are zinc metalloproteases (Komander et al., 2009). The cysteine proteases contain three conserved amino acids for the nucleophilic attach of the catalytic cysteine residue to the peptide bond formed (Storer and Menard, 1994, Komander et al., 2009), whereas the zinc metalloproteases use two zinc ions for the recruitment and activation of a water molecule, which attacks the peptide bond (Sato et al., 2008). The de-ubiquitinases have diverse functions in the cell, including the processing of the ubiquitin precursors after translation, the recycling of ubiquitin and the removal of ubiquitin from the protein substrates for proteosomal degradation rescue (Komander et al., 2009). De-ubiquitinases show some substrate specificity between the different types of ubiquitination and the type or structure of the different chain linkages (Komander et al., 2009), but the exact mechanisms for this are still unclear. For instance, UCHs are known to cleave mono-ubiquitinated, but not poly-ubiquitinated chains (Pfoh et al., 2015), and members of the UPS (Hu et al., 2005) and OTU (Edelmann et al., 2009) families have been described to be specific for K48 ubiquitinated chains (Komander et al., 2009).

1.3.2. RPRS27a- and RPL40-ubiquitin fusion ribosomal proteins

In mammals, there are four Ub-encoding genes. *Ubb* and *Ubc* encode for a 4- and 9-tandem repeat array of ubiquitin respectively, whereas RPS27a (*Uba52* in mouse) and RPL40 (*Uba80* in mouse) are produced as ubiquitin-ribosomal protein precursors, encoding for one ubiquitin (Redman and Rechsteiner, 1989). In humans, the majority of the ubiquitin pool is made up by the ubiquitins transcribed by *Ubb* and *Ubc* genes. In contrast, in yeast, only one gene, *UBI4*, encodes for a poly-ubiquitin chain, and the ubiquitin encoded by the ubiquitin-fusion ribosomal proteins genes *UBI1*, *UBI2* and *UBI3* make up the majority of the ubiquitin pool (Finley et al., 1987). The ubiquitin in the cell is not produced in excess, but the levels of the free ubiquitin are sufficient for the cellular functions (Kimura and Tanaka, 2010).

RPS27a and RPL40 are produced as ubiquitin-ribosomal protein precursors throughout eukaryotes, which are then cleaved to separate the ribosomal proteins and ubiquitin component (Kimura and Tanaka, 2010), but their functions and significance remains unclear. RPS27a and RPL40 are part of the small and large ribosomal subunit respectively (Kimura and Tanaka, 2010), but they are not produced from 5' TOP mRNAs as most of the ribosomal proteins (Levy et al., 1991). However, not much is known about their functions in humans or yeast. RPS27a was firstly identified as a ribosomal protein in 1989 (Redman and Rechsteiner, 1989) and the RPS27a protein was later found to be expressed in high levels in solid tumours, and up-regulated in patients with chronic myeloid leukaemia (CML) or acute myeloid leukaemia (AML). Confirming its role in CML, the expression of RPS27a in the CML cell line K562 was found to be elevated, which induced cell cycle and proliferation, while inhibiting apoptosis (Wang et al., 2014). Finally, RPS27a was found to be involved in the regulation of the tumour suppressor p53, which is normally targeted for proteosomal degradation by the E3 ubiquitin ligase MDM2. Upon ribosomal stress, RPS27a was found to directly interact with MDM2, inhibiting its activity, resulting in p53 activation (Sun et al., 2011). These studies indicate that RPS27a could be an important target for future anti-cancer treatment therapies.

1.4. Modifications of ribosomal RNA

1.4.1. Pseudouridylation and methylation of rRNA

The most prelavent rRNA modifications are the 2'-*O*-methylation and pseudouridylation. It is hypothesized that there are more than 100 2'-*O*-methylation sites and around 100 pseudouridines in human rRNAs (Maden, 1990). These modifications are mainly found in the well-conserved regions of the ribosome, such as the peptidyl-transferase centre and the decoding centre (Decatur and Fournier, 2002). Most individual modifications are not essential, but loss of the total 2'-*O*-methylation or pseudouridines is lethal (Higa-Nakamine et al., 2012, Decatur and Fournier, 2002) and clusters of modifications are important for the cell (Gigova et al., 2014, Esguerra et al., 2008).

2'-*O*-methylation involves the addition of a methyl group on the 2' hydroxyl group of the ribose of the rRNA by methyltransferases (Figure 1.5A). This modification is important for the stability of single base pairs, since there are increased base-base interactions in the presence of a methyl group at 2'-OH, because of its ability to change the polarization of the bases (Agris, 1996). The stability of single base pairs is further aided by the presence of the methyl group, since it prevents hydrolysis from various nucleases because of chemical and steric block (Helm, 2006). Furthermore, 2'-*O*-methylation encourages the formation of a thermodynamically stable RNA structure (Kierzek and Kierzek, 2003). Pseudouridylation involves the isomerization of uridine to pseudouridine (Ψ) by pseudouridine synthases (Figure 1.5B). Pseudouridine is less flexible than uridine due to its conformation (Charette and Gray, 2000). Furthermore, in uridine, the N1 atom of the uracil interacts with the the C1 atom of the ribose, whereas in pseudouridine the C5 atom of the uracil interacts with the C1 atom of the ribose (Figure 1.5B). This allows pseudouridine to form more stable interactions, because of the presence of an additional hydrogen donor of N1 atom (Charette and Gray, 2000).

The 2'-*O*-methylation is catalyzed by the box C/D snoRNPs in eukaryotes, whereas pseudouridylation is catalyzed by the H/ACA snoRNPs (Watkins and Bohnsack, 2011). The crystal structures of the snoRNPs have been solved in archaea and the eukaryotic structures are predicted based on sequence similarities of the snoRNAs and proteins.

In bacteria, even though the rRNA modifcations are highly conserved, they are catalyzed by protein enzymes instead of snoRNP complexes (Bachellerie et al., 2002). Therefore, it is widely believed that the eukaryotic snoRNP complexes were most likely evolved from archaea, rather than bacteria, due to structural and mechanistical similarities (Bachellerie et al., 2002).

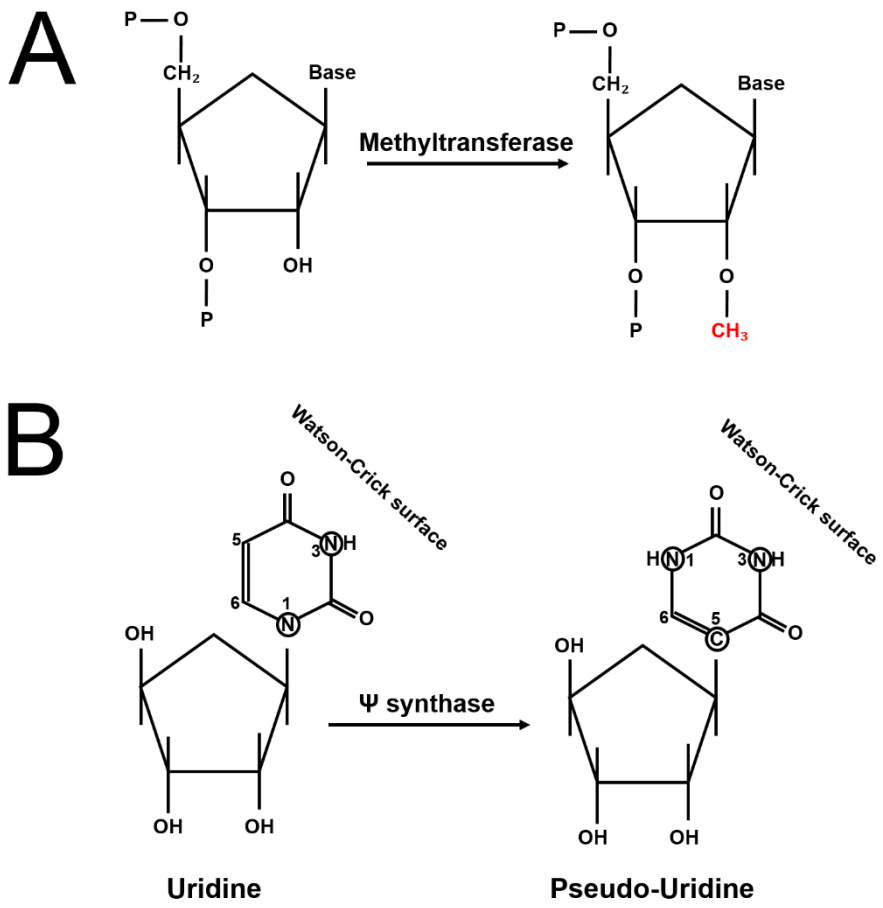

Figure 1.5. Schematic representation of methylation and pseudouridylation. (A) The addition of a methyl group (shown in red) on the 2' OH of the ribose by a methyltransferase. **(B)** The isomerization of uridine to pseudouridine (Ψ) by a pseudouridine synthase. The atom positions on the uracil rings and the Watson-Crick surface are indicated (Adapted from: (Kiss and Jady, 2004)).

1.4.2. The Box C/D snoRNP

The archaeal box C/D sRNP consists of the proteins L7Ae (NHPX or 15.5K in humans, Snu13 in yeast), Nop5 (Nop56, Nop58 in eukaryotes) and Fibrillarin (Nop1 in yeast) (Watkins and Bohnsack, 2011), as well as a sRNA component (Figure 1.6). Fibrillarin is a methyltransferase and it is essential for the catalysis of 2'-*O*-methyation of the rRNA (Watkins and Bohnsack, 2011). The archaeal and eukaryotic box C/D snoRNAs contain a conserved C/D box at the 5' and 3' ends of the RNA, and a C'/D' box, which

is found in the middle of the RNA (Watkins and Bohnsack, 2011). A stem-loop structure, called the K-turn, is formed by the C/D motif, whereas another stem-loop structure, called the K-loop, is formed by the C'/D' motif (Reichow et al., 2007).

The archaeal box C/D sRNPs are thought to contain one copy of the sRNA, although there is some debate about this, and two copies of each of the box C/D proteins. After the crystal structure of the archaeal complex was solved (Bleichert et al., 2009), the two Nop5 molecules were found to interact forming a homo-dimer (Lin et al., 2011), providing the basis for the formation of the box C/D sRNP (Figure 1.6). The C-terminal of Nop5 interacts with L7Ae, which binds the K-turn motif of the sRNA, whereas the N-terminal of Nop5 interacts with Fibrillarin, so that the active site of Fibrillarin is in close proximity to the substrate ribose (Lin et al., 2011) (Figure 1.6). It is the L7Ae that initially binds the K-turn motif of the sRNA (Kuhn et al., 2002), and the L7Ae-snoRNA complex is then recognized by the Nop5/Fibrillarin complex, which subsequently binds on the sRNA (Omer et al., 2002). The modification nucleotide is selected by base-pairing to the target site and the target nucleotide base pairs in a proximity of 5 base pairs from the D or D' box (Kiss-Laszlo et al., 1996).

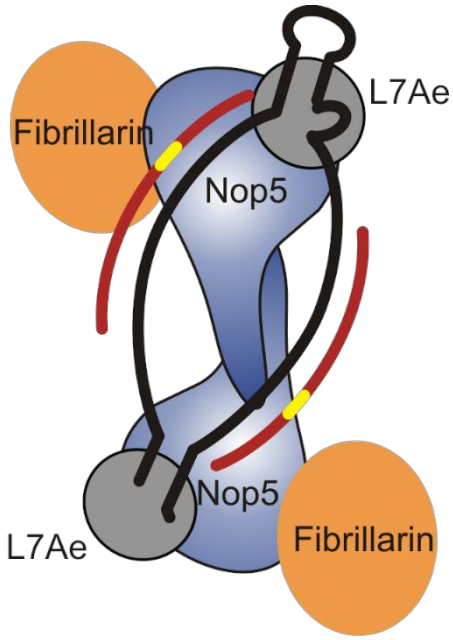

Figure 1.6. Graphical representation of the archaeal box C/D sRNP. Nop5 is indicated in blue, Fibrillarin in orange and L7Ae in grey. The box C/D snoRNA is shown in black and the substrate RNA is shown in red. The target nucleotide in shown in yellow (From: (Watkins and Bohnsack, 2011)).

The structure of the eukaryotic box C/D snoRNP has been recently solved and it was shown that it is highly similar to the archaeal complex (Kornprobst et al., 2016). In eukaryotes, the Nop56/Nop58 heterodimer is formed instead of the Nop5 homodimer, which is predicted to bind at the same positions on the snoRNA as the Nop5 dimer (Aittaleb et al., 2003). Nop56 is more often found to bind the C/D motif, whereas Nop58

most often binds the C'/D' motif (Cahill et al., 2002) (van Nues et al., 2011). On the other hand, 15.5K in humans or Snu13 in yeast was initially found to bind the K-turn formed by the C/D motif (Szewczak et al., 2005), but not the K-loop. Recent data have indicated that Snu13 in yeast also binds the C'/D' motif (Qu et al., 2011); hence, it is possible that Snu13 can stably bind the C/D motif and, in the presence of Nop56, the C'/D' motif. Snu13 interacts with the snoRNA component first in eukaryotes (Rothe et al., 2014) (Dobbyn and O'Keefe, 2004) and it is predicted that Fibrillarin (Nop1 in yeast) is near the catalytic side, similarly to archaea.

A number of box C/D snoRNAs are involved in rRNA methylation. For example, U16 is involved in the methylation of the 18S rRNA, whereas U24 snoRNA is predicted to guide the methylation of nucleotides of the 28S rRNA (Kiss-Laszlo et al., 1996). Furthermore, some box C/D snoRNAs were found to be involved in both rRNA processing and methylation, such as U14 which is involved in 18S rRNA processing (Li et al., 1990, Enright et al., 1996) and methylation (Kiss-Laszlo et al., 1996) in yeast. Finally, a number of box C/D snoRNAs are solely involved in rRNA processing. U3 snoRNA is involved in 18S rRNA processing in eukaryotes (Phipps et al., 2011) and U22 is involved in 18S rRNA in *Xenopus* oocytes (Tycowski et al., 1994), whereas U8 is involved in 28S rRNA processing in *Xenopus* oocytes (Peculis and Steitz, 1993). Most of the box C/D snoRNAs contain complementary sequences to the rRNA substrate, which are important not only for guiding methylation, but also for rRNA processing and folding (Henras et al., 2008). Interestingly, there are more than 200 box C/D snoRNAs, but only 100 2'-*O*-methylation sites (Jorjani et al., 2016).

1.4.3. The H/ACA snoRNP

The H/ACA sRNP complex consists of the proteins Dyskerin (Cbf5 in yeast and archaea), NOP10, NHP2, GAR1 and an RNA component (Figure 1.7) (Kiss et al., 2010, Watkins and Bohnsack, 2011). Dyskerin is the pseudouridine synthase of the complex, important for the isomerisation of uridine to pseudouridine (Lafontaine et al., 1998, Zebarjadian et al., 1999). All of the H/ACA RNAs have a similar structure and two very well conserved motifs: the ANANNA motif (called the H box), found in the hinge region (Balakin et al., 1996), and the ACA motif (Ganot et al., 1997b) found three positions downstream from 3' end (Balakin et al., 1996, Meier, 2005). The H/ACA snoRNA forms a stem-loop structure where the nucleotide for catalysis is found, flanked by P1 and P2

stems, and a loop structure, called the K-loop or K-turn (Figure 1.7). Most of structural and biochemical studies on the H/ACA sRNP have been performed on archaeal proteins, where it was found that most H/ACA RNAs are found as a single hairpin structure and the eukaryotic complexes are thought to be similar (Watkins and Bohnsack, 2011).

In archaea, it was found that the Cbf5, Nop10 and L7Ae (Nhp2) bind that H/ACA RNA directly, whereas Gar1 does not (Duan et al., 2009, Liang et al., 2009). Cbf5 binds the ACA motif and the P1 stem of the H/ACA RNA (Figure 1.7A), whereas L7Ae itneracts with the K-loop or K-turn formed at the top of the snoRNP (Baker et al., 2005, Rozhdestvensky et al., 2003). The P2 stem loop of the H/ACA RNA is bound by the surface formed after interactions between Cbf5, Nop10 and L7Ae (Figure 1.7A) (Li and Ye, 2006). In contrast, Gar1 does not bind the H/ACA RNA directly. Rather, it interacts with a conserved motif of Cbf5 called the thumb loop (Figure 1.7A). The interaction of Gar1 with the thumb loop of Cbf5 is important for keeping the substrate in place during catalysis and for the release of the final product (Duan et al., 2009).

Based on the solved archaeal structure, the proposed model for the eukaryotic H/ACA snoRNP complex suggests that there are two copies of each of the proteins on the H/ACA RNA, where the two Dyskerin copies interact with each other (Figure 1.7B) (Watkins and Bohnsack, 2011). Furthermore, it was found that the eukaryotic H/ACA RNAs do not contain a K-turn motif and, therefore, NHP2 does not bind independently of Dyskerin, as in archaea. It is thought that binding of Dyskerin and NOP10 to the H/ACA RNA, and the protein-protein interactions between them are important for NHP2 binding in eukaryotes (Watkins and Bohnsack, 2011). In yeast, it was shown that the Cbf5-Nop10-Gar1 complex is structurally similar to the archaeal complex (Li et al., 2011), further confirming the proposed model. Similarly, in eukaryotes, GAR1 interacts with Dyskerin but not with the H/ACA snoRNA, and is important for the organization of the complex to help keep the substrate in place during catalysis and for the release of the for the final product (Duan et al., 2009).

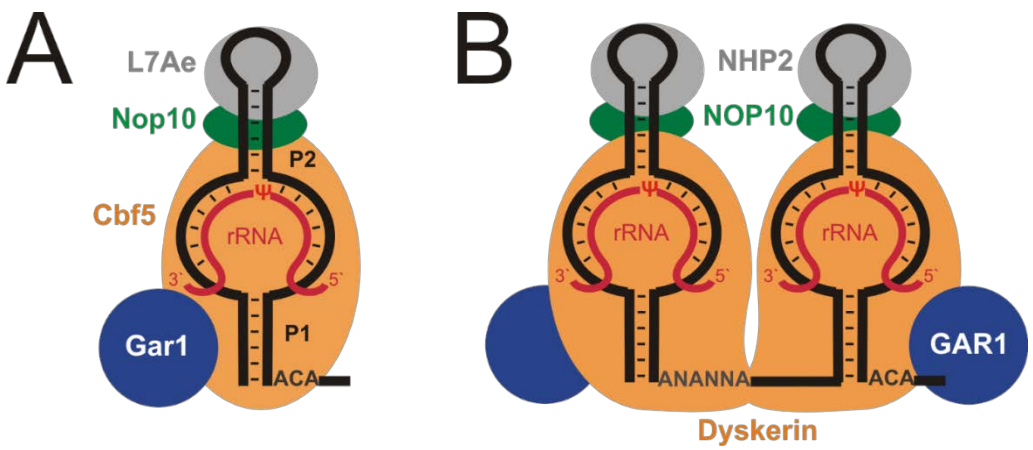

Figure 1.7. Graphical representation of the H/ACA snoRNP. (A) The archaeal H/ACA snoRNP consists of Cbf5 (orange), Nop10 (green), L7Ae (grey) and Gar1 (blue). The H/ACA snoRNA is shown in black and the ACA motif, the P1 and P2 loops are indicated. The substrate rRNA is shown in red and the target nucleotide is indicated by Ψ, showing pseudouridylation. **(B)** The human H/ACA snoRNP consists of Dyskerin (orange), NOP10 (green), NHP2 (grey) and GAR1 (blue). The H/ACA snoRNA is shown in black and the target rRNA is shown in red, with the target nucleotide to be marked with Ψ/ The H box is indicated by ANANNA sequence and the ACA motif is shown (From: (Watkins and Bohnsack, 2011)).

Most H/ACA snoRNAs are required for rRNA modification. For example, U64 H/ACA snoRNA is required for pseudouridylation of the 28S rRNA, whereas U66 was found to be guide pseudouridylation of the 18S rRNA (Ganot et al., 1997a). However, some H/ACA snoRNAs were shown to be involved in rRNA processing rather than modification. For example, U17 (snR30 in yeast) is important in 18S rRNA processing. Depletion of U17 in frog oocytes caused the accumulation of the 20S rRNA precursor, indicating that it is required for the 5' end processing for the production of the mature 18S rRNA (Mishra and Eliceiri, 1997), which was similar to the phenotype shown in yeast (Morrissey and D.Tollervey, 1993, Atzorn et al., 2004). In particular, snR30 in yeast base pairs directly with 18S rRNA, and this interaction is essential for 18S rRNA processing and production (Fayet-Lebaron et al., 2009). Furthermore, the human U17 H/ACA snoRNA has sequence similarity with its yeast homologue snR30 (Atzorn et al., 2004) and was found to have direct interactions with 18S rRNA precursors (Rimoldi et al., 1993), indicating a role in 18S rRNA processing. Another example of a H/ACA snoRNA not involved in modification is snR10 in yeast, which was found to be involved in 18S rRNA processing (Tollervey, 1987). Most of the H/ACA snoRNAs have complementary sequences to rRNA, which are important for both the modification and processing of the substrate rRNA (Henras et al., 2008).

1.4.4. Other functions of the H/ACA RNP

The H/ACA RNP is also a component of other RNP complexes in the cell and are predicted to be important for pre-mRNA splicing, by pseudouridylation of the small nuclear RNAs, and telomere maintenance, as well as ribosome biogenesis. It is also interesting that some H/ACA snoRNAs, called orphan snoRNAs, do not contain complementary sequences to any of the rRNA targets, as box C/D RNPs (Cavaillé et al., 2000).

The H/ACA RNP guides the pseudouridylation of the small nuclear (sn)RNAs as a scaRNP, which are key players in pre-mRNA splicing for the production of the mature mRNA. The H/ACA scaRNP was found or predicted to be involved in the pseudouridylation of U1, U2, U4 and U5 snRNAs (Darzacq et al., 2002). For example, the U100 scaRNA is predicted to be important for the pseudouridylation of U54 in U2 snRNA and U53 of U5 snRNA (Kiss et al., 2002, Schattner et al., 2006). Most scaRNAs contain H box and ACA motifs, such as U92 (Darzacq et al., 2002) and U93 (Kiss et al., 2002), which contain one and two H/ACA box domains respectively (Lestrade and Weber, 2006). However, some scaRNAs were also identified that contained both box C/D and H/ACA box domains, such as U85 (Jady and Kiss, 2001) and U87 (Darzacq et al., 2002), or only box C/D motifs, such as U90 and U91 (Darzacq et al., 2002). The H/ACA scaRNP complexes localize mainly to Cajal bodies, where the snRNPs are produced. This is achieved by binding of the Cajal body RNA chaperon protein TCAB1 on the H/ACA scaRNP (Figure 1.8), which aids the localization of the complex in Cajal bodies (Tycowski et al., 2009).

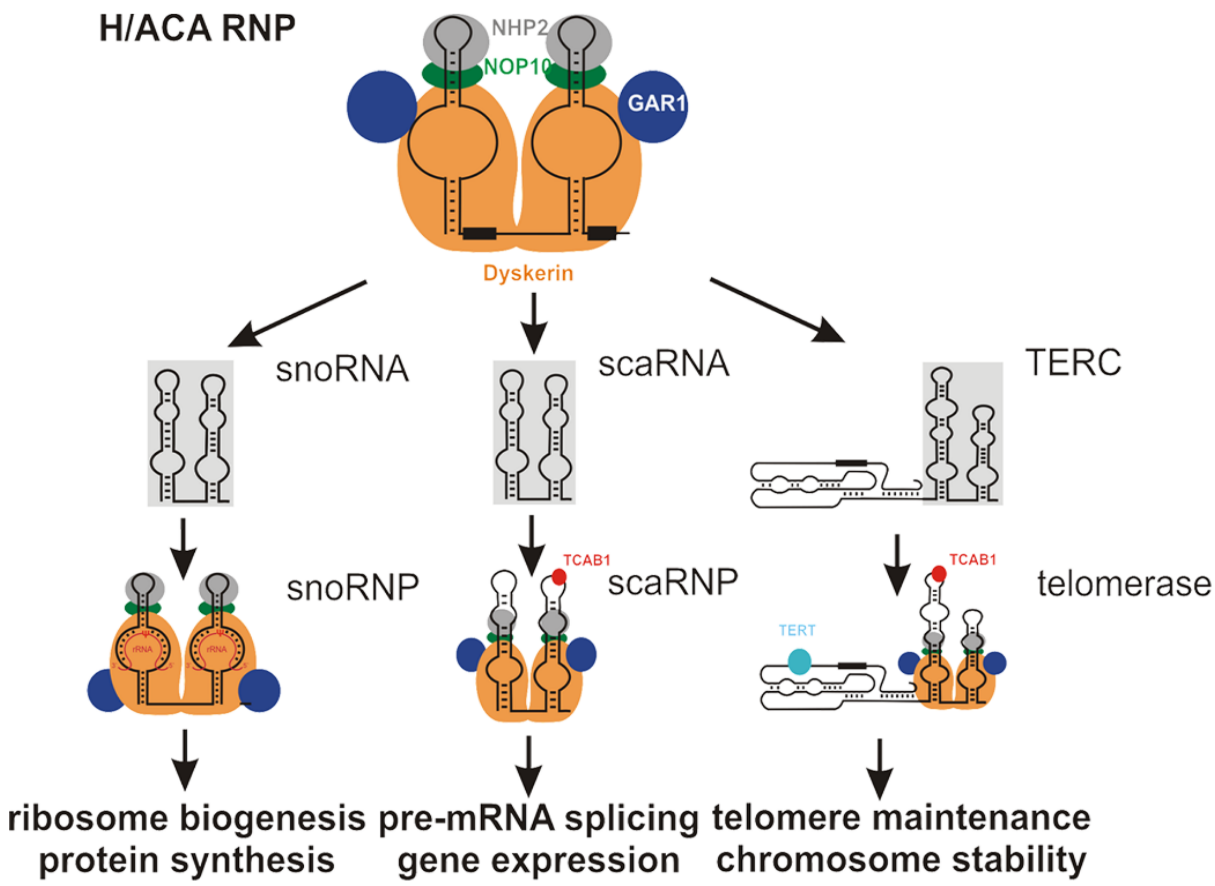

Figure 1.8. Schematic representation of the functions of the H/ACA RNP. The human H/ACA RNP consists of Dyskerin (orange), NOP10 (green), NHP2 (grey), GAR1 (blue) and an RNA component (black), and is involved in ribosome biogenesis, mRNA splicing and telomere maintenance. The Cajal-body chaperone protein TCAB1 is shown in red and the protein component of telomerase (TERT) is show in light blue

The H/ACA RNP is also part of the telomerase RNP and was found to have an important role in telomere maintenance (Figure 1.8) (Meier, 2005). Telomerase is a ribonucleoprotein enzyme, which is important for the addition of DNA sequence repeats at the telomeric ends. Telomerase consists of a protein component (hTERT) and an RNA component (hTR or TERC) which acts as a template (Feng et al., 1995). The RNA chaperone TCAB1 is associated with the telomerase complex for the localization of the H/ACA RNP complex on telomerase (Figure 1.8) (Stern et al., 2012). The H/ACA RNP and the Shelterin complex, which consists of six proteins (TRF1, TRF2, POT1, RAP1, TIN2, TPP1) (Xin et al., 2008), are important for the assembly and the stability of the telomerase complex (Meier, 2005, Podlevsky et al., 2008). Furthermore, Dyskerin may also play a functional role in telomere assembly, since mutations in Dyskerin were shown to cause a decreased accumulation of TERC

leading to telomere defects (Brault et al., 2013), which were restored after the addition of the catalytic domain of Dyskerin (Machado-Pinilla et al., 2012).

1.4.5. The pseudouridine synthase Dyskerin

Dyskerin (*Cbf5* in yeast, *NOP60B* in *Drosophila melanogaster*), the pseudouridine synthase of the H/ACA RNP, is a 58kD evolutionary conserved protein (Angrisani et al., 2014). Cbf5 in yeast (Cadwell et al., 1997) and NOP60B in Drosophila (Giordano et al., 1999) were the first to be identified in being involved in rRNA processing and pseudouridylation. Later on, mutations on the human *DKC1* gene, which encodes for Dyskerin, were identified in X-linked Dyskeratosis Congenita (DC) patients, a rare genetic disease (Podlevsky et al., 2008). Dyskerin is a highly conserved protein evolutionarily, especially the aspartic acid residue important for its catalytic activity. Furthermore, mutations on the yeast *Cbf5* gene were rescued by expression of either the Drosophila (Phillips et al., 1998) or rat (Yang et al., 2000) Dyskerin, also underlying its high conservation. In addition, the protein levels of Dyskerin were found to be elevated in different neuroblastoma cell lines independently of the telomerase functions, showing that Dyskerin might also have functions outside the H/ACA RNP (O'Brien et al., 2016a).

Dyskerin consists of multiple domains: the nuclear localization signals, the Dyskerin-specific domain, the TruB and the PUA domain. There are two nuclear localization signals (NLS), one at the N-terminus and one at the C-terminus of the protein (Figure 1.9), to ensure the nuclear, and nucleolar, localization of Dyskerin. In humans, there is a small extension of approximately 30 amino acids in the N-terminal NLS, which is not found in yeast Cbf5 (Angrisani et al., 2014). This indicates that the N-terminal NLS may have additional roles in humans, which is further supported by the identification of a few mutations in this domain, giving rise to X-linked DC (Podlevsky et al., 2008).

Dyskerin contains a Dyskerin-specific domain (Figure 1.9), which is conserved amongst the Dyskerin protein family, but its functions are still unknown (Angrisani et al., 2014). Mutations in this domain have been identified in DC patients (Podlevsky et al., 2008), showing that it might be important for the function or structure of Dyskerin. In addition, TruB is the catalytic domain of Dyskerin (Figure 1.9) important for its pseudouridylation activity (Angrisani et al., 2014). A highly conserved aspartic acid is

found in this domain (D125 in humans, D96 in yeast) (Figure 1.9), required the isomerization of uridine to pseudouridine (Cerrudo et al., 2014). Inactivation of the catalytic activity of Dyskerin by mutation of D125 site does not support growth in yeast (Zebarjadian et al., 1999). Finally, Dyskerin contains a PUA domain (Figure 1.9), which recognizes and binds the H/ACA snoRNA component of the H/ACA RNP (Angrisani et al., 2014). Interestingly, a few mutations in the PUA domain have been linked with X-linked DC, whereas only two mutations, S121G and R158W, in the TruB domain have been identified in X-linked DC patients (Figure 1.9) (Podlevsky et al., 2008). It is likely that many mutations in the TruB domain of Dyskerin completely block the activity of Dyskerin, resulting in cell death and, therefore, cannot be identified.

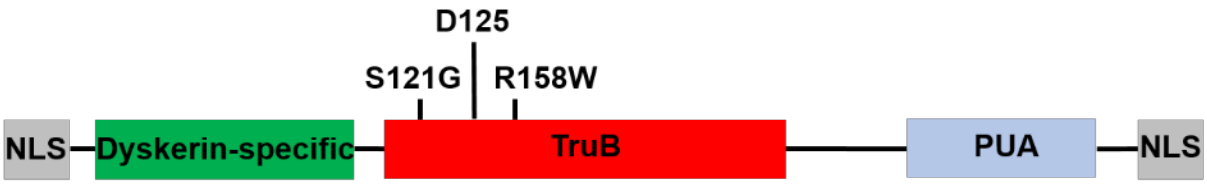

Figure 1.9. Schematic representation of the domains of Dyskerin. The nuclear-localization signals (NLS) are shown in grey, the Dyskerin-specific domain in green, the TruB catalytic domain in red and the PUA RNA-binding domain in light blue. The conserved catalytic aspartic acid is indicated (D125 in humans), as well as the mutations S121G and R158W found in X-linked DC patients (Adapted from: (Angrisani et al., 2014)).

1.5. Ribosomopathies

1.5.1. Introduction

Ribosomopathies are rare genetic diseases caused by mutations on genes encoding ribosomal proteins or ribosome biogenesis factors (Narla and Ebert, 2010). There are 18 ribosomopathies characterized, including Diamond-Blackfan Anaemia (DBA), 5q syndrome, Treacher-Collins (TC) syndrome, Dyskeratosis Congenita (DC), Shwachman-Diamond Syndrome (SDS), Cartilage Hair Hypoplasia (CHH) and Bowen-Conradi syndrome (Table 1.1). Ribosomopathies arise due to mutations in genes encoding for SSU ribosomal proteins (Lipton and Ellis, 2010, Ebert et al., 2008b), LSU ribosomal proteins (Cmejla et al., 2009) or ribosome biogenesis factors, such as *TCOF1* (Gonzales et al., 2005, Weiner et al., 2012), Dyskerin (Heiss et al., 1998, Knight et al., 2001, Angrisani et al., 2014) or *SBDS* (Boocock et al., 2003).

Ribosomopathy	Prevalence	Gene defect	Clinical manifestations	Cancer risk	p53 involvement
Diamond-Blackfan anaemia	1:100,000 to 1:200,000 live births	RPS19, RPS24, RPS17, RPS7, RPS15, RPS27A, RPL36, RPL35A, RPL5, RPL11	Hypoplastic macrocytic anaemia Skeletal, urogenital and cardiac defects Short stature	AML MDS osteosarcoma	p53-dependent anaemia
5q syndrome	Less than 1 in 200,000	RPS14	Macrocytic anaemia	MDS AML	p53-dependent anaemia
Treacher-Collins Syndrome	1 in 50,000 live births	TCOF1, POLR1C, POLR1D	Craniofacial anomalies Hearing difficulties	None reported	p53-dependent craniofacial defects
Dyskeratosis Congenita	1 in 1million people	DKC1, NOP10, NHP2, TERT, TERC, TINF2	Cytopenias Anaemia Skin hyperpigmentation Nail dystrophy Oral leukoplakia	AML Head and neck tumours	p53-dependent anaemia
Shwachman-Diamond Syndrome	1 in 50,000 births	SBDS	Exocrine pancreatic insufficiency Neutropenia Neurocognitive impairment Liver abnormalities	MDS AML	p53-dependent hematopoietic defects
Cartilage Hair Hypoplasia	1 in 1,300 (Old Older Amish), 1 in 20,000 (Finnish descent)	RMRP	Short stature Bone deformities Hair growth abnormalities	Non-Hodgkin Lymphoma Basal cell carcinoma	p53-dependent symptoms
Bowen-Conradi syndrome	1 in 355 births (Hutterite population) to 1 in 1million	EMG1	Growth retardation Early childhood death	None reported	None reported

Table 1.1. Clinical representation of Ribosomopathies. The table presents the most well-studied Ribosomopathies Diamond-Blackfan Anaemia, 5q syndrome, Treacher-Collins syndrome, Dyskeratosis Congenita, Shwachman-Diamond Syndrome, Cartilage Hair Hypoplasia and Bowen-Conradi syndrome. The prevalence, the genes mutated, the clinical manifestations, the cancer risk and the p53 involvement in each ribosomopathy are shown (Adapted from: (Narla and Ebert, 2010)).

Interestingly, even though mutations in genes encoding for different proteins involved in different stages of ribosome biogenesis result in ribosomopathies, most patients present with similar phenotypes. These include macrocytic anaemia, skeletal defects and pre-disposition to cancer, especially acute myeloid leukaemia (AML) (Table 1.1)

(Narla and Ebert, 2010). Despite the fact that all tissues require an efficient ribosome biogenesis pathway, it is clear that ribosome biogenesis defects mostly affect the haematopoietic cells after embryonic development, as seen by ribosomopathy patients as well as animal models (Yelick and Trainor, 2015). Furthermore, the tumour suppressor p53 was found to be involved in the development of some of the phenotypes in animal models (Amsterdam et al., 2004, Jaako et al., 2015) (Table 1.1), which is directly regulated by ribosome biogenesis defects (Golomb et al., 2014), as discussed later on. Surprisingly, not much is known about the levels of p53 in ribosomopathy patients, as most of our knowledge on p53 involvement comes from cell and animal models.

1.5.2. Diamond-Blackfan Anaemia

Diamond-Blackfan Anaemia is a congenital bone marrow failure syndrome, which presents with macrocytic anaemia and, sometimes, short stature (Delaporta et al., 2014), that is estimated to affect 4-5 cases per million births (Narla and Ebert, 2010). Approximately 30-50% of the patients present with craniofacial and limb abnormalities, similar to TC syndrome patients (Yelick and Trainor, 2015). Diamond-Blackfan anaemia is caused by mutations in genes encoding for SSU or LSU ribosomal proteins; indeed rRNA processing defects are used for DBA diagnosis (Ellis, 2014). The main therapeutic strategy for DBA is the use of steroids (Khanna-Gupta, 2013). However, this cannot be maintained in most cases, hence regular blood transfusions are needed, and bone marrow transplantation is frequently needed (Vlachos et al., 2001).

Diamond-Blackfan anaemia patients often have a family history and most cases in an autosomal dominant manner (Narla and Ebert, 2010). The most commonly mutated gene is RPS19 (Lipton and Ellis, 2010), but mutations on other genes encoding for the SSU proteins RPS24, RPS17, RPS7 and RPS15, or LSU proteins RPL35A, RPL5, RPL11 and RPL36 have also been identified (Cmejla et al., 2009, Lipton and Ellis, 2010). Patients with mutations on RPL5 were found to have higher frequency of physical abnormalities, and patients with RPL11 mutations were found to have more thumb abnormalities than those with RPS19 mutations (Gazda et al., 2008). Hence, mutations in different genes may cause different phenotypes in DBA patients.

DBA presents with an increased risk of development of myelodysplastic syndrome (MDS), AML or osteosarcoma (Table 1.1). In mouse models resembling DBA phenotypes, some symptoms were found to be dependent on the levels of the tumour suppressor p53. More specifically, the development of anaemia in these models was shown to be dependent upon the interaction of the ribosome assembly intermediate 5S RNP with MDM2, the main p53 suppressor in the cell (discussed later) (Jaako et al., 2015), suggesting that ribosome biogenesis defects are linked to cancer development in these patients.

1.5.3. 5q- syndrome

5q- syndrome has been characterized as a subtype of myelodysplastic syndrome (MDS) (Narla and Ebert, 2010) and it is caused by a deletion on the long arm of chromosome 5 (Van den Berghe et al., 1974). 5q- syndrome is characterized by severe macrocytic anaemia and it is presented with a lower rate of progression to AML in comparison to other MDS patients (Vardiman et al., 2002). The 5q-syndrome symptoms can be effectively managed with the drug Lenalidomide (List et al., 2006), which promotes erythropoiesis for production of healthy blood cells (Ebert et al., 2008a, Narla and Ebert, 2010, Wei et al., 2009).

5q- syndrome was identified to be caused by haploinsufficiency of *RPS14* gene (Ebert et al., 2008b), which encodes for the small ribosomal protein RPS14. Haploinsufficiency of RPS14 was shown to cause defective SSU biogenesis and impaired erythropoiesis, probably due to ribosome biogenesis defects (Ebert et al., 2008b). As with DBA syndrome, the tumour suppressor p53 was found to be involved in 5q- syndrome as well. There was a high expression of p53 in erythroid cells of 5q-syndrome patients, where the p53 pathway was found to be deregulated (Pellagatti et al., 2010). Finally, p53 gene inactivation in mice models having RPS14 haploinsufficiency rescued the erythroid defects observed (Yelick and Trainor, 2015).

1.5.4. Treacher-Collins syndrome

Treacher-Collins (TC) syndrome is an autosomal dominant disorder and it is presented once every 50,000 live births (Posnick and Ruiz, 2000). Patients with TC syndrome have no haematological abnormalities, but they present with craniofacial defects as

well as problems with brain development and hearing (Narla and Ebert, 2010). These craniofacial abnormalities can be managed by doctors with a series of surgeries and speech development therapies (Sakai and Trainor, 2009).

Mutations on *TCOF1* gene, which encodes for treacle protein, have been found to cause the development of Treacher-Collins syndrome (Weiner et al., 2012). Treacle is involved in ribosome biogenesis, in the methylation of the rRNA precursors, as well as transcription of the rDNA. Furthermore, it was found to be localized in the nucleolus along with the upstream binding factor (UPF) and RNA polymerase I (Gonzales et al., 2005, Valdez et al., 2004). Mutations on the RNA polymerase I and III subunits were also found to cause TC syndrome (Yelick and Trainor, 2015).

The p53 tumour suppressor was found to be involved in TC syndrome pathogenesis. Mouse models with the TC phenotype were found to have an upregulated p53, resulting in the apoptosis of almost 25% of the neuronal crest cells (NCC) when *TCOF1* was mutated (Dixon et al., 2006). Furthermore, inhibition of p53 in *TCOF1*-deficient mice prevented the development of craniofacial defects (Jones et al., 2008), further providing a link between p53 and ribosomopathies.

1.5.5. Dyskeratosis Congenita

Dyskeratosis Congenita (DC) is a rare genetic disorder with clinical manifestations including bone marrow failure, nail dystrophy, immune deficiencies, tumours (Mason and Bessler, 2011). Hoyeraal-Hreidarsson Syndrome is a more severe variant of DC (Yaghmai et al., 2000), which is characterized by intra-uterine growth retardation, microcephaly, mental retardation, mucocutaneous lesions and a higher mortality rate (Ohga et al., 1997, Yaghmai et al., 2000). DC patients present with shortened telomeres, which is detected by clinical testing (Savage, 2009).

DC is acquired with different modes of inheritance (Table 1.2). X-linked DC arises due to mutations in *DKC1* gene (Table 1.2), which encodes of Dyskerin, the pseudouridine synthase of the H/ACA snoRNP complex (Heiss et al., 1998, Knight et al., 1998). Mutations in the genes encoding for the other H/ACA proteins NOP10 (Walne et al., 2007) and NHP2 (Vulliamy et al., 2008) give rise to the autosomal recessive form of DC (Table 1.2). No mutations in the gene encoding for GAR1 have been identified so

far. The autosomal dominant form of DC arises due to mutations in the genes encoding for the protein (TERT) (Armanios et al., 2005) or the RNA (TERC) (Vulliamy et al., 2001) component of the telomerase complex (Table 1.2). Furthermore, mutations in the gene encoding for the Cajal body-localization protein TCAB1, which is associated with telomerase, result to the autosomal recessive form of the disease (Table 1.2) (Mason and Bessler, 2011).

The exact cause of DC is still unclear. It was initially thought that DC arises because of telomere defects, since telomere shortening is observed in all forms (Mason and Bessler, 2011). Nevertheless, there are a few problems with this theory. Firstly, the DC phenotype is similar to the one observed in other ribosomopathies, such as DBA, especially the anaemia and increased cancer risk (Narla and Ebert, 2010). Secondly, clinical features of the disease were seen in mice (Ruggero et al., 2003, Gu et al., 2008) and zebrafish models (Ying Zhang et al., 2012), before any telomere defects were observed. These studies show that DC might not be caused by telomere defects, but rather, be due to ribosome biogenesis defects. This was further confirmed in a recent study, where the authors showed that Dyskerin levels were elevated in neuroblastoma patients, which were independent of the telomerase functions in these cells (O'Brien et al., 2016a).

Dyskeratosis Congenita			
Complexes	**Mutations**		
	Genes	**Inheritance**	**Presentation**
H/ACA snoRNP	Dyskerin	X-linked recessive	X-linked recessive Dyskeratosis Congenita Hoyeraal Hreidarsson syndrome
H/ACA snoRNP	NOP10	Autosomal recessive	Autosomal recessive Dyskeratosis Congenita
H/ACA snoRNP	NHP2	Autosomal recessive	Autosomal recessive Dyskeratosis Congenita
H/ACA scaRNP	TCAB1	Autosomal recessive	Autosomal recessive Dyskeratosis Congenita
Telomerase	TERT	Autosomal dominant	Idiopathic pulmonary fibrosis Aplastic anaemia Autosomal recessive Dyskeratosis Congenita
Telomerase	TERC	Autosomal dominant	Aplastic anaemia Pulmonary fibrosis Dyskeratosis Congenita

Table 1.2. Clinical presentation of Dyskeratosis Congenita.

As with other ribosomopathies, the levels of the tumour suppressor p53 were found to be de-regulated in DC as well. Depletion of Dyskerin in mice (Ge et al., 2010b) or zebrafish (Ying Zhang et al., 2012) resulted in an increase in p53 levels. Finally, suppression of Dyskerin in neuroblastoma human cells was shown to lead to a p53-dependent cell cycle arrest due to ribosome biogenesis defects, but not telomerase defects (O'Brien et al., 2016a). These studies suggest that DC is most likely due to ribosome biogenesis defects rather than telomere defects.

1.5.6. Ribosomes, Ribosomopathies and cancer

Most ribosomopathies appear with increased cancer risk, especially for AML, which is likely to be linked with anaemia (Orsolic et al., 2015). DC patients from a National Cancer Institute cohort presented an 11-fold higher ratio of observed to expected cancers as compared to general population (Alter et al., 2009). Patients with SDS have an estimated cancer risk of 19% at 20 years old, which reaches 36% at the age of 30 years old, according to the French Severe Chronic Neutropenia Registry (Donadieu et al., 2005). In the case of DBA, the situation is less clear, but patients were found to develop AML and, in some cases, osteosarcoma, as well as other types of tumours (Vlachos et al., 2012).

It is thought that the tumour development in ribosomopathy patients is directly linked to ribosome biogenesis defects. Mutations in genes encoding for either ribosome biogenesis factors or ribosomal proteins are the main cause of ribosomopathies (Yelick and Trainor, 2015). A study in 2004 have used zebrafish cell lines which were heterozygous for a recessive embryonic lethal mutation. An elevated cancer incident was observed in 12 cell lines, 11 of which had a mutation in a gene encoding for ribosomal proteins (Amsterdam et al., 2004). Furthermore, the transcription factor RUNX1 was found to be involved in the development of AML, MDS (Behrens et al., 2016) as well as breast cancer (Browne et al., 2015), and its depletion in hematopoietic stem and progenitor cells was found to cause an inhibition of ribosome biogenesis (Cai et al., 2015). Mutations in *NPM1* gene, encoding for nucleophosmin, a nucleolar protein involved in ribosome biogenesis, are found in approximately 30% of AML patients (Federici and Falini, 2013). Furthermore, It was found that translocation or heterozygous deletion of *NPM1* gene is commonly found in hematopoietic cancers, such as APL (acute promyelocytic anaemia) or MDS (Lindstrom, 2011).

1.6. The tumour suppressor p53

1.6.1. p53

p53 was identified by three independent studies in 1979 (DeLeo et al., 1979, Lane and Crawford, 1979, Linzer and Levine, 1979) and it was firstly thought to be an oncogene, whilst later it became clear that it acts as a tumour suppressor (Levine, 1989). p53 is found as a monomer or as a homotetramer in the cell (McLure and Lee, 1998). The *TP53* gene, which encodes for p53, consists of 11 exons, and the p53 protein contains 5 domains: the N-terminal transactivation domain (TAD), the proline-rich domain (PRD), the central DNA binding domain (DBD), the tetramerization domain (TD) and C-terminal basic domain (BD) (Figure 1.10) (Kamada et al., 2015). The transactivation domain (TAD) is involved in the transcriptional activity of p53, as well as interactions with other proteins (Kamada et al., 2015). The proline-rich domain is important for p53 stability and activity (Green and Kroemer, 2009). The DNA-binding domain binds directly on DNA consensus sequences for p53 binding (Zhao et al., 2001). The binding of DBD on the DNA is regulated by the C-terminal basic domain. Finally, the tetramerization domain is important for p53 tetramerization, which is required for DNA binding, post-translational modifications and interactions with other proteins (Kamada et al., 2015).

Figure 1.10. Schematic representation of the domains of p53. The N-terminal transactivation domain (TAD) is shown in green, the proline-rich domain (PRD) in yellow, the DNA-binding domain (DBD) in red, the tetramerization domain (TD) in light blue and the C-terminal basic domain (BD) in light grey (Adapted from: (Kamada et al., 2015)).

Other members of the p53 family include p63 and p73 transcription factors, which have similar structure, but a longer C-terminal on their tetramerization domain. In p63 and p73, this forms a helical structure, which is, presumably, involved in stabilisation (Joerger et al., 2009). The DNA binding nucleotide recognition motif is conserved amongst the p53 family members (Brandt et al., 2009) and hetero-tetramers of p53, p63 or p73 have been found in cells involved in transcriptional regulation of cell cycle and development (Joerger et al., 2009). Finally, p63 and p73 have been shown to have

p53-independent roles in the cells, such as epithelial or neuronal development (Dotsch et al., 2010).

1.6.2. p53 regulation and activation

p53 is a transcription factor and the major tumour suppressor in humans, widely known as the "guardian of the genome". Mutations in the gene encoding for p53 or deregulation of p53 levels have been reported in a variety of cancers (Wade et al., 2013), as well as other diseases including ribosomopathies (Drygin et al., 2014). The levels of p53 are mainly controlled by the ubiquitin ligase MDM2 (or HDMX) (Momand et al., 1992), which homodimerizes via its RING domain (Fang et al., 2000) and binds to p53 (Wade et al., 2013). This leads to p53 ubiquitination so that it is targeted for proteosomal degradation (Vogelstein et al., 2000). Furthermore, p53 activity is also inhibited by MDM2. The p53-binding domain of MDM2 binds on the transactivation (TAD) domain of p53 (Poyurovsky et al., 2010) and the central domain of MDM2, including the acidic domain and zinc finger domain, binds on the transactivation domain of p53 (Ma et al., 2006) (Cross et al., 2011). This results in p53 inhibition (Figure 1.11). A positive feedback loop mechanism exists between MDM2 and p53, where MDM2 expression is activated by p53 (Wu and Levine, 1997), ensuring that the p53 levels remain low in unstressed cells.

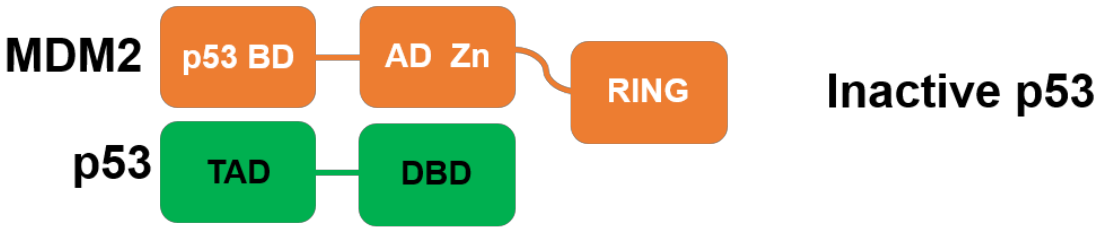

Figure 1.11. The inhibition of p53 by MDM2. The p53 binding domain (BD), the acidic domain (AD), the Zinc-finger domain (Zn) and the RING domain of MDM2 are shown in orange. The transactivation domain (TAD) and DNA-binding domain (DBD) of p53 are shown in green.

Apart from MDM2, a related MDM protein called MDMX (or HDM4) was found to be another important regulator of p53 levels in human cells (Linares et al., 2003). MDMX does not have a ubiquitin-ligase activity like MDM2 (Linares et al., 2003). However, MDM2-MDMX hetero-dimers are formed via interaction between their RING domains, which provides a stronger inhibition mechanism for p53 regulation (Uldrijan et al.,

2007). Finally, inhibition of p53 by the MDM2-MDMX heterodimer was found to be particularly important during embryonic development (Pant et al., 2011), and a lot of targeted cancer treatments are now focused on MDM2 and MDMX (Wade et al., 2013).

Activation of p53 in the cell after stress responses (Brown et al., 2009) takes places by various mechanisms. Firstly, phosphorylation of p53 leads to p53 activation due to a block in MDM2-p53 interaction (Momand et al., 2000). For example, phosphorylation of serine 15 is the main mechanism for p53 activation after DNA damage responses (Meek and Anderson, 2009). Furthermore, phosphorylation of MDM2 can also take place, blocking the MDM2-p53 interaction, which leads to p53 stabilisation (Momand et al., 2000). Finally, oligomerization of p53 can also lead to p53 activation by blocking the MDM2-p53 interaction due to post-transcriptional modifications on p53, such as phosphorylation or acetylation (Meek and Anderson, 2009).

A number of upstream pathways, both intrinsic and extrinsic, result in p53 activation (Figure 1.12) (Brown et al., 2009). DNA damage responses, which result in double strand breaks, lead to the activation of ATM (ataxia telangiectasia mutated) kinase, whereas UV irradiation leads to the activation of ATR kinase (serine/threonine kinase) or Casein Kinase II (Vogelstein et al., 2000) (Figure 1.12). ATM, ATR or Casein Kinase II kinases activate Chk2 kinase, which in turns phosphorylates p53 on serine 20 (Hirao et al., 2000). This modification prevents MDM2 binding, resulting in p53 stabilisation. Furthermore, growth signals also result in p53 activation. Oncogenic signals, such as expression of Ras or Myc oncogenes (Sherr and Weber, 2000), result in activation of the tumour suppressor $p14^{ARF}$, an alternative reading frame protein of *CDKN2A* locus (Stott et al., 1998). $p14^{ARF}$ inhibits the proteosomal degradation of p53 by preventing its ubiquitination by MDM2 (Xirodimas et al., 2001), leading to p53 activation (Figure 1.12), via the 5S RNP complex (discussed later) (Sloan et al., 2013a).

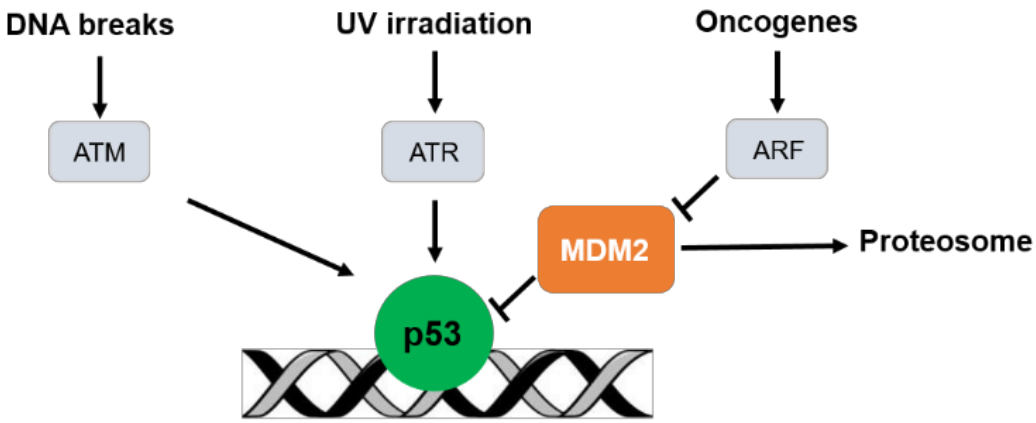

Figure 1.12. The activation of p53 after DNA breaks, UV irradiation and oncogene over-expression. Activation of downstream targets is indicated with an arrow and inhibition of downstream targets is indicated by a line. p53 is shown in green, MDM2 in orange and ATM (ataxia telangiectasia mutated), ATR (serine/threonine kinase) and ARF are indicated in light grey (Adapted from: (Brown et al., 2009)).

1.6.3. Cell cycle regulation by p53

p53 has a variety of functions in the cell for maintenance of the genome integrity (Bieging et al., 2014), including cell cycle control, apoptosis and DNA damage repair.

The cell cycle consists of interphase, which contains the G1, S and G2 phase, and mitosis, which contains the prophase, metaphase, anaphase and telophase. During G1 phase, the cell is prepared for DNA replication, which takes places during S phase, whereas the cell prepares for mitosis during G2 phase (Schafer, 1998). The cell cycle is mainly regulated by the cyclin-dependent serine/threonine kinases (CDKs) along with cyclins (Nigg, 1995), by activating enzymes required for progression to the next cell cycle phase and inhibiting enzymes that prevent this. In brief, Cdk4 or 6 along with cyclin D (Bates et al., 1994) are required for the progression of cell cycle through G1 phase, whereas Cdk2-cyclin E (Dulic et al., 1992) complex is required for the progression from G1 to S phase. Cdk2-cyclin A complex (Tsai et al., 1991) is necessary for progression of cell cycle from S phase to G2 phase and, finally, Cdk1-cyclin B complex (Nurse, 1990) is required for progression to mitosis (Schafer, 1998).

Activation of p53 promotes the expression of p21 ($p21^{WAF1/CIP1}$) (Figure 1.13), which results in inhibition of several CDKs (Karimian et al., 2016), apart from Cdk1 presumably (Harper et al., 1995). Cdk4/6-cyclin D complex activate transcription factors important for the expression of genes involved in G1 to G2 phase promotion.

Active p21 binds cyclins, preventing the activation of downstream transcription factors (Hall et al., 1995a), resulting in G1 cell cycle arrest (Figure 1.13). Furthermore, p53 activation results in G1 cell cycle arrest by activation of a DNA damage checkpoint (Bakalkin et al., 1995), which prevents the progression of cell cycle to the S phase. Activation of p53 also results in G2/M cell cycle arrest in some cases (Vogelstein et al., 2000). Active p53 promotes the expression of the 14-3-3σ protein, especially in epithelial cells. 14-3-3σ blocks Cdk1-cyclin B complex, required for the transition of G2 phase to mitosis, thus resulting in G2 cell cycle arrest (Figure 1.13) (Laronga et al., 2000).

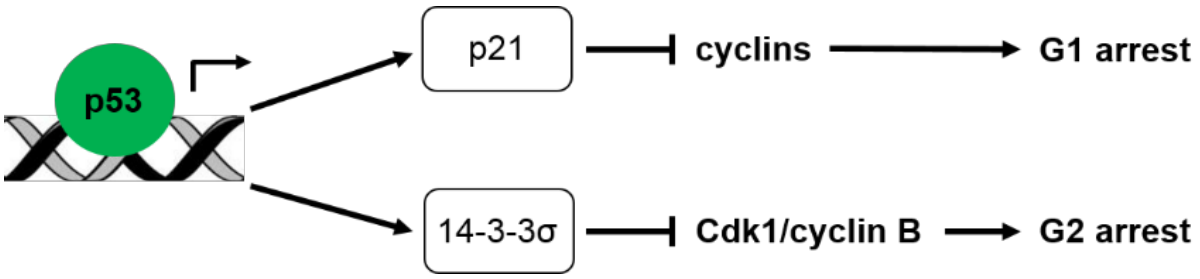

Figure 1.13. Schematic representation of the cell cycle regulation by p53. Activation of downstream targets is shown by an arrow and inhibition of downstream targets is shown by a line. p53 is shown in green, p21 and 14-3-3σ in white. Cdk1=cyclin-dependent kinase 1 (Adapted from: (Brown et al., 2009)).

1.6.4. p53 function in apoptosis

Apoptosis is a programmed cell death which takes place normally for maintenance of cell numbers in tissues, or as a defence mechanism under stress conditions (Elmore, 2007). Caspases, cysteine-aspartic proteases, are the key players in apoptosis, which cleave polypeptide chains upon activation, resulting in cell death (Goodsell, 2000). Activation of apoptosis occurs by the intrinsic, mitochondrial pathway, or the extrinsic, death receptor pathway. Intracellular signals, such as toxin accumulation or hypoxia, result in changes in mitochondria and the opening of the mitochondria permeability transition (MPT) pore (Chalah and Khosravi-Far, 2008). This leads to the release of several proteins, forming the apoptosome, resulting in activation of caspase-9, which, in turn, activates the execution caspase-3 (Elmore, 2007). On the other hand, the extrinsic pathway is activated by the association of extracellular ligands with the transmembrane death receptors, such as TNF (Locksley et al., 2001). Activation of death receptors results in the formation of a death-inducing signalling complex (DISC), resulting in the activation of caspase-8, which leads to the activation of the execution

caspase-3 (Fuchs and Steller, 2011). In both cases, caspase-3 activates other caspases, proteases and endonucleases, leading to apoptosis (Elmore, 2007).

p53 has been found to act as pro-apoptotic transcription factor, leading to the induction of apoptosis, mainly via the activation of the intrinsic pathway. p53 leads to the transcriptional activation of various pro-apoptotic proteins of the Bcl-2 protein family (Fridman and Lowe, 2003), such as Bax (Figure 1.14) (Miyashita et al., 1994). Upon activation, Bax binds on the mitochondrial membrane in association with other pro-apoptotic proteins (Gross et al., 1998), leading to the release of cytochrome c and caspases, which form the apoptosome, resulting in apoptosis (Figure 1.14) (Weng et al., 2005). Other pro-apoptotic proteins that are transcriptionally activated by p53 include PUMA (Nakano and Vousden, 2001) and NOXA (Figure 1.14) (Oda et al., 2000). Furthermore, p53 activation can also result in the activation of the extrinsic pathway. p53 was found to activate PIDD protein (Figure 1.14), which contains a death-domain and resembles other death-signal receptors, like TNF and Fas (Lin et al., 2000). Finally, p53 plays a non-transcriptional role in apoptosis (Fridman and Lowe, 2003), potentially by interactions with the mitochondrial membrane for cytochrome c release (Figure 1.14) (Mihara et al., 2003).

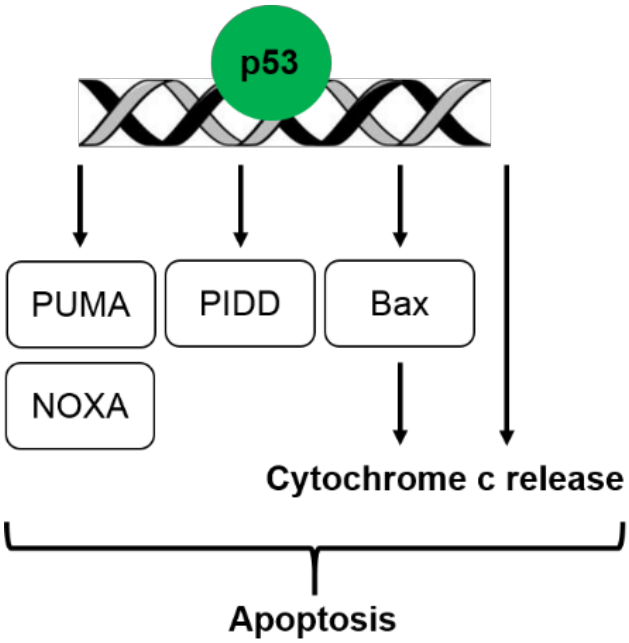

Figure 1.14. Schematic representation of the regulation of apoptosis by p53. Activation of downstream targets is indicated by an arrow, p53 is shown in green and the proteins PUMA, NOXA, PIDD and Bax are show in white (Adapted from: (Brown et al., 2009)).

1.6.5. p53 function in DNA damage repair

DNA damage occurs for a number of reasons and various mechanisms exist in the cell for DNA damage repair. In outline, DNA damage caused by reactive oxygen species (ROS) or X-rays results in the formation of base oxidation or single strand breaks, which is repaired by the Base Excision Repair (BER) machinery. Errors during DNA replication may lead to insertions, deletions or mismatches, which is repaired by Mismatch Repair (MMR), whereas bulk DNA adducts caused by UV light are repaired by Nucleotide Excision Repair (NER) enzymes. Finally, double strand breaks caused by ionizing radiation or anti-tumour drugs are repaired by Homologous Recombination (HR) or Non-Homologous End Joining (NHEJ) (Sancar et al., 2004).

Active p53 can lead to the transcriptional activation of downstream targets involved in DNA damage repair (Figure 1.15). For example, p53 is responsible for induction of GADD45α (Figure 1.15), which is involved in recruiting DNA damage repair enzymes (Carrier et al., 1999). GADD45α has been found to interact with PCNA (proliferating cell nuclear antigen) (Hall et al., 1995b), which binds on DNA and recruits other enzymes involved in BER (Shivji et al., 1992) and homologous recombination (Pfander et al., 2005). Furthermore, p53 results in activation of XPC (Figure 1.15), which senses DNA bulky adducts during nucleotide excision repair (NER) (Adimoolam and Ford, 2002).

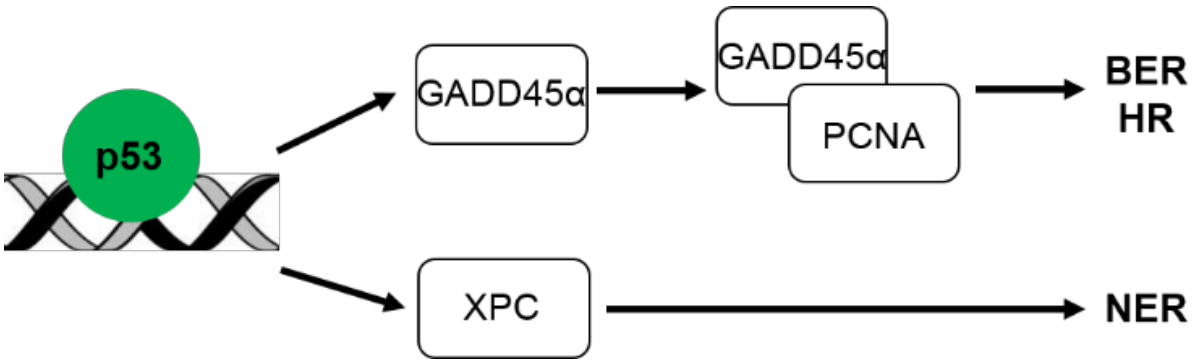

Figure 1.15. Schematic representation of the regulation of DNA damage repair by p53. Activation of downstream targets is indicated by an arrow, p53 is shown in green and the proteins GADD45α, PCNA (proliferating cell nuclear antigen) and XPC in white. BER=base-excision repair, HR=homologous recombination, NER=nucleotide-excision repair (Adapted from: (Brown et al., 2009)).

1.6.6. The 5S RNP-MDM2 pathway for p53 regulation and ribosomopathies

Ribosome biogenesis was shown to be directly linked to the regulation of the levels of p53 (Freed et al., 2010a, Narla and Ebert, 2010). The 5S RNP, consisting of the ribosomal proteins RPL5, RPL11 and the 5S rRNA, is normally integrated in the large ribosomal subunit (Sloan et al., 2013a). However, ribosome biogenesis defects result in the accumulation of the free 5S RNP in the nucleoplasm, since it can no longer be integrated in the large ribosomal subunit. This results in the binding of the 5S RNP to MDM2, inhibiting its function in ubiquitinating p53, leading to p53 stabilisation (Figure 1.16) (Pelava et al., 2016). It was recently found that all three components of the 5S RNP are required for its binding to MDM2 (Sloan et al., 2013a, Donati et al., 2013). Furthermore, the structures of the MDM2-RPL11 and ribosome-bound 5S RNP have shown that the same binding site on RPL11 is used for binding of the 5S RNP complex to either MDM2 or the ribosome (Zheng et al., 2015). Finally, it is believed that the interaction of the 5S RNP with MDM2 prevents the association of MDMX in the complex, leading to p53 activation (Figure 1.16) (Li and Gu, 2011). It is of particular interest that other ribosomal proteins have also been shown to bind to MDM2 *in vivo*, including RPL23 (Dai et al., 2004), RPS3 (Yadavilli et al., 2009) and RPS27a (Sun et al., 2011), suggesting that there are multiple pathways regulation p53 levels after ribosome biogenesis defects.

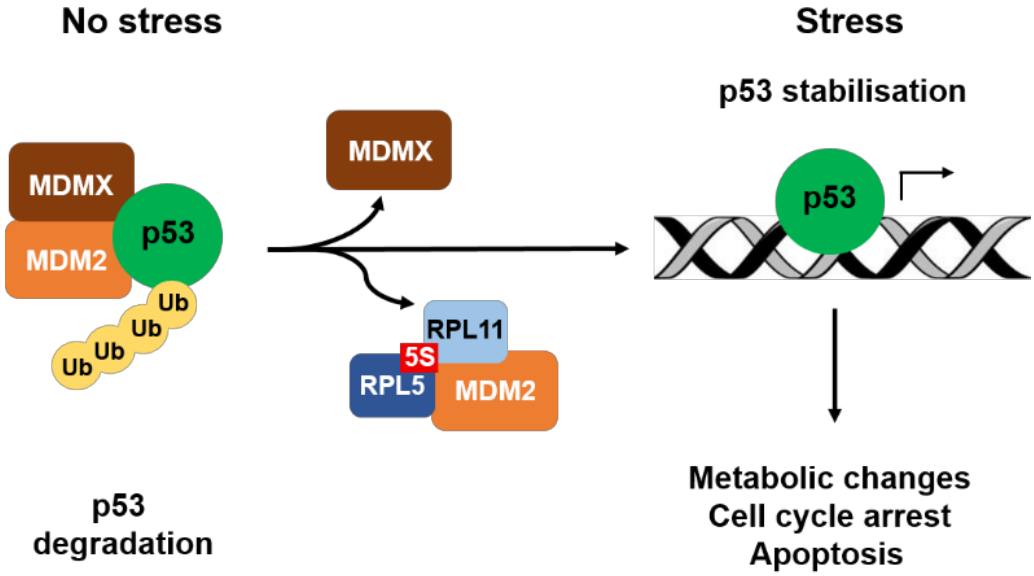

Figure 1.16. Schematic representation of the stabilisation of p53 via the 5S RNP-MDM2 interaction. MDM2 (orange), with MDMX (brown), binds and ubiquitinates p53 (green), targeting it for proteosomal degradation. The free 5S RNP (blue) binds and inactivates MDM2, causing p53 stabilisation, which leads to metabolic changes, cell cycle arrest, and apoptosis.

Defects in LSU production have been shown to cause the accumulation of the 5S RNP in the nucleoplasm, which results in p53 stabilisation by binding MDM2 (Donati et al., 2013, Marechal et al., 1994, Sloan et al., 2013a, Dai and Lu, 2004, Horn and Vousden, 2008). However, defects in SSU production have also been linked with the stabilisation of p53 via the 5S RNP-MDM2 pathway (Fumagalli et al., 2009, Fumagalli et al., 2012, Dutt et al., 2011), but the mechanism for this is still unclear. It was recently proposed that defects in SSU production are linked with the levels of the tumour suppressor p53 by the up-regulation of the ribosomal protein mRNAs (Fumagalli et al., 2012). In this paper, the authors propose that defects in 40S synthesis result in an up-regulation of translation of the ribosomal proteins (Fumagalli et al., 2012). This results in the production of more 5S RNP to bind MDM2 in order to compete the requirement of the 60S subunit for the RPL11 protein as part of the 5S RNP. However, when both the 40S and the 60S synthesis are co-impaired, it is predicted that there is both an up-regulation on 5S RNP production and a block in 5S RNP integration into the 60S, leading to p53 supra-induction (Fumagalli et al., 2012).

The 5S RNP has been implicated in other signalling pathways in the cell as well. Firstly, RPL5 and RPL11, presumably as a part of the 5S RNP, were shown to bind p73, blocking its interaction with MDM2, leading to p73 activation (Zhou et al., 2015). Furthermore, it was found that the 5S RNP might be important for the regulation of the levels and stability of the proto-oncogene c-Myc. RPL11 binds c-Myc after ribosome biogenesis defects, resulting in the suppression of its transcriptional activity. Additionally, RPL5 and RPL11 were shown to recruit the RNA-induced silencing complex (RISC) for c-Myc mRNA degradation (Liao et al., 2014). Finally, it was shown that RPL11 also binds the tumour suppressor $p14^{ARF}$, forming the RPL11/$p14^{ARF}$/MDM2/p53 complex, leading to p53 stabilisation because of MDM2 inhibition (Dai et al., 2012). It was recently found that RPL5 and the 5S rRNA, presumably as part of the 5S RNP complex, are also important for this process, since depletion of RPL5 or RPL11 in cells overexpressing $p14^{ARF}$ eliminated the p53 response (Sloan et al., 2013a).

To date, there is no evidence on how ribosome biogenesis defects lead to ribosomopathies, but it is widely thought that p53 plays an important role in this process (Narla and Ebert, 2010), even though not much research has been carried out using patient tissues. The main hypothesis so far is that p53 levels are up-regulated in

ribosomopathy patients via the 5S RNP-MDM2 pathway after ribosome biogenesis defects as described, leading to cell cycle arrest and apoptosis, which, subsequently, results in anaemia (McGowan et al., 2008, Fumagalli et al., 2009). Another possibility is that the defective ribosome biogenesis causes a delay in translation of globin mRNA, leading to the accumulation of excess heme, which results in cell-specific apoptosis due to oxidative stress and, therefore, anaemia (Keel et al., 2008). Lastly, it was suggested that abnormal translation might occur due to defective ribosome production, leading to the phenotypes observed (Blazquez-Domingo et al., 2005).

1.7. Aims and Objectives

Ribosome biogenesis is an essential cellular process, which is down-regulated during cell division and differentiation, and controlled by various stimuli, such as DNA damage, hypoxia and oncogene expression (Gentilella et al., 2015). Defects in ribosome biogenesis are associated with ribosomopathies, and the ribosome biogenesis pathway was found to be up-regulated in a variety of cancers (Orsolic et al., 2015). Ribosome biogenesis is directly linked with the regulation of the tumour suppressor p53 via the 5S RNP-MDM2 pathway (Pelava et al., 2016), and most of the previous and current anti-cancer chemotherapeutic treatments target ribosome biogenesis (Burger et al., 2010), highlighting its importance in cancer development.

The work in this PhD thesis covers three key areas of ribosome biogenesis and p53 regulation:

1) Ribosomopathies, a set of rare genetic diseases, arise due to mutations in genes encoding for ribosomal proteins or ribosome biogenesis factors. X-linked Dyskeratosis Congenita (DC) arises due to mutations in the gene encoding for Dyskerin, which is important for the pseudouridylation of rRNAs as part of the H/ACA snoRNP (Knight et al., 2001). However, very little is known about its function in humans, since most studies have been performed in yeast, where the H/ACA snoRNP is only involved in SSU biogenesis (Atzorn et al., 2004, Henras et al., 2004, Lafontaine et al., 1998). The catalytic activity of Dyskerin was shown to be essential for rRNA processing and modification in yeast (Zebarjadian et al., 1999), but not in mice, where it is more likely that pseudouridines are important for rRNA stability (Gu et al., 2013). In humans, the importance of Dyskerin in H/ACA snoRNP formation and rRNA

processing is yet to be determined. Furthermore, zebrafish (Ying Zhang et al., 2012) and mice models (Ge et al., 2010b, Gu et al., 2008) of X-linked DC were presented with elevated p53 levels when Dyskerin was depleted, presumably due to ribosome biogenesis defects. Despite its high important in X-linked DC and, possibly, cancer development in these patients, not much is known about the role of Dyskerin in p53 regulation in humans.

2) Diamond-Blackfan Anaemia (DBA), another ribosomopathy, arises due to mutations in genes encoding for either LSU or SSU ribosomal proteins (Ellis, 2014). As with most ribosomopathies, DBA patients present with an increased cancer risk, where de-regulation of p53 levels is thought to be important. This is supported by DBA mouse models where most of the symptoms were dependent on p53, and the anaemia development was dependent on the interaction of the 5S RNP and MDM2 (Jaako et al., 2015). It is known for a few years that defects in LSU production lead to the accumulation of the free 5S RNP, leading to MDM2 binding and inhibition, and, subsequently, p53 activation (Pelava et al., 2016, Sloan et al., 2013a, Nicolas et al., 2016). Surprisingly, various studies have shown that defects in SSU production also lead to p53 accumulation via the 5S RNP-MDM2 pathway (Fumagalli et al., 2009, Fumagalli et al., 2012, Golomb et al., 2014). However, it still remains unclear how defects in the SSU feedback to the recruitment of the 5S RNP in the LSU, with no obvious defects in LSU production. Furthermore, ribosome biogenesis takes place in different compartments in the cell with a number of ribosomal proteins and ribosome biogenesis factors to be involved. Depletion of LSU or SSU ribosomal proteins (Fumagalli et al., 2009, Fumagalli et al., 2012, Golomb et al., 2014) or depletion of ribosome biogenesis factors important for LSU production (Sloan et al., 2013a) was shown to result in p53 activation via the 5S RNP-MDM2 pathway. Whether defects in early or late stages of either LSU or SSU production affect the regulation of p53 via the same pathway is unclear.

3) The majority of ribosomal proteins are transcribed by 5'-TOP mRNAs (Levy et al., 1991). Instead, RPS27a and RPL40 are transcribed as ubiquitin-ribosomal protein precursors (Kimura and Tanaka, 2010), which are then processed for the release of the ubiquitin and the ribosomal protein. Yet, there is not much information on when this processing step occurs. It is known that RPS27a and RPL40 are part of the SSU and LSU respectively (Finley et al., 1989, Redman and Rechsteiner, 1989), but their role

in ribosome biogenesis during rRNA processing is still unclear. Interestingly, RPS27a is up-regulated in a variety of cancers and leukaemia (Wang et al., 2014) and was described as a potential new regulator of p53 by binding and inhibiting MDM2 when over-expressed (Sun et al., 2011). However, not much is known about the function of RPS27a or RPL40 in p53 homeostasis.

Therefore, this PhD project aimed to:

- Investigate the functions of Dyskerin in human ribosome biogenesis and p53 regulation
- Explore how defects on different stages of SSU or LSU production affect p53 regulation
- Study the processing of RPS27a and RPL40, and their function in human ribosome biogenesis and p53 regulation

2. Chapter Two. Materials and Methods

2.1 DNA methods

2.1.1 Construct introduction

The open reading frame (ORF) of Dyskerin, Ubiquitin-RPS27a or Ubiquitin-RPL40 was cloned in a pcDNA5/FRT/TO vector as described below (Figure 2.1). The pcDNA5/FRT/TO vector contained a FLAG-tag sequence so that all the proteins were expressed with a FLAG-tag on the N-terminus. For RPS27a- and RPL40- ubiquitin fusion ORFs, an HA tag was added to the C-terminus.

2.1.2 Polymerase Chain Reaction (PCR) for cloning

The ORF of each construct was amplified by Polymerase-Chain Reaction (PCR) using the Phusion DNA Polymerase (New England Biolabs) in order to create PCR products with blunt-ends. A cDNA library of the total mRNA, made using a reverse-transcription (RT) PCR (discussed later), was used as a template in all cases. A final concentration of 1x HF (High-Fidelity) Phusion Buffer (New England Biolabs) was used in a 50 µl reaction, along with 200 µM dNTPs, 1 µM of each of the Forward and Reverse primers (Table 2.1), approximately 100 ng of the template DNA and 0.5 µl of the Phusion Polymerase (New England Biolabs).

Name	Forward primer (5' to 3')	Reverse Primer (5' to 3')
Dyskerin	CGCGAGATCTATGGCGGATGCGGAAGTAAT	CGCGCTCGAGTCACTCAGAAACCAATTCTACC
RPS27a	GATCGGATCCATGCAGATTTTCGTGAAAACCCTTAC	1:GGATAGCCCGCATAGTCAGGAACATCGTATGGGTACTTGTCTTCTGGTTTGTTGAAACAGTAAGTCAG
		2:GCCGTCGACTCATGCATAGTCCGGGACGTCATACGGATAGCCCGCATAGTCAGGAAC
RPL40	GATCGGATCCATGCAGATCTTTGTGAAGACCCTCAC	1:GGATAGCCCGCATAGTCAGGAACATCGTATGGGTATTTGACCTTCTTCTTGGGACGC
		2:GCCCTCGAGTCATGCATAGTCCGGGACGTCATACGGATAGCCCGCATAGTCAGGAAC

Table 2.1. Primers used for cloning.

The PCR conditions (Table 2.2) were according to the manufacturer's instructions, where the annealing temperature was 3°C below the primer melting temperature (Tm).

Phusion PCR			
Step	**Temperature (°C)**	**Time (sec)**	**Cycles**
Initial activation	98	30	1
Denaturation	98	10	20-25
Annealing	Tm - 3	30	
Extension	72	15/kb	
Final Extension	72	600	1

Table 2.2. PCR conditions using the Phusion DNA polymerase for cloning.

2.1.3 DNA visualization and extractions

The PCR products were diluted in 6x DNA loading buffer (0.4 % orange G, 0.03 % bromophenol blue, 0.03 % xylene cyanol FF, 15 % Ficoll400, 10 mM Tris-HCl pH 7.5, 50 mM EDTA pH 8.0), to a final concentration of 1x. Products bigger than 500kb were loaded on a 1% agarose gel, whereas products smaller than 500kb were loaded on a 2% agarose gel. The agarose gels were made in 1x TBE solution (TRIS/Borate/EDTA: 90 mM Tris-HCl, 90 mM Boric acid, 2 mM EDTA, pH 8.0) with the addition of 1x SYBRSafe dye (Life Technologies). Gels were visualized using a UV transilluminator and the GelDoc system or a Typhoon Phosphorimager. For cloning, DNA was extracted from the agarose gel using the Wizard® SV gel and PCR Clean-Up System Kit (Promega), according to the manufacturer's instructions. To remove any excess ethanol from the sample after extractions, the samples were dried using the speed-vac for 30minutes.

2.1.4 Ligation in pJET1.2 vector

1 µl of the DNA PCR product (approximately 10 ng) was added to 0.5 µl of pJET1.2 vector (approximately 50 ng) (Promega), with 0.5 µl of T4 DNA ligase (Promega) and 5 µl of 2x Ligase Reaction Buffer (Promega). The mixture was incubated at room temperature for 30 minutes, before being transformed in DH5α *E. coli* competent cells.

2.1.5 Transformations in Escherichia coli and DNA extractions

Plasmid DNA was transformed into DH5α *E. coli* competent cells, which were prepared based on the Inoue Method (Brown et al., 2009).Up to 100 ng of plasmid DNA or up to 10 µl of the ligation mixture was added to 100 µl of DH5α *E. coli* competent cells and placed on ice for 30 minutes. The cells were then heat-shocked at 42°C for 1 minute

before they were placed on ice for 1 minute. 1 ml of Luria Broth (LB) (15.5 g LB / 1 L water) medium was added and the cells were incubated at 37°C for 1 hour while shaking. The cells were then centrifuged at 3,000rpm on a benhctop centrifuge for 2 minutes and 900 µl of the LB medium was removed. The cells were resuspended in the remaining LB medium and placed on ampicillin-containing plates overnight at 37°C. One colony was picked up from each plate and added to 3 ml of ampicillin-containing LB medium, which was grown overnight at 37°C. DNA was extracted from the cells using the GeneJet Plasmid Miniprep Kit (ThermoScientific) according to the manufacturer's instructions.

2.1.6 DNA sequencing

The identity of the plasmids was confirmed by DNA sequencing at GATC Biotech or Source Biosciences. The primers used for DNA sequencing corresponded to the vector sequences upstream and downstream the open reading frame.

2.1.7 Restriction Digest

The cDNA of interest was released, using restriction digest, from pJET1.2 vector for its cloning in the pcDNA5/FRT/TO vector. Approximately 2 µg of DNA was digested with 10 U of the relevant restriction enzymes and buffers (Promega) according to the manufacturer's instructions, producing sticky-ended products. Table 2.3 summarizes the restriction enzymes used for each of the constructs.

ORF	Restriction Enzyme 1	Restriction Enzyme 2
Dyskerin	BglII	XhoI
RPS27a	BamHI	SalI
RPL40	BamHI	XhoI

Table 2.3. Restriction enzymes used for construct digestion.

2.1.8 Ligation in pcDNA5/FRT/TO vector

The cDNAs were cloned into a modified pcDNA5/FRT/TO vector (Andrew Knox, Nick Watkins, personal communication) (Figure 2.1). A 5:1 molar ration (DNA insert:vector) was used along with 0.3 U of T4 DNA ligase (Promega) in 1x T4 DNA ligase Buffer (Promega). The samples were incubated at 18°C overnight and transformed in DHA5α *E. coli* competent cells. DNA was extracted as described above and the samples were sent for DNA sequencing in order to confirm the construct sequence.

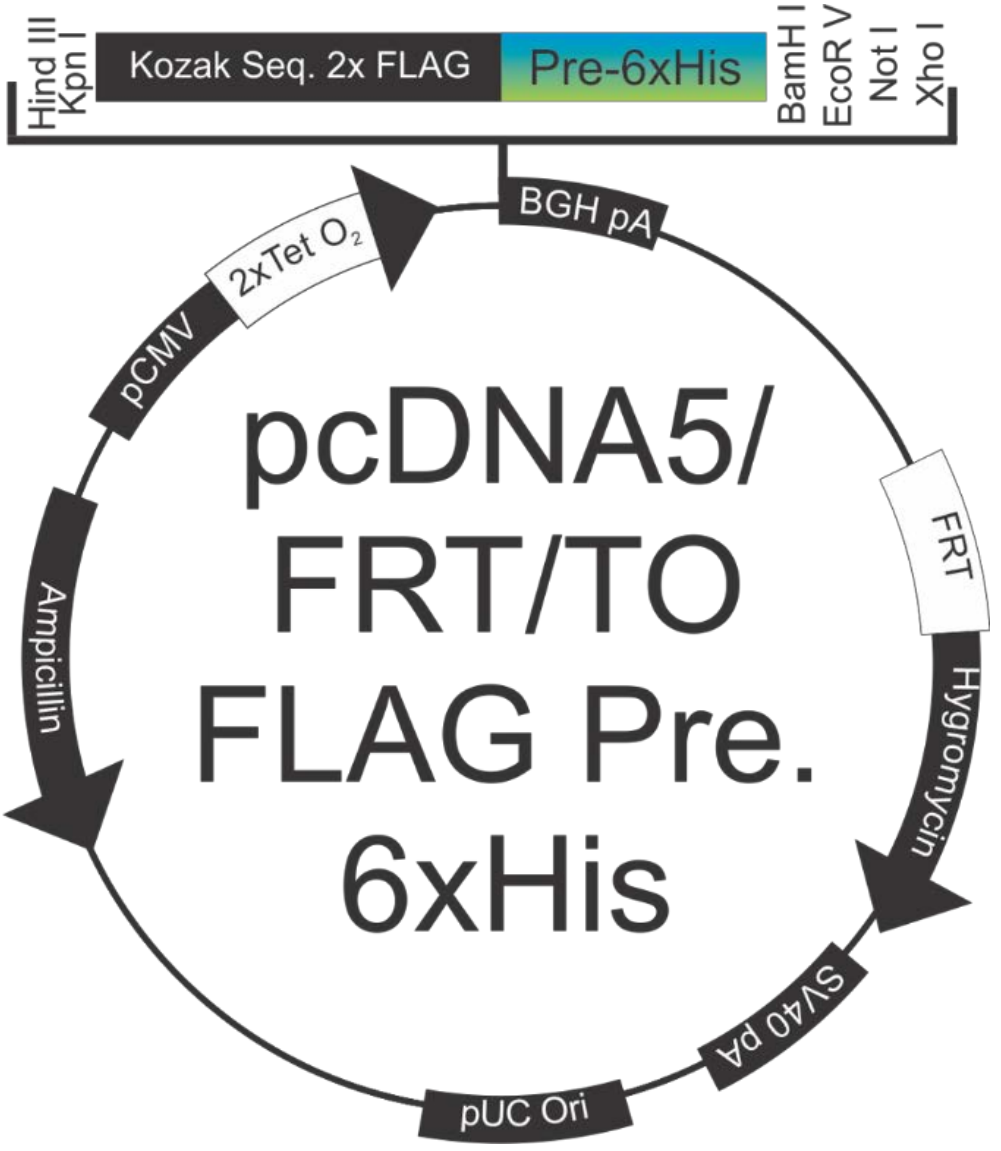

Figure 2.1. The modified pcDNA5/FRT/TO vector used for cloning. Two repeats of FLAG-tag sequence and six copies of the His-tag sequence were found upstream the cloned cDNA, which was under a tetracycline promoter. On the pcDNA5/FRT/TO vector are shown in order: the CMV promoter, the multiple cloning sites, the BGH reverse priming site and polyadenylation signal (pA), the Flp recombination site (FRT), the Hygromycin-resistance gene, the SV40 early polyadenylation (pA) signal, the pUC origin and Ampicillin resistance gene (From A.A Knox).

2.1.9 Site-directed mutagenesis

Site-Directed mutagenesis was used to introduce mutations in the pcDNA5/FRT/TO-cloned Dyskerin. 200 ng DNA, 1x Pfu Turbo Buffer (Stratagene), 100 ng of each primer (Forward and Reverse) (Table 2.4), 200 nM dNTPs and 2.5 U Pfu Turbo (Stratagene) were added to the reaction, which was performed according to the manufacturer's instructions. Next, the PCR products were digested with DpnI (Promega) for 1 hour at 37°C in order to remove the template DNA, since DpnI digests the methylated DNA. 5 µl out of the 100 µl reaction were transformed in 50 µl of DHA5α *E. coli* competent cells. Cells were grown and DNA was purified as described above.

Dyskerin	**Forward Primer (5' to 3')**	**Reverse Primer (5' to 3')**
RNAi resistant	GATTGGGGACTATATCAGGACA GGTTTCATTAATCTTGACAAGCC CTCTAACCCCTC	GAGGGGTTAGAGGGCTTGTCAA GATTAATGAAACCTGTCCTGATA TAGTCCCCAATC
D125A	GGAGAAGACAGGGCACAGTGGT ACTCTGGACCCCAAGGTGACTG GTTGTTTAATCG	CGATTAAACAACCAGTCACCTTG GGGTCCAGAGTACCACTGTGCC CTGTCTTCTCC

Table 2.4. Primers used for site-directed mutagenesis.

The PCR conditions used were according to the manufacturer's instructions as described in Table 2.5.

Pfu Turbo PCR			
Step	**Temperature (°C)**	**Time (sec)**	**Cycles**
Initial activation	95	30	1
Denaturation	95	10	17
Annealing	55	60	
Extension	72	60/kb+60	

Table 2.5. PCR conditions using the Pfu Turbo DNA polymerase.

2.2 Human Cell Culture methods

2.2.1 Human Cell lines

HEK293 (human embryonic kidney) cells Flp-In™ T-REX™-293 (Invitrogen), HeLa human cell line SS6 (cervical carcinoma) and U2OS (human osteosarcoma) Flp-In™ cells (gift from Dr Laurence Pelletier, Samuel Lunenfeld Research Institute, Toronto,

Canada) were cultured using Dulbecco's Modified Eagles Medium (DMEM) containing 4500 mg/L glucose, L-glutamine and sodium bicarbonate, without pyruvate (Sigma Aldrich) with additional 10 % Fetal Bovine Serum (FBS) (Sigma Aldrich) and 1 % Penicillin/Streptomycin (Sigma Aldrich). MCF7 (human breast cancer) cells were cultured using Gibco™ DMEM/F12 media with Glutamax (Life Technologies) with the addition of 10 % FCS (Sigma Aldrich). LNCaP prostate cancer cells (from Neil Perkins) were grown in RPMI 1640 (Lonza) with L-Glutamine and 25 mM HEPES, supplemented with 10 % Fetal Bovine Serum (FBS) (Sigma Aldrich). All cells were grown as a monolayer in a humidified incubator at 37°C with 5 % CO_2. When 70-80 % confluent, the cells were passaged using 1x Trypsin-EDTA (Sigma Aldrich) in sterile Phosphate Buffer Saline (PBS) (Sigma Aldrich) for 5 minutes at 37°C and re-seeded with the appropriate medium. LNCaP cells were centrifuged at 3,000 g for 2-3 minutes after trypsinization, in order to remove any leftover trypsin, and re-seeded with the appropriate medium.

HEK293 Flp-In™ T-REX™-293 and U2OS Flp-In™ cells both contain an integrated pFRT/*lac*Zeo vector which provides a Flp-In Recombinase site (FRT). They also contain a pcDNA6/TR vector which provides a tetracycline-regulated gene, where the ORF of each gene of interest was cloned. This allowed for the control of the expression of the gene of interest with different concentrations of tetracycline. Finally, they contain a Blasticidin-S resistant sequence, whereas the pcDNA5/FRT/TO vector contain a Hygromycin B resistance gene upstream the ORF of the gene of interest cloned. These cells were therefore used to generate tetracycline-inducible stable cell lines (details below) by selection with 100 µg/ml Hygromycin B every passage and 10 µg/ml Blasticidin S every third passage.

Cell stocks were prepared using a Freezing Media made by the corresponding media for each cell line with the addition of 20 % FBS and 10 % DMSO. Approximately $4x10^6$ cells were resuspended in the freezing media and the cell stocks were cooled to -80°C before being stored in liquid nitrogen. Reviving of cell stocks was performed by thawing of cells at 37°C and washing the cells in 5 ml of the corresponding media before resuspending them in 10 ml of media for normal growth.

2.2.2 Cell harvesting by trypsinization

Cells were harvested by trypsinization, followed by centrifugation at 800rpm for 3 minutes (swing bucket centrifuge) or 3,000rpm for 5 minutes (benchtop microcentrifuge).

2.2.3 Actinomycin D and MG132 treatments

Low levels of actinomycin D (ActD) block RNA polymerase I, resulting in ribosome biogenesis inhibition (Casse et al., 1999), whereas MG132 was used for inhibition of the proteasome (Guo and Peng, 2013). The cells were treated with 5 ng/µl ActD (in ethanol) or 25 µM of MG132 (in ethanol) (Lam et al., 2007) for approximately 18 hours.

2.2.4 siRNA transfections

Knockdowns were performed using the lipid transfection method for reverse transfection of siRNA duplexes. The Lipofectamine RNAiMAX transfection Reagent (5 µl for a 6-well plate or 1 µl for a 24-well plate) (Life Technologies) and Optimem I (500 µl for a 6-well plate or 100 µl for a 24-well plate) (Invitrogen) were incubated along with the siRNA for 15 minutes at room temperature. The different concentrations of siRNAs used are described on Table 2.6. Note that 5 times less siRNA was used when a 24-well plate was used. Approximately $3x10^5$ cells (6-well plate) or $5x10^4$ cells (24-well plate) in antibiotic-free media were added to each well. siRNA transfections were performed for 48 hours unless otherwise stated.

siRNA	Source	Reference	Sequence (5' to 3')	µM	µl (6-well)
Control	Eurofins MWG	Elbashir et al., 2001	CGUACGCGGAAUACUUCGAdTdT	20	7.5
DKC-2	EUROGENTEC	N/A	GGACAGGUUUCAUUAAUCUdTdT	20	20
PICT1	Eurofins MWG	N/A	GAAGAAGUCACUGCUUCUCdTdT	20	10
PNO1	Eurofins MWG	N/A	CAGUCCCAGCUAACAGAUATT	20	10
RIO2	Eurofins MWG	N/A	GGAUCUUGGAUAUGUUUAAdTdT	20	7.5
RPL18	ThermoScientific Pharmacon	N/A	GAGGCUGUUGGUCAAGU UAUACAGGdTdT	2	1
RPL21	Dharmacon Smartpool	N/A	N/A	2	1
RPL40	Dharmacon Smartpool	Sun et al., 2011	N/A	20	7.5
RPL5	Eurofins MWG	N/A	GGUUGGCCUGACAAAUUAUdTdT	20	7.5
RPL7	ThermoScientific Pharmacon	N/A	N/A	2	7.5
RPL7a	Eurofins MWG	Fumagalli et al., 2009	CACCACCTTGGTGGAGAACAAdTdT	20	7.5
RPS19	Eurofins MWG	Idol et al., 2007	GAUGGCGGCCGCAAACUGAdTdT	20	7.5
RPS27a	Eurofins MWG	Sun et al., 2011	CAGACATTATTGTGGCAAAdTdT	20	7.5
RPS6	Eurofins MWG	Fumagalli et al., 2009	TTGTAAGAAAGCCCTTAAATAdTdT	20	7.5

Table 2.6. The siRNA sequences used for siRNA transfections.

2.2.5 DNA transfections for stable cell lines

Stable cell lines were created using the Flp-In recombination system (Life Technologies, (Sauer, 1994)). The open reading frame of the protein of interest was cloned in a pcDNA5/FRT/TO plasmid as described previously, which contains an FRT recombination site. Both the HEK293T and U2OS cells also contain an FRT specific recombination site in the chromatin (Figure 2.2). pOGG44 vector, which was co-transfected with the pcDNA5/FRT/TO plasmid, contains the Flp-In recombinase. Expression of the recombinase results in the homologous recombination of the two FRT sites on the vector and host cell line, so that the gene of interest is integrated in the host (Figure 2.2). The gene of interest is cloned downstream a tetracycline

promoter, so that its expression can be induced. The host cell line contains a Hygromycin B resistance gene, so that selection with Hygromycin B was performed to identify the transfected cells (Figure 2.2).

Cells were plated on a 6-well plate for 18-24 hours, aiming for 30-60 % confluence. 1.8 µg of pOGG44 were added to 0.6 µg of pcDNA5/FRT/TO plasmid, for each well, in a microcentrifuge tube. In the meantime, 9 µl of FuGene 6 (Promega) were added to 91 µl Optimem I (Life Technologies) for each well, in a separate microcentrifuge tube, and incubated at room temperature for 5 minutes. The DNA mixture containing both the pOGG44 and pcDNA5/FRT/TO vectors was added to the Optimem mixture and incubated at room temperature for 15 minutes. The whole mixture was added to the cells in each well in a drop-wise manner. The cells were left to grow for 72h before transferred in a T75 flask (Sarstedt). Selection with Hygromycin B and Blasticidin S was performed as described above, to select for stable transformants.

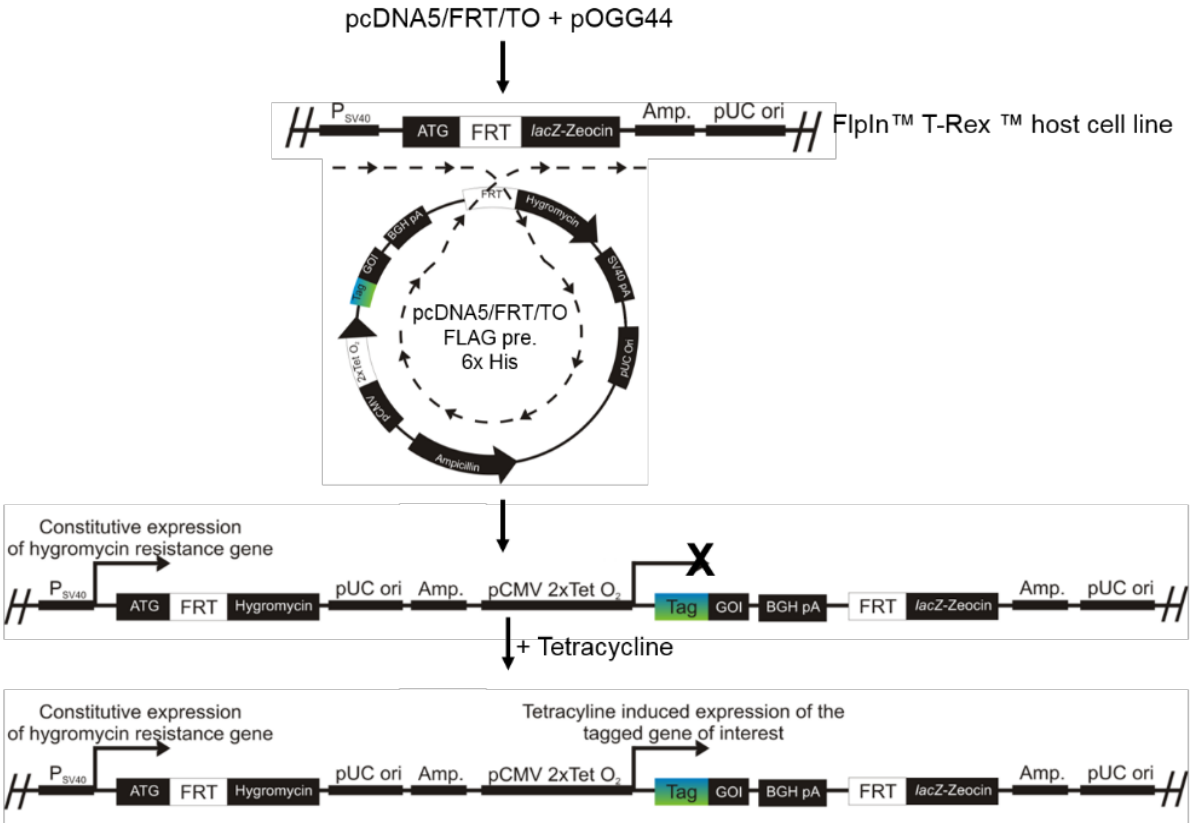

Figure 2.2. Schematic representation of the FlpIn recombination system for stable cell line generation. Homologous recombination between the Flp recombination (FRT) sites of the pcDNA5/FRT/TO vector and the HEK293T host cell line is shown by the dotted line and the Flp-In recombinase needed is encoded by the pOGG44 vector. Addition of tetracycline results in the expression of the FLAG-tagged gene of interest. In order, the following are shown on the figure: the SV40 polyadenylation signal, the ATG initiation codon, the Flp recombination site (FRT), the Hygromycin-resistance gene, the pUC origin, the ampicillin-resistance gene, the CMV promoter, the tetracycline promoter, the FLAG-tag, the cloned cDNA of the gene of interest (GOI) and the *lacZ* fused with zeocin resistance gene (*lacZ*-zeocin) (based on a figure from Invitrogen, adapted from K.E. Sloan).

2.2.6 Flow cytometry for cell cycle analysis

Cells were harvested by trypsinization and centrifuged at 3,000rpm on a bench-top centrifuge for 5 minutes. The cell pellet was washed with 500 µl of PBS/0.1 % FCS before centrifuged again at 3,000rpm on a bench-top centrifuge for 5 minutes. Cells were fixed using 1 ml of ice-cold 70 % ethanol and incubated on ice for 30 minutes. Cells were centrifuged again at 3,000rpm on a bench-top centrifuge for 5 minutes and the cell pellet was resuspended in 50 µl of 100 µg/ml of RNase A diluted in water. Addition of 200 µl of propidium iodide to a final concentration of 50 µg/ml (diluted in PBS) took place before incubation of cells in the dark at 4°C for 20 minutes. The

samples were transferred to Flow Cytometry tubes and analysed using the FACS Canto II software (BD Biosciences).

2.2.7 Immunofluorescence

Cells were plated on coverslips in a 24-well plate and treated as stated in each experiment. U2OS, but not HEK293T, cells were washed once with Phosphate Buffer Saline (PBS). 200 µl of 4 % parafolmadehyde in PBS was added to the cells for 20 minutes in room temperature, for fixing the cells on the coverslip. The cells were washed once with PBS before the addition of 200 µl of PBS/0.1 % Triton for 15 minutes, followed by 4 washes with 500 µl of PBS. The cells were blocked for 1-2 hours using PBS/0.1% Triton/10% fetal calf serum (FCS) solution before being transferred to a clean well for the addition of 50 µl of the primary antibody (Table 2.7), which was diluted in the blocking solution, for 1-2 hours. The coverslip was transferred back to the original well for the cells to be washed 3 times with 500 µl of PBS followed by three 10-minute washes with 500 µl PBS. The coverslip was transferred to the second well to be probed with 50 µl of the secondary antibody, which was also diluted in the blocking solution (Table 2.7), for 1-2 hours in the dark. The coverslip was again transferred to the original well to be washed three times with PBS followed by one 10-minute wash with PBS, one 10-minute wash with DAPI (0.1 µg/ml, Sigma) diluted in PBS (1 in 10,000 dilution) and a final 10-minute wash with PBS. All washes after the addition of the secondary antibody were performed in the dark. The coverslip was then immerged 5 times in water and 5 times in ethanol, air-dried and mounted on a glass slide using Moviol. The cells were visualized using a Zeiss Axiovert 200M inverted microscope and analysed using the Axiovert software.

Antibody	**Source**	**Reference**	**# number**	**Dilution**
α-Fibrillarin	Mouse	SantaCruz	G2808	1 in 200
α-FLAG	Rabbit	Sigma	F7425-2MG	1 in 100
α-HA	Mouse	Perkeley Antibody Company	N/A	1 in 200
α-Rabbit Alexa Fluor 555	Donkey	Invitrogen	N/A	1 in 500
α-Mouse Alexa Fluor 647	Donkey	Invitrogen	N/A	1 in 500

Table 2.7. The primary and secondary antibodies used for immunofluorescence.

2.2.8 Pulse chase labelling

Cells were plated on a 6-well plate and treated as described in each experiment. They were then incubated at 37°C/5 % CO_2 for 1 hour with Phosphate-Free Media (Life Technologies) for phosphate depletion before being incubated for 1 hour with Phosphate-Free Media with added ^{32}P-orthophosphate (0.5 µl per ml) at 37°C/5 % CO_2. Incubation with normal DMEM media (Sigma Aldrich) followed for 3 or 4 hours (chase) as stated in each experiment. RNA was extracted using Tri-reagent and loaded on a glyoxal-agarose gel as described below. The membrane was exposed to a phosphorimager screen before visualization of RNA using a Typhoon Phosphorimager (Life Technologies). ImageQuant software was used for quantitation of RNA bands and each RNA value was normalized against the loading control as stated in each experiment.

2.3 Protein Methods

2.3.1 Western Blotting

Cells were harvested by trypsinization and centrifuged at 3,000rpm on a benchtop centrifuge for 2-5 minutes. The pellet was resuspended in 2x Protein Loading Dye (74 mM Tris-HCl pH 6.8, 1.25 mM EDTA, 20 % glycerol, 2.5 % SDS, 0.125 % bromophenol blue, 50 mM DTT) and mixed, before incubated at 95°C for 5-10 minutes. The sample was loaded on an SDS polyacrylamide (PAGE) gel, consisting of 13 % separating gel (4.33 ml 30 % acrylamide (37.5:1), 2.5 ml 4x resolving gel buffer (1.5 M Tris pH 8.8, 0.4% SDS), 33 µl 10% ammonium persulfate, 33 µl TEMED, water up to 10 ml) and 4 % stacking gel (1.7 ml 30 % acrylamide (37.5:1), 2.5 ml 4x stacking gel buffer (0.5 M Tris pH 6.8, 0.4 % SDS), 100 µl 10% ammonium persulfate, 10 µl TEMED, water up to 10 ml). Electrophoresis was carried out for 40 minutes at 200V in 1x Protein Running Buffer (25 mM Tris-HCl pH 8.3, 250 mM glycine, 0.1 % SDS (w/v)) in a BioRad Western Electrophoresis tank. The samples were transferred on a nitrocellulose membrane (Protran, GE Healthcare) for 1,5 hour at 65V in Western Transfer Buffer (25 mM Tris-HCl pH 8.3, 150 mM glycine, 10 % methanol) in a BioRad Western Transfer tank. The membranes were stained with Ponceau S solution (Sigma) confirming efficient transfer of the sample. Next, the membranes were blocked, in order to avoid any unspecific antibody binding, using 2 % non-fat milk (Marvel) in 1x Phosphate Buffer Saline

(PBS)/0.1 % Triton for 1-2 hours at room temperature. The membranes were then probed with the primary antibodies diluted in blocking solution (Table 2.8) overnight at 4°C before washed for 5-10 minutes for 3 times with 1x PBS/0.1 % Triton.

Antibody	Source	Reference	# number	Dilution
α-CSL4	Rabbit	Watkins Lab, raised against peptides, ref: 1390	1390	1 in 500
α-Dyskerin	Rabbit	SantaCruz	sc-48794	1 in 1,000
α-FLAG	Rabbit	Sigma	F7425-2MG	1 in 1,000
α-HA	Mouse	Perkeley Antibody Company	N/A	1 in 5,000
α-Karyopherin	Rabbit	SantaCruz	SC-11367	1 in 1,000
α-p21	Rabbit	SantaCruz	sc-397	1 in 200
α-p53	Mouse	SantaCruz	sc-126	1 in 500
α-PICT1	Goat	SantaCruz	sc-46615	1 in 500
α-PNO1	Rabbit	Watkins Lab, raised against peptides	N/A	1 in 500
α-RIO2	Goat	SantaCruz E-14	E-14	1 in 200
α-RPL5	Rabbit	SantaCruz	A0912	1 in 5,000
α-RPL7	Rabbit	Abcam	ab72550	1 in 2,000
α-RPS19	Rabbit	P. Mason (Idol et al, 2007), Sloan et al, 2013 (JCB)	N/A	1 in 1,000
α-Tubulin	Mouse	Cell Signalling	3873	1 in 1,000

Table 2.8. The primary antibodies used for Western Blotting.

The membranes were subsequently probed with the secondary antibodies diluted in blocking solution (Table 2.9) for 1-2 hours at room temperature before washed again for 5-10 minutes for 3 times with 1x PBS/0.1 % Triton.

Antibody	Source	Reference	# number	Dilution
Donkey α-Goat HRP conjugated	Donkey	SantaCruz	sc-2020	1 in 10,000
Donkey α-Mouse CD800	Donkey	LICOR	926-32212	1 in 10,000
Donkey α-Mouse HRP conjugated	Donkey	SantaCruz	sc-2314	1 in 10,000
Donkey α-Rabbit CD680	Donkey	LICOR	926-60073	1 in 10,000
Donkey α-Rabbit HRP conjugated	Donkey	SantaCruz	sc-2313	1 in 10,000

Table 2.9. The secondary antibodies used for Western Blotting.

The membranes probed with Horseradish Peroxidase (HRP)-conjugated secondary antibodies were developed on an ECL film (GE Healthcare) using the Automatic Developer after the addition of ECL solution (Thermo Scientific). The membranes

probed with fluorescently-labelled secondary antibodies (CD680 or CD800) were visualized using the Odyssey-LICOR system (LICOR). Quantitation of the western blots was performed using the ImageQuant software (GE Healthcare), followed by normalization against the loading control.

2.3.2 Luciferase assay

U2OS cells expressing luciferase under the control of a p53-regulated promoter (kindly provided from Dr Neil Perkins, Newcastle University) were plated on a 24-well plate (approximately $5x10^4$ cells) and treated appropriately before washed once with Phopshate Buffer Saline (PBS) (Sigma Aldrich). The cells were harvested using 1x Lysis Buffer (Promega) and the luciferase reaction was carried out according to the manufacturer's instructions using the Promega Luciferase Kit. Measurements of the luciferase intensity were taken using the Lumat 100 Luminometer (Berthold). Bradford assay was also performed in order to identify differences in cell numbers, where 10 µl of cell extract was added to 790 µl of water (800 µl of water was used as a blank control) before the addition of 200 µl of Bradford Reagent. The samples were incubated for 5 minutes at room temperature before the Optimal Density (OD) was measured at 595 nm using a Spectrophotometer (Ultrospec 2000). In order to calculate the fold difference in p53 activity, the luciferase intensity values were normalized against the OD values from the Bradford assay for each sample.

2.3.3 Glycerol gradients

10-40 % glycerol gradient (v/v) were prepared by adding approximately 2 ml of 10 % Glycerol solution (10 % Glycerol, 0.15 M KCl, 20 mM HEPES pH 8, 1.5 mM $MgCl_2$, 1 mM DTT, 0.2 % Triton X-100) to an Ultra-Clear Centrifuge Tube (Beckman). Using a long needle, 40 % Glycerol solution (40 % Glycerol, 0.15 M KCl, 20 mM HEPES pH 8, 1.5 mM $MgCl_2$, 1 mM DTT, 0.2 % Triton X-100) was under the 10% gradient solution. A rubber lid was placed at the top and the gradients were rotated at 83° angle for 1 minute and 10 seconds at 22rpm on a BioComp Gradient master (BioComp), before being stored in the fridge for 1h. In the meantime, approximately $5\text{-}7x10^6$ cells were resuspended in 0.5 ml of Gradient Buffer E (20 mM HEPES pH 8, 150 mM KCl, 0.5 mM EDTA, 0.1 mM DTT, 5 % Glycerol) on ice. The cells were disrupted by sonication twice for 15sec with a 30sec interval at 20 % amplitude/0.3sec pulse. 0.2 % Triton-X

100 was added to the samples before centrifuging for 10min at 4°C at 13,000rpm to remove any insoluble material. 400 µl were removed from the top of the gradient, which was then placed on a pre-cooled swTi60 bucket, where 400 µl of the extract were loaded. 40 µl of the sample before centrifugation were stored in -20^{0}C, representing the 10 % total sample. The buckets were then balanced using Gradient Buffer E. Centrifugation took place in a swTi60 rotor (Beckman L7-80) for 1,5h at 52,000rpm at 4°C with brakes to slow acceleration. Each gradient was then fractionated using 200 µl from top to bottom and frozen in liquid nitrogen before being stored in -80°C. For Western Blot analysis, 20 µl of each fraction was added to 5 µl of 5x Protein Loading Dye and 5 µl of the total sample was added to 5 µl of 2x Protein Loading Dye, before loaded on an SDS-PAGE gel and analysed as described above.

2.4 RNA methods

2.4.1 RNA extractions

RNA was extracted for total cell pellets using Tri-Reagent. 1 ml of Tri Reagent (Ambion) was added to whole cell pellet from a 6-well plate and incubated for 5 minutes at room temperature. 200 µl of chloroform were added and the samples were vortexed for approximately 15 seconds until mixed. The samples were incubated at room temperature for 2 minutes before being centrifuged at 12,000g for 15 minutes for separation of RNA (top layer), DNA (middle layer) and protein (bottom layer). The RNA (top layer) was transferred to a clean microcentrifuge tube and 500 µl of isopropanol (Sigma Aldrich) were added. The sample was vortexed for 1-2 seconds and incubated at room temperature for 5 minutes before being centrifuged at 12,000g for 10 minutes. The supernatant was discarded and the RNA pellet was washed with 1 ml of 75 % ethanol before centrifuged for 5 minutes at 13,000rpm. The supernatant was again discarded and the RNA pellet was dried using the speed-vac for 1 minute. The RNA pellet was diluted in 12-13 µl of water and incubated at 55°C for 10 minutes. The RNA was stored at -20°C until needed.

2.4.2 Reverse-Transcription (RT)-PCR

RT-PCR was performed in order to identify the levels of the mRNAs where no antibodies were available either commercially or in the lab. RNA was extracted from

the cells using Tri-reagent as described above. DNase treatment followed in order to remove any DNA that was potentially left in the sample, where 8 µl of the total RNA were added to 8 µl of water before the addition of 2 µl of DNase Turbo (ThermoScientific) and 2 µl of DNase Turbo Buffer (ThermoScientific). The samples were incubated at 37°C for 1 hour followed by incubation at 80°C for 5 minutes to denature the DNase. Next, reverse transcription was carried out, where 1 µl of the DNase-treated RNA (approximately 400 ng) was added to 9 µl of water before the addition of 1 µl of 2 µM of an oligo-dT primer and 1 µl of 10 mM dNTPs. The samples were incubated at 65°C for 5 minutes and in ice for 1 more minute. After the addition of 4 µl of 5x First-Strand (FS) Buffer (ThermoScientific), 2 µl of 0.1 M DTT (ThermoScientific) and 1 µl of rRNAsin (Promega), the samples were gently mixed and incubated at 42°C for 2 minutes. 1 µl of Superscript III Reverse Transcriptase (ThermoScientific) was added to the mixture, whereas 1 µl of water was added as a negative control. The samples were incubated at 42°C for 50 minutes, followed by incubation at 70°C for 15 minutes. The primers used for the final PCR step are described on table 2.10.

Name	**Forward primer (5' to 3')**	**Reverse Primer (5' to 3')**
GAPDH	GTCGTATTGGGCGCCT GGTCACCC	ACACCCATGACGAACATGGGGGC
RPL18	CTACCTGAGGCTGTTGG TCAAG	CGAAATGCCGGTACACCTCTC
RPL21	GGAAAGAGGAGAGGC ACCCG	GCTGGCGCTTTAGTTGAACC
RPL40	GATCGGATCCATGCAGATCTT TGTGAAGACCCTCAC	GGATAGCCCGCATAGTCAGGAACATCGTATGGGTA TTTGACCTTCTTCTTGGGACGC
RPS27a	GATCGGATCCATGCAGATTTT CGTGAAAACCCTTAC	GGATAGCCCGCATAGTCAGGAACATCGTATGGGTA CTTGTCTTCTGGTTTGTTGAAACAGTAAGTCAG

Table 2.10. Primers used for RT-PCR.

GoTaq D2 DNA polymerase was used for the final PCR according to the manufacturer's instructions (Table 2.11).

GoTaq G2 (RT-PCR)			
Step	**Temperature (°C)**	**Time (min)**	**Cycles**
Initial activation	95	5	1
Denaturation	95	1	20-25
Annealing	Tm - 3	1/kb	
Extension	72	2	
Final Extension	72	5	1

Table 2.11. The PCR conditions using Go-Taq D2 DNA polymerase

2.4.3 Northern Blotting

RNA was extracted from the cells and diluted in 1x Glyoxal Loading Buffer (61.2 % DMSO (v/v), 20.4 % glyoxal (v/v), 12.2 % 1x BPTE buffer (28.7 mM Bis-Tris, 9.9 mM PIPES, 1 mM EDTA) (v/v), 4.8 % glycerol (v/v), and 0.02 mg/ml ethidium bromide), before being incubated at 55°C for 1 hour. The sample was loaded on a glyoxal-agarose gel consisting of 1.2 % Agarose (Melford) in 1x BPTE (30 mM Bis-Tris free acid pH 7.0, 10 mM PIPES free acid, 1 mM EDTA) diluted in 1x BPTE buffer. The RNA was separated for 3,5 hours at 185V in 1x BPTE buffer and visualized using a UV light or the Typhoon Phosphorimager. The gel was then washed once with 75 mM NaOH at room temperature for 20 minutes, twice with Tris-Salt pH 7.4 (0.5 mM Tris-HCl pH 7.4, 1.5 M NaCl) at room temperature for 15 minutes and once with 6x SSC (1 M NaCl, 0.1 M $Na_3C_6H_5O_7$) at room temperature for 20 minutes. The RNA was transferred on a Hybond N membrane (Amersham) in 6x SSC overnight at room temperature using the capillary action method. The RNA was then cross-linked on the membrane using the auto-crosslinking option on the Stratalinker UV Crosslinker (Stratagene).

Alternatively, RNA was extracted and diluted in 1x RNA loading dye (40 % formamide, 0.5 mM EDTA, 50 µg/ml bromophenol blue, 50 µg/ml xylene cyanol). The sample was incubated for 2-5 minutes at 95°C and loaded on an 8 % Acrylamide/7 M Urea gel. Electrophoresis was performed for approximately 1 hour at 400V in 1x TBE solution, following RNA transfer on a Hybond N membrane (Amersham) in 0.5x TBE solution for 1,5 hour at 65V in a transfer tank. The RNA was cross-linked on the membrane using the auto-crosslinking option the Stratalinker UV Crosslinker (Stratagene).

The RNA membranes were pre-hybridized using 10 ml of SESI buffer (0.5 M sodium phosphate pH 7.2, 7 % SDS (w/v), 1 mM EDTA) for 5'-oligo probes for 30 minutes at 37°C. After pre-hybridization, the membranes were incubated with the respective probes for 1-2 days at 37°C. After decanting of the 5'-oligo labelled probes, the membranes were washed for 20 minutes twice at 37°C using 1x SSC/0.1 % SDS solution before exposed to a phosphorimager screen. Alternatively, hybridization (Pre-Hyb) buffer (25 mM $NaPO_4$ pH 6.5, 6x SSC, 5x Denhardts, 0.5 % SDS (w/v), 50 % deionised formamide, 100 µg/ml denatured salmon sperm DNA) was used for random-prime labelled probes, where the membrane was incubated for 2 hours at 42°C. After pre-hybridization, the membranes were incubated with the respective probes for 1-2

days at 42°C. After decanting of the random-prime labelled probes, the membranes were washed twice for 5 minutes at 42°C with 2x SSC/0.5 %SDS, twice for 5 minutes at 42°C with 2x SSC/0.1 % SDS and finally for 20 minutes at 50°C with 2x SSC/0.1 % SDS, before exposed to a phosphorimager screen and visualized using a Typhoon Phosphorimager.

2.4.4 ^{32}P-Labelled probes for Northern Blotting

Oligo probes (Table 2.12) were labelled using a ^{32}P-labelled γ-ATP (Perkin Elmer), by adding 1 µl of the oligo-primer (10 µM), 1 µl of Polynucleotide Kinase Buffer (New England Biolabs), 2-3 µl of ^{32}P-labelled γ-ATP and 1 µl of T4 Polynucleotide Kinase (New England Biolabs) in 10 µl reaction. The mixture was incubated at 37°C for 45 minutes before the addition of 40 µl of water. Any excess radioactive material was removed using a G50 column (Life Technologies) by centrifugation of the mixture at 3,000rpm for 2 minutes on a benchtop centrifuge. The probe was incubated at 95°C for 2 minutes before added to the SESI buffer for membrane hybridization.

Name	**Sequence**
18S	GGGCGGTGGCTCGCCTCGCG
28S	TGGTCCGTGTTTCAAGACGGGT
5'-ITS1	CCTCGCCCTCCGGGCTCCGTTAATGATC
ITS1	AGGGGTCTTTAAACCTCCGCGCCGGAACGCGCTAGGTAC
ITS2	GCGCGACGGCGGACGACACCGCGGCGTC
pre-5.8S	ATTGATCGGCAAGCGAC

Table 2.12. The oligo rRNA probes used for Northern Blotting.

Random-primed labelled probes (Table 2.13) were made using a random hexamer mix. 25-50 ng of template DNA, which was PCR-amplified from a plasmid template (Madhumalar et al., 2009), was placed in a microcentrifuge tube and water was added to a final volume of 9 µl. The mixture was incubated at 95°C for 5 minutes and then placed on ice for 1 minute. Next, 3 µl random hexamer mix (250 mM Tris pH 7.5, 50 mM $MgCl_2$, 5 mM DTT, 500 µM dATP, 500 µM dGTP, 500 µM dTTP), 2 µl of ^{32}P-labelled dCTP (Perkin Elmer) and 1 µl of Klenow Polymerase (Promega) were added to the sample. The mixture was incubated at 37°C for 30 minutes before the addition of 35 µl of water. Similarly to the oligo-labelled probes, the excess radioactive material was removed using a G50 column (Life Technologies), by centrifugation of the sample at 3,000rpm for 2 minutes on a benchtop centrifuge. The probe was finally incubated at 95°C for 2 minutes before added to the Pre-Hyb Buffer for membrane hybridization.

Name	Vector	Forward Primer (5' to 3')	Reverse primer (5' to 3')
U1	pUC18	GGGGAAAGCGCGAACGCAGdTdT	TACTTACCTGGCAGGGGAGdTdT
U17	pBS+HU17	T7	T3
U64	pUC19	ACTCTCTCGGCTCTGCATAGTTGCdTdT	GCCTGTTTGCACCCCTCAAGGdTdT
U19	N/A	ATCCAGCGGTTGTCAGCTATCCdTdT	AATTGTTTGCACCCAGACTAGGdTdT
U70	N/A	CCGCAGCCAATTAAGCCGACdTdT	GCCTGTCTCCAAGGTCCCTTAGAGCdTdT

Table 2.13. The PCR products used for random-prime labelling of rRNA probes for Northern Blotting.

2.5 Other assays

2.5.1 Immunoprecipitation

Approximately $2x10^7$ cells were harvested by trypsinization and centrifuged at 800rpm (swing bucket centrifuge) for 3 minutes. 2 ml of Gradient Buffer E (150 mM KCl, 20 mM HEPES pH 8.0, 0.5 mM EDTA, 0.1 mM DTT) was added to each sample before vortexing for a few seconds until the cell pellet was dissolved. The samples were kept on ice throughout the whole procedure. The samples were sonicated at 20 % amplitude/0.3sec pulse/1sec off, 3x 20 sec on-20 sec off intervals before the addition of 100 µl of 20 % Triton-X (final concentration of 0.2 %), 222 µl of 87 % Glycerol (final concentration of 10 %) and 3 µl of 1 M $MgCl_2$ (final concentration of 1.5 mM). The samples were mixed gently and divided into two microcentrifuge tubes before centrifugation at 12,000g for 10 minutes at 4°C. The supernatant was transferred to a clean microcentrifuge tube. 100 µl of sample was stored in -20^0C representing the 5 % of the total sample.

The beads were prepared the day before using 10 µl of Protein G-sepharose beads (GE Healthcare) for each reaction by washing them 3 times in 1 ml of ice-cold immunoprecipitation (IP) buffer (10 % Glycerol, 0.15 M KCl, 20 mM HEPES pH 8.0, 1.5 mM $MgCl_2$, 1 mM DTT, 0.2 % Triton X) and resuspending them in 1 ml of IP buffer before the addition of 2 µl of α-FLAG antibody (Sigma Aldrich) per sample. The antibody was bound on the Protein G-sepharose beads by gently rotating the mixture overnight at 4°C. Control beads were used, which contained no antibody. Both control- and FLAG-beads were again washed 3 times in 1 ml of ice-cold IP buffer and resuspended in 1 ml of ice-cold IP buffer. 100 µl of the beads were added in a

microcentrifuge tube for each reaction. 1 ml of the lysate was added to either the α-FLAG or the control beads and the mixture was gently rotated for 2 hours at 4°C. The samples were centrifuged at 3,000rpm at 4°C for 1 minute and washed 3 times using 1 ml of ice-cold IP buffer, before diluted in 1ml of ice-cold IP buffer and transferred to a clean microcentrifuge tube.

RNA was extracted by adding 180 µl of Homogenization Buffer (1 % SDS, 50 mM Tris, 50 mM NaCl, 0.5 mM EDTA) to each sample and 200 µl of Phenol/Chloroform (Sigma Aldrich). The samples were vortexed for 2-3 minutes and centrifuged at 13,000rpm for 5 minutes. The RNA was transferred to a clean microcentrifuge tube, where 1 µl of 20 mg/ml Glycogen Blue (Fisher Scientific), 12.5 µl of 3 M NaOAc pH 5.3 (final concentration of 1 in 10) and 500 µl of 100 % ethanol (final concentration of 2.5x) were added. The samples were incubated at -80°C for 1 hour or -20°C overnight before being centrifuged at 12,000g for 20 minutes at 4°C. The RNA pellet was washed in 1 ml of ice-cold 75 % ethanol and further centrifuged at 12,000g for 20 minutes at 4°C. The RNA pellet was air-dried before resuspended in 8 µl of water. RNA analysis was performed using Northern Blotting as described above.

2.5.2 Statistical Analysis

Statistical analysis took place using Microsoft Excel, where the T-test function was used. Unpaired t-test using a two-tailed distribution was performed.

3. Chapter Three. The role of Dyskerin in human ribosome biogenesis and p53 regulation

3.1 Introduction

Ribosome biogenesis is a tightly regulated pathway that involves more than 200 proteins, including nucleases and helicases (Henras et al., 2008). The 28S, 18S and 5.8S rRNAs are transcribed as a single (47S) rRNA precursor by RNA polymerase I in the nucleolus, whereas the 5S rRNA is transcribed by RNA polymerase III in the nucleoplasm (Granneman and Baserga, 2004). The mature rRNAs are produced after a series of cleavage events and they incorporate a number of modifications necessary for their stability and function. One of the main rRNA modifications is the conversion of uridine to the isomer pseudouridine (Figure 3.1A). This process is catalysed by pseudouridine synthases. A conserved aspartic acid residue found in all pseudouridine synthases acts as a nucleophile (Ramamurthy et al., 1999) and interacts with the uracil to promote a break in the glycosyl bond between the uracil and the ribose, followed by the rotation of the uracil before being attached back on the ribose (Boschi-Muller and Motorin, 2013). In uridine, the C1 atom of the ribose interacts with the N1 atom of the uracil via the formation of a glycosyl bond. In contrast, in pseudouridine the C1 atom of the ribose interacts with the C5 atom of the uracil (Figure 3.1A). This C-C bond in pseudouridine allows for an increased rotation ability and for additional base pairing with other molecules by interactions with the N1 atom, so that more stable structures are formed when pseudouridine is present (Charette and Gray, 2000).

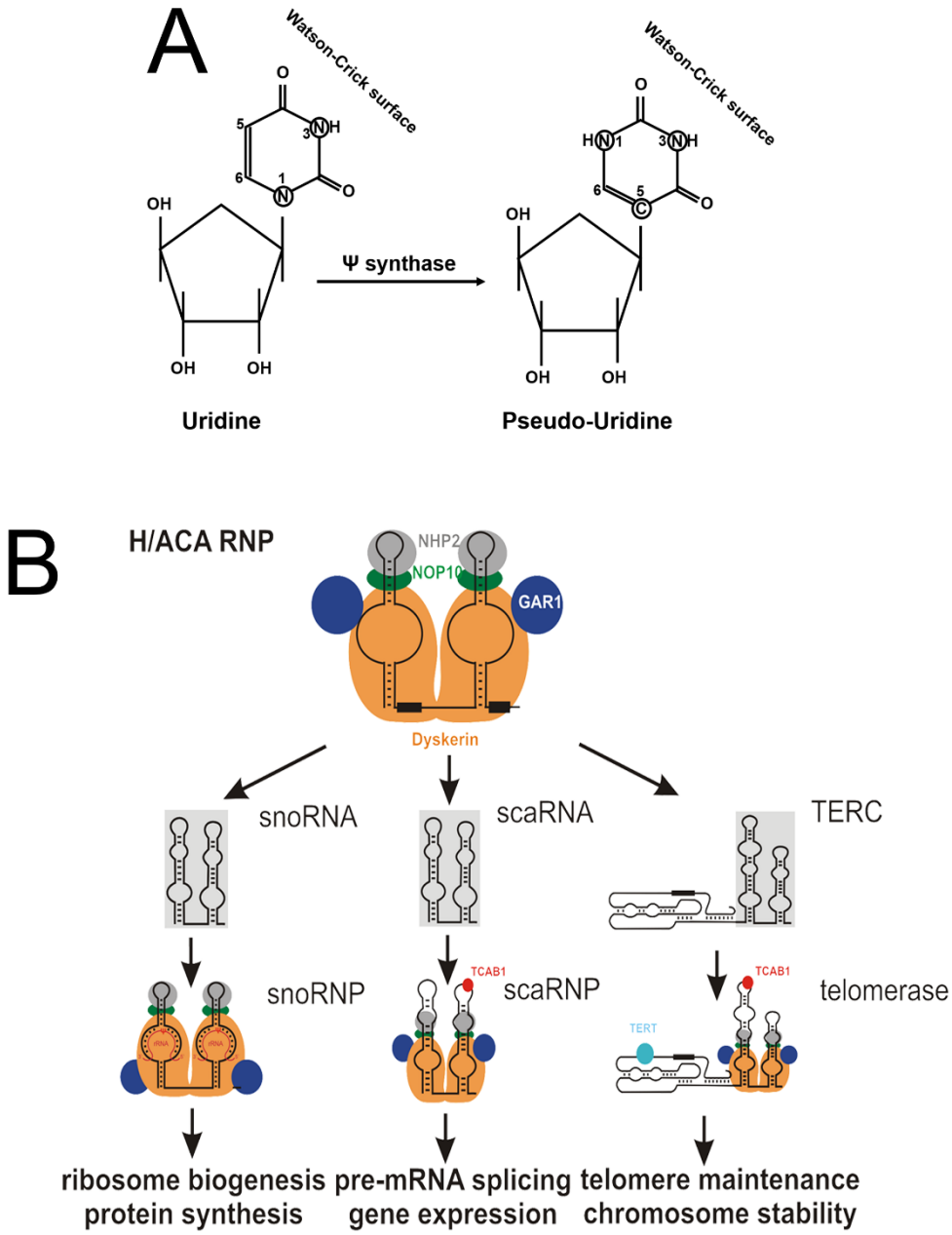

Figure 3.1. The pseudouridylation and the H/ACA snoRNP. (A) Schematic representation of the differences between uridine and pseudouridine. The atom positions on the uracil rings and the Watson-Crick surface is indicated in each case. Ψ=pseudouridine. **(B)** Schematic representation of the functions of the H/ACA RNP. The H/ACA RNP consists of Dyskerin (orange), NOP10 (green), NHP2 (grey), GAR1 (blue) and an RNA component (black), and is involved in ribosome biogenesis, mRNA splicing and telomere maintenance. The Cajal-body chaperone protein TCAB1 is shown in red and the protein component of telomerase (TERT) is show in light blue.

The process of pseudouridylation is catalysed by the H/ACA small nucleolar (sno)RNPs, which consist of the pseudouridine synthase Dyskerin (Cbf5 in yeast and archaea), the core proteins NOP10, NHP2 (L7Ae in archaeal) and GAR1, and a snoRNA component (Figure 3.1B) (Watkins and Bohnsack, 2011). The structure of the H/ACA snoRNP has been solved in archaea, where the H/ACA snoRNA consists of one stem loop, containing the ACA motif at the bottom, the P1 and P2 stems and a K-turn at the top (Watkins and Bohnsack, 2011). Cbf5 interacts with the H/ACA snoRNA, by binding on the ACA motif (Baker et al., 2005), L7Ae binds the K-turn (Rozhdestvensky et al., 2003) and the surface between the P2 stem and the K-turn is bound by the Cbf5-Nop10-L7Ae complex. Gar1 does not interact directly with the H/ACA snoRNA and it binds the thumb loop of Cbf5 (Watkins and Bohnsack, 2011).
In eukaryotes, the structure of the H/ACA snoRNP is yet to be solved, but the similarities between the H/ACA snoRNAs and proteins (Reichow et al., 2007) indicate that the eukaryotic complex shows structural similarity to the archaeal complex. Indeed, it was shown in yeast that the Cbf5-Nop10-Gar1 complex is structurally similar to the archaeal complex (Li et al., 2011). It is thought that the eukaryotic H/ACA snoRNAs consist of two stem loops instead of one (Figure 3.1B) (Ganot et al., 1997b) which are important for the formation and function of the H/ACA RNP. Presumably, the two Dyskerin molecules interact with each other (Figure 3.1B) (Watkins et al., 1998) and binding of Dyskerin to NOP10 is required for the recruitment of NHP2 to the complex because of the lack of a K-turn in eukaryotic H/ACA snoRNAs (Watkins and Bohnsack, 2011). GAR1 interacts with Dyskerin but not with the H/ACA snoRNA, and is important for the organization of the complex to help keep the substrate in place during catalysis and for the final product to be released (Duan et al., 2009).

Most H/ACA snoRNAs interact with the RNA substrate by base-complementarity (Henras et al., 2008), which is important for both the modification and the positioning of the rRNA substrate during catalysis (Henras et al., 2008). The majority of H/ACA snoRNAs are involved in LSU or SSU rRNA pseudouridylation. For example, the U64 H/ACA snoRNA is important for pseudouridylation of U4975 of the 28S rRNA, whereas the U66 H/ACA snoRNA guides the pseudouridylation of U119 of the 18S rRNA in humans (Ganot et al., 1997a). Notably, a number of H/ACA snoRNAs have been found to be involved in rRNA processing rather than modification, such as U17/E1 (snR30 in yeast) (Enright et al., 1996, Morrissey and D.Tollervey, 1993, Mishra and Eliceiri, 1997) and snR10 (Tollervey, 1987), both of which have been shown to be important for 18S

rRNA processing. U17 depletion in frog oocytes resulted in a decrease of mature 18S rRNA and an accumulation of the 18S rRNA precursors (Mishra and Eliceiri, 1997), which was similar to the phenotype shown in yeast after snR30 depletion (Morrissey and D.Tollervey, 1993). Furthermore, it was shown that snR30 base pairs directly with 18S pre-rRNA sequences in yeast, which is important for its processing resulting in the production of the mature 18S rRNA (Fayet-Lebaron et al., 2009). Similarly, the human U17 H/ACA snoRNA was found to interact directly with 18S rRNA precursors (Rimoldi et al., 1993, Atzorn et al., 2004), suggesting that it might be involved in SSU processing. Depletion of snR10 was also shown to affect 18S rRNA processing in yeast (Tollervey, 1987) and it is likely that base pairing of snR10 with the precursor rRNA is required for processing (Liang et al., 2010). To date, no H/ACA snoRNAs were found to be solely involved in LSU rRNA processing in higher eukaryotes that resemble the mechanism of action of U17/snR30 or snR10. TB11Cs2C2 snoRNA in *Trypanosoma brucei*, a protozoan parasite, was suggested to have specific roles in LSU rRNA processing (Gupta et al., 2010) and bioinformatics analysis of the snoRNAs in *Leishmania major,* another protozoan parasite, suggested that some snoRNAs might be involved in both SSU and LSU rRNA processing (Eliaz et al., 2015). For example, LM35Cs3C5, a *L.major*-specific snoRNA, is likely to be involved in LSU rRNA processing and SSU rRNA modification (Eliaz et al., 2015). Whether this is the case with some H/ACA snoRNAs in higher eukaryotes remains to be demonstrated.

Apart from its role in human ribosome biogenesis, the H/ACA RNP has additional roles in the cell. Firstly, it is involved in mRNA splicing, by pseudouridylation of small nuclear (sn)RNAs (Figure 3.1B) (Darzacq et al., 2002, Karijolich and Yu, 2011, Fernandez et al., 2013). The H/ACA proteins bind to the H/ACA small Cajal (sca)RNAs, forming the H/ACA scaRNP, which was found or predicted to be involved in the pseudouridylation of U1, U2, U4, U5 and U6 snRNAs involved in mRNA splicing (Darzacq et al., 2002). For example, U93 H/ACA scaRNA was predicted to be important for pseudouridylation of both U2 and U5 snRNAs (Kiss et al., 2002, Schattner et al., 2006). The localization of the H/ACA scaRNP complex to the Cajal body, a nuclear sub-organelle, is aided by the binding of the chaperone protein TCAB1 (Tycowski et al., 2009). Furthermore, the H/ACA snoRNP is an essential part of telomerase and important for telomere maintenance (Figure 3.1B). Telomerase is a ribonucleoprotein complex consisting of a protein (TERT) and an RNA (TERC) component, which adds DNA sequence repeats at the ends of telomeres (Feng et al., 1995). The H/ACA snoRNP part of telomerase is

important for both the assembly and stability of the telomerase complex (Meier, 2005). The involvement of the H/ACA snoRNP in ribosome biogenesis, splicing and telomere maintenance may provide a regulatory link between these three processes.

A number of genetic diseases, called ribosomopathies, arise because of mutations in genes encoding for ribosomal proteins or ribosome biogenesis factors. Examples of these diseases include Diamond-Blackfan anaemia, Dyskeratosis Congenita and 5q syndrome (Freed et al., 2010b). Dyskeratosis Congenita (DC) is a rare genetic disorder characterized by bone marrow failure, nail dystrophy, immune deficiencies and tumour development (Mason and Bessler, 2011). DC is presented with different modes of inheritance. X-linked DC is caused by mutations in *DKC1* gene, which encodes for Dyskerin (Heiss et al., 1998, Knight et al., 1998), whereas autosomal recessive DC is caused by mutations in *NOP10* (Walne et al., 2007) or *NHP2* (Vulliamy et al., 2008) genes. Interestingly, autosomal dominant DC arises because of mutations in genes encoding for TERT (Armanios et al., 2005) or TERC (Vulliamy et al., 2001) component of human telomerase. A more severe form of DC, called Hoyeraal-Hreidarsson syndrome, presents with a higher mortality rate (Yaghmai et al., 2000). Several mutations in *DKC1* gene were found to cause Hoyeraal-Hreidarsson syndrome, such as P10L, found in the Dyskerin-specific domain of Dyskerin (Figure 3.2) (Vulliamy et al., 2006). Interestingly, mutations found on domain encoding for the catalytic TruB domain of Dyskerin all result in both X-linked Dyskeratosis Congenita and Hoyeraal-Hreidarsson syndrome (Podlevsky et al., 2008). More specifically, S121G (Knight et al., 1999) and R158W (Knight et al., 2001) mutations found in the catalytic site of Dyskerin (Figure 3.2) were identified in DC patients.

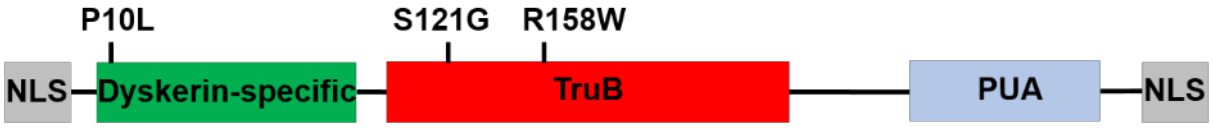

Figure 3.2. Schematic representation of the domain organization of *DKC1* gene and the site of mutations. The nuclear localization signals (NLS) are shown in grey, the Dyskerin-specific domain is shown in green, the RNA-binding domain (PUA) is shown in light blue and the catalytic domain (TruB) is shown in red. The P10L, S121G and R158W mutations found in DC patients are clearly indicated.

It was originally thought that DC arises due to telomere defects, since telomere shortening is observed in all forms (Podlevsky et al., 2008). This idea was enforced after the discovery of mutations in the genes encoding for TERT (Armanios et al., 2005)

or TERC (Vulliamy et al., 2001) that were shown to cause DC. However, clinical features of the disease, such as anaemia, are common to other ribosomopathies, similar to Diamond-Blackfan Anaemia and 5q syndrome (Narla and Ebert, 2010). The DC phenotype has been found to present before telomere shortening in mouse models (Ruggero et al., 2003, Gu et al., 2008) and in zebrafish (Ying Zhang et al., 2012), supporting the theory that ribosome biogenesis defects might be responsible for DC as well as telomere shortening. Furthermore, a recent study showed that increased cell proliferation in neuroblastoma patient samples was due to Dyskerin-related ribosome biogenesis defects but independent of telomerase inhibition (O'Brien et al., 2016a).

Most ribosomopathies, including DC, present with a high risk of developing cancer, especially Acute Myeloid Leukaemia (AML) (Narla and Ebert, 2010). In mice and zebrafish models of ribosomopathies, the clinical symptoms of some of these diseases were shown to be dependent on the tumour suppressor p53 (Yelick and Trainor, 2015). Ribosome biogenesis is directly involved in the regulation of p53 in the cell (Pelava et al., 2016). p53 is controlled by MDM2, an E3 ubiquitin ligase, which binds and ubiquitinates p53, targeting it for proteosomal degradation (Figure 3.3) (Meek, 2015). MDM2 was found to be regulated by the 5S RNP, an LSU intermediate complex consisting of the ribosomal proteins RPL5 and RPL11 along with the 5S rRNA (Donati et al., 2013, Sloan et al., 2013a, Nishimura et al., 2015). Under normal conditions, the 5S RNP is integrated in the large ribosomal subunit during ribosome biogenesis. Under stress conditions, ribosome biogenesis is blocked, resulting in an increase in the levels of the free 5S RNP in the nucleoplasm, since it can no longer be integrated into the large ribosomal subunit. The free 5S RNP, but not the individual RPL5, RPL11 or 5S rRNA (Sloan et al., 2013a), binds and inactivates MDM2, resulting in p53 stabilization (Figure 3.3) (Sloan et al., 2013a, Dai and Lu, 2004, Dai et al., 2008, Sun et al., 2010, Zhang et al., 2003, Lu, 2006, Nishimura et al., 2015). Being a major transcription factor in the cell, stabilization of p53 leads to transcriptional activation of downstream targets, such as p21, which is involved in cell cycle arrest, and Bax, which is involved in apoptosis (Brown et al., 2009).

As with most ribosomopathies, p53 was found to be involved in models of X-linked DC where Dyskerin levels were significantly reduced. In zebrafish models, it was found that Dyskerin knockdown resulted in p53 activation, which led to the development

hematopoietic defects (Ying Zhang et al., 2012). Furthermore, depletion of Dyskerin in mouse livers was shown to cause an induction of p53, leading to cell cycle arrest (Ge et al., 2010b). On another study, hemizygous male mice carrying a mutation in the gene encoding for Dyskerin (*DKC1*) were shown to present with an induction in the p53-dependent DNA damage repair pathway (Gu et al., 2008).

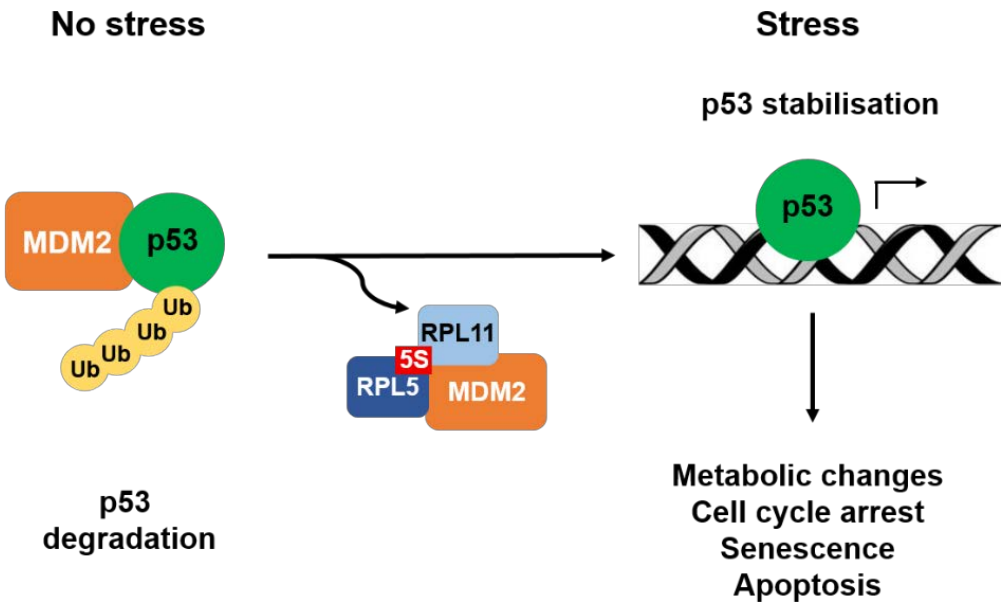

Figure 3.3. Schematic representation of the regulation of p53 levels by the 5S RNP-MDM2 pathway. MDM2 (orange) binds and ubiquitinates p53 (green), targeting it for proteosomal degradation. The free 5S RNP (blue) binds and inactivates MDM2, causing p53 stabilisation, which leads to metabolic changes, cell cycle arrest, senescence and apoptosis.

It is clear that Dyskerin plays a key role in the development of DC. In order to understand the exact causes of DC and how tumour development might occur, it is of vital importance to study the functions of Dyskerin in human cells. In yeast, it was shown that the H/ACA snoRNPs are mainly involved in the biogenesis of the small ribosomal subunit (Atzorn et al., 2004, Henras et al., 2004, Lafontaine et al., 1998). However, not many studies have been performed in human cells exploring the role of Dyskerin in ribosome biogenesis. Furthermore, mutations in the catalytic domain of Dyskerin result in the development of Hoyeraal-Hreidarsson syndrome and the presentation of severe clinical symptoms of X-linked Dyskeratosis Congenita (Podlevsky et al., 2008). These mutations only affect the pseudouridine synthase activity of Dyskerin, which was shown to be essential for both rRNA processing and modification in yeast (Zebarjadian et al., 1999) but, presumably, only for rRNA stability in mouse embryonic fibroblast cells (Gu et al., 2013). Therefore, I aimed to investigate

the functions of Dyskerin in human ribosome biogenesis pathway and to identify whether the catalytic activity of Dyskerin is essential for rRNA processing in humans. Finally, since ribosome biogenesis defects are linked with the regulation of the p53 tumour suppressor via the 5S RNP-MDM2 pathway (Pelava et al., 2016), I investigated whether p53 levels were affected when Dyskerin was knocked-down or inactive.

3.2 Results

3.2.1 Dyskerin is likely to be essential for H/ACA snoRNP accumulation in HEK293T cells

In order to study the functions of Dyskerin in human cells, a knockdown system was established in HEK293T human embryonic kidney cells using reverse transfection of siRNA complexes. The knockdown efficiency was evaluated by Western Blotting, after the whole cell extract was loaded on an SDS-PAGE gel. The levels of Dyskerin were analysed using an α-Dyskerin antibody and the exosome component CSL4 was used as a loading control (Figure 3.4A). Even though the lane with the Dyskerin knockdown was under-loaded, the siRNA treatment resulted in a reduction of the Dyskerin levels by approximately 60% (Figure 3.4A), as shown after quantitation using the ImageQuant software, and often worked more efficiently (see later).

In yeast, Cbf5 is essential for the accumulation of the H/ACA snoRNP, since its loss results in a decrease in snoRNA levels (Zebarjadian et al., 1999). It was, therefore, expected that knockdown of Dyskerin in human HEK293T cells would also result in a reduction of the levels of the H/ACA snoRNAs. To confirm this, knockdown of Dyskerin was performed for 48h, and RNA was extracted and loaded on an 8% Acrylamide/7M Urea gel. The RNA was transferred on a Hybond N membrane, which was incubated with radiolabelled (^{32}P) probes against the U17, U64, U19 and U70 H/ACA snoRNAs, with the U1 snRNA used as a loading control (Figure 3.4B). U17 is involved in SSU rRNA processing (Atzorn et al., 2004), U64 and U19 are involved in LSU modification (Ganot et al., 1997a) and U70 is involved in SSU rRNA modification (Ganot et al., 1997a). In comparison to the control, knockdown of Dyskerin resulted in a reduction of the levels of all four H/ACA snoRNAs tested (Figure 3.4B). These data demonstrated that the Dyskerin-knockdown system in HEK293T showed the expected phenotype with Dyskerin being required for the accumulation of the H/ACA snoRNAs in humans.

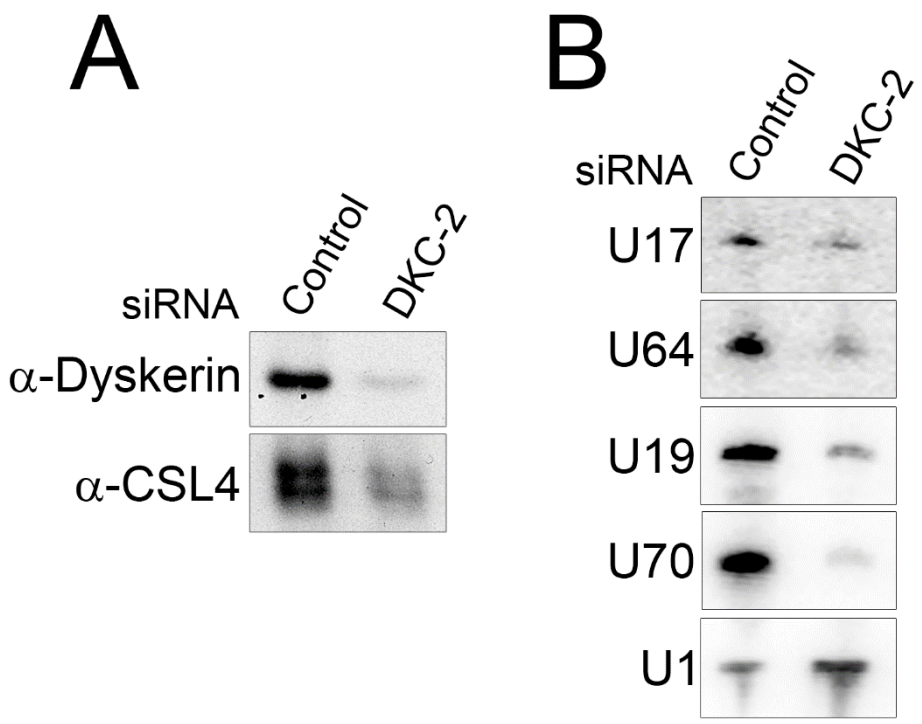

Figure 3.4. Dyskerin knockdown results in a reduction in the levels of the H/ACA snoRNAs tested. siRNA-mediated knockdown using Control or Dyskerin (DKC-2) siRNAs was performed in HEK293T cells for 48h. **(A)** Whole cell extracts were loaded on an SDS-PAGE gel, analyzed by Western Blotting and visualized using ECL. The antibodies, used to detect the levels of Dyskerin, and CSL4, used as a loading control, are indicated on the left of the panel. **(B)** RNA was extracted, separated on an 8% Acrylamide/7M Urea gel, and analyzed by Northern Blotting. Radiolabelled (^{32}P) probes, indicated on the left of the panel, were used to detect the levels of U17, U64, U19 or U70 H/ACA snoRNAs. The U1 snRNA was used as a loading control.

3.2.2 Dyskerin is required for ribosome biogenesis in HEK293T cells

In yeast, it was shown that the H/ACA snoRNPs are required for biogenesis of the small ribosomal subunit (Lafontaine et al., 1998, Girard et al., 1992). Having established a knockdown system in HEK293 cells, I next investigated the function of Dyskerin in human ribosome biogenesis. Pulse-chase labelling was used to characterize the newly-synthesized rRNAs, after Dyskerin knockdown. HEK293T cells were incubated in phosphate-free media for 1h, followed by the addition of radiolabelled phosphate (^{32}P) for 1h. The cells were then grown in normal media for 3h or 4h (chase) (Figure 3.5A). RNA was extracted, loaded on a 1.2% agarose-glyoxal gel and transferred on a Hybond N membrane. The ethidium bromide staining (UV) of the 28S rRNA was used as a loading control (Figure 3.5A).

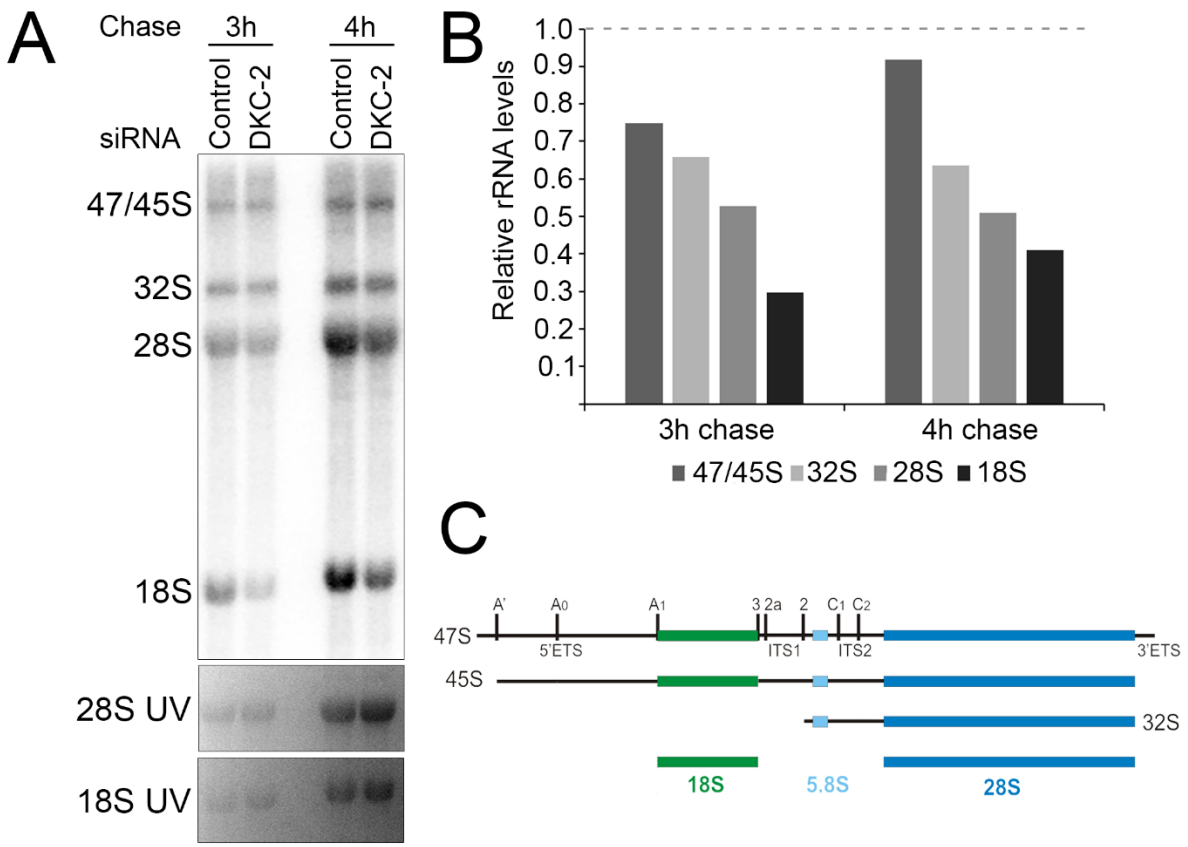

Figure 3.5. Dyskerin knockdown results in defects in both large and small ribosomal subunit biogenesis in HEK293T cells. (A) 48h after knockdowns using control or Dyskerin (DKC-2) siRNAs, the cells were incubated in a phosphate-free media for 1h. Addition of radiolabelled phosphate (^{32}P) took place for 1h before the cells were left to grow under normal conditions for 3h or 4h (chase). RNA was extracted and loaded on a glyoxal-agarose gel, before being transferred on a Hybond N membrane and visualized using a Phosphorimager. The 28S rRNA levels after ethidium bromide staining (UV) were used as a loading control. **(B)** ImageQuant was used for quantitation of the rRNAs and the data were normalized against the loading control (28S UV). The graph represents the averages of two experimental repeats, and the rRNA levels after Dyskerin knockdown (DKC-2) were normalized to the rRNA levels using the control siRNA for 3h or 4h of chase. The dotted line represents the rRNA precursor levels in control cells. **(C)** Schematic representation of the rRNA processing intermediates seen in pulse labelling experiments in humans. The SSU precursors and mature rRNA are shown in green and the LSU precursors and mature rRNA are shown in blue. The cleavage sites are shown on the top (Adapted from (Sloan et al., 2013c)).

At 3h of chase after Dyskerin knockdown, there was an approximately 15% decrease in the 47/45S rRNA precursor levels and a 35% decrease in the levels of the 32S rRNA precursor as compared to the control (Figure 3.5A, B, 3h chase). Furthermore, the levels of the newly-synthesized 28S rRNA were decreased by approximately 50% after Dyskerin knockdown as compared to the control, whereas the levels of the newly-synthesized 18S rRNA were decreased by approximately 70% (Figure 3.5A, B, 3h chase). By comparison, 4h of chase after Dyskerin knockdown, not much difference

was observed in the levels of the 47/45S rRNA precursor as compared to the control (less than 10% decrease), but the levels of the 32S rRNA precursor were decreased by approximately 35% (Figure 3.5A, B, 4h chase). Similarly to the 3h chase, the levels of the newly-synthesized 28S and 18S were decreased by approximately 50% and 60% respectively when Dyskerin was knocked down as compared to the control, after 4h of chase (Figure 3.5A, B, 4h chase).

Taken together, these data indicate that Dyskerin knockdown results in defects in the biogenesis of both the large and small ribosomal subunit, as opposed to yeast where Dyskerin plays an important role in small ribosomal subunit biogenesis (Lafontaine et al., 1998).

Since Dyskerin knockdown surprisingly affected both the LSU and SSU newly-synthesized rRNAs, I used Northern blotting to investigate the effects of Dyskerin knockdown on pre-rRNA processing. Dyskerin was knocked down for 48h in HEK293T cells before RNA was extracted. The RNA was loaded on a glyoxal-agarose gel and analysed by Northern Blotting. Radiolabelled (^{32}P) probes against the Internal Transcribed Spacer 1 (ITS1) and 2 (ITS2) (Sloan et al., 2013c) regions were used in order to analyse the levels of the precursor rRNAs (Figure 3.6A). The 5'-ITS1 probe identifies the 18SE rRNA precursor, the ITS1 probe identifies the 47/45S, 41S, 30S, 26S and 21S precursors whereas the ITS2 probe identifies the 47/45S, 32S and 12S precursors (Figure 3.6A) (Sloan et al., 2013c).

Dyskerin knockdown resulted in a significant decrease in the levels of 41S, 26S, 21S and 18SE rRNA precursors as compared to the control, but no significant difference were observed in the levels of 30S rRNA precursor after Dyskerin knockdown as compared to the control (Figure 3.6B, D). Furthermore, the 32S rRNA precursor levels were significantly increased after Dyskerin knockdown as compared to the control, but no significant difference was observed on the levels of the 12S rRNA precursor (Figure 3.6 C, D). Taken together, these data show that Dyskerin contributes to pre-rRNA processing for both large and small ribosomal subunit biogenesis. This agrees with the previous data showing that Dyskerin knockdown results in a decreased accumulation of both 28S and 18S rRNAs in pulse-chase labelling experiments (Figure 3.5).

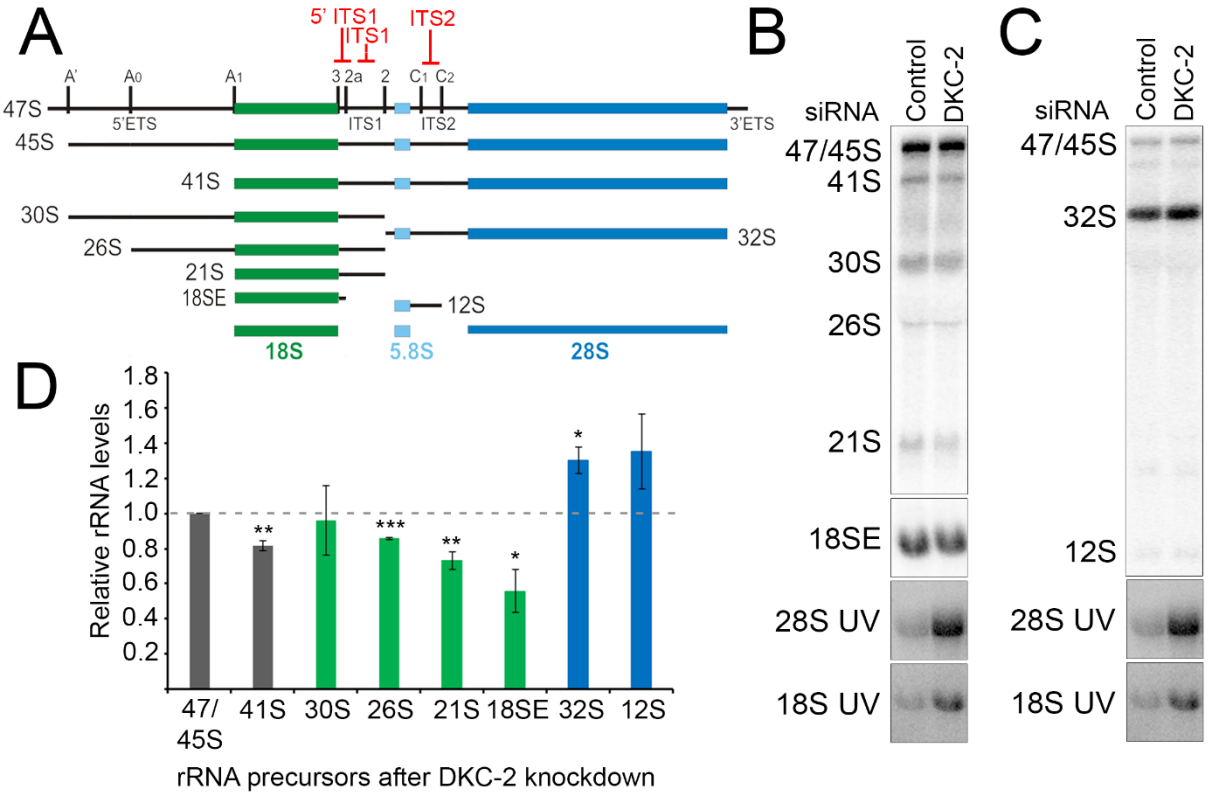

Figure 3.6. Dyskerin knockdown results in both LSU and SSU early rRNA processing defects. (A) Schematic representation of the rRNA precursors in humans. The SSU precursors and mature 18S rRNA are shown in green and the LSU precursors and mature 28S rRNA are shown in blue. The cleavage sites are shown at the top and the ITS1 and ITS2 sites recognized by the radiolabeled (^{32}P) probes are marked in red (Adapted from (Sloan et al., 2013c) **(B-C)** RNA was extracted 48h after siRNA transfection using control or Dyskerin (DKC-2) siRNAs in HEK293T. The RNA was separated on a 1.2% glyoxal-agarose gel and analyzed by Northern blotting. The membranes were incubated with ^{32}P-labelled-oligo probes against ITS1 or 5'ITS1 (18SE) **(B)** and ITS2 **(C)** The ethidium bromide staining of 28S rRNA (UV) was used as a loading control. The rRNA precursors are indicated on the left of each panel. **(D)** ImageQuant software was used for quantitation of the rRNA levels, which were normalized to the loading control (28S UV). The levels of the rRNA precursors were normalized to control and to the 47/45S rRNA levels. The graphs represent the averages of three experimental repeats and the error bars show the standard error (+/- SEM). Statistical analysis was performed using an unpaired t-test. The unmarked bars indicate non-significant differences as compared to the control and the dotted line represents the rRNA precursor levels in control cells. *p value < 0.05, **p value < 0.01, ***p value < 0.001.

3.2.3 Dyskerin knockdown results in p53 accumulation via the 5S RNP-MDM2 pathway in U2OS cells

Defects in ribosome biogenesis result in the accumulation of the tumour suppressor p53 (Freed et al., 2010b) via the 5S RNP-MDM2 pathway. The 5S RNP, an LSU intermediate consisting of the ribosomal proteins RPL5, RPL11 and the 5S rRNA,

accumulates in the nucleoplasm when ribosome biogenesis is defective. The free 5S RNP binds the ubiquitin ligase MDM2, which normally binds and inhibits p53, targeting it for proteosomal degradation. Upon 5S RNP binding, the function of MDM2 is inhibited, leading to p53 stabilisation (Pelava et al., 2016). Since Dyskerin knockdown resulted in defects in both LSU and SSU ribosome biogenesis, I wanted to investigate whether Dyskerin knockdown had an effect on p53 levels in the cell. For this, U2OS human osteosarcoma cells were used instead of HEK293T, because HEK293T cells do not contain an active p53 due to their transformation method with adenovirus E1A and E1B, as E1B inhibits activation of transcription of p53 by decreasing its DNA-binding capacity (Lin et al., 2014, Steegenga et al., 1996). Knockdown of Dyskerin was performed in U2OS cells for 48h and the whole cell extract was loaded on an SDS-PAGE gel before analysed by Western Blotting using α-p53 and α-p21 antibodies. The p21 gene is a target of p53 and provides an indication of p53 activity. It is worth noting that p21 levels can be regulated post-translationally (Jung et al., 2010) and p21 mRNA levels were not checked here, neither were other downstream targets of p53 (Gottlieb and Vousden, 2010). Karyopherin was used as a loading control (Figure 3.7A).

Dyskerin knockdown resulted in an almost 2-fold significant increase in p53 levels (Figure 3.7A, B) and to an increase in p21 protein levels. In order to investigate whether the p53 increase observed after Dyskerin knockdown was a result of MDM2 inhibition by the 5S RNP, RPL5 was co-depleted with Dyskerin to block p53 activation by the 5S RNP (Donati et al., 2013). Note that expression levels of Dyskerin or RPL5 were not checked after the double knockdowns, so less efficient depletion of the targets might have occurred. After co-depletion of RPL5, p53 was at similar levels to the control and significantly decreased as compared to the p53 levels after Dyskerin knockdown (Figure 3.7A, B). Furthermore, the p21 levels were also decreased as compared to the single Dyskerin knockdown (Figure 3.7A) which was consistent in all experimental repeats. Finally, RPL5 knockdown resulted in a 60% decrease in RPL5 levels (Figure 3.7C), although this decrease was often bigger. RPL5 knockdown alone did not result in a significant change in p53 levels as compared to the control, as expected (Figure 3.7A, B) (Donati et al., 2013, Sloan et al., 2013a). In conclusion, these data indicate that defects in ribosome biogenesis caused by Dyskerin knockdown result in p53 accumulation via the 5S RNP-MDM2 pathway.

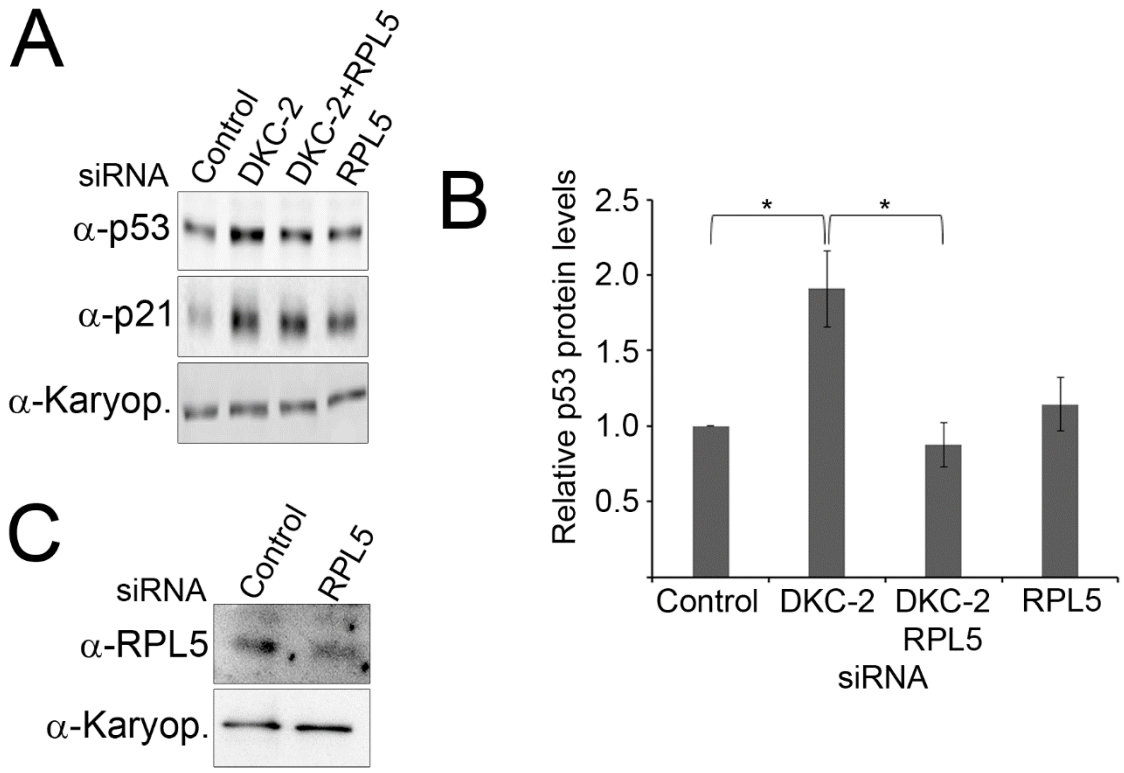

Figure 3.7. Dyskerin knockdown results in an induction of p53 via the 5S RNP-MDM2 pathway. (A) Knockdowns of control, Dyskerin (DKC-2) or RPL5 were performed in U2OS cells for 48h. The whole cell extract was loaded on an SDS-PAGE gel and analyzed by Western Blotting using α-p53 and α-p21 antibodies (shown on the left of the panel). Karyopherin (Karyop.) was used as a loading control. The membranes were visualized using the LICOR system. **(B)** The ImageQuant software was used for quantitation of the Western blots. The graphs represent the averages from three experimental repeats and the error bars show the standard error (+/-SEM). Statistical analysis was performed using an unpaired t-test. The unmarked bars indicate non-significant differences as compared to the control. *p value < 0.05. **(C)** siRNA treatment was performed in U2OS cells for 48h. The whole cell extract was loaded on an SDS PAGE gel and analysed by Western Blotting using the antibodies shown on the left of the panel. Karyopherin (Karyop.) was used as loading control and Western blots were visualized using ECL.

3.2.4 Creation of RNAi resistant stable cell lines of Dyskerin WT and D125A catalytic mutant in HEK293T and U2OS cells

I have shown that Dyskerin knockdown results in defects in both large and small ribosomal subunit biogenesis, which leads to p53 accumulation via the 5S RNP-MDM2 pathway. In yeast, the catalytic activity of Dyskerin is important for rRNA processing and modifications (Zebarjadian et al., 1999), but not in mouse embryonic fibroblasts where it was shown it affects rRNA stability rather than processing (Gu et al., 2013). Therefore, I next wanted to investigate whether the catalytic activity of Dyskerin is

important for ribosome biogenesis in humans. HEK293T and U2OS cells that stably expressed Dyskerin were created using the Flp-In recombination system (Life Technologies). The open reading frame (ORF) of Dyskerin was mutated so that it would be resistant to the siRNA sequence (DKC-2) with no change in the amino acid sequence (Figure 3.8D). Furthermore, the ORF of Dyskerin was mutated to inactivate the catalytic activity of Dyskerin by replacing the aspartic acid essential for Dyskerin activity with an alanine (D125A) (Figure 3.8A). This mutation was shown to cause rRNA processing or stabilisation defects in yeast and mouse models due to inactivation of Dyskerin (Gu et al., 2013, Zebarjadian et al., 1999). The aspartic acid at position 125 is a well-conserved residue found at the catalytic domain of Dyskerin (TruB) amongst species (Figure 3.8B) and it is also conserved in four classes of pseudouridine synthases (Gu et al., 2013). The expressed protein contained a FLAG-tag sequence on the N-terminus and was under the control of a titratable tetracycline promoter.

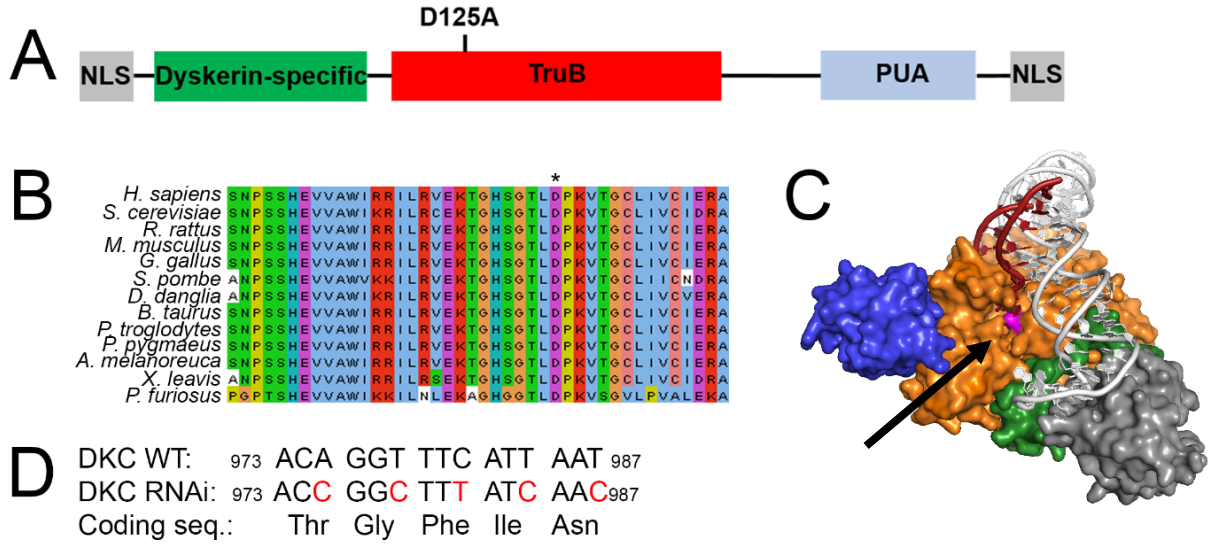

Figure 3.8. Dyskerin domains and mutagenesis. (A) Schematic representation of the domain organization of Dyskerin. The nuclear localization signals (NLS) are shown in grey, the Dyskerin-specific domain is shown in green, the RNA-binding domain (PUA) is shown in light blue and the catalytic domain (TruB) is shown in red. The position of the catalytic mutant D125A is marked. **(B)** Sequence alignment of the conserved catalytic site of Dyskerin in 13 species: human (*H. sapiens*), budding yeast (*S. cerevisiae*), rat (*R. rattus*), mice (*M. musculus*), chicken (*G. gallus*), fission yeast (*S. pombe*), fish (*D. danglia*), cow (*B. taurus*), chimpanzee (*P. troglodytes*), orangutan (*P. pygmaeus*), giant panda (*A. melanoleuca*), frog (*X. leavis*) and archaea (*P. furiosus*). The conserved aspartate necessary for the catalytic activity of Dyskerin is indicated with an asterix. **(C)** Structure of the H/ACA snoRNP. Dyskerin is shown in orange, NOP10 in green, NHP2 in dark grey and GAR1 in blue. The H/ACA snoRNA is shown in light grey and the rRNA substrate in red. The position of the D125 catalytic nucleotide is shown in pink (indicated by the arrow). **(D)** Outline of the mutations on the Dyskerin ORF for creation of the RNAi resistant plasmids. The nucleotide and amino acid sequences are clearly marked on the sequence.

The cells were grown in normal media and induction of the FLAG-tagged protein was performed for 48h using a range of tetracycline concentrations (0-1000 ng/µl). Whole cell extract was then loaded on an SDS-PAGE gel and analysed using Western Blotting. The levels of both the endogenous and FLAG-tagged Dyskerin were determined using an α-Dyskerin antibody and the levels of the FLAG-tagged Dyskerin were revealed using an α-FLAG antibody. The exosome complex protein CSL4 was used as a loading control (Figure 3.9).

Expression of the FLAG-tagged proteins was optimised to result in an equal or slightly higher levels to that seen for the endogenous. The expression of the RNAi resistant WT FLAG-tagged Dyskerin in HEK293T was optimal using 100ng/µl tetracycline (Figure 3.9A, top panel), whereas expression of the RNAi resistant D125A mutant FLAG-tagged Dyskerin in HEK293T cells was optimal using 1000ng/µl tetracycline (Figure 3.9A, bottom panel). It is not clear why this difference in tetracycline concentrations was seen in HEK293T cells. In U2OS cells expressing the RNAi resistant WT or the D125A mutant FLAG-tagged Dyskerin, 1000ng/µl tetracycline was used for optimal expression of the FLAG-tagged protein (Figure 3.9B). It was expected that expression of the FLAG-tagged Dyskerin would result in a slight decrease in the levels of the endogenous protein, since the cells would compensate for the over-expression of Dyskerin.

Dyskerin localizes to the nucleolus, where ribosome biogenesis takes place, and in the nucleoplasm, in humans (Heiss et al., 1999) and in yeast (Bertrand et al., 1998). Immunofluorescence was performed to confirm that the RNAi resistant FLAG-tagged Dyskerin was localized as normal in cells expressing either the WT or the D125A mutant Dyskerin (Figure 3.9C). HEK293T cells expressing the RNAi resistant WT or D125A mutant FLAG-tagged Dyskerin were grown in normal media for 48h with the addition of 100ng/µl or 1000ng/µl tetracycline respectively. The cells were then fixed on a coverslip using 4% paraformaldehyde and incubated with α-FLAG antibody for visualization of the FLAG-tagged protein expressed. The nucleolus was stained using α-Fibrillarin antibody and HEK293T cells were used as a control. The RNAi resistant WT FLAG-tagged Dyskerin was found to mainly localize to the nucleolus and, to a lesser extent, to the nucleoplasm, as expected (Figure 3.9C, WT panel). Similarly, the RNAi resistant D125A FLAG-tagged Dyskerin also localized to the nucleolus and, to a

lesser extent, to the nucleoplasm (Figure 3.9C, D125A panel). The RNAi resistant WT or D125A mutant FLAG-tagged Dyskerin, therefore, localized as expected.

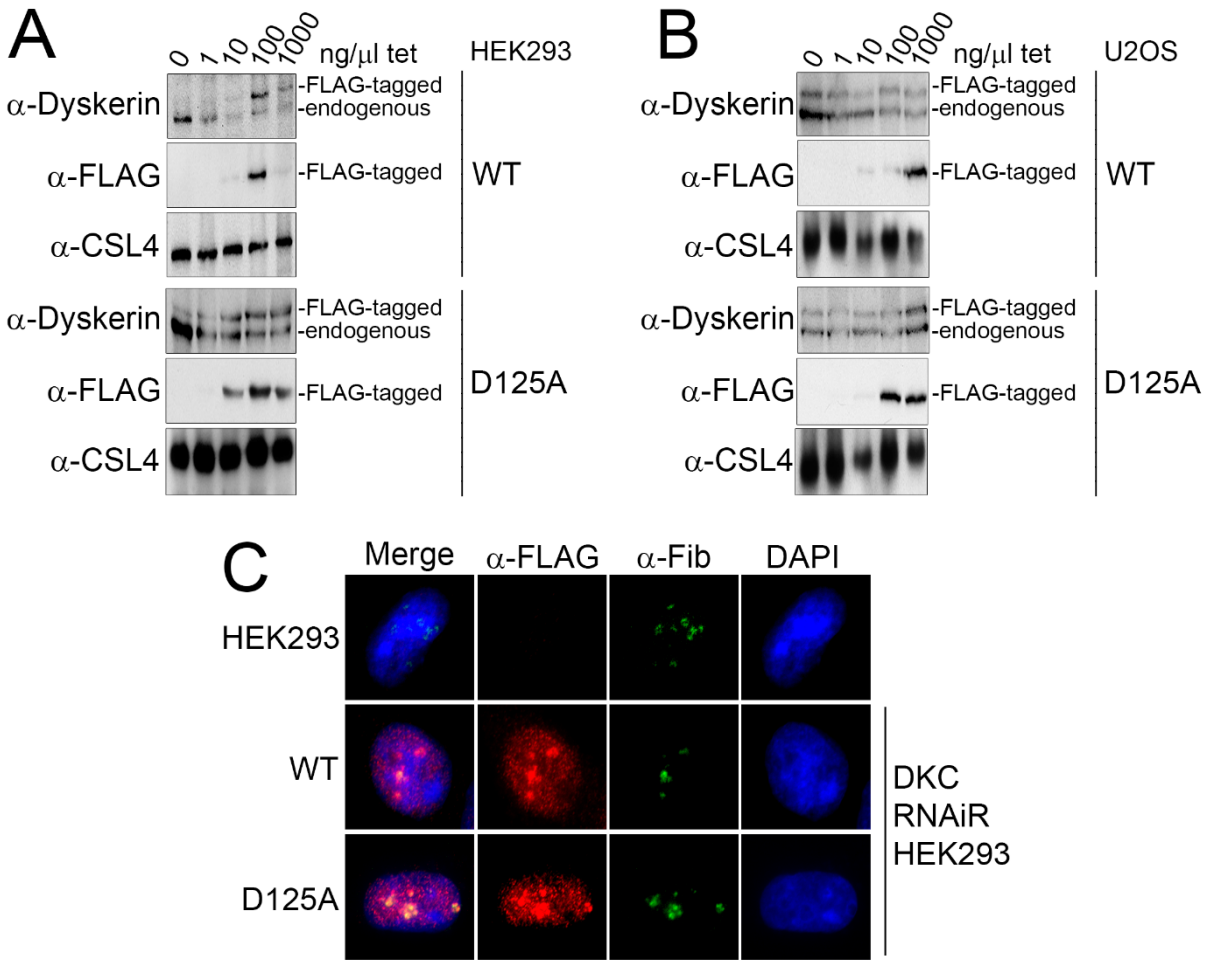

Figure 3.9. Expression of the WT or D125A Dyskerin in HEK293T and U2OS cells. **(A-B)** The cells were grown in normal media in addition to different concentrations of tetracycline (0-1000 ng/µl) in HEK293T **(A)** or U2OS **(B)** cells stably expressing the RNAi resistant WT or D125A mutant Dyskerin. Whole cell extracts were loaded on an SDS-PAGE gel and analysed by Western Blotting, visualized by ECL. α-Dyskerin antibody was used to detect the levels of the endogenous and the FLAG-tagged protein, whereas α-FLAG antibody was used to detect the levels of the FLAG-tagged protein only. CSL4 was used as a loading control. The antibodies used are indicated on the left of the panels and the FLAG-tagged or endogenous Dyskerin are indicated on the right of the panels. **(C)** Immunofluorescence was performed after 48h of induction of HEK293T cells expressing the RNAi resistant (RNAiR) WT or the D125A mutant FLAG-tagged Dyskerin using 100ng/µl or 1000ng/µl tetracycline respectively. Plain HEK293T cells were used as a control. The FLAG-tagged Dyskerin is shown by the α-FLAG antibody (red). Nucleolar staining was performed using the α-Fibrillarin (Fib) antibody (green), whereas the DNA was stained with DAPI (blue). Visualization of the cells was performed using the Zeiss Axiovision inverted microscope and software.

Next, the RNAi rescue system was tested, where the siRNA duplexes were transfected for 48h in HEK293T or U2OS cells expressing the RNAi resistant WT or D125A mutant FLAG-tagged Dyskerin for 48h, with the addition of tetracycline. Whole cell extracts were loaded on an SDS-PAGE gel and analysed by Western Blotting. In HEK293T cells containing the empty pcDNA5 vector, the Dyskerin knockdown resulted in approximately 70% decrease in the levels of the endogenous protein compared to the control, taking in mind the differences in loading as seen by the CSL4 levels (Figure 3.10A). Two bands were visible in these cells when the α-Dyskerin antibody was used, but there was no visible band when the α-FLAG antibody was used. It is not clear why this was sometimes seen. Dyskerin knockdown in HEK293T cells expressing either the RNAi resistant WT or the D125A mutant FLAG-tagged Dyskerin resulted in an a 90% and 95% reduction of the endogenous protein respectively as compared to the control knockdown (Figure 3.10A, B). However, no reduction was observed in the levels of the FLAG-tagged protein in HEK293T expressing the RNAi resistant WT FLAG-tagged Dyskerin (Figure 3.10A), showing that the endogenous protein was mostly replaced by the FLAG-tagged Dyskerin. Even though an increase was observed in the levels of the FLAG-tagged protein in HEK293T cells expressing the RNAi resistant D125A mutant FLAG-tagged Dyskerin (Figure 3.10A), this was not always seen, indicating that the D125A mutant protein replaced the endogenous one.

In U2OS cells containing the empty pcDNA5 vector, the knockdown of Dyskerin resulted in an efficient 70% decrease in the levels of the endogenous protein, as expected (Figure 3.10C). Even though there were differences in loading, Dyskerin knockdown in U2OS cells expressing either the RNAi resistant WT or D125A mutant FLAG-tagged Dyskerin resulted in a 40% and 30% reduction of the endogenous protein levels respectively, but not in any reduction in the levels of the FLAG-tagged protein (Figure 3.10C, D). Even though the reduction in the levels of the endogenous Dyskerin in U2OS cells expressing the RNAi resistant WT or D125A mutant was not as high as expected, the cells contained the RNAi resistant FLAG-tagged protein while the endogenous Dyskerin was decreased, which allowed us to study the effects of the inactivation of Dyskerin nevertheless. The minor increase in the levels of the RNAi resistant D125A FLAG-tagged Dyskerin was not always seen and it might be an experimental variation (Figure 3.10C, D).

Taken together, these data indicated that the RNAi rescue system enabled the replacement of the endogenous Dyskerin with the FLAG-tagged protein in both HEK293T and U2OS cells.

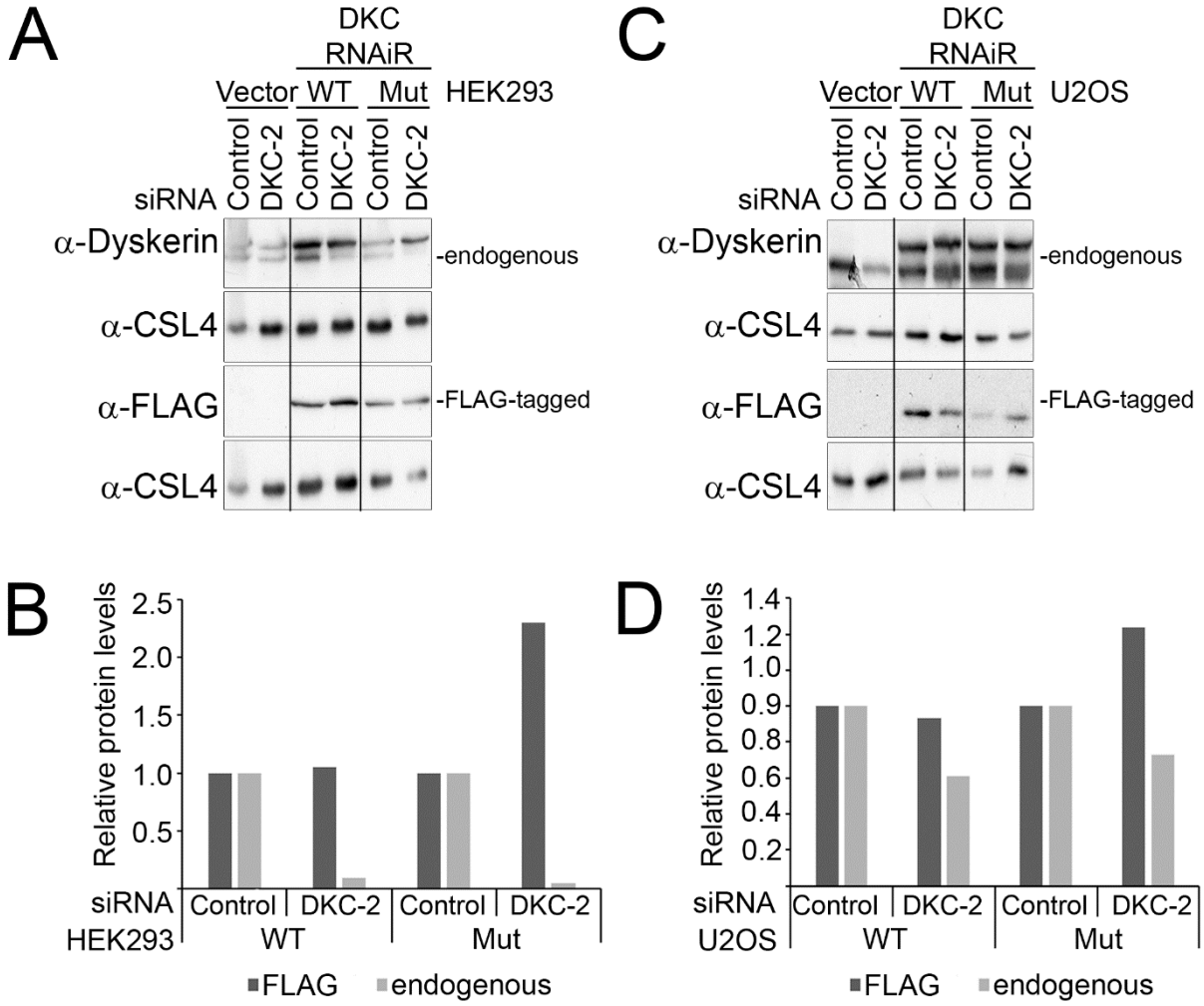

Figure 3.10. The RNAi rescue system in HEK293T and U2OS cells. (A, C) HEK293T **(A)** or U2OS **(C)** cells containing the empty pcDNA5 vector (marked as "Vector") or expressing the RNAi resistant WT or D125A mutant FLAG-tagged Dyskerin were treated with control or Dyskerin (DKC-2) siRNAs for 48h. 100ng/µl tetracycline was used for 48h in WT-expressing cells and 1000ng/µl tetracycline was used in pcDNA5-containing and D125A-expressing cells. The whole cell extract was loaded on an SDS-PAGE gel and analysed by Western Blotting, visualized by ECL. α-Dyskerin antibody was used to detect the levels of the endogenous and the FLAG-tagged Dyskerin, whereas α-FLAG antibody was used to detect only the FLAG-tagged protein. CSL4 was used as a loading control. The antibodies used are shown on the left of the panels and the endogenous and FLAG-tagged Dyskerin are indicated on the right of the panels. **(B, D)** ImageQuant software was used for quantitation of the levels of the endogenous and FLAG-tagged Dyskerin in HEK293T **(B)** or U2OS **(D)** cells expressing the RNAi resistant (RNAiR) WT or D125A mutant Dyskerin, which were normalized to the loading control (CSL4).

3.2.5 The catalytic activity of Dyskerin is not required for accumulation of the H/ACA snoRNP

Dyskerin knockdown resulted in a decrease in the levels of U17, U64, U19 and U70 H/ACA snoRNAs (Figure 3.4B). It was shown that mutations in the catalytic domain of the yeast Cbf5 resulted in a decreased accumulation of the H/ACA snoRNAs (Zebarjadian et al., 1999). I, therefore, wanted to investigate whether this was also the case in humans. Knockdowns of control and Dyskerin (DKC-2) were performed for 48h in HEK293T cells expressing the RNAi resistant WT or D125A mutant FLAG-tagged Dyskerin, or in HEK293T cells containing pcDNA5 vector. RNA was extracted and separated on an 8% acrylamide/7M Urea gel, and the membranes were incubated with radiolabelled (^{32}P) probes specific for the U17, U64, U19 or U70 snoRNAs and the U1 snRNA, which was used as a loading control (Figure 3.12A).

In HEK293T cells containing the empty pcDNA5 vector, the levels of all four H/ACA snoRNAs were decreased by approximately 80% after Dyskerin knockdown (Figure 3.11A, B), consistent with earlier results (Figure 3.4B). Expression of the RNAi resistant WT FLAG-tagged Dyskerin resulted in more than 90% rescue of U17, U64 and U70 after Dyskerin knockdown as compared to the control knockdown, and in approximately 70% rescue of U19 H/ACA snoRNA (Figure 3.11A). This further confirmed that the RNAi rescue system worked as expected and that the FLAG-tagged Dyskerin can function in snoRNP biogenesis as normal. Expression of the RNAi resistant D125A catalytic mutant FLAG-tagged Dyskerin also rescued all four H/ACA snoRNAs, even though there was a slight increase in U64, U19 and U70 snoRNA levels (Figure 3.11A). These results indicated that the catalytic activity of Dyskerin is not required for the accumulation of H/ACA snoRNAs in human cells. Analysis of further H/ACA snoRNAs, such as U66, U69 and U72, will be performed in the future in order to understand the involvement of Dyskerin and its catalytic activity in the accumulation of other H/ACA snoRNAs.

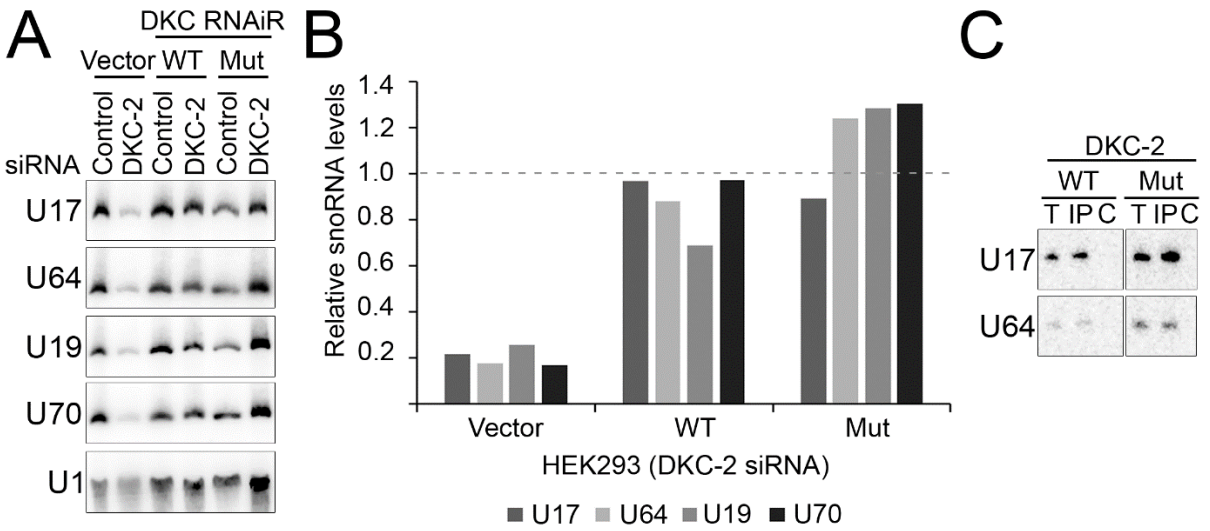

Figure 3.11. Dyskerin, but not its catalytic activity, is required for the accumulation of the H/ACA snoRNAs in HEK293T cells. (A) Knockdowns using Control or Dyskerin siRNA (DKC-2) were performed for 48h in HEK293T cells containing the empty pcDNA5 vector, or expressing the RNAi resistant WT or the D125A mutant FLAG-tagged Dyskerin for 48h. 100ng/μl tetracycline was used in WT-expressing cells and 1000ng/μl tetracycline was used in pcDNA5-containing and D125A-expressing cells. RNA was extracted and loaded on an acrylamide gel and analysed by Northern Blotting. Radiolabelled (^{32}P) probes specific for U17 and U64 H/ACA snoRNAs and U1 snRNA were used, as indicated on the left of the panel. The U1 snRNA was used as a loading control. **(B)** Quantitation of two experimental repeats was performed using the ImageQuant Software and the levels U17 and U64 H/ACA snoRNAs were normalized against the loading control levels (U1 snRNA). The graphs represent the averages from two experimental repeats and the dotted line represents the snoRNA levels in control cells. **(C)** Knockdowns using Dyskerin siRNA (DKC-2) were performed for 48h in HEK293T cells expressing the WT or the D125A mutant FLAG-tagged Dyskerin. Immunoprecipitation followed, where α-FLAG beads were used for pull down of complexes associated with Dyskerin, and control beads, containing no antibody, were used as a control. RNA was extracted using the phenol-chloroform method and loaded on an 8% acrylamide/7M Urea gel before analysed by Northern Blotting. Radiolabelled (^{32}P) probes were used to detect the levels of U17 and U64 H/ACA snoRNAs (shown on the left of the panel). T=total, IP=α-FLAG beads, C=control beads.

To further investigate the importance of the Dyskerin catalytic domain mutants on H/ACA snoRNP formation, I determined the association of the FLAG-tagged proteins with the snoRNAs using immunoprecipitation. The endogenous protein was replaced by the WT or D125A mutant FLAG-tagged Dyskerin as described previously and the whole cell extract was lysed using sonication. Sepharose beads containing the α-FLAG antibody were used for the pull down and beads containing no antibody were used as a control. RNA was extracted from the beads and loaded onto an acrylamide gel, transferred on a membrane and probed with radiolabelled (^{32}P) probes for U17 and U64 (Figure 3.11C). Both WT and D125A mutant FLAG-tagged proteins efficiently

pulled down the U17 and U64 snoRNAs (Figure 3.11C), indicating the absence of the catalytic activity of Dyskerin does not affect the formation of the H/ACA snoRNP.

In conclusion, these data showed that the catalytic activity of Dyskerin is not required for the accumulation or snoRNP formation of either U17, U64, U19 or U70 H/ACA snoRNAs, indicating that the catalytic activity of Dyskerin is not likely to be required for H/ACA snoRNP accumulation. This is different from yeast data showing that inactivation of the catalytic activity of Cbf5 (yeast Dyskerin) resulted in a decreased accumulation of the H/ACA snoRNAs interacting with Cbf5, which are involved in either rRNA processing (snR10), LSU rRNA pseudouridylation (snR8, snR37) or SSU rRNA pseudouridylation (snR31) (Zebarjadian et al., 1999). Finally, inactivation of the catalytic activity of Dyskerin in mouse embryonic fibroblast cells also showed a similar phenotype to yeast, where several H/ACA snoRNAs, including U17 and U64, were significantly decreased in the cell (Gu et al., 2013), which differs from my data here. It will be interesting to investigate the interactions of the WT and the catalytic mutant Dyskerin with other H/ACA snoRNAs in human cells as well, in order to understand the function of Dyskerin in H/ACA snoRNP accumulation. It is worth noting that I have established here the first system in humans which allows us to investigate for rRNA processing defects affected by the absence of the catalytic activity of Dyskerin without affecting the levels of the snoRNAs in the cell.

3.2.6 The catalytic activity of Dyskerin is essential for rRNA processing

Inactivation of the catalytic activity of Dyskerin did not affect the accumulation of the tested H/ACA snoRNAs (Figure 3.11). This is different from yeast where the catalytic activity of Dyskerin is required for both H/ACA snoRNP accumulation and rRNA processing (Zebarjadian et al., 1999). This, therefore, provided us with the opportunity to investigate whether the catalytic activity of Dyskerin is important for human ribosome biogenesis. The endogenous protein was replaced by the WT or the D125A FLAG-tagged Dyskerin in HEK293T cells as previously, and HEK293T cells containing the empty pcDNA5 vector were used as a control. RNA was extracted and loaded on a glyoxal-agarose gel and analysed by Northern Blotting using radiolabelled (^{32}P) probes for 5'-ITS1, ITS1 or ITS2 regions (Figure 3.12A).

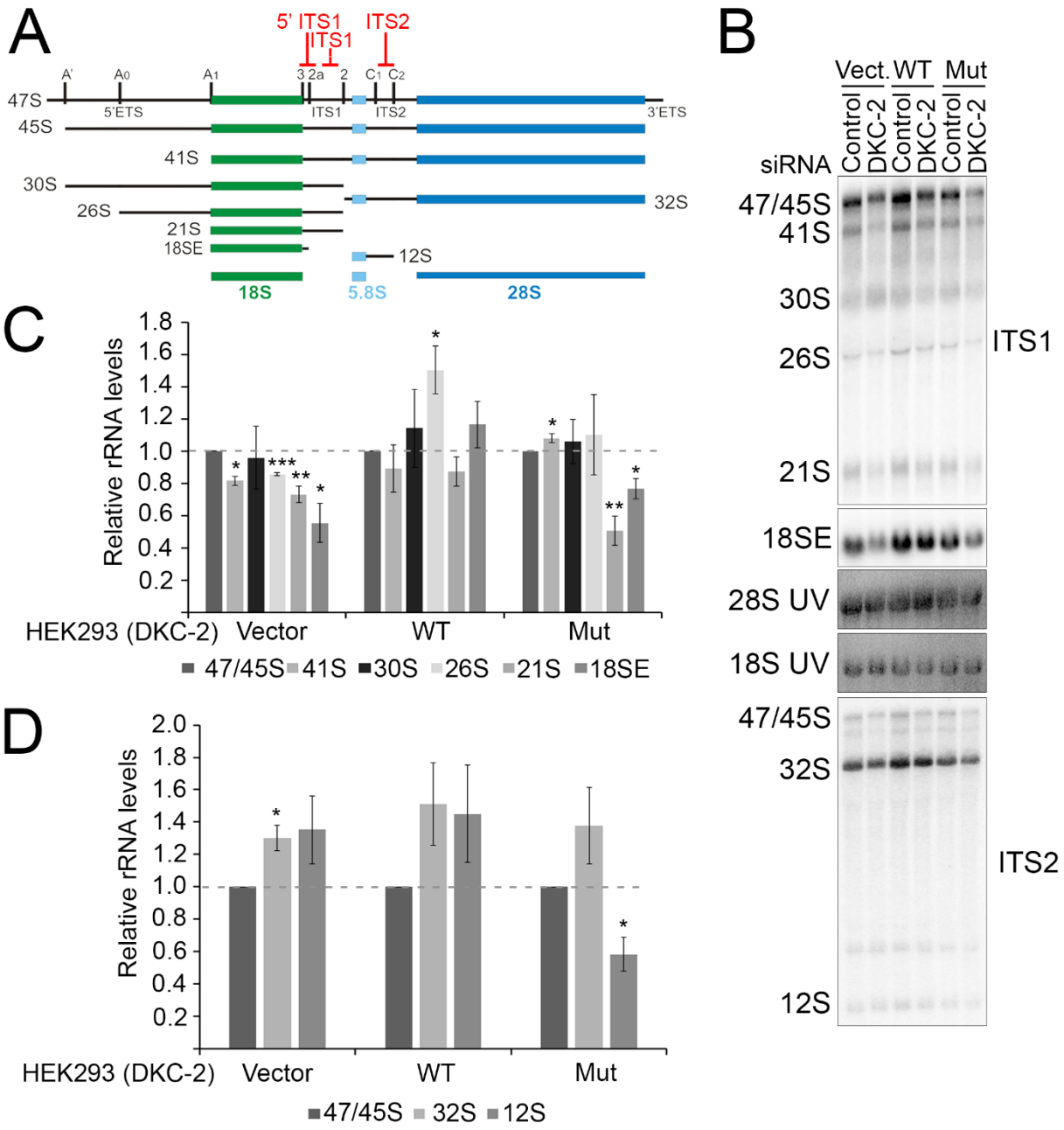

Figure legend on the next page.

Figure 3.12. Inactivation of the catalytic activity of Dyskerin results in LSU late processing defects. (A) Schematic representation of the rRNA precursors in humans. The SSU precursors and mature rRNA are shown in green and the LSU precursors and mature rRNA are shown in blue. The cleavage sites are shown at the top and the 5'ITS1, ITS1 and ITS2 sites recognized by the radiolabeled (^{32}P) probed are shown in red (Adapted from (Sloan et al., 2013c)) **(B)** Knockdowns using Control or Dyskerin (DKC-2) siRNAs were performed for 48h in HEK293T cells containing the empty pcDNA5 vector or expressing the RNAi resistant FLAG-tagged WT or D125A mutant Dyskerin. 100ng/µl or 1000ng/µl tetracycline was used for 48h in WT-expressing cells or pcDNA5 and D125A-expressing cells respectively. RNA was extracted from the cells and separated on a 1.2% glyoxal-agarose gel. The RNA was transferred on a Hybond N membrane and incubated with radiolabeled-(^{32}P)-oligo probes against ITS1, 5'ITS1 (18SE) or ITS2, as indicated on the right of each membrane. A phosphorimager was used for visualization of the rRNAs, and ethidium bromide staining of 28S rRNA (UV) was used as a loading control. **(C-D)** ImageQuant software was used for quantitation of the northern blots. The graphs represent the relative levels of the rRNAs as averages of three independent experimental repeats, which were normalized to the loading control (28S UV) and the control knockdown in each case. Further normalization of the rRNA precursor levels to the 47/45S rRNA precursor was performed. The error bars represent the standard error (+/-SEM) and statistical analysis took place using an unpaired t-test. Lack of significance values indicates significant differences as compared to the control and the dotted line represents the rRNA precursor levels in control cells. The vector values are the same as the ones presented on Figure 3.6D. *p value < 0.05, **p value < 0.01, ***p value < 0.001.

Knockdown of Dyskerin in HEK293T cells resulted in an accumulation of the 32S rRNA precursor, whereas the levels of 41S, 26S, 21S and 18SE rRNA precursors were significantly decreased (Figure 3.12, vector). The levels of the 41S, 21S and 18SE rRNA precursors were restored to normal in HEK293T expressing the RNAi resistant WT FLAG-tagged Dyskerin after Dyskerin knockdown (Figure 3.12B, C, WT). Furthermore, the levels of 30S rRNA remained unaffected after Dyskerin knockdown in these cells as compared to the control, whereas the levels of 26S rRNA precursor were slightly increased (Figure 3.12B, C, WT). Since no significant change was observed in the levels of 21S rRNA, it is unlikely that 26S rRNA accumulation is indicative of rRNA processing defects here. Expression of the RNAi resistant WT FLAG-tagged Dyskerin rescued the levels of the increased levels of 32S rRNA precursor after Dyskerin knockdown as compared to the control, whereas the levels of the 12S rRNA were not significantly altered (Figure 3.12 B, D, WT). These data indicated that expression of the RNAi resistant WT FLAG-tagged Dyskerin rescued the rRNA processing phenotype caused by Dyskerin knockdown in HEK293T cells.

Expression of the RNAi resistant D125A FLAG-tagged Dyskerin resulted in a very slight increase in 41S rRNA precursor levels after Dyskerin knockdown as compared

to the control, but no change was observed in the levels of 30S or 26S rRNA precursors (Figure 3.12B, C, Mut). Importantly, the levels of 21S and 18SE rRNAs were significantly decreased by approximately 50% and 30% respectively after Dyskerin knockdown in HEK293T cells expressing the RNAi resistant D125A FLAG-tagged Dyskerin as compared to the control (Figure 3.12B, C, Mut), as well as the levels of the 12S rRNA precursors, which were approximately 40% lower (Figure 3.12B, D, Mut panel). No significant difference was observed in the levels of 32S rRNA precursor after Dyskerin knockdown as compared to the control in HEK293T cells expressing the RNAi resistant D125A FLAG-tagged Dyskerin (Figure 3.12B, D, Mut panel). Taken together, these data indicate that inactivation of the catalytic activity of Dyskerin rescues the early rRNA processing defects observed when Dyskerin is knocked-down, but results in late rRNA processing defects.

I next used pulse-chase labelling to further characterize the effects of the catalytically inactive Dyskerin on rRNA production. HEK293T cells containing the empty pcDNA5 vector were used as a control and the endogenous protein was replaced by the WT or D125A mutant FLAG-tagged Dyskerin as previously. The cells were then incubated with phosphate-free media for 1h, followed by the addition of radiolabelled phosphate (^{32}P) for 1h. The cells were left to grow in normal media for 3h (chase) for detection of the newly-synthesized rRNAs. RNA was extracted, separated on an agarose gel and transferred on a Hybond N membrane. As seen previously (Figure 3.5), knockdown of Dyskerin in HEK293T cells containing the empty pcDNA5 vector resulted in a decrease in 47/45S and 32S rRNA precursors as well as a decrease in the newly-synthesized 28S and 18S rRNA after 3h of chase (Figure 3.13A, B, vector). Expression of the RNAi resistant WT FLAG-tagged Dyskerin after Dyskerin knockdown rescued the levels of the 47/45S and 32S rRNA precursors and the levels of the newly-synthesized 28S and 18S rRNAs as compared to the control knockdown in these cells after 3h (Figure 3.13A, B WT). A slight accumulation of the 47/45S rRNA precursor was observed after expression of the RNAi resistant WT FLAG-tagged Dyskerin (Figure 3.13A, B, WT), which might be due to experimental variation. Taken together, these data further support the previous data, showing that expression of the RNAi resistant WT FLAG-tagged Dyskerin rescues the rRNA processing phenotype caused by Dyskerin knockdown. It is worth noting that this experiment was only performed twice due to time limitations. However, since the levels of the H/ACA snoRNAs (Figure 3.11) and rRNA precursors (Figure 3.12) were rescued after expression of the RNAi resistant WT

FLAG-tagged Dyskerin in cells where Dyskerin was knocked down, I am confident that the RNAi rescue system worked as expected.

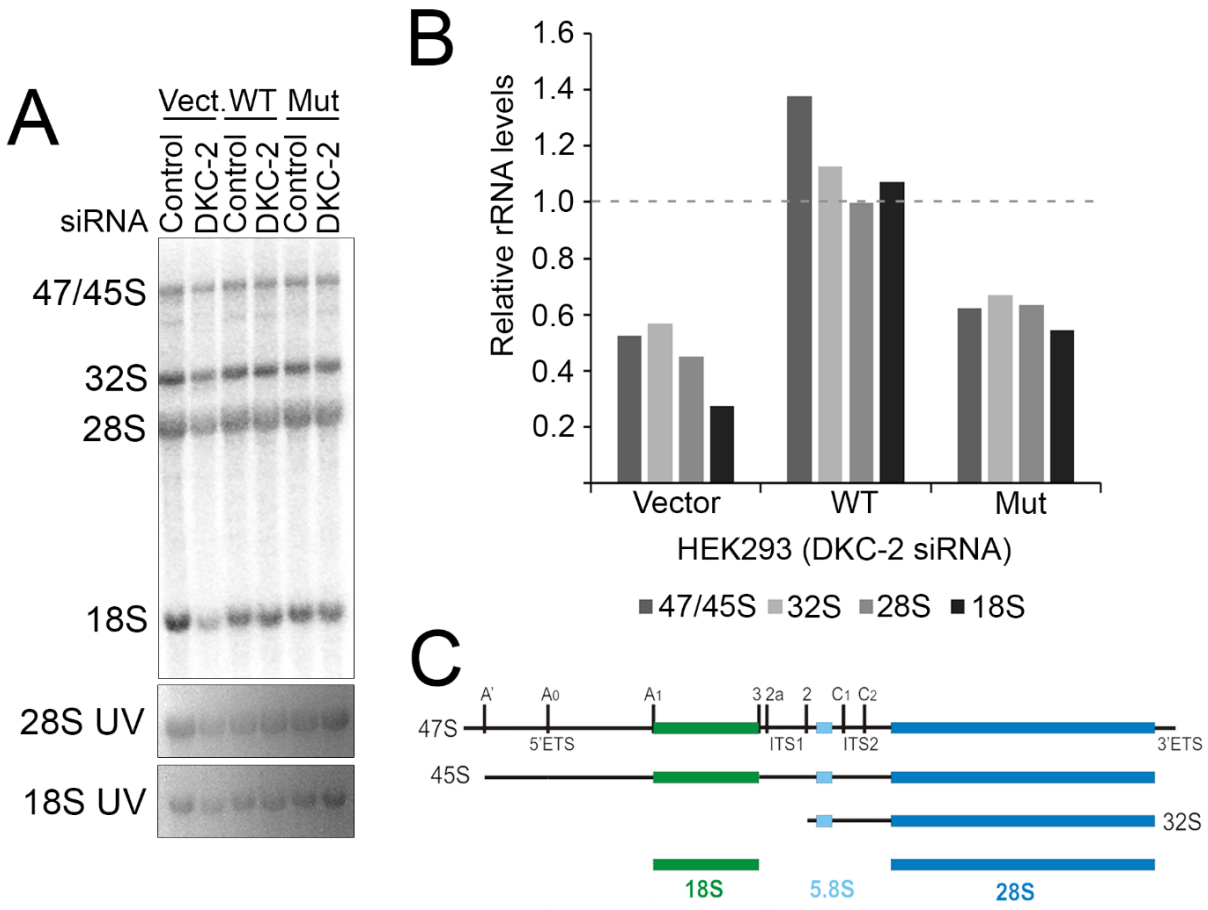

Figure 3.13. Inactivation of the catalytic activity of Dyskerin is likely to result in slower accumulation of the newly-synthesized LSU and SSU rRNAs. (A) Knockdowns using Control and Dyskerin (DKC-2) siRNAs were performed for 48h in HEK293T cells containing the empty pcDNA5 vector or expressing the RNAi resistant FLAG-tagged WT or D125A mutant Dyskerin using 100ng/µl or 1000ng/µl tetracycline respectively for 48h. 1000ng/µl tetracycline was used in pcDNA5-containing cells for 48h. During pulse chase labelling, phosphate depletion was performed followed by addition of radiolabelled phosphate (^{32}P) for 1h. The cells were left to grow under normal conditions for 3h (chase), before RNA was extracted and separated on a glyoxal-agarose gel. The RNA was transferred on a Hybond N membrane and visualized using a Phosphorimager. The 28S rRNA levels after ethidium bromide staining (UV) were used as a loading control. **(B)** ImageQuant software was used for quantitation of the Northern blots. The graph represents the relative rRNA levels of one experimental repeat after Dyskerin knockdown and normalization against the loading control (28S UV) and the control knockdown for each cell line. The dotted line represents the rRNA precursor levels in control cells. **(C)** Schematic representation of the rRNA processing precursors and mature rRNAs in humans. The cleavage sites are indicated on the top (Adapted from (Sloan et al., 2013c)).

Knockdown of Dyskerin in HEK293T cells expressing the RNAi resistant D125A mutant FLAG-tagged Dyskerin resulted in approximately 35% and 40% decrease in the levels of the 47/45S and 32S rRNA precursors respectively, and approximately 40% and 45%

decrease in the levels of the newly-synthesized 28S and 18S rRNAs respectively, as compared to the control knockdown after 3h of chase (Figure 3.13A, B, Mut). These data indicate that inactivation of the catalytic activity of Dyskerin causes a slower accumulation of the newly-synthesized rRNAs, which further supports the theory that it is required for late rRNA processing in humans.

3.2.7 Inactivation of the catalytic activity of Dyskerin does not activate p53

Cells expressing the D125A mutated FLAG-tagged Dyskerin showed a reduction in the accumulation of the 28S and 18S rRNAs (Figures 3.12, 3.13). Since ribosome biogenesis defects are known to activate the p53 tumour suppressor, I investigated whether inactivation of the catalytic activity of Dyskerin resulted in p53 accumulation. U2OS cells containing the empty pcDNA5 vector were used as a control and the endogenous protein was replaced by the WT or D125A mutant FLAG-tagged Dyskerin as previously. Whole cell extracts were loaded on an SDS-PAGE gel and analysed by Western blotting, using α-p53 and α-p21 antibodies. The p21 gene is a target of p53, indicating p53 activity, even though the p21 mRNA levels were not assessed as p21 can also be regulated post-translationally (Jung et al., 2010). Karyopherin was used as a loading control.

Knockdown of Dyskerin in U2OS cells containing the pcDNA5 vector resulted in a 2-fold increase in p53 levels as expected, due to defects in ribosome biogenesis. Furthermore, the levels of p21 were increased by approximately 3.5-fold, indicating an increase in p53 activity (Figure 3.14). Dyskerin knockdown in U2OS cells expressing the RNAi resistant WT FLAG-tagged Dyskerin did not result in a significant difference in p53 levels as compared to the control knockdown in these cells (Figure 3.14). However, there was an approximately 2-fold increase in p21 levels (Figure 3.14). This could be due to the fact that there is some over-expression of Dyskerin in U2OS cells, since the endogenous protein was still found at approximately 60%, as previously shown (Figure 3.10B). Dyskerin knockdown in cells expressing the RNAi resistant FLAG-tagged D125A mutant Dyskerin resulted in slightly lower p53 levels as compared to the control, and an increase in p21 levels (Figure 3.14). This p21 increase was similar to the one observed in U2OS cells expressing the RNAi resistant WT FLAG-tagged Dyskerin.

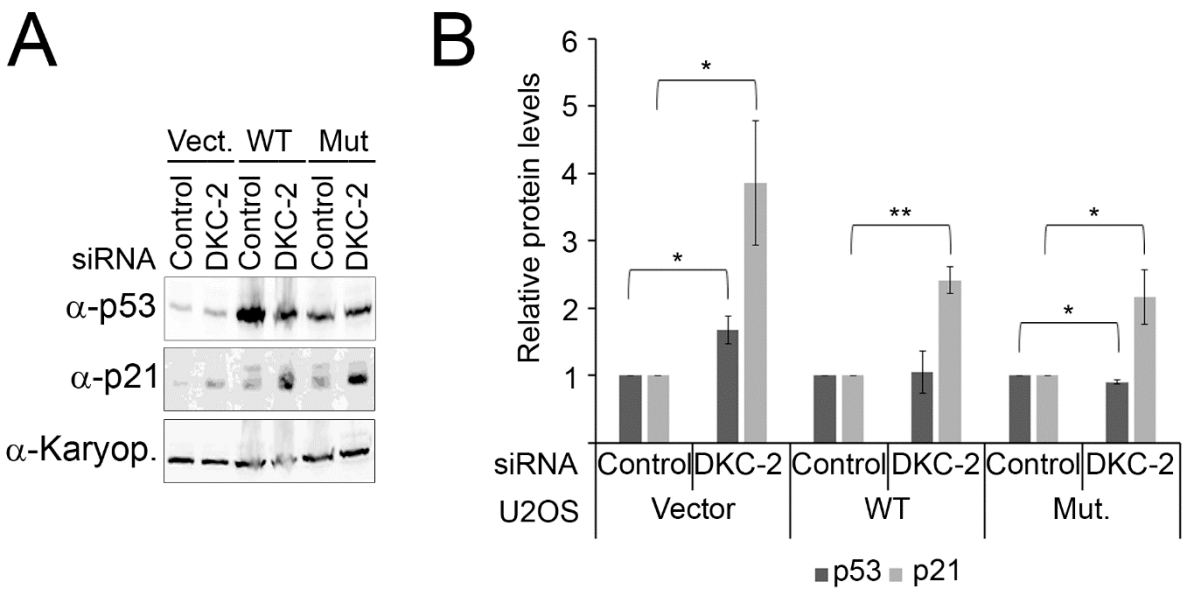

Figure 3.14. The catalytic activity of Dyskerin is not required for p53 accumulation in U2OS cells. Knockdowns using control or Dyskerin siRNAs (DKC-2) were performed in U2OS cells containing the pcDNA5 vector or expressing the RNAi resistant FLAG-tagged WT or the D125A mutant Dyskerin for 48h using 1000ng/µl tetracycline. **(A)** Whole cell extracts were loaded on an SDS-PAGE and analysed by Western Blotting, using the antibodies indicated on the left of the panel. Results were viewed using the LICOR system. Karyopherin (Karyop.) was used as a loading control. The antibodies used are indicated on the left of the panel. **(B)** Quantitation of Western Blots was performed using the ImageQuant Software. The graphs represent the average p53 and p21 protein levels from three experimental repeats and the error bars show the standard error (SEM). Statistical analysis was performed using an unpaired t-test. Absence of significance values indicates no significant differences. *p value < 0.05, **p value < 0.01.

It is worth noting that the p53 levels were consistently higher in U2OS cells expressing the RNAi resistant FLAG tagged WT or D125A mutant Dyskerin. However, the p21 levels were consistently low in control cells, resembling the levels of p21 in U2OS cells containing the pcDNA5 vector after control knockdowns. This indicated that there might be an induction in p53 levels in the cells expressing the RNAi resistant FLAG-tagged Dyskerin, but not p53 activity. Since p21 levels were not induced after control knockdowns, indicating that p53 activity was probably at normal levels, it is unlikely that p53 levels are saturated in these cells. Due to time constraints, it was not possible to explore this further (see Discussion). In conclusion, these results indicate that inactivation of the catalytic activity of Dyskerin does affect the levels of p53 in U2OS cells as compared to the WT Dyskerin.

3.3 Discussion

The H/ACA snoRNP, consisting of the pseudouridine synthase Dyskerin (Cbf5 in yeast), the core proteins NOP10, NHP2 and GAR1, and a snoRNA component, catalyses the pseudouridylation of the rRNA during ribosome biogenesis (Watkins and Bohnsack, 2011). Mutations in the gene encoding for Dyskerin have been found to cause X-linked Dyskeratosis Congenita (DC), a rare genetic disease characterized by bone marrow failure and tumour development (Mason and Bessler, 2011). The tumour suppressor p53 has been shown to be involved in the development of the majority of the clinical symptoms of DC in mouse (Ruggero et al., 2003, Ge et al., 2010b) and zebrafish (Ying Zhang et al., 2012) models. Ribosome biogenesis defects directly regulate the levels of p53 (Pelava et al., 2016) via inhibition of MDM2, the main suppressor of p53 through the 5S RNP. The 5S RNP is an LSU intermediate consisting of the ribosomal proteins RPL5, RPL11 and the 5S rRNA (Sloan et al., 2013a, Dai and Lu, 2004, Donati et al., 2013, Marechal et al., 1994, Nishimura et al., 2015). Despite the importance of Dyskerin in DC patients and, probably, in tumour development, not much is known about its function in humans. Therefore, the first part of this PhD aimed to investigate the roles of Dyskerin in human ribosome biogenesis and p53 regulation. I have shown that Dyskerin is required for rRNA processing for both large and small ribosomal subunit, and defects in ribosome biogenesis after Dyskerin knockdown caused p53 induction via the 5S RNP-MDM2 pathway. Interestingly, the catalytic activity of Dyskerin is not required for the accumulation of the H/ACA snoRNP in humans and it is likely to only be necessary for late stages of rRNA processing and potentially, rRNA stability. Finally, inactivation of the catalytic activity of Dyskerin indicated a slower accumulation of the newly-synthesized LSU and SSU rRNAs, but did not result in a change in p53 levels.

Here, were have established an RNAi rescue system in HEK293T and U2OS human cells, where the RNAi resistant WT or D125A mutant FLAG-tagged Dyskerin replaced the endogenous protein, in order to study the effects of the inactivation of the catalytic activity of Dyskerin. This system was quite efficient in HEK293T, where the endogenous Dyskerin was decreased by more than 90% after siRNA transfections in cells expressing the RNAi resistant WT or D125A mutant FLAG-tagged Dyskerin (Figure 3.10A). Furthermore, expression of the RNAi resistant WT FLAG-tagged Dyskerin resulted in a rescue of the rRNA processing defects observed after Dyskerin

knockdown (Figure 3.12). However, the RNAi rescue system was not as efficient in U2OS cells, since the endogenous protein was only decreased by 30-40% in cells expressing the RNAi resistant WT or D125A mutant FLAG-tagged Dyskerin (Figure 3.10B). This was only observed in some cases, since this decrease was often seen at 50-60%. It is unclear why there were differences in the endogenous Dyskerin levels in HEK293T and U2OS cells as other knockdowns that have been performed in the lab were equally efficient in both cell lines. The RNAi rescue system established in HEK293T cells could be also used for studying the effects of other Dyskerin mutants found in DC patients. For example, S121G (Knight et al., 1999) and R158W (Knight et al., 2001) mutants, found in the catalytic domain of Dyskerin, have been shown to lead to the development of X-linked DC and Hoyeraal-Hreidarsson syndrome, which is a more severe form of the disease (Ohga et al., 1997). It would be interesting to identify whether these mutations affect the accumulation of the H/ACA snoRNP or rRNA processing in humans similarly to the catalytic mutant D125A studied here, possibly revealing molecular mechanisms on the way DC progresses, which could potentially lead to the development of future therapies. However, since the endogenous protein is only replaced by 40% in U2OS cells expressing the RNAi resistant FLAG-tagged proteins, the use of the RNAi rescue system in these cells for studying the effects of other mutants on p53 levels is probably not feasible. It would be beneficial to search for another cell line to be used instead of U2OS for studying p53 involvement after expression of DC mutations, which might present with a better knockdown efficiency and expression of the RNAi resistant FLAG-tagged Dyskerin. For example, HCT-116 is a colorectal cancer cell line which expresses a wild-type p53, or A549 lung carcinoma cell line, which was used in previous studies for p53 function (Krzesniak et al., 2014, Fumagalli et al., 2012).

I have shown here that Dyskerin knockdown in human HEK293T cells results in a decrease in the levels of the U17, U64, U19 and U70 H/ACA snoRNAs (Figure 3.4), which was expected, since Cbf5 depletion in yeast was shown to cause a decrease in the H/ACA snoRNAs levels (Zebarjadian et al., 1999). Furthermore, these data agree with recent micro-array data showing that depletion of Dyskerin in mouse livers resulted in a decrease in the H/ACA snoRNA levels (Ge et al., 2010a). In yeast, it was shown that expression of the Cbf5 catalytic mutant (D65A) resulted in a decreased interaction of Cbf5 with the tested H/ACA snoRNAs and a decrease in H/ACA snoRNA levels (Zebarjadian et al., 1999). The snoRNAs affected included the snR10, which is

involved in 18S rRNA processing (Tollervey, 1987), snR31, which is involved in 18S rRNA pseudouridylation (Balakin et al., 1993), and snR8 (Ni et al., 1997) and snR37 (Ganot et al., 1997a), which are involved in 28S rRNA pseudouridylation. A similar pattern was observed in mouse embryonic fibroblast cells, where inactivation of the catalytic activity of Dyskerin resulted in a decrease in the levels of several H/ACA snoRNAs, including U17, U64 and U19 (Gu et al., 2013), which are involved in SSU rRNA processing (Enright et al., 1996), 28S rRNA pseudouridylation and processing (Ganot et al., 1997a) respectively. On the contrary, my data indicated that the catalytic activity of Dyskerin is not required for the accumulation of either U17, U64, U19 or U70 H/ACA snoRNAs in human HEK293T cells and the interaction of Dyskerin with the H/ACA snoRNAs is not likely to be affected by inactivation of its catalytic activity (Figure 3.11). These results indicate that Dyskerin, but not its catalytic activity, is likely to be required for the accumulation of the H/ACA snoRNP complex in humans, as opposed to previous yeast and mouse models. Furthermore, the establishment of the RNAi rescue system in HEK293T cells allowed us to analyse the role of pseudouridine formation on rRNA processing for the first time.

There are two types of H/ACA snoRNAs involved in processing or modification of the rRNA (Watkins and Bohnsack, 2011). The majority of the H/ACA snoRNAs bind to the substrate RNA by base complementarity, which is essential for both the positioning and modification of the rRNA substrate, and for bringing the complex to the appropriate conformation for catalysis (Henras et al., 2008). Examples of snoRNAs involved in rRNA modifications include the U64 H/ACA snoRNA, which is important for pseudouridylation of U4975 of the 28S rRNA, and the U66 H/ACA snoRNA guides the pseudouridylation of U119 of the 18S rRNA (Ganot et al., 1997a). The U17/E1 (snR30 in yeast) H/ACA snoRNA is required for the 18S rRNA processing in yeast (Morrissey and D.Tollervey, 1993) and in frog oocytes (Mishra and Eliceiri, 1997), and it is presumed that it has the same function in humans since it was found to directly interact with 18S rRNA precursors (Rimoldi et al., 1993). U17 is important for the early rRNA cleavage at A’ site (Enright et al., 1996) in mammals and contains a conserved pseudouridine loop, which is essential for its binding to the 18S rRNA on the eukaryotic-specific region ES6 (Atzorn et al., 2004, Fayet-Lebaron et al., 2009). This mechanism of action is unique to snR30 (Watkins and Bohnsack, 2011), as no other H/ACA snoRNAs have been found to function in the same mode yet. The snR10 H/ACA snoRNA is also involved in SSU rRNA processing in yeast (Tollervey, 1987),

where the 5' hairpin on the snR10 base pairs with the 5' ETS region of the 18S rRNA precursor (Liang et al., 2010). To date, no H/ACA snoRNAs were found to be important for LSU rRNA processing in either yeast or higher eukaryotes that resemble the mechanism of action of U17/snR30 or snR10. However, TB11Cs2C2 snoRNA in *Trypanosoma brucei*, a protozoan parasite, was suggested to have specific roles in LSU rRNA processing (Gupta et al., 2010) and bioinformatics analysis of the *Leishmania major* snoRNAs, another protozoan parasite, suggested that some snoRNAs might be involved in both LSU and SSU rRNA processing (Eliaz et al., 2015). For example, LM35Cs3C5 is a snoRNA that is specific to *Leishmania major* and is likely to be involved in LSU rRNA processing and SSU rRNA modification (Eliaz et al., 2015). My data suggest that there are H/ACA snoRNAs involved in LSU processing in humans, since absence of the catalytic activity of Dyskerin resulted in a significant decrease in 12S LSU rRNA precursor (Figure 3.12), while the H/ACA snoRNP still accumulated (Figure 3.11). However, the specific H/ACA snoRNAs involved in this are yet to be identified.

In yeast, the H/ACA snoRNP is essential for the early steps of small ribosomal subunit biogenesis (Lafontaine et al., 1998), and for modifications on both the LSU and SSU rRNAs (Torchet et al., 2005). On the contrary, in human HEK293T cells, I have shown that knockdown of Dyskerin results in defects in early stages of LSU and SSU rRNA processing (Figures 3.5, 3.6). Interestingly, no A' cleavage defects were observed after Dyskerin knockdown (Figure 3.6), even though the levels of the U17 H/ACA snoRNA were decreased (Figure 3.4). It was recently shown that A' cleavage can be bypassed naturally in cells, as this is an extra step in pre-rRNA processing in eukaryotes (Sloan et al., 2014). It is, therefore, possible that Dyskerin depletion does not result in rRNA defects because of the lack of A' cleavage because cleavage at A0 site occurs after the bypass of A' cleavage. Inactivation of the catalytic activity of Dyskerin in human cells resulted in late rRNA processing defects (Figure 3.12) and a slower accumulation of the newly-synthesized LSU and SSU rRNAs (Figure 3.13). These data agree with previously published results where mouse embryonic fibroblast (MEF) cells expressing the D125A mutant Dyskerin appeared with a delayed accumulation of the newly-synthesized 28S and 18S rRNA species and an accumulation of the precursor rRNAs (Gu et al., 2013). In this study, the authors have shown that the mature rRNAs produced were also very unstable, and the cell growth was significantly decreased in MEFs expressing the catalytically inactive Dyskerin (Gu et al., 2013). It is, therefore,

likely that the pseudouridines are required for rRNA stability rather than processing in humans. Furthermore, it is possible that the H/ACA snoRNP is involved in recruiting factors essential for ribosome biogenesis, since rRNA processing still occurs when the catalytic activity of Dyskerin is inactive.

Mutations on the catalytic domain of Dyskerin (TruB) were shown to cause X-linked DC and, in some cases, the development of Hoyeraal-Hreidarsson syndrome (Podlevsky et al., 2008). Since the catalytic activity of Dyskerin is likely to be involved in the function, but not the accumulation, of the H/ACA snoRNP in humans, it is possible that the clinical symptoms of DC arise due to the production of unstable rRNAs. It was previously suggested that inactivation of the catalytic activity of Dyskerin results in a slow growth of mouse embryonic fibroblast (MEF) cells and the production of unstable rRNAs (Gu et al., 2013). It is possible that mutations in the catalytic site of Dyskerin found in DC patients, such as S121G (Knight et al., 1999) or R158W (Knight et al., 2001), or other domains of Dyskerin (Podlevsky et al., 2008), might affect the function of the H/ACA snoRNP. Since Dyskerin binds the snoRNA, NOP10 and GAR1 (Watkins and Bohnsack, 2011), the mutations on Dyskerin could affect interactions with other processing factors, but it is more likely that the lack of pseudouridylation causes the observed defects. A high rate of ribosome biogenesis occurs during red blood cell development (Danilova and Gazda, 2015). Thus, a slower accumulation rate of mature rRNAs during embryogenesis could affect haematopoiesis, resulting in the anaemia seen in DC and other ribosomopathies, as well as the development of cancers, especially AML. It would be interesting to identify whether Dyskerin is involved in erythroid cell differentiation, causing the clinical symptoms of DC, perhaps by using an erythroid progenitor cell line, such as CD34+, which contains both hematopoietic and epithelial progenitor cell populations (Kuranda et al., 2011).

Ribosome biogenesis defects result in p53 induction via the 5S RNP-MDM2 pathway (Sloan et al., 2013a, Nishimura et al., 2015). Here, I have shown that Dyskerin knockdown results in a p53 accumulation via the 5S RNP-MDM2 pathway (Figure 3.7), which agrees with previous studies showing that reduction of Dyskerin levels resulted in the activation of p53 in zebrafish (Ying Zhang et al., 2012) and mouse models (Ge et al., 2010b, Gu et al., 2008). It is possible that the LSU and SSU rRNA defects observed after Dyskerin knockdown, likely due to low levels of the H/ACA snoRNPs, lead to the accumulation of the free 5S RNP in the nucleoplasm. As a result, the free

5S RNP binds MDM2, leading to its inactivation, resulting in p53 stabilization. If this is the case in DC patients, the 5S RNP or MDM2 could be used as a target for future therapeutic treatments to reduce p53 tumour suppressor levels in patients. Furthermore, inactivation of the catalytic activity of Dyskerin did not result in an alteration on p53 levels in U2OS cells (Figure 3.14), even though a block in rRNA processing occurred. Presumably, the 5S RNP can still be integrated in the LSU so that MDM2 binds and inhibits p53. Interestingly, the levels of p53 were elevated when the RNAi resistant FLAG-tagged WT Dyskerin was expressed in U2OS cells, but the levels of its downstream target p21 were found to be normal. Since p21 levels were not induced after control knockdowns, it is unlikely that p53 levels are saturated in these cells. Due to time constraints, it was not possible to explore this further. However, treatment with Actinomycin D (ActD) in U2OS cells expressing the RNAi resistant FLAG-tagged WT Dyskerin would be an important control in order to test whether p53 levels are induced as expected or whether p53 levels are saturated in these cells. ActD is an inhibitor of RNA polymerase I resulting in ribosome biogenesis block, and it is known to induce p53 levels and activity (Sloan et al., 2013a, Nishimura et al., 2015). It is also possible that Dyskerin over-expression might lead to p53 induction with a reduced activity. If this is the case, it would be important to identify whether this is due to other possible functions of Dyskerin in the cell, which are currently unknown, making Dyskerin a novel regulator of the p53 pathway in humans. It would be interesting to identify whether this is the case, probably by using other cell lines in order to identify whether this is a cell line-specific phenotype.

The H/ACA RNP pseudouridylates the snRNAs, a modification needed for pre-mRNA splicing, and it is involved in telomere maintenance, by promoting telomere stability (Meier, 2005). However, not much is known about the functions of the complex in these processes. The H/ACA scaRNPs are required for the pseudouridylation of the small nuclear (sn)RNA during splicing, including U1, U2, U4, U5 and U6 snRNAs (Reichow et al., 2007). For example, the U85 H/ACA scaRNA is involved in the pseudouridylation of U46 residue of the U2 snRNA (Jady and Kiss, 2001). The H/ACA scaRNPs are mainly localized in Cajal bodies in the nucleus since they contain a Cajal body localization sequence, called the CAB box (Richard et al., 2003), and they are bound by TCAB1, a Cajal-body chaperone protein (Stern et al., 2012). It would be interesting to identify the levels of the H/ACA scaRNAs in the cell after knockdown of Dyskerin or inactivation of its catalytic activity. Given that the H/ACA snoRNAs accumulate in the

presence of the catalytically inactive Dyskerin, it is hypothesized that the H/ACA scaRNAs would be stable. It would be interesting to determine whether the activity of specific snRNAs are affected after Dyskerin knockdown or inactivation of its catalytic activity. In mouse embryonic fibroblast (MEF) cells, it was shown that the catalytic activity of Dyskerin was only required for the accumulation of the H/ACA snoRNAs in the cell, but not for H/ACA scaRNAs or snRNAs (Gu et al., 2013). Apart from its importance to pre-mRNA splicing, the H/ACA snoRNP was found to be important for maintenance of the telomerase complex. The human telomerase RNA (hTERC) contains an H/ACA box-like domain on its 3' end (Mitchell et al., 1999), which is essential for its nuclear localization (Lukowiak et al., 2001). Furthermore, the H/ACA box-like domain of hTERC is important for interactions with the other H/ACA snoRNP components (Cohen et al., 2007) and for the recruitment of TCAB1 protein in the complex (Venteicher et al., 2009, Venteicher and Artandi, 2009). The presence of the H/ACA snoRNP complex was found to promote telomere maintenance and potentially assembly (Egan and Collins, 2012). Therefore, mutations in the gene encoding for Dyskerin found in DC patients, which presumably affect the accumulation and function of the H/ACA snoRNP in humans, might affect splicing and telomere maintenance as well as ribosome biogenesis. It is possible that these mutations may result in a slower accumulation of the H/ACA snoRNP complex in humans, leading to a decreased rate of snRNA pseudouridylation and, therefore, mRNA splicing, as well as telomere defects by affecting telomere stability.

There is still some debate on whether DC is caused by ribosome biogenesis defects or telomere maintenance defects, since telomere shortening is observed in all forms (Podlevsky et al., 2008). Studies on induced pluripotent stem (iPS) cells from X-linked DC patients have shown that telomere maintenance was severely defective, whilst the ribosome biogenesis pathway was mostly unaffected (Gu et al., 2015). However, other studies showed that Dyskerin reduction did not correlate to telomere maintenance or length in mouse or zebrafish models (Ge et al., 2010b, Gu et al., 2008, Ying Zhang et al., 2012) and the disease phenotype occurred before any telomere defects were visible in mice (Gu et al., 2008). Furthermore, a recent study has showed that Dyskerin was over-expressed in cell lines from neuroblastoma patients, and Dyskerin depletion resulted in p53-dependent cell cycle arrest due to ribosome biogenesis defects, but not telomere maintenance defects (O'Brien et al., 2016b). These studies support the theory that defects in ribosome biogenesis, rather than telomere defects, are more

likely to be responsible for the accumulation of p53 in DC patients. In patients where mutations on TERT or TERC are found, it is possible that the H/ACA snoRNP has normal functions in ribosome biogenesis pathway, and therefore telomere maintenance defects could be the primary cause of DC. The possibility that the DC phenotype results from both ribosome biogenesis and telomere maintenance defects if both pathways are affected cannot be excluded. Whether Dyskerin depletion affects telomere maintenance in humans, due to low accumulation of the H/ACA snoRNPs, remains to be seen. One possibility is that inactivation of Dyskerin could cause p53-dependent telomere maintenance defects after p53 induction due to ribosome biogenesis defects, leading to cell cycle arrest and apoptosis. Another possibility is that inactivation of Dyskerin would directly cause defects in telomere stability and maintenance, perhaps due to weaker interactions of the H/ACA snoRNP with the human telomerase complex, which would lead in a p53 induction via both ribosome biogenesis and telomere maintenance defects. Since U2OS cells do not express a wild type telomerase and use alternative lengthening of telomeres (ALT) to maintain telomere length, another human cell line has to be used for studying the involvement of Dyskerin in telomere maintenance and p53 induction, such as the human colorectal cancer cell line HCT-116.

In conclusion, in the past few years, it was shown that Dyskerin plays a key role in the development of the clinical symptoms of DC and carcinogenesis. However, most studies have been done in yeast, where Dyskerin appears to have different functions in ribosome biogenesis pathway. Here, I have showed that Dyskerin is required for both LSU and SSU rRNA processing, and inactivation of its catalytic activity is likely to result in a slower production of, perhaps, unstable rRNAs. Furthermore, I have shown that Dyskerin depletion causes p53 accumulation via the 5S RNP-MDM2 pathway in humans, possibly due to ribosome biogenesis defects, which is in agreement with previous studies in mouse and zebrafish models. It is clear that further investigation of the functions of Dyskerin in both ribosome biogenesis and p53 accumulation in humans is necessary for the development of novel therapeutic treatments for DC patients. Finally, it would be interesting to explore the roles of the 5S RNP in tumour development in DC patients, which could be used as a target for future targeted treatments, not only for DC, but for other ribosomopathies as well.

4. Chapter Four. Defects in large or small ribosomal subunit production result in p53 accumulation

4.1 Introduction

Ribosomes consist of two subunits: the large (60S; LSU) and the small (40S; SSU). In humans, the LSU contains the 28S, 5.8S and 5S rRNAs and approximately 46 ribosomal proteins, whereas the SSU contains the 18S rRNA and approximately 33 ribosomal proteins (Freed et al., 2010b). The 28S, 5.8S and 18S rRNAs are transcribed in the nucleolus as a single transcript (47S) by RNA polymerase I, and the mature rRNAs are produced after a series of cleavage and modification steps (Figure 4.1) (Gamalinda and Woolford, 2015). In contrast, the 5S rRNA is transcribed in the nucleoplasm by RNA polymerase III, and is bound by the ribosomal proteins RPL5 and RPL11, resulting in the formation of the mature 5S RNP (Gamalinda and Woolford, 2015), before being integrated in the LSU (Figure 4.1). Early steps of ribosome biogenesis take place in the nucleolus and the nucleoplasm, whereas subunit maturation is completed in the cytoplasm (Figure 4.1) (Gamalinda and Woolford, 2015).

The 47S rRNA precursor is cleaved at ITS1 for separation of the LSU and SSU rRNA precursors (Figure 4.1). A number of factors are involved in this cleavage step in humans, including the RNA-binding protein RRP5 and the ribosome biogenesis factors NOL12, BOP1 and RBM28 (Sloan et al., 2013c). Further processing of the 30S SSU rRNA precursor results in the formation of the 21S rRNA precursor, which is processed in the nucleoplasm, leading to the formation of the 18SE rRNA precursor (Figure 4.1). In turn, the 18SE rRNA precursor is exported to the cytoplasm (Henras et al., 2015) where it is further processed, by NOB1 endonuclease (Sloan et al., 2013c), producing the mature 18S rRNA (Figure 4.1). The 32S rRNA LSU rRNA precursor is processed in the nucleolus and nucleoplasm for the production of the mature 28S and 5.8S rRNAs (Figure 4.1) (Ansel et al., 2008). It is unclear whether the last stages of the pre-28S and pre-5.8S rRNA processing occur in the cytoplasm in humans, as it is in yeast (Thomson and Tollervey, 2010). It was originally thought that the biogenesis of LSU and SSU are two independent processes, but, in yeast, it was shown that the mature

LSU is required for the last stages of SSU rRNA precursor processing in the cytoplasm (Lebaron et al., 2012), suggesting that the two processes are likely to be linked.

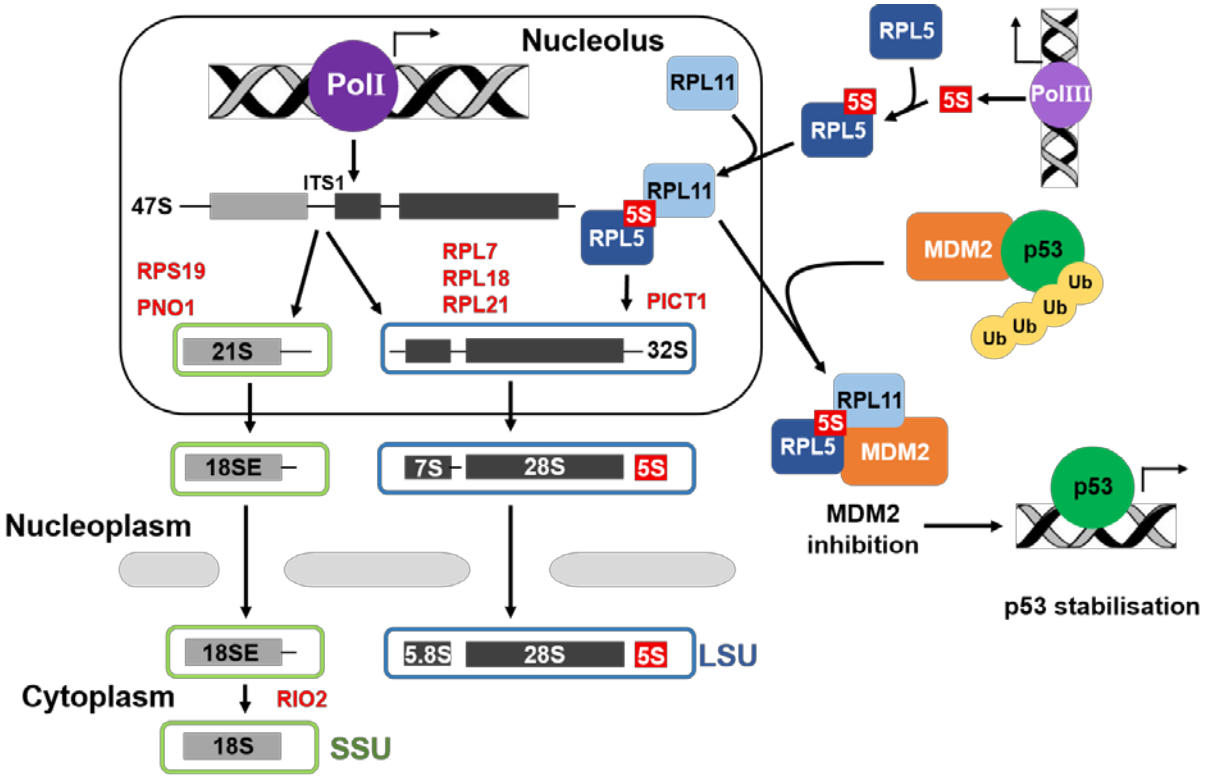

Figure 4.1. The ribosome biogenesis pathway and p53 induction via the 5S RNP-MDM2 pathway. Schematic representation of the small (SSU) and large (LSU) ribosomal subunit biogenesis pathway in humans. p53 induction via the 5S RNP-MDM2 pathway after ribosome biogenesis defects is shown. The stages where the ribosomal proteins (RSP19, RPL7, RPL18, RPL21) or ribosome biogenesis factors (PNO1, RIO2, PICT1), proteins focused on in this chapter, act are shown in red (Adapted from (Kressler et al., 2010)).

Ribosome biogenesis is directly linked with the levels of the tumour suppressor p53 in the cell (Figure 4.1) (Orsolic et al., 2015). p53 is a transcription factor, which, upon activation, causes the transcriptional activation of downstream targets involved in cell cycle arrest, metabolic changes, senescence and apoptosis (Brown et al., 2009). For example, p21 is a downstream target of p53 involved in cell cycle arrest (Karimian et al., 2016). The activation of p53 is controlled by various intracellular stimuli, such as DNA damage (Vogelstein et al., 2000), or extracellular stimuli, such as growth factors (Sherr and Weber, 2000). p53 is normally found in low levels in the cell, being targeted and inhibited for proteosomal degradation by the ubiquitin ligase MDM2, the main p53 suppressor (Wade et al., 2013). Defects in ribosome biogenesis cause the accumulation of the free 5S RNP in the nucleoplasm, which binds MDM2, inhibiting its activity, leading to p53 stabilisation (Figure 4.1) (Pelava et al., 2016). It is clear that LSU production defects lead to p53 induction via the 5S RNP-MDM2 pathway (Sloan

et al., 2013a, Donati et al., 2013, Nishimura et al., 2015), but there is minimal evidence of the mechanism by which SSU production defects lead to p53 induction.

A number of rare genetic diseases, called ribosomopathies, arise due to defects in ribosome production (Narla and Ebert, 2010), from mutations in genes encoding for ribosome biogenesis factors or ribosomal proteins (Yelick and Trainor, 2015). Most of the genes mutated in ribosomopathies encode for SSU ribosomal proteins or ribosome biogenesis factors (Narla and Ebert, 2010). The most well-studied ribosomopathies include Diamond-Blackfan Anaemia (DBA), 5q syndrome and Treacher-Collins (TC) syndrome (Table 4.1). DBA arises due to mutations in genes encoding for SSU ribosomal proteins, such as RPS19 and RPS24, or LSU ribosomal proteins, such as RPL5 and RPL11 (Lipton and Ellis, 2010). 5q syndrome arises due to mutations in the gene encoding for the SSU ribosomal protein RPS14 (Ebert et al., 2008b), whereas TC syndrome arises mainly due to mutations in the gene encoding for a ribosome biogenesis factor, TCOF1 (Weiner et al., 2012) (Table 4.2). The majority of ribosomopathies appear with common phenotypes, such as the development of macrocytic anaemia, craniofacial defects and, in most cases, increased cancer risk, especially for acute myeloid leukaemia (AML) (Yelick and Trainor, 2015). Interestingly, in mouse models of DBA the development of anaemia was found to be dependent on the 5S RNP-MDM2 interaction (Jaako et al., 2015) and RPS19 depletion in a DBA zebrafish model resulted in p53-dependent defective erythropoiesis (Danilova et al., 2008). In 5q syndrome mouse models, the development of anaemia due to haploinsufficiency of RPS14 was shown to be dependent on p53 (Table 4.2) (Schneider et al., 2016). Furthermore, depletion of either RPS14 or RPS19 in human erythroid progenitor cells resulted in p53 activation (Dutt et al., 2011). Moreover, the craniofacial defects observed in a mouse model where TCOF1 was mutated were also p53-dependent (Table 4.2) (Jones et al., 2008).

Ribosomopathy	Gene defect	Clinical manifestations	Cancer risk	p53 involvement
Diamond-Blackfan anaemia	RPS19, RPS24, RPS17, RPS7, RPS15, RPS27A, RPL36, RPL35A, RPL5, RPL11	Hypoplastic macrocytic anaemia Skeletal, urogenital and cardiac defects Short stature	AML MDS osteosarcoma	p53-dependent anaemia
5q syndrome	RPS14	Macrocytic anaemia	MDS AML	p53-dependent anaemia
Treacher-Collins Syndrome	TCOF1, POLR1C, POLR1D	Craniofacial anomalies Hearing difficulties	None reported	p53-dependent craniofacial defects

Table 4.1. The most well-known ribosomopathies. The genes mutated in each ribosomopathy, the clinical symptoms, the cancer risk and the involvement of p53 are shown in each case (Adapted from (Narla and Ebert, 2010).

The evidence from ribosomopathy animal models indicate that SSU production defects lead to p53 induction. Further confirming this, depletion of other SSU ribosomal proteins, apart from the ones involved in ribosomopathies, was also shown to cause p53 induction. For instance, RPS6 inactivation in mice resulted in the development of p53-dependent anaemia and other erythropoiesis defects (McGowan et al., 2011), and knockdowns of RPS6 or RPS7 in human cells resulted in p53 induction (Fumagalli et al., 2012). These studies raised the question on how defects on SSU production result in p53 induction. A few papers have reported that this is a result of binding of the 5S RNP on MDM2 (Fumagalli et al., 2009, Fumagalli et al., 2012, Golomb et al., 2014). If this is the case, it is unclear how defects on the SSU production feedback to the recruitment of the 5S RNP in the LSU, leading to p53 accumulation.

It was proposed that there are two different pathways leading to p53 induction after either LSU or SSU defects (Figure 4.2) (Fumagalli et al., 2012). LSU defects directly lead to the accumulation of the free 5S RNP in in the nucleoplasm, resulting in its binding and inhibition of MDM2, and p53 induction (Figure 4.2) (Fumagalli et al., 2012), as previously suggested (Sloan et al., 2013a). The authors have proposed that defects in SSU biogenesis lead to low levels of the mature SSU, which results in changes in the translation dynamics in the cell. This leads to the up-regulation of the translation of ribosomal proteins, such as RPL11 (Figure 4.2) (Fumagalli et al., 2012). This is proposed to result in the production of more 5S RNP, which binds MDM2 and inhibits MDM2 (Figure 4.2). For either LSU- or SSU-mediated p53 accumulation, it has been proposed that p53 induction leads to G1 cell cycle arrest (Fumagalli et al., 2012).

However, when both the LSU and the SSU biogenesis are co-impaired, it was predicted that there was both an up-regulation on 5S RNP production and a block in 5S RNP integration into the LSU, leading to p53 supra-induction due to the two pathways being affected (Figure 4.2). This resulted in a stronger p53 response and both G1 and G2/M cell cycle arrest (Fumagalli et al., 2012).

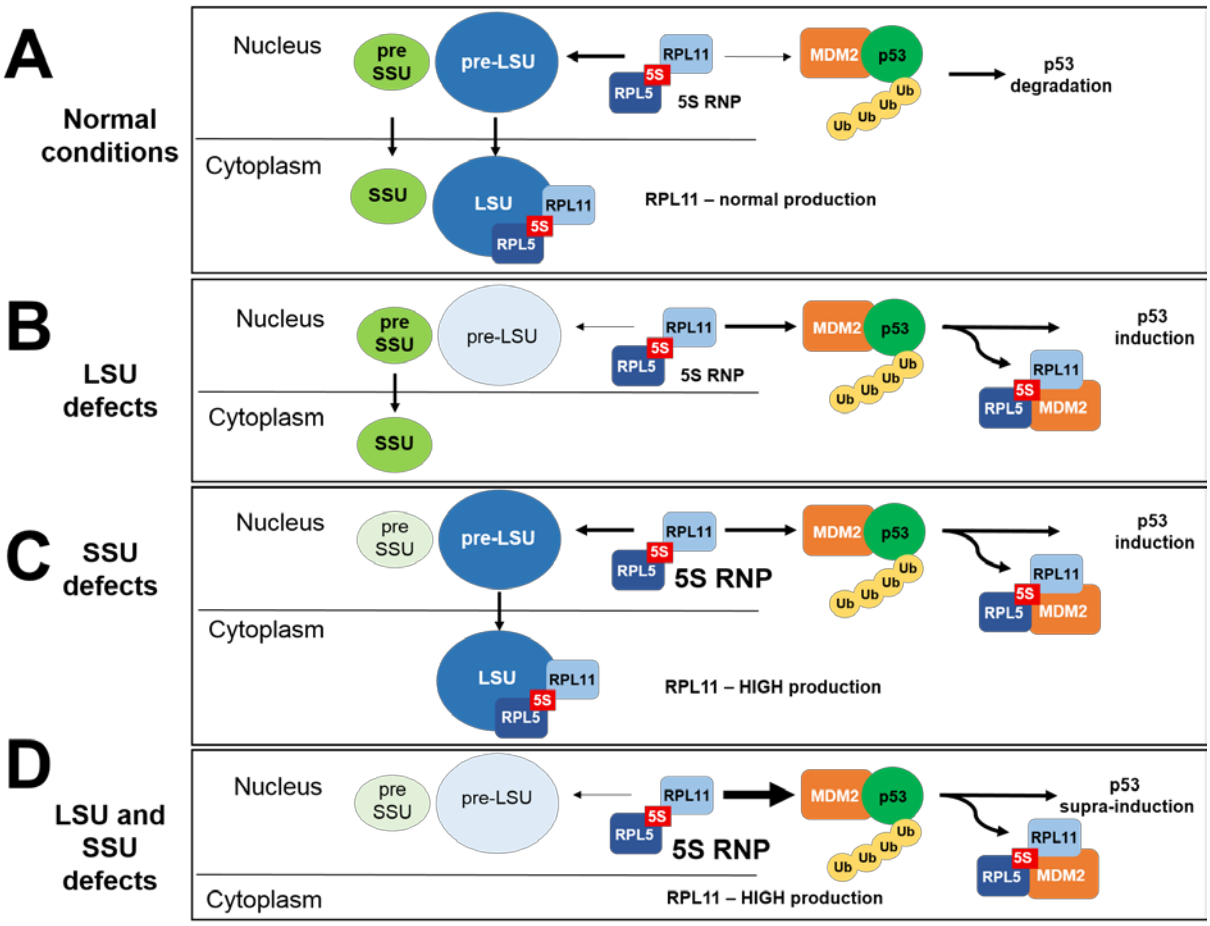

Figure 4.2. Schematic representation of the proposed model for the regulation of p53 after ribosome biogenesis defects. Large ribosomal subunit (LSU) defects lead to the accumulation of the free 5S RNP, which binds MDM2 resulting in p53 induction. Small ribosomal subunit (SSU) defects lead to the upregulation of ribosomal protein production, resulting in the increased production of the 5S RNP, which binds both the LSU and MDM2, leading to p53 induction. Defects on both the LSU and SSU lead to the upregulation of ribosomal protein production and the accumulation of the increased 5S RNP produced, which only binds MDM2, resulting in p53 supra-induction (Adapted from: (Fumagalli et al., 2012)).

Even though a number of studies have investigated how defects in early, nucleolar stages of ribosome biogenesis, result in p53 induction, not much is known about how p53 levels are affected when later rRNA processing stages are affected. Furthermore, the pathway in which defects in SSU lead to p53 accumulation via the 5S RNP-MDM2 is far from clear. Therefore, in this part of the PhD, I aimed to investigate:

- Whether defects in early or late stages of the LSU or SSU biogenesis lead to p53 accumulation via the 5S RNP-MDM2 pathway
- Whether p53 is induced because of ribosome production defects or a reduction in ribosomes
- Whether SSU biogenesis defects lead to LSU production defects and activation of p53 through the 5S RNP-MDM2 pathway

4.2 Results

4.2.1 Identification of targets to analyse ribosome biogenesis defects

I firstly wanted to study whether defects in different stages of LSU or SSU production lead to p53 induction. For this, the ribosomal protein RPS19 and the ribosome biogenesis factors PNO1 and RIO2 proteins were studied for SSU rRNA processing, and the ribosomal proteins RPL7, RPL18, RPL21 and the ribosome biogenesis factor PICT1 were studied for LSU rRNA processing. siRNA-mediated knockdowns, targeting these proteins, were performed in human osteosarcoma U2OS cells for 48h. In order to establish knockdown efficiency, the whole cell extract was loaded on an SDS-PAGE gel and analysed by Western Blotting (Figure 4.3) using the corresponding antibodies. In the case of RPL21, where there was no available antibody in the lab, RT-PCR was performed after RNA was extracted from the cells (Figure 4.3). A reduction in protein levels was seen for all knockdowns, ranging from 60% (RPL5, Chapter 3) to 80% (RPS19, RIO2, PICT1) reduction (Figure 4.3A, B). Furthermore, the mRNA levels of RPL21 after knockdowns were approximately 95% decreased (Figure 4.3C), indicating that the protein levels were probably low after the knockdown.

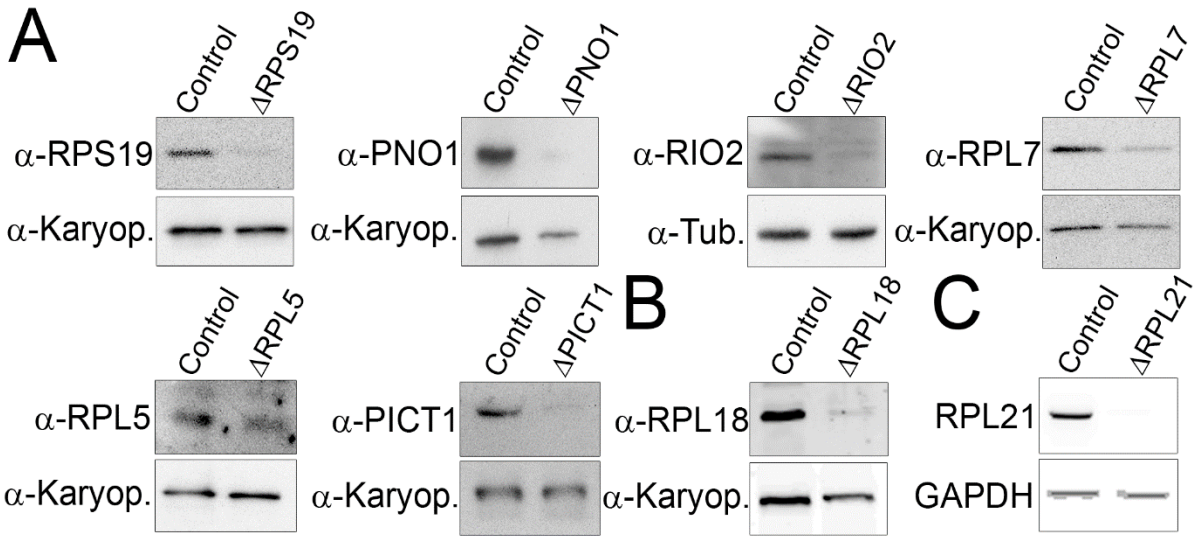

Figure 4.3. The chosen proteins were efficiently knocked down in U2OS cells. Knockdowns were performed in U2OS cells for 48h. **(A-B)** The whole cell extract was loaded on an SDS PAGE gel and analysed by Western Blotting using the corresponding antibodies (shown on the left). α-Tubulin (Tub.) and α-Karyopherin (Karyop.) were used as loading controls. Western Blots were visualized using ECL **(A)** or the LICOR system **(B)**. **(C)** RNA was extracted from the cells and RT-PCR was performed. The samples were loaded on a 2% agarose/1X TBE gel and visualized using a Typhoon Phosphorimager. Primers specific for RPL21 or GAPDH (loading control) were used for detection of the mRNA (shown on the left).

I next addressed whether the knockdown of these proteins resulted in rRNA processing defects. As I was particularly interested in SSU defects, I wanted to identify the specific stages of SSU production that RPS19, PNO1 and RIO2 are involved in U2OS cells. RPL5, PICT1 (Sloan et al., 2013a), RPL7, RPL18 and RPL21 (Loren Gibson, Nick Watkins, personal communication) knockdowns all resulted in 28S rRNA processing defects. Knockdowns of RPS19, PNO1 or RIO2 were performed in U2OS cells for 48h, the RNA was extracted and loaded on a glyoxal-agarose gel before transferred to a Hybond N membrane. Incubation of the membrane with a radio-labelled (^{32}P) probe specific for the 5'-ITS1 (Figure 4.4A) was performed, and the RNAs were visualized using a Typhoon Phosphorimager (Figure 4.4B). Knockdown of RPS19 resulted in a major accumulation of the 21S rRNA precursor and a decrease of the 18SE rRNA precursor levels as compared to the control (Figure 4.4B). Furthermore, an accumulation of the 21SC rRNA precursor was observed, no differences were observed in the levels of 47/45S or 41S precursors, and the levels of 30S and 26S rRNA precursors were slightly decreased (Figure 4.4B). Knockdown of RIO2 did not result in a significant change in the levels of the 47/41S, 41S, 30S or 26S rRNA precursors as compared to the control, but it caused a slight decrease in the levels of 21S rRNA precursor and an accumulation of the 18SE rRNA precursor (Figure 4.4B). Finally, knockdown of PNO1 resulted in an accumulation of the 47/45S, 41S and 30S rRNA precursors, and to an ever greater accumulation of the 26S rRNA precursor as compared to the control. The levels of 21S and 18SE rRNA precursors were slightly decreased and there was an accumulation of the 21SC rRNA precursor (Figure 4.4B). Taken together, these data showed that RPS19, PNO1 and RIO2 knockdowns resulted in the expected rRNA processing phenotype in U2OS cells as previously shown in other cell lines (Choesmel et al., 2007, Vanrobays et al., 2004, Geerlings et al., 2003), further confirming the efficiency of the knockdowns.

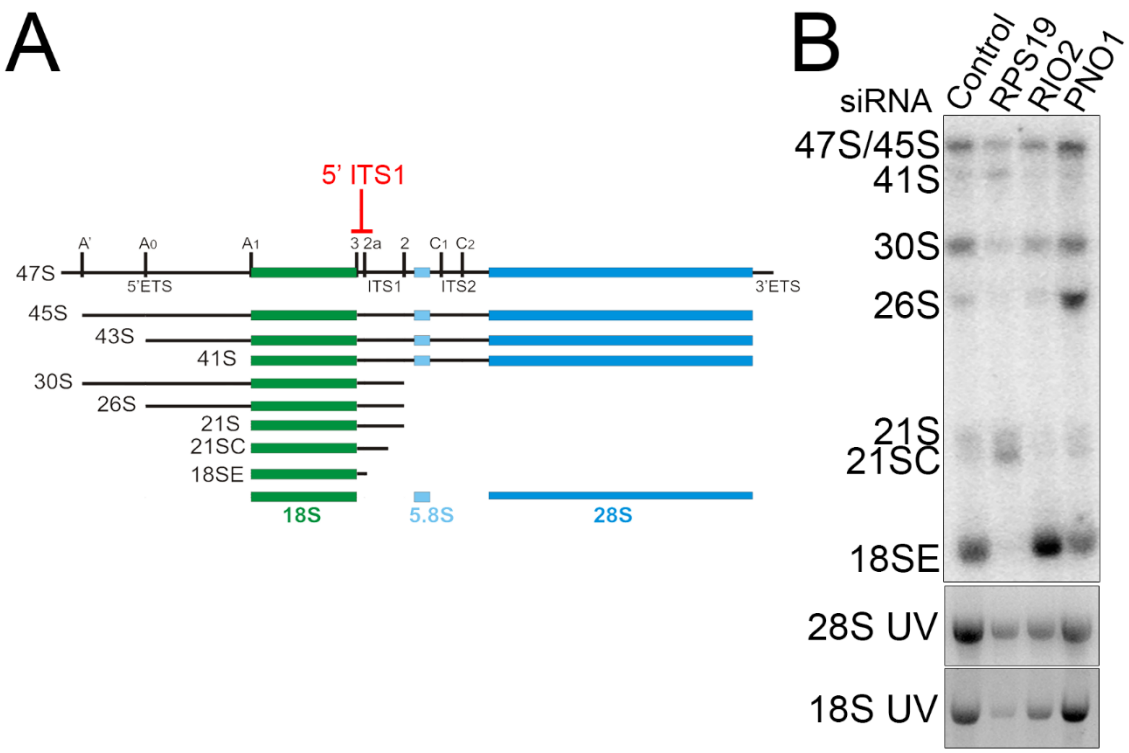

Figure 4.4. RPS19, PNO1 and RIO2 knockdowns result in SSU rRNA processing defects. (A) Schematic representation of the human ribosome biogenesis pathway. The LSU precursor and mature rRNA are shown in blue, and the SSU precursor and mature rRNA are shown in green. The 5'-ITS1 site recognized by the radiolabelled (^{32}P) probe is indicated in red (Adapted from (Sloan et al., 2013c)). **(B)** Knockdowns were performed for 48h in U2OS cells before the RNA was extracted and loaded on a 1.2% agarose-glyoxal gel. The RNA was transferred on a Hybond N membrane, incubated with radiolabelled (^{32}P) probe specific for the 5'-ITS1 site and visualized using a Typhoon Phosphorimager. The ethidium bromide staining (UV) of the 28S rRNA was used as a loading control.

4.2.2 Defects in different stages of LSU or SSU production lead to p53 induction via the 5S RNP-MDM2 pathway

Defects in either LSU (Sloan et al., 2013a, Donati et al., 2013) or SSU (Fumagalli et al., 2012) biogenesis were shown to cause p53 accumulation via the 5S RNP-MDM2 pathway. I, therefore, wanted to investigate whether p53 was induced after inhibition of different stages of rRNA processing. Knockdowns were performed in U2OS cells for 48h and the whole cell extract was loaded on an SDS-PAGE gel before analysed by Western Blotting using antibodies for p53 or its downstream target p21, indicating p53 activity (Figure 4.5), even though other downstream targets of p53 were not examined. It is worth noting that p21 mRNA levels were not examined here due to time constraints, as p21 is regulated post-translationally as well (Jung et al., 2010). RPS19, RPL7, RPL18 and RPL21 are found in the nucleolus and the cytoplasm, PNO1 mainly

functions in the nucleoplasm and RIO2 is found in both the nucleoplasm and cytoplasm.

Either RPS19 or RIO2 knockdown resulted in a significant induction in p53 levels as compared to the control (Figure 4.5A, B). Furthermore, the levels of p21 also increased when RPS19 or RIO2 were knocked down (Figure 4.5A), indicating an increase in p53 activity. Since all three components of the 5S RNP are required for its binding on MDM2 (Sloan et al., 2013a), RPL5 knockdown was performed in order to investigate whether this p53 accumulation was mediated by the 5S RNP-MDM2 pathway. RPL5 knockdown alone did not result in a significant change in p53 or p21 levels as compared to the control (Figure 4.5A, B). Note that the efficiency of the double knockdowns on the target levels was not examined due to time constraints and, therefore, a slight variation in the knockdown efficiency might have occurred. Double knockdown of RPL5 and RPS19 resulted in a rescue of the p53 levels as compared to the RPS19 knockdown (Figure 4.5A, B). The same was observed when RIO2 and RPL5 were knocked down as compared to the RIO2 knockdown (Figure 4.5A, B). Finally, the levels of p21 were also decreased when double knockdowns of RPS19 or RIO2 with RPL5 were performed (Figure 4.5A), indicating a rescue in p53 activity. These results indicated that inhibition of SSU production in either early, nuclear steps, as seen by RPS19 knockdown, or late, cytoplasmic steps, as seen by RIO2 knockdown, resulted in p53 induction via the 5S RNP-MDM2 pathway.

Either RPL7, RPL18 or PICT1 knockdown resulted in a significant increase in p53 levels (Figure 4.5A, B). Furthermore, knockdowns of RPL7, RPL18 or PICT1 resulted in a p21 increase, indicating an increase in p53 activity as well (Figure 4.5A). In order to investigate whether this increase in p53 levels and activity was due to the 5S RNP-MDM2 pathway, double knockdowns of RPL7, RPL18 or PICT1 with RPL5 were performed (Figure 4.5). As previously, knockdown of RPL5 did not result in a significant change in p53 or p21 levels as compared to the control (Figure 4.5A, B). Double knockdown of RPL5 with RPL7, RPL18 or PICT1 resulted in a significant decrease on p53 levels as compared to the single knockdowns of these proteins (Figure 4.5A, B). Furthermore, the p21 levels were also decreased when double knockdowns with RPL5 were performed, showing that both p53 levels and activity were rescued. These results indicated that defects in early or late stages of LSU biogenesis result in p53 induction

via the 5S RNP-MDM2 pathway, further confirming previous studies (Sloan et al., 2013c, Golomb et al., 2014)

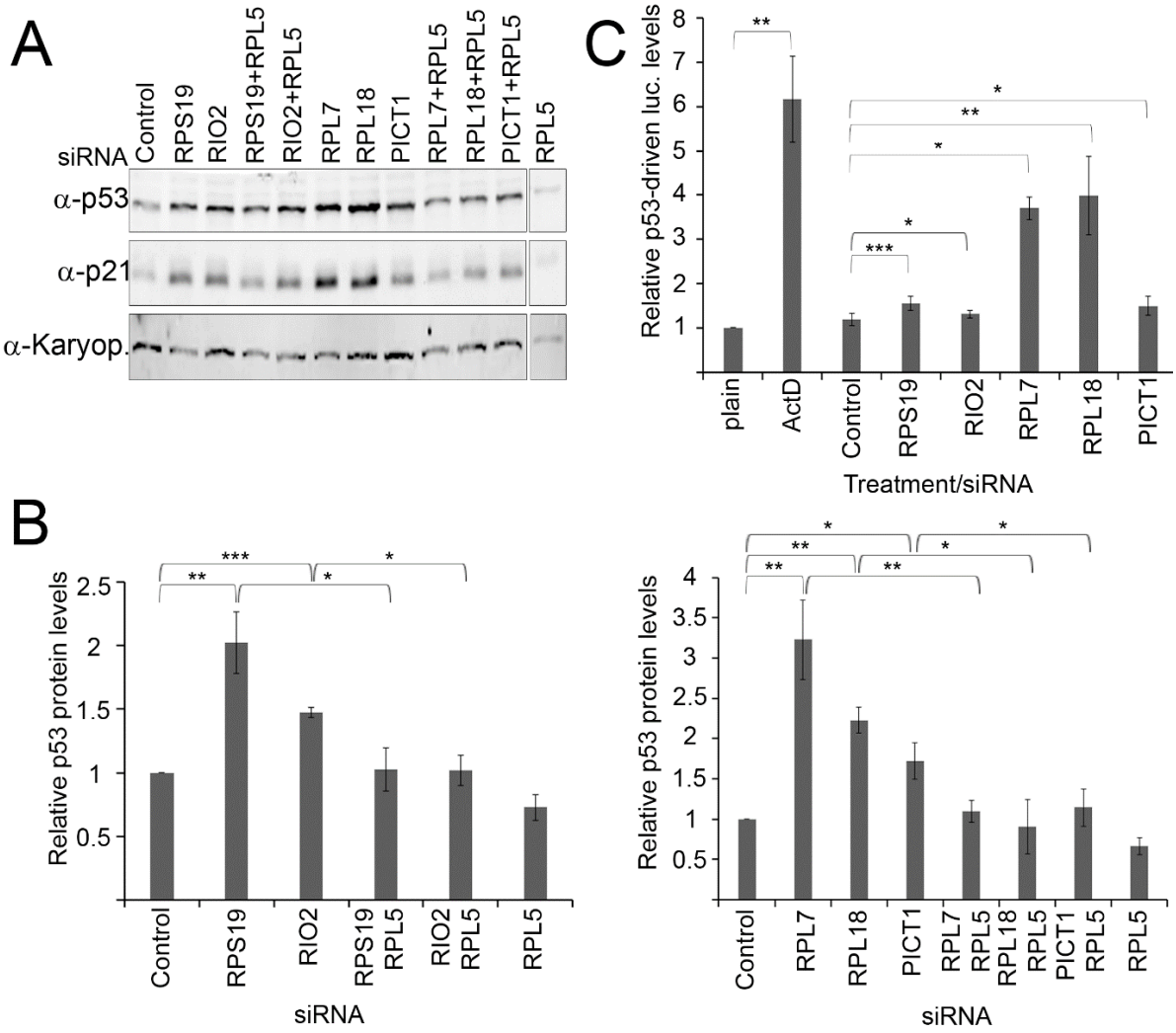

Figure 4.5. Defects on different stages of SSU or LSU production lead to p53 accumulation via the 5S RNP-MDM2 pathway. (A) Knockdowns were performed for 48h in U2OS cells and the whole cell extract was loaded on an SDS-PAGE gel, followed by Western blot analysis using the LICOR system. The antibodies used are shown on the left and Karyopherin (Karyop.) was used as a loading control. **(B)** ImageQuant software was used for quantitation of the p53 levels of the Western Blot membranes, which were normalised against the loading control values (α-Karyopherin). The graphs represent the average p53 protein levels of three experimental repeats and the error bars show the standard error (+/-SEM). Statistical analysis was performed using unpaired t-test. **(C)** Knockdowns were performed for 48h in U2OS cells expressing p53-driven luciferase. ActD treatment was performed for 18h and untreated cells are presented as "plain". The p53-driven luciferase levels were analysed using a luminometer and cell numbers were measured using a Bradford assay. The luciferase values were normalized against the Bradford assay values. The graph shows the average luciferase intensity of three experimental repeats and the error bars represent the standard error (+/-SEM). Statistical analysis was performed using an unpaired t-test and absence of significance values indicates no significant differences as compared to the control. *p value<0.05, **p value<0.01, ***p value<0.0001.

In order to directly address the levels of p53 activity, knockdowns were also performed in U2OS cells expressing luciferase, regulated by a p53-promoter. The luciferase levels were analysed using a Luminometer (Figure 4.5C). Overnight treatment with Actinomycin D was used as a positive control, since it is a known ribosome biogenesis inhibitor that blocks RNA polymerase I, which leads to p53 induction via the 5S RNP-MDM2 pathway (Sloan et al., 2013a). Indeed, the p53-driven luciferase levels were significantly induced after ActD treatment as compared to the plain, untreated cells (Figure 4.5C). RPS19 or RIO2 knockdowns resulted in a small, but significant increase in the p53-driven luciferase levels (Figure 4.5C) in comparison to the control knockdown. A significant increase in p53-driven luciferase levels was also observed after RPL7, RPL18 or PICT1 knockdowns (Figure 4.4D). These results indicated that defects in early or late stages of SSU or LSU production lead to an increase in both p53 levels and activity. In summary, these results showed that defects in early or late stages of either LSU or SSU production lead to p53 accumulation via the 5S RNP-MDM2 pathway.

4.2.3 Defects on different stages of LSU or SSU production have different effects on cell cycle

It was recently reported that p53 activation after defects in either LSU or SSU production led to G1 cell cycle arrest (Fumagalli et al., 2012). Since p53 was induced after defects in different stages of human ribosome biogenesis, I wanted to investigate how the cell cycle might have been affected. Knockdowns were performed for 48h in U2OS cells or treated with ActD for 18h. ActD treatment was used as a positive control, since it was previously shown to result in G1 and G2/M cell cycle arrest (Fumagalli et al., 2012). The cells were fixed in 70% ethanol and the DNA was stained using propidium iodide. The cell cycle analysis was performed using the FACS Canto II flow-cytometer and software.

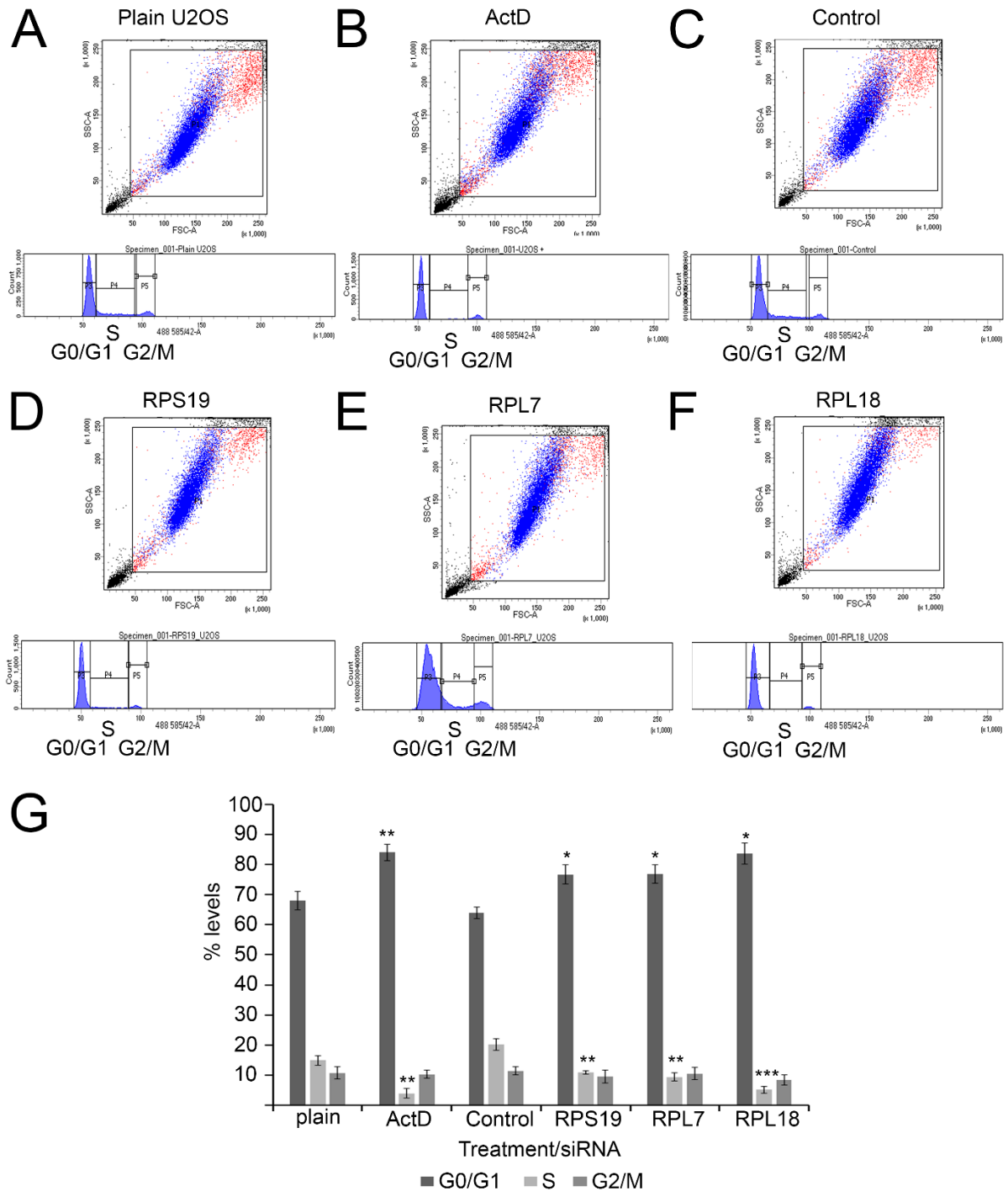

Figure 4.6. SSU or LSU defects result in G1 and a slight G2/M cell cycle arrest in U2OS cells. (A-F) ActD treatment was performed overnight, whereas knockdowns (control, RPS19, RPL7 and RPL18) were performed for 48h in U2OS cells. The cells were fixed using 70% ethanol and DNA was stained using propidium iodide. Cell cycle analysis was performed using the FACS Canto II flow cytometer and software. **(G)** The graph represents the average percentage levels of G1/G0 (dark grey), S (light grey) or G2/M (grey) phase of three experimental repeats. The error bars represent the standard error (+/-SEM) and statistical analysis was performed using an unpaired t-test. Comparison of significance was performed against the plain U2OS cells for ActD or against the control knockdown for RPS19, RPL7, RPL18 knockdowns. Absence of significance values indicates no significant differences to the control. *p value<0.05, **p value<0.01, ***p value<0.0001.

Firstly, I investigated the effects of the ribosomal protein knockdowns on cell cycle. ActD treatment, as compared with the non-treated (plain) U2OS cells, resulted in a significant G1 cell cycle arrest and a significant reduction in S phase, showing a G2/M arrest, even though the levels of G2 phase were not significantly altered (Figure 4.6A, B, G). Knockdowns of either RPS19, RPL7 or RPL18 all resulted in a significant increase in G1 phase and a significant decrease in S phase (Figure 4.6). Even though the levels of G2/M phase were not significantly changed, these results indicate that p53 induction after RPS19, RPL7 or RPL18 knockdown results in a significant G1 and a mild G2/M cell cycle arrest, presumably due to p53 induction. This phenotype is similar to the one observed after ActD treatment, but the cell cycle arrest after ribosomal protein knockdowns RPS19 and RPL7 is not as strong as the cell cycle arrest observed after ActD treatment. This is consistent with the fact that ActD treatment resulted in a bigger increase in p53 activity than the ribosomal protein knockdowns.

Additionally, I investigated the effects of knockdowns of the SSU and LSU ribosome biogenesis factors RIO2 and PICT1 on cell cycle regulation. As previously seen, ActD treatment resulted in a significant increase in G1 levels and a significant decrease in S phase levels, but not in a significant G2 phase levels change as compared with the non-treated (plain) U2OS cells (Figure 4.7A, B, F). Neither RIO2 nor PICT1 knockdowns resulted in a significant change in either G1, S or G2/M phase in cell cycle (Figure 4.7). These results showed that knockdown of RIO2 or PICT1 ribosome biogenesis factors did not result in cell cycle arrest, even though p53 was significantly induced in both cases, although to a lesser extent than the p53 induction observed after ribosomal protein knockdowns (see discussion).

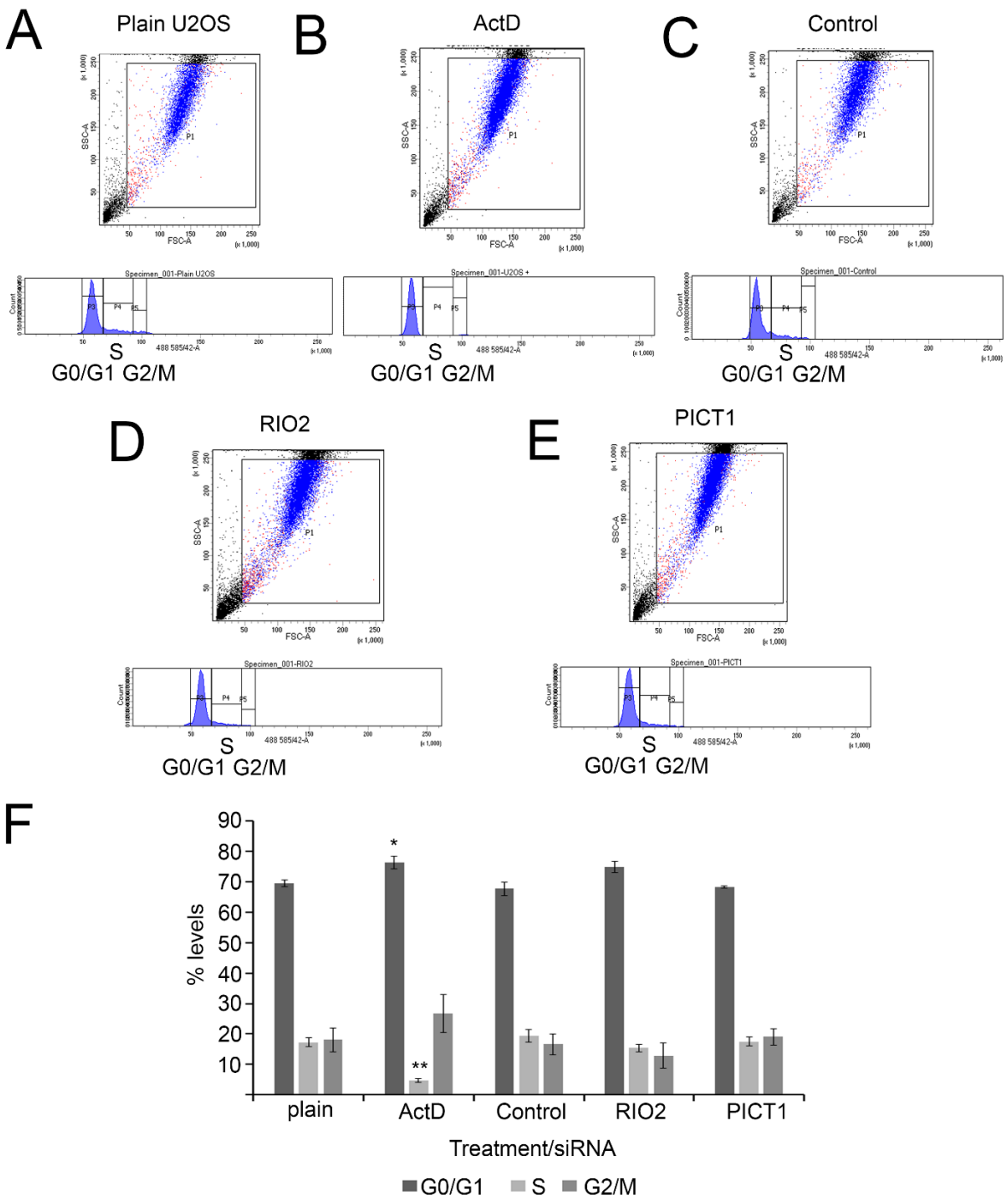

Figure 4.7. Knockdowns of RIO2 or PICT1 do not affect the cell cycle in U2OS cells. (A-E) ActD treatment was performed overnight, whereas knockdowns using siRNAs against control, RIO2 or PICT1 were performed for 48h in U2OS, before being fixed using 70% ethanol. The DNA was stained using propidium iodide and the cell cycle was analysed using the FACS Canto II flow cytometer and software **(F)** The graph represents the average percentage levels of G1/G0 (dark grey), S (light grey) or G2/M (grey) phase of three experimental repeats. The error bars represent the standard error (+/-SEM) and statistical analysis was performed using an unpaired t-test. Comparison of significance was performed against the plain U2OS cells for ActD or against the control knockdown for RIO2 and PICT1 knockdowns. Lack of significance values indicates no significant differences. *p value<0.05, **p value<0.01.

4.2.4 p53 levels increase as a result of ribosome production block

It was previously suggested that changes in the steady-state levels of ribosomes, rather than defects in rRNA processing, result in p53 accumulation (Fumagalli et al., 2012). In this paper, the authors suggest that defects in LSU result in the accumulation of the free 5S RNP in the nucleoplasm, whereas defects in SSU result in the up-regulation of translation of the ribosomal proteins, which then results in high levels of the free 5S RNP in the nucleoplasm (Fumagalli et al., 2012). This would imply that the kinetics of LSU or SSU defects on p53 activation would be different, as the free 5S RNP accumulates by two different pathways. I, therefore, decided to test this by performing knockdowns of RPS19, RPL7, RPL18 or RPL21 in U2OS cells for 24h, 48h or 72h. Note that the RPL21 knockdown was previously shown in the lab to majorly decrease the 28S rRNA levels (Loren Gibson, Nick Watkins, personal communication). The whole cell extract was loaded on an SDS-PAGE gel, and analysed by Western blotting using p53 and p21 antibodies (Figure 4.8).

RPS19 knockdown resulted in a significant 2-fold increase in p53 levels after 24h as compared to the control, which was sustained after 48h and 72h (Figure 4.8). Furthermore, the levels of p21 were also slightly increased after 24h, and further increased after 48h and 72h, suggesting an increase in p53 activity over time. Knockdown of either RPL7, RPL18 or RPL21 resulted in a significant, approximately 5-fold p53 increase after 24h (Figure 4.8). The levels of p21 were also increased, indicating an increase in p53 activity after RPL7, RPL18 or RPL21 knockdowns (Figure 4.8). p53 levels were still significantly increased after 48h or 72h as compared to the control after RPL7, RPL18 or RPL21 knockdowns, as were the p21 levels (Figure 4.8). However, the p53 levels decreased over time after knockdowns of the LSU ribosomal proteins (Figure 4.8). These results showed that p53 levels increased as early as 24h after a block in either LSU or SSU production.

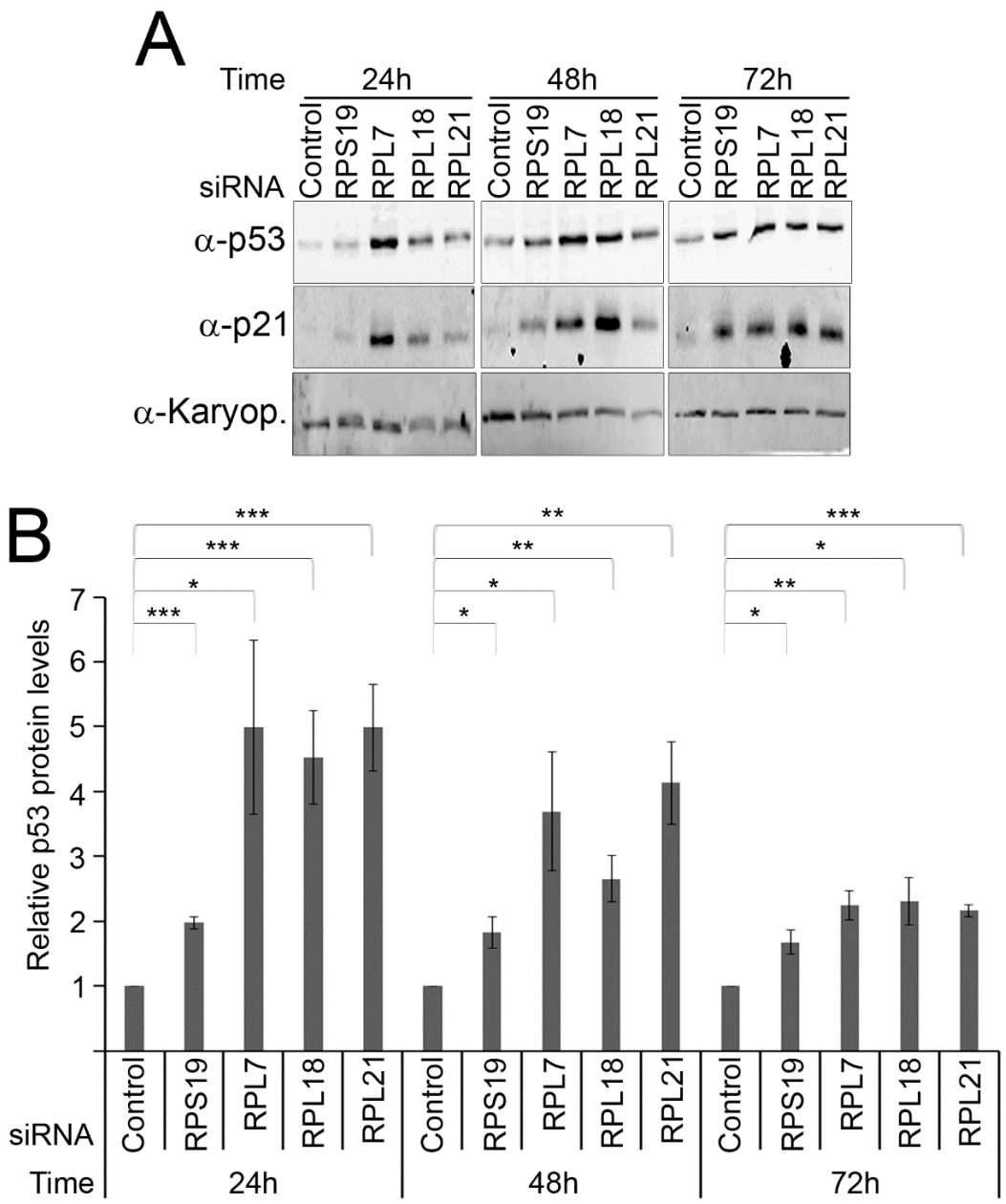

Figure 4.8. p53 induction after SSU or LSU defects occurs in less than 24h. (A) Knockdowns were performed for 24h, 48h or 72h in U2OS cells and the whole cell extract was loaded on an SDS-PAGE gel, followed by Western blot analysis. The antibodies used are shown on the left and Karyopherin (Karyop.) was used as a loading control. The membranes were visualised using the LICOR system. **(B)** ImageQuant software was used to quantitate the levels of p53, followed by normalization against the values of the loading control (α-Karyopherin). The graph represents the p53 protein level averages of three experimental repeats and the error bars show standard error (+/-SEM). Statistical analysis was performed using unpaired t-test. *p value<0.05, **p value<0.01, ***p value<0.001.

Next, I investigated whether the levels of the mature 28S or 18S rRNAs correlated with the levels of p53 induction in the cell. RNA was extracted after knockdown or ribosomal proteins, loaded on a glyoxal-agarose gel and then analysed with Northern Blotting. The membrane was incubated with radio-labelled (^{32}P) probes that recognize the

mature 28S or 18S rRNA (Figure 4.9). The levels of the mature 18S rRNA were compared to 28S rRNA for RPS19 knockdown, whereas the levels of the mature 28S rRNA were compared to the 18S rRNA for the RPL7, RPL81 and RPL21 knockdown

RPS19 knockdown resulted in a significant 40% decrease in the levels of the mature 18S rRNA after 24h of siRNA treatment, 60% decrease after 48h of siRNA treatment and a striking 75% decrease after 72h of siRNA treatment (Figure 4.9A, B). A similar pattern was observed after knockdowns of RPL7, RPL18 and RPL21 for 28S rRNA. An approximately 60-70% significant decrease on 28S rRNA levels was observed after RPL7, RPL18 or RPL21 knockdowns after 24h of treatment, 70% decrease after 48h and 85% after 72h (Figure 4.9A, C). These results showed that the mature 18S or 28S rRNA decrease in a linear manner after small or large ribosomal subunit defects respectively.

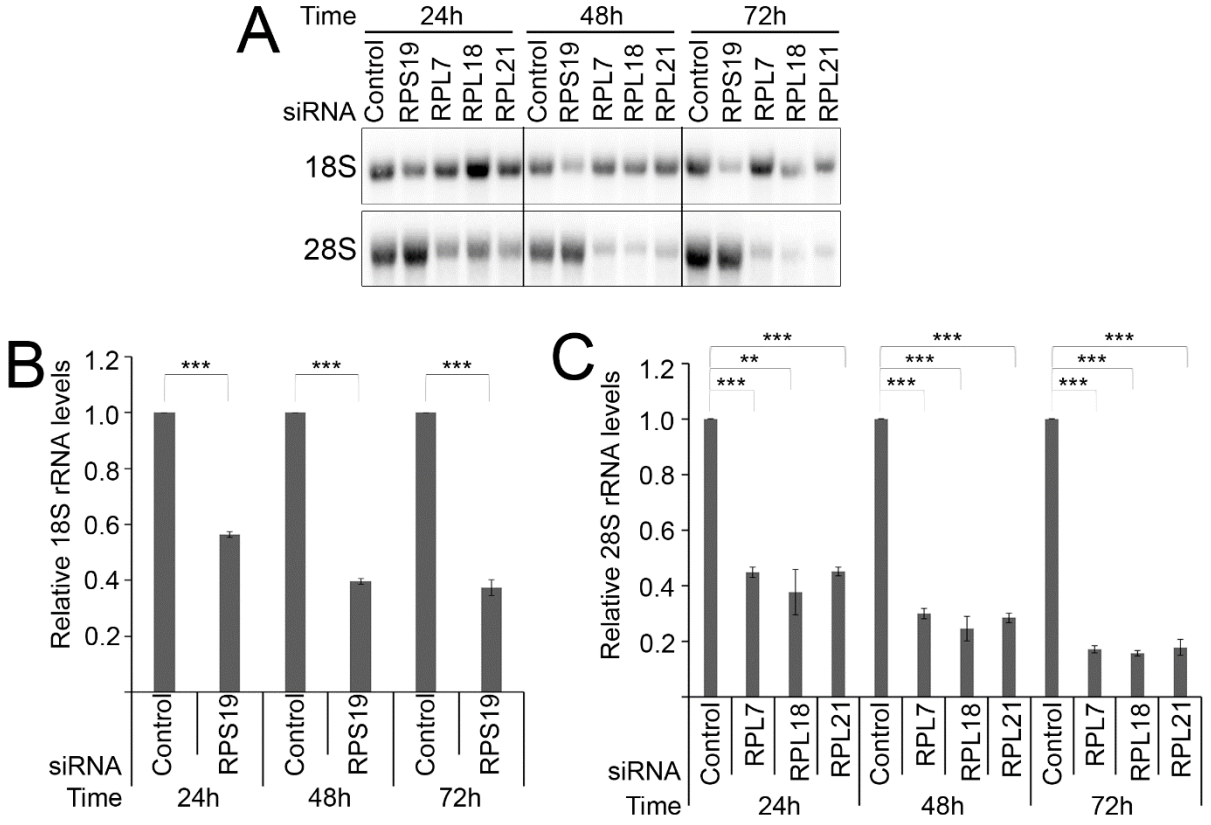

Figure legend on the next page.

Figure 4.9. The levels of the mature rRNAs decrease linearly over time after SSU or LSU defects. (A) Knockdowns were performed for 24h, 48h or 72h in U2OS cells and RNA was extracted and loaded on a 1.2% agarose/glyoxal gel. The membranes were incubated with radio-labelled (^{32}P) probes that recognize the mature 18S or 28S rRNA, and visualized using the Typhoon Phosphorimager. **(B-C)** Quantitation of Northern Blots was performed using the ImageQuant software. The 18S rRNA was normalized to the 28S rRNA levels for RPS19 knockdown, whereas the 28S rRNA was normalized to the 18S rRNA levels after RPL7, RPL18 or RPL21 knockdowns. The graphs represent the average relative levels of 18S **(B)** or 28S **(C)** rRNA of three experimental repeats and the error bars show standard error (SEM). Statistical analysis was performed using unpaired t-test. **p value<0.01, ***p value<0.001.

4.2.5 p53 levels increase independently of the levels of 18S rRNA in the cell

It was previously proposed that p53 induction after defects in SSU production is due to a decrease of the mature 18S rRNA levels in the cell (Fumagalli et al., 2012). Since p53 levels were induced after only 24h of either LSU or SSU block (Figure 4.8) when the 18S rRNA levels were already low (Figure 4.9), I decided to look at shorter time-points after the knockdowns. Knockdowns of RPS19, RPL7, RPL18 or RPL21 were performed in U2OS for 12h or 24h. Cells were analysed by Western blotting using α-p53 or α-p21 antibodies (Figure 4.10).

RPS19 knockdown resulted in a significant p53 induction after 12h of siRNA treatment as compared to the control, as well as in a slight p21 increase (Figure 4.10). RPL7, RPL18 or RPL21 knockdown also resulted in a significant p53 induction as compared to the control, and a p21 increase as well (Figure 4.10). After 24h of siRNA treatment, RPS19 knockdown resulted in a significant p53 increase as compared to the control and an increase in p21 (Figure 4.10), as expected. Similarly, knockdowns of RPL7, RPL18 or RPL21 also resulted in a significant p53 increase and in an increase in p21 levels, indicating an increase in p53 activity (Figure 4.10). These results showed that p53 levels were increased as early as 12h after block in either SSU or LSU production.

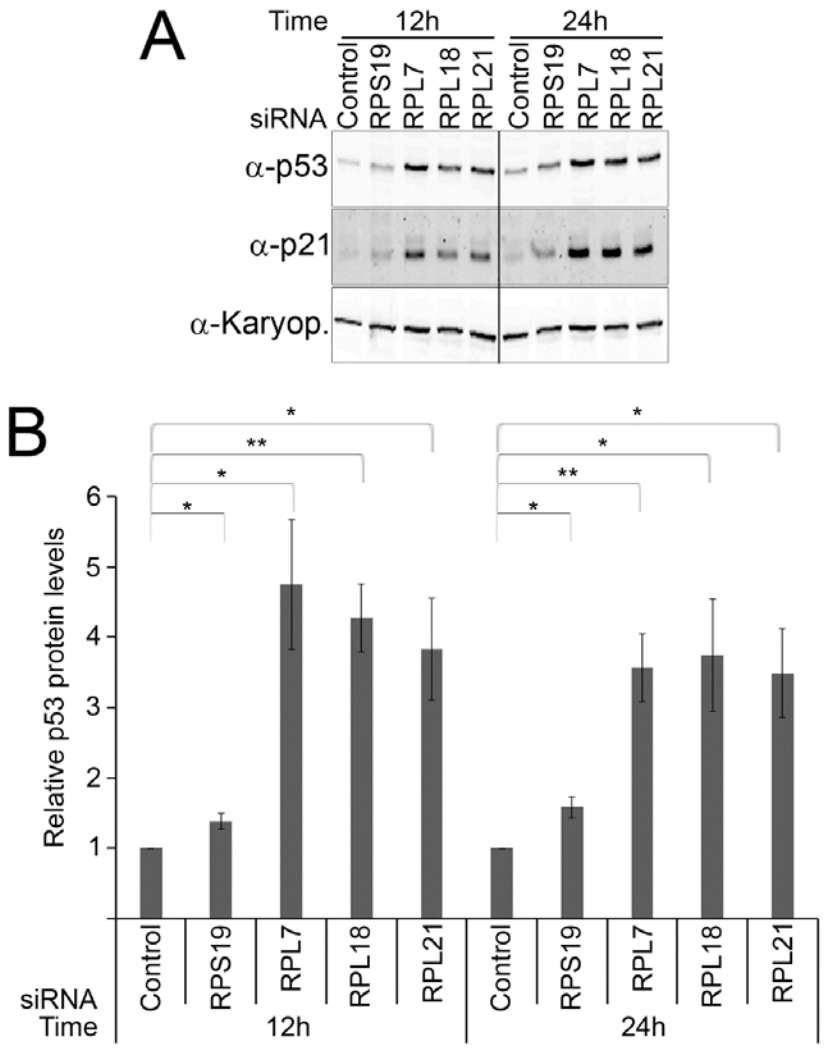

Figure 4.10. p53 is induced as soon as 12h after SSU or LSU defects. (A) Knockdowns of control, RPS19, RPL7, RPL18 or RPL21 were performed in U2OS cells for 12h or 24h. The whole cell extract was loaded on an SDS-PAGE gel and analysed by Western Blotting. The antibodies used are shown on the left and Karyopherin (Karyop.) was used as a loading control. Visualization of the Western blot membrane was performed using the LICOR system. **(B)** The ImageQuant software was used for quantitation of Western Blots. The protein levels of p53 were normalized against the levels of the loading control (α-Karyopherin). The graph represents the averages of the relative p53 protein levels after each knockdown to the control of 12h or 24h respectively, of three experimental repeats. The standard error (+/-SEM) is shown by the error bars. Statistical analysis was performed using unpaired t-test. *p value<0.05, **p value<0.01.

Next, I investigated whether the levels of the mature 18S or 28S rRNA has already changed after 12h of SSU or LSU production defects. RNA was extracted from cells after knockdowns, loaded on a glyoxal-agarose gel and analysed by Northern Blotting (Figure 4.11).

RPS19 knockdown resulted in a slight, but not significant reduction of the levels of the mature 18S rRNA after 12h of siRNA treatment as compared to the control (Figure 4.11A, B). However, RPS19 knockdown resulted in a significant 40% decrease in the levels of 18S rRNA after 24h of siRNA treatment (Figure 4.11A, B), as expected. In contrast, knockdowns of RPL7, RPL18 or RPL21 resulted in a significant decrease of the levels of the mature 28S rRNA after 12h of siRNA treatment as compared to the control, which was approximately 30-40% (Figure 4.11A, C). Similarly to the previous time-course (Figure 4.9), knockdowns of RPL7, RPL18 or RPL21 resulted in an approximately 60% significant decrease of the levels of the mature 28S rRNA after 24h of siRNA treatment as compared to the control (Figure 4.11A, C).

In conclusion, these data indicated that p53 induction occurs very rapidly in the cell, in less than 12h, after block of either SSU or LSU. Furthermore, these results indicated that p53 induction, at least after RPS19 knockdown, does not correlate with the levels of the mature 18S rRNA in the cell after SSU block as previously suggested (Fumagalli et al., 2012), but rather, it is more likely to occur due to ribosome production defects. Finally, these data indicated that induction of p53 is more likely to occur due to ribosome biogenesis defects rather than the reduction of functional ribosomes as previously suggested, since it occurred before the newly-synthesized ribosomes were fully produced.

Since RPS19 knockdown resulted in a p53 induction without a significant reduction in the mature 18S rRNA levels, I next investigated whether this was the case when the SSU biogenesis was blocked by ribosome biogenesis factor knockdowns. For this, RIO2 and PNO1 knockdowns were performed, for block of the late or middle SSU rRNA processing respectively, for 48h in U2OS cells (Figure 4.12). The proteins were analysed by Western Blotting, where the whole cell extract was loaded on an SDS-PAGE gel, using p53 and p21 antibodies. The RNA was extracted from cells, loaded on a glyoxal-agarose gel, and analysed by Northern Blotting with radiolabelled (^{32}P) probes targeting the mature 18S or 28S rRNA.

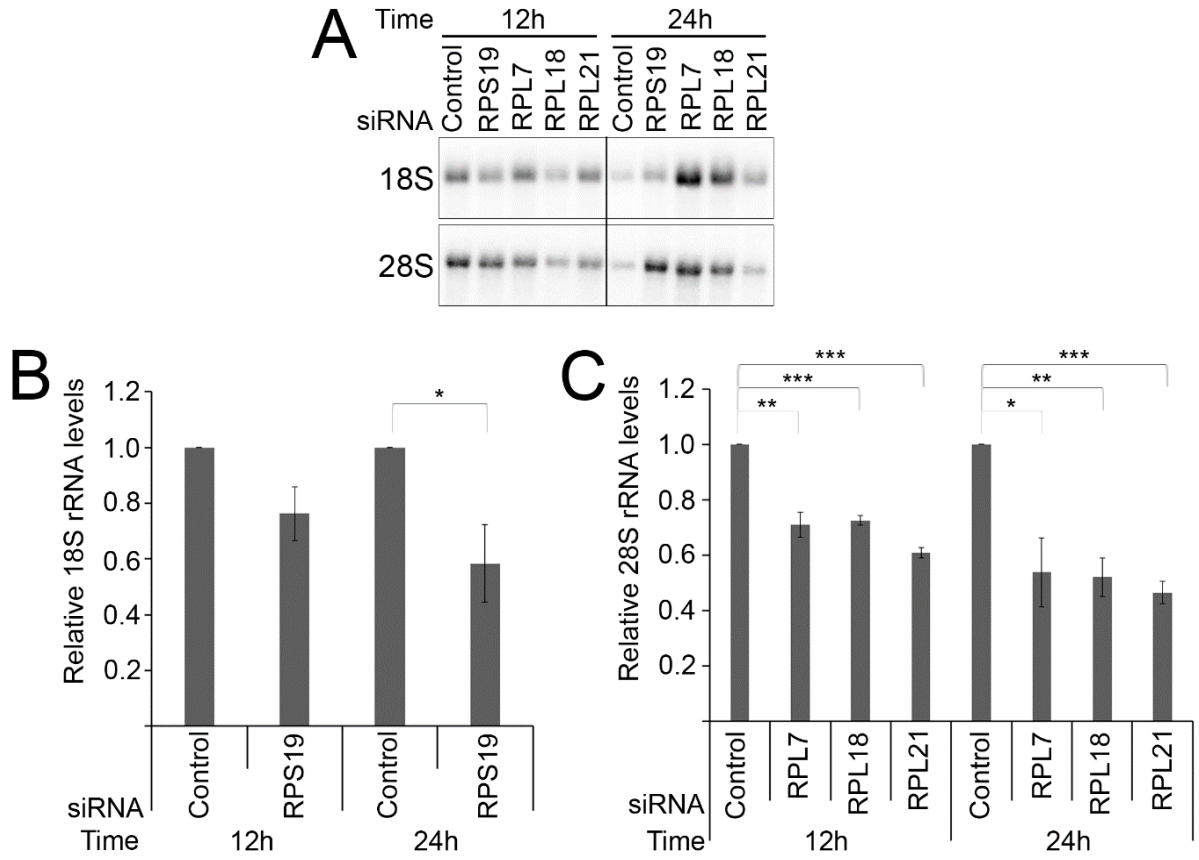

Figure 4.11. Defects in LSU or SSU rRNA processing occur over time. (A) Knockdowns of control, RPS19, RPL7, RPL18 and RPL21 were performed for 12h or 24h in U2OS cells, before RNA was extracted and loaded on a 1.2% agarose-glyoxal gel, before being transferred on a Hybond N membrane. The membranes were incubated with radiolabelled (^{32}P) probes against the mature 28S or 18S rRNA, and visualized using a Typhoon Phosphorimager. **(B-C)** ImageQuant software was used for quantitation of Northern Blots. The 18S rRNA after RPS19 knockdown was normalized to the levels of 28S rRNA **(B)**, whereas the 28S rRNA after RPL7, RPL18 or RPL21 knockdowns was normalized to the 18S rRNA **(C)**. The graphs represent the average relative rRNA levels of three experimental repeats and the standard error is shown by the error bars (+/-SEM). Statistical analysis was performed using unpaired t-test and absence of significance values indicates no significant differences as compared to the control. *p value<0.05, **p value<0.01, ***p value<0.001.

The levels of the 18S rRNA were compared to the 28S rRNA (Figure 4.12). RIO2 or PNO1 knockdowns did not result in a change of the mature 18S rRNA levels as compared to the control (Figure 4.12). However, p53 was induced after knockdown of RIO2 or PNO1 (Figure 4.12). p21 was also increased after RIO2 or PNO1 knockdowns (Figure 4.12A), indicating an increase in p53 activity. These results indicated that defects in early or late stages of SSU rRNA processing result in p53 induction independently of the levels of the mature 18S rRNA.

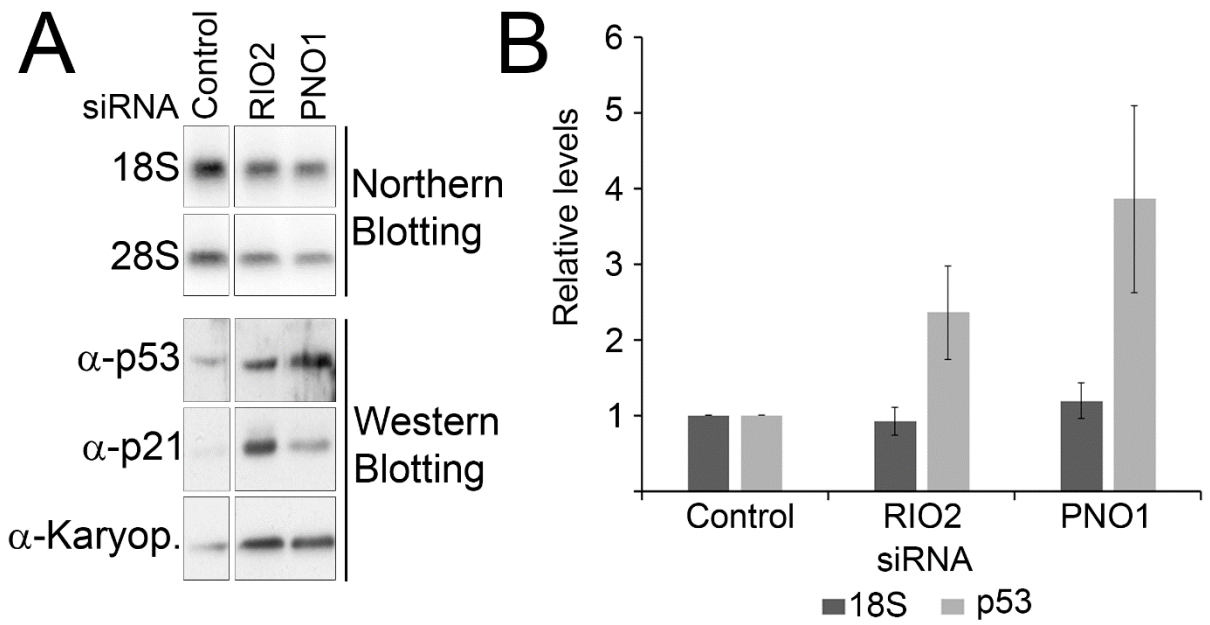

Figure 4.12. Defects in early or late stages of SSU rRNA processing result in p53 induction independently of the levels of the mature 18S rRNA. (A) Knockdowns were performed for 48h in U2OS cells. Half of the cells were analysed by Northern Blotting (indicated on the right) after RNA was extracted, loaded on a 1.2% glyoxal-agarose gel, and transferred on a Hybond N membrane. Radiolabelled (^{32}P) probes recognizing the mature 28S and 18S rRNA were used (shown on the left) and visualized using a Typhoon Phosphorimager. The remaining cells were analysed by Western Blotting (indicated on the right), where the whole cell extract was loaded on an SDS-PAGE gel. The antibodies used are shown on the left and Karyopherin (Karyop.) was used as a loading control. **(B)** ImageQuant software was used for quantitation of the northern or western blots. The 18S rRNA values were normalized to the 28S rRNA values and the p53 protein levels were normalized against the Karyopherin levels. The graph represents the relative 18S rRNA (dark grey) and p53 protein (light grey) averages of four experimental repeats and the error bars show the standard error (+/-SEM).

4.2.6 Combined defects on both the large and small ribosomal subunit result in p53 supra-induction in only a few cases

It was previously proposed that combined defects in both the large and small ribosomal subunit result in p53 supra-induction, leading to a G1 and G2/M cell cycle arrest (Fumagalli et al., 2012). I investigated this further in U2OS cells using RPS19 knockdown for a SSU production block and RPL7 or RPL18 knockdowns for an LSU production block. Even though the efficiency of the single knockdowns was tested previously (Figure 4.3), the expression levels of the targets were not tested after the double knockdowns; therefore a variation in the knockdown efficiency might have occurred. Knockdowns were performed for 48h and the whole cell extract was loaded

on an SDS-PAGE gel. Western Blotting analysis was used, using the LICOR system, to monitor the levels of p53 and p21 (Figure 4.13).

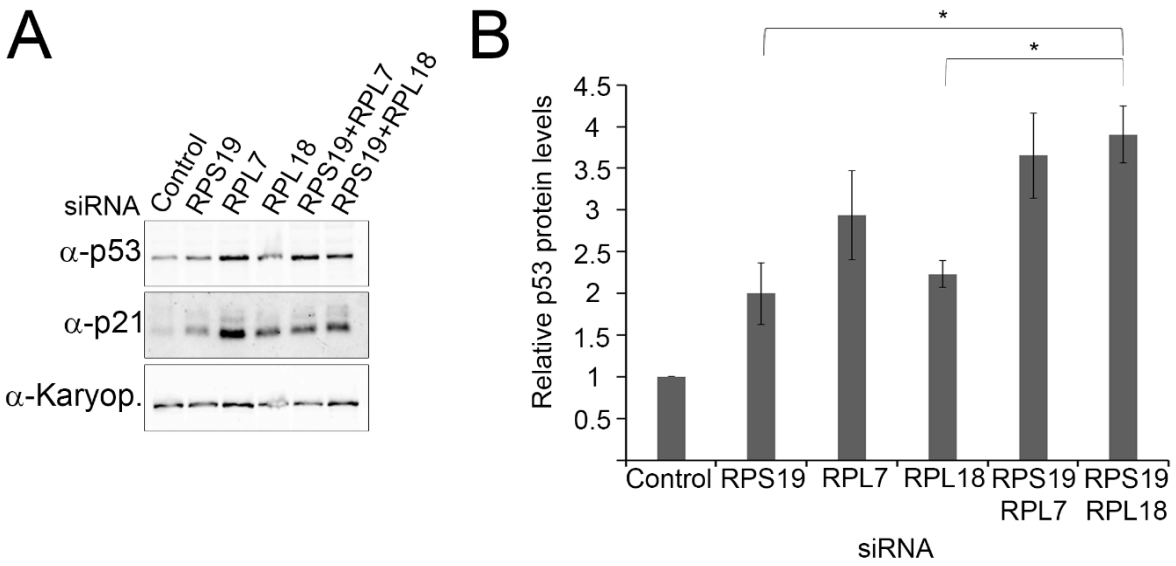

Figure 4.13. Combined LSU and SSU defects lead to p53 induction in U2OS cells, and supra-induction is only observed in one case. (A) Knockdowns of control, RPS19, RPL7 or RPL18 were performed in U2OS cells for 48h and the whole cell extract was loaded on an SDS PAGE gel, before being analysed by Western Blotting using the LICOR system. The antibodies used are shown on the left and. α-Karyopherin (Karyop.) was used as a loading control. **(B)** The ImageQuant software was used for quantitation of the western blots and the levels of p53 were normalised against the loading control levels (α-Karyopherin). The graph represents the average p53 relative levels from three experimental repeats and the error bars show the standard error (+/-SEM). The p53 levels after RPS19, RPL7 or RPL18 knockdowns were compared to the control and p53 levels after the double RPS19 and RPL7 or RPL18 knockdowns were compared to the single knockdowns. Statistical analysis was performed using an unpaired t-test and absence of significance values on RPS19+RPL7 indicates no significant difference as compared to the single knockdowns. *p value<0.05.

As expected, there was a significant p53 induction after RPS19, RPL7 or RPL18 knockdown as compared to the control (Figure 4.13). Furthermore, there was an increase in the levels of p21 in all three cases, especially after RPL7 knockdown (Figure 4.13A), indicating an increase in p53 activity. Note that p21 can be regulated post-translationally, but p21 mRNA levels was not tested here and neither did other p53 downstream targets to measure p53 activity. After RPS19 and RPL7 double knockdowns, there was a significant p53 induction as compared to the control (Figure 4.13). Comparing the levels of p53 of the double knockdown with either RPS19 or RPL7 single knockdowns, there was no significant difference between them (Figure 4.13), indicating no supra-induction. Furthermore, the levels of p21 resembled those

seen with the single knockdowns, further supporting that there was no p53 supra-induction. In contrast, knockdown of both RPS19 and RPL18 led to a significant p53 induction as compared to the control (Figure 4.13), but comparing the double knockdown with either RPS19 or RPL18 single knockdowns, there was a significant increase in p53 levels (Figure 4.13), indicating a p53 supra-induction. However, the levels of p21 resembled the ones of the single knockdowns, especially the p21 levels observed after RPL18 knockdown (Figure 4.13). Taken together, these results showed that p53 supra-induction is not constantly seen after combined knockdowns of LSU or SSU ribosomal proteins, but might be seen with specific combinations of knockdowns.

Next, I investigated whether p53 induction or supra-induction observed after the double RPS19 and RPL7 or RPL18 knockdowns resulted in a G1 and G2/M cell cycle arrest as previously suggested (Fumagalli et al., 2012). Knockdowns were performed for 48h in U2OS cells before the cells were fixed using 70% ethanol. The DNA was stained using propidium iodide and the cell cycle was analysed using the FACS Canto II flow-cytometer and software. ActD overnight treatment was used as a positive control as previously (Figure 4.14). As shown earlier, treatment with Actinomycin D (ActD) resulted in a G1 and a G2/M cell cycle arrest (Figures 4.6, 4.7, 4.14). Furthermore, RPS19, RPL7 or RPL18 knockdowns resulted in an increase in cells in G1 and, to a lesser extent, G2/M stage, indicating arrest (Figures 4.6, 4.7, 4.14). After RPS19 and RPL7 or RPS19 and RPL18 double knockdowns, there was a significant G1 cell cycle arrest as compared with the control and a slight reduction in S phase, indicating a slight G2/M cell cycle arrest. No significant change was observed in the levels of G2 phase as compared to the control (Figure 4.14A, C). However, no major differences were observed between the single and double knockdowns in G1 or G2/M phase (Figure 4.14). After RPS19 and RPL7 or RPS19 and RPL18 double knockdowns, the S phase levels were lower than the single RPS19 knockdown or RPL7 or RPL18 knockdowns respectively (Figure 4.14). Taken together, these data indicated that the p53 supra-induction observed after RPS19 and RPL18 knockdown resulted in a G1 and a mild G2/M cell cycle arrest, similar to the one observed after RPS19 or RPL18 single knockdowns.

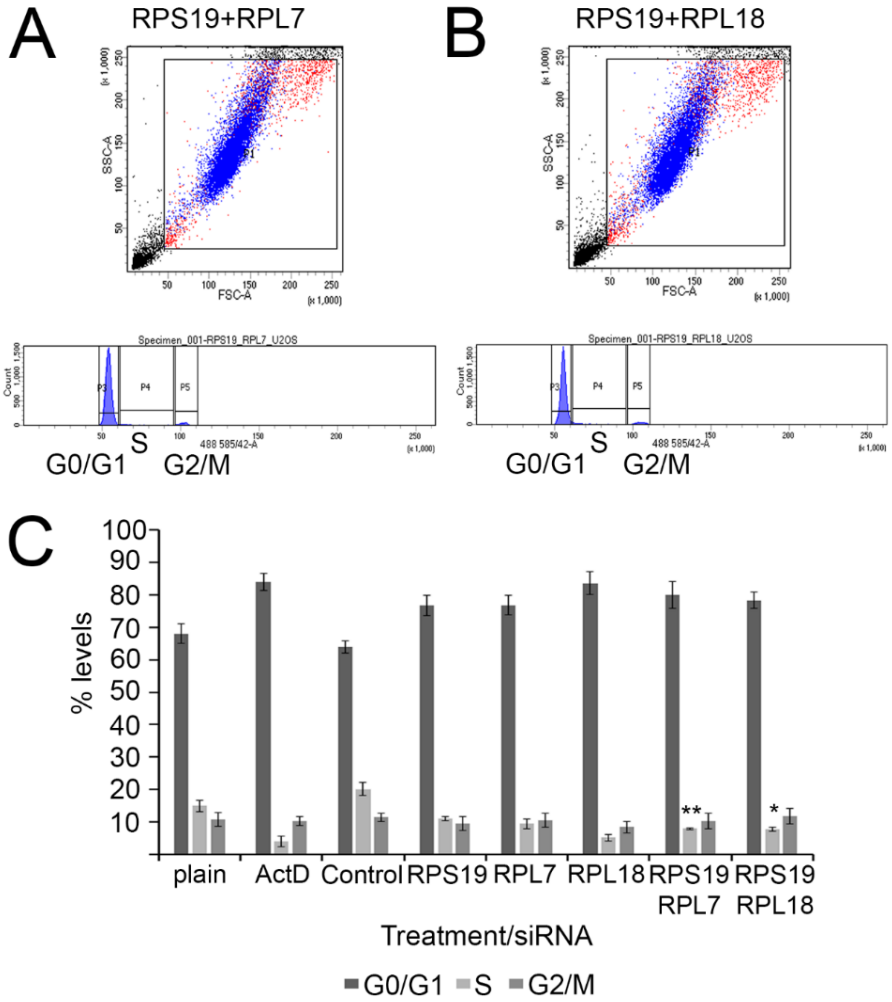

Figure 4.14. Combined defects in LSU and SSU production lead to a G1 and a slight G2/M cell cycle arrest. (A-B) Knockdowns were performed for 48h in U2OS cells, which were then fixed using 70% ethanol. The DNA was stained with propidium iodide and cell cycle analysis was performed using the FACS Canto II flow cytometer and software. **(C)** The average percentage levels of G1 (dark grey), S (light grey) or G2/M (grey) phases of three experimental repeats are shown on the graph. The error bars represent the standard error (+/-SEM) and statistical analysis was performed using an unpaired t-test. The first six samples are the same as the ones used on Figure 4.6. The RPS19 and RPL7 or RPL18 knockdowns were compared to the single RPS19 knockdown and absence of significance values on indicates no significant differences. p value<0.05, **p value<0.01.

Since my results were different from those published (Fumagalli et al., 2012), I next investigated whether this was specific to U2OS cells. For this, I have used the human breast cancer cell MCF7 and the human prostate cancer cell line LNCaP, which both confer a wild-type and active p53. Firstly, the knockdown efficiency in MCF7 cells was assessed by Western blotting after the knockdowns were performed for 48h. The protein levels of RPS19, RPL7 and RPL18 were decreased after knockdowns from 60% (RPS19, RPL7) to 80% (RPL18) (Figure 4.15). Even though the knockdown

efficiency could not be analysed in LNCaP cells due to time limitations, taking in consideration that the knockdowns were efficient in both U2OS and MCF7, it was assumed that the siRNA treatment was efficient in LNCaP cells as well.

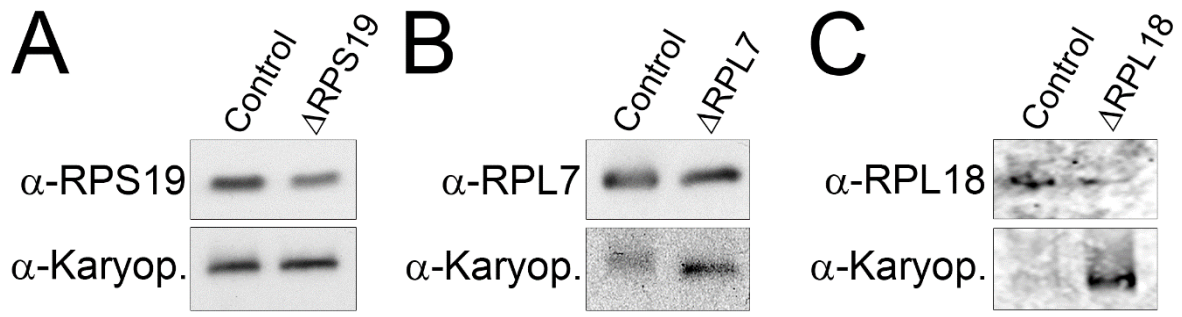

Figure 4.15. The knockdown efficiency of siRNAs in MCF7 cells. Knockdowns were performed for 48h in MCF7 cells and the whole cell extract was loaded on an SDS-PAGE gel before analysed with Western Blotting. Visualization with ECL **(A-B)** or the LICOR system **(C)** was performed. Antibodies for RPS19 **(A)**, RPL7 **(B)** or RPL18 **(C)** were used to detect the levels of the ribosomal proteins, whereas α-Karyopherin was used as a loading control in all cases (shown on the left of the panel).

I next investigated the levels of p53 after single or double knockdowns of RPS19, RPL7 or RPL18 in MCF7 or LNCaP cells (Figure 4.16). Note that the knockdown efficiency of the double knockdowns on the expression levels of the targets was not assessed, which could have led to less efficient depletion of each target. Knockdowns were performed as usual for 48h and the whole cell extract was loaded on an SDS-PAGE gel, which was then analysed by Western Blotting using for p53 and p21 levels (Figure 4.16). In both MCF7 and LNCaP cells, the levels of p53 were significantly increased after RPS19, RPL7 or RPL18 knockdowns as compared to the control (Figure 4.16). Furthermore, the p21 levels were also increased after the ribosomal protein knockdowns in both cell lines (Figure 4.16A, C). Double knockdowns of RPS19 and RPL7 or RPS19 and RPL18 resulted in a significant p53 induction as compared to the control. However, the p53 increase observed after the double knockdowns was not significant as compared to the single RPS19, RPL7 or RPL18 knockdowns in either MCF7 or LNCaP cell lines (Figure 4.16). Furthermore, the p21 levels after the double RPS19 and RPL7 or RPS19 and RPL18 knockdowns resembled those of the single knockdowns (Figure 4.16A, C). These results indicated that p53 is induced after either SSU or LSU block in MCF7 and LNCaP cells, as it was observed in U2OS cells (Figure 4.5). However, defects in both SSU and LSU production resulted in p53 induction but not supra-induction in MCF7 or LNCaP cells, as opposed to previously published data (Fumagalli et al., 2012). Whether this induction was also seen on p53 activity cannot

be concluded, as p21 can be regulated post-translationally, but p21 mRNA levels or other p53 downstream targets were not assessed here.

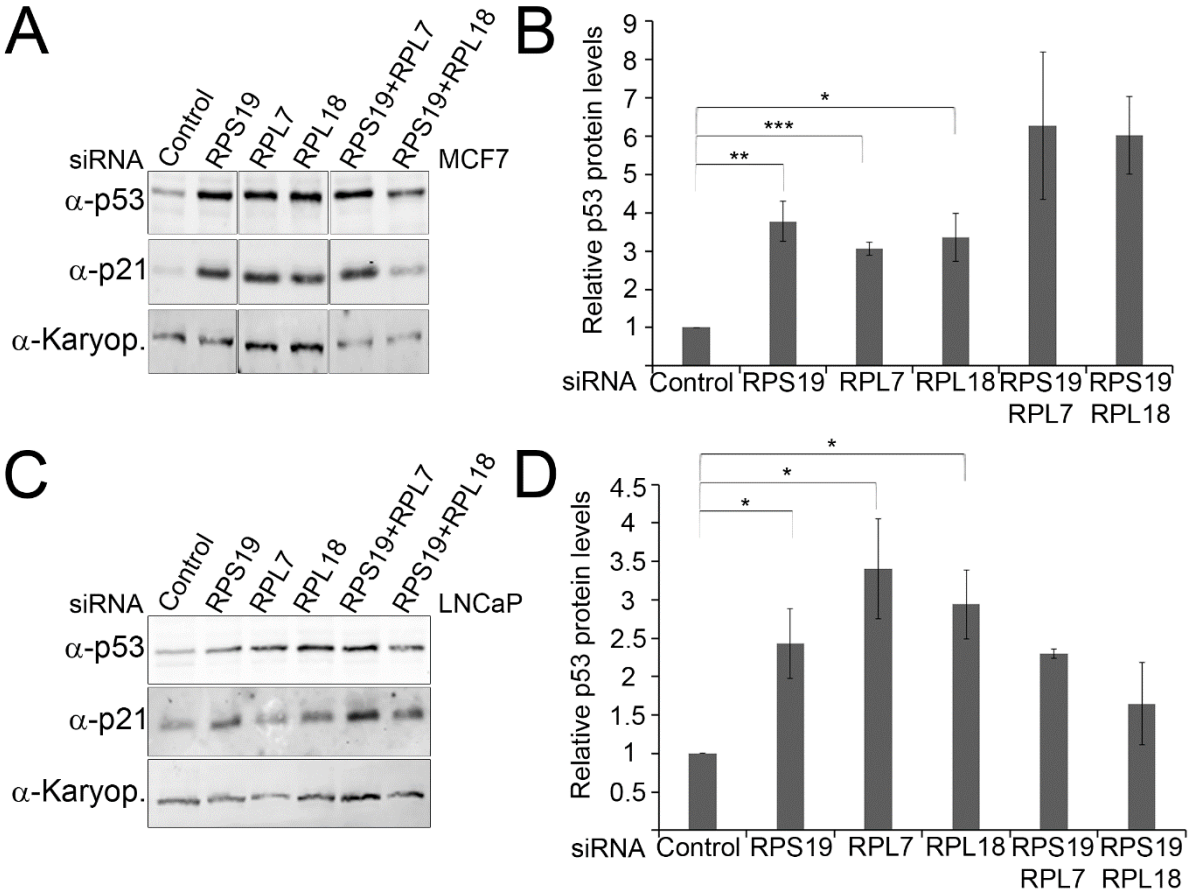

Figure 4.16. Combined defects in LSU and SSU result in p53 induction, but not supra-induction, in MCF7 or LNCaP cells. (A, C) Knockdowns were performed for 48h in MCF7 **(A)** or LNCaP **(C)** cells and the whole cell extract was loaded on an SDS-PAGE gel, before Western Blot analysis was performed using the LICOR system. The antibodies used are shown on the left and Karyopherin (Karyop.) was used as a loading control. **(B, D)** ImageQuant software was used for quantitation of the Western Blots and p53 levels were normalized to the levels of the loading control (α-Karyopherin). The graph represents the average p53 relative levels from three different experimental repeats in MCF7 **(B)** or LNCaP **(D)** cells and the error bars represent the standard error (+/-SEM). The p53 levels after RPS19, RPL7 or RPL18 knockdowns were compared to the control and p53 levels after the double RPS19 and RPL7 or RPL18 knockdowns were compared to the single knockdowns. Statistical analysis was performed using an unpaired t-test and absence of significance values indicates no significant differences. *p value<0.05, **p value<0.01, ***p value<0.0001.

In the published paper, the authors have targeted different proteins using siRNAs against RPS6 or RPL7a ribosomal proteins for SSU or LSU block respectively. I, therefore, performed these knockdowns for 48h, using the siRNAs from the report (Fumagalli et al., 2012), for SSU or LSU block, in U2OS, MCF7 or LNCaP cells. The whole cell extract was loaded on an SDS-PAGE gel and analysed by Western Blotting for p53 and p21 levels (Figure 4.17).

Knockdown of RPS6 resulted in a significant increase in p53 levels in U2OS, MCF7 and LNCaP cells as compared to the control (Figure 4.17). Knockdown of RPL7a resulted in a significant increase in p53 levels in U2OS and MCF7 cells, and in an increase in p53 levels in LNCaP cells, which did not appear to be significant (Figure 4.17). This might be due to differences in knockdown efficiencies between the cell lines. Furthermore, the p21 levels were also increased after RPS6 or RPL7a knockdowns (Figure 4.17A), indicating an increase in p53 activity. Double knockdowns of RPS6 and RPL7a resulted in an increase in p53 levels as compared to the control in all three cell lines. However, the p53 levels after the double RPS6 and RPL7a knockdowns were not significantly increased as compared to the single RPS6 or RPL7a knockdown in neither U2OS, MCF7 nor LNCaP (Figure 4.17). Moreover, p21 levels after the double RPS6 and RPL7a knockdown resembled those after the single RPS6 or RPL7a knockdowns (Figure 4.17A).

These data indicated that double RPS6 and RPL7a knockdowns do not result in p53 supra-induction in U2OS, MCF7 or LNCaP cell lines. My data show little evidence of p53 supra-induction after combined defects in LSU and SSU, except one case and only in U2OS cells, as opposed to previously published data (Fumagalli et al., 2012).

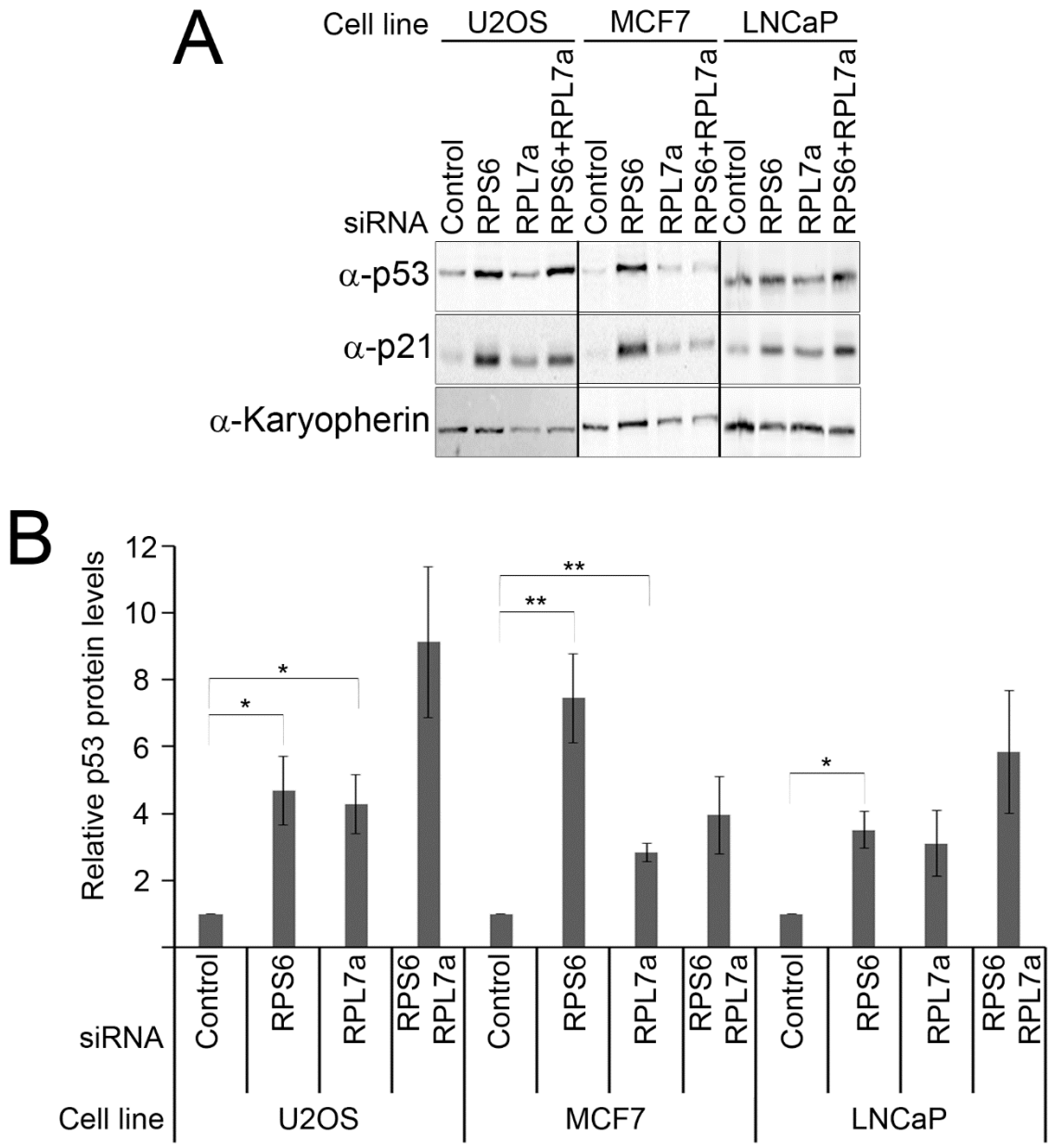

Figure 4.17. Combined defects in LSU and SSU after RPS6 and RPL7a knockdown result in p53 induction, but not supra-induction, in U2OS, MCF7 or LNCaP cells. (A) siRNA treatment was performed for 48h in U2OS, MCF7 or LNCaP cells and the whole cell extract was loaded on an SDS-PAGE gel, before being analysed with Western Blotting using the LICOR system. The antibodies used are shown on the left and Karyopherin (Karyop.) was used as a loading control. **(B)** ImageQuant software was used for quantitation of the western blots and p53 levels were normalized to the loading control (α-Karyopherin). The average relative p53 protein levels of three experimental repeats are shown on the graph and the error bars show the standard error (+/-SEM). The p53 levels after RPS6 or RPL7a knockdowns were compared to the control and p53 levels after the double RPS6 and RPL7a knockdowns were compared to the single knockdowns. Statistical analysis was performed using an unpaired t-test and absence of significance values indicates no significant differences. *p value<0.05, **p value<0.01.

In the study by Fumagalli et al (2012) it was suggested that the combined LSU and SSU defects result in both G1 and G2/M cell cycle arrest after p53 supra-induction, using RPS6 and RPL7a siRNAs in A549 and U2OS cells. Since I did not observe any p53 supra-induction with these knockdowns, I investigated whether there was also no effect on cell cycle in U2OS cells. For this, knockdowns were performed for 48h in U2OS cells before being fixed using 70% ethanol. The DNA was then stained using propidium iodide and the cell cycle was analysed using the FACS Canto II flow cytometer and software (Figure 4.18).

Single knockdown of either RPS6 or RPL7a resulted in a significant increase in G1 phase as compared to the control (Figure 4.18), showing a G1 cell cycle arrest. The levels of the S phase were significantly decreased as compared to the control after knockdowns of RPS6 or RPL7a (Figure 4.18) and the levels of G2/M phase were significantly decreased (Figure 4.18). These results indicated a G1 and a slight G2/M cell cycle arrest after SSU or LSU block using RPS6 or RPL7a siRNAs in U2OS cells. After the double knockdown of RPS6 and RPL7a, there was a significant increase in G1 phase as compared to either RPS6 or RPL7a single knockdowns (Figure 4.18). Furthermore, there was a significant reduction in S phase after RPS6 and RPL7a double knockdowns in comparison to RPS6 or RPL7a single knockdowns (Figure 4.18). The levels of G2 phase were not significantly changed after RPS6 and RPL7a double knockdown as compared to the single RPS6 knockdown, but they were significantly decreased as compared to the RPL7a single knockdown (Figure 4.18).

These results show that RPS6 and RPL7a double knockdowns result in a bigger G1 cell cycle arrest as compared to the single RPS6 or RPL7a, which is not seen with other combinations of siRNAs.

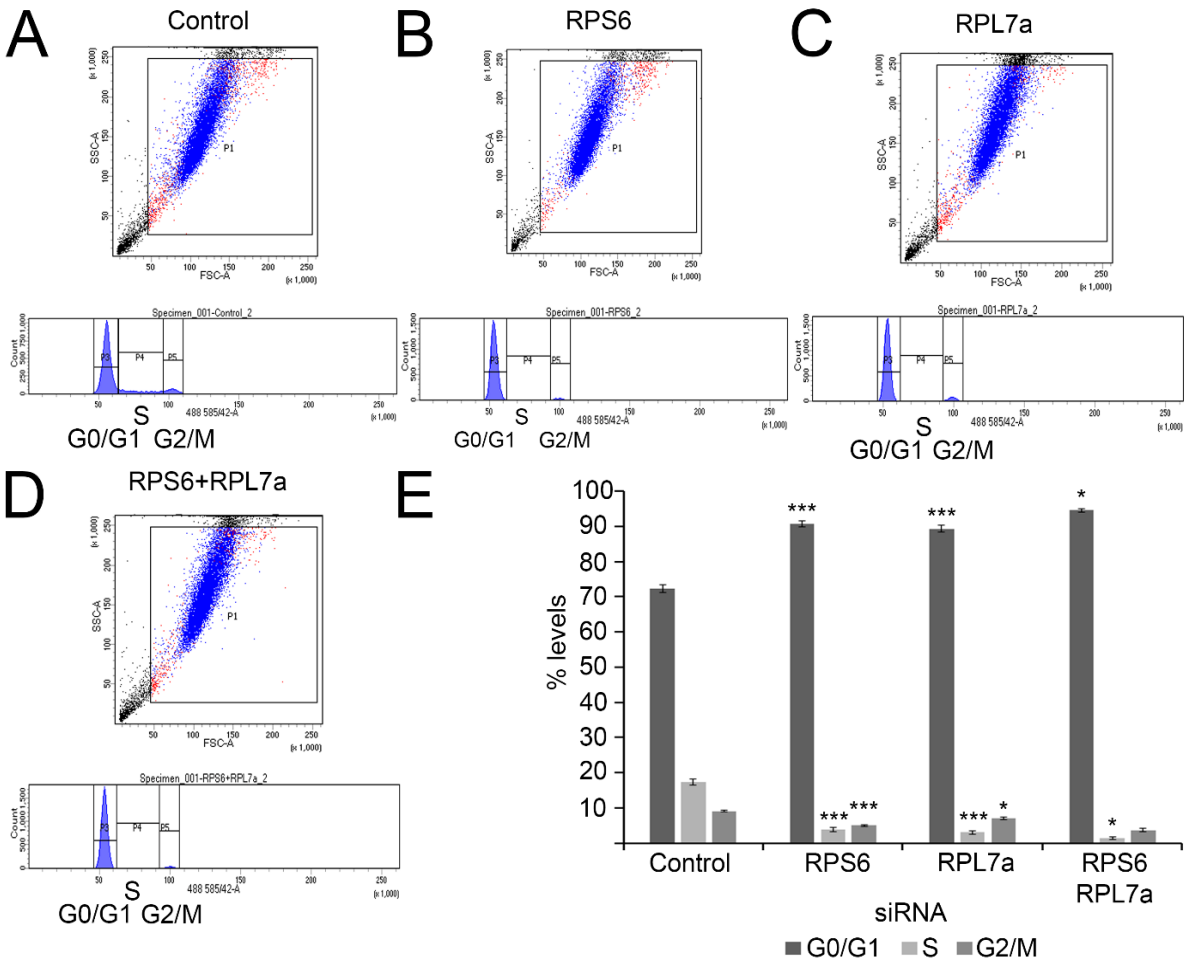

Figure 4.18. SSU and LSU defects after RPS6 and RPL7a knockdowns result in G1 and a G2/M cell cycle arrest in U2OS cells. (A-D) Knockdowns of control, RPS6 and RPL7a were performed in U2OS cells for 48h before the cells were fixed using 70% ethanol. Propidium iodide was used for DNA staining and cell cycle analysis was performed using the FACS Canto II flow-cytometer and software. **(E)** The average values of the percentage levels of the G1 (dark grey), S (light grey) and G2/M (grey) phases of three experimental repeats are indicated on the graph. The error bars represent the standard error (+/-SEM) and the statistical analysis was performed using an unpaired t-test. The % levels of each phase after RPS6 or RPL7a knockdowns were compared to the control values, and the levels of each phase after the double RPS6 and RPL7a knockdown were compared to RPS6 single knockdown values. Lack of significance values indicates no significant differences. *p value<0.05, **p value<0.01, ***p value<0.001.

4.2.7 Block in SSU production results in an accumulation of the free 5S RNP

I have shown that defects in SSU biogenesis result in p53 accumulation via the 5S RNP-MDM2 pathway, independently of the levels of the 18S rRNA. However, no obvious defects on the LSU biogenesis were observed after knockdowns of the SSU factors RPS19, RIO2 or PNO1 in assays performed so far. Therefore, how defects in SSU production resulted in an accumulation of the free 5S RNP in the nucleoplasm

with no obvious LSU defects is unclear. It is possible that the LSU might still be produced, but there is an inhibition or retardation of its export from the nucleus to the cytoplasm if SSU production is blocked. This would result in a reduction in the integration of the 5S RNP into pre-LSU complex and would lead to its accumulation in the nucleoplasm and its binding on MDM2. To test this hypothesis, U2OS cell lines stably expressing tetracycline-inducible FLAG-tagged RPL11 were used (kindly provided by Dr Loren Gibson, Nick Watkins). Knockdowns of RPS19 and RPL7 were performed for 48h in these cells and tetracycline was also added for 48h. The whole cell extract was analysed by gradient analysis, using a 10%-40% glycerol gradient, to separate the small (free) and large (ribosomal) cellular complexes. The gradient was then fractionated and each of the fractions was loaded on an SDS-PAGE gel and analysed by Western Blotting using an α-FLAG antibody (Figure 4.19).

In control cells, approximately 65% of the FLAG-tagged RPL11 was found in the ribosomal complexes and almost 35% in the free complexes (Figure 4.19). Knockdown of RPL7 resulted in a major accumulation of RPL11 in the free pool as compared to the control (almost 80%) (Figure 4.19) and a decrease of the FLAG-tagged RPL11 that was integrated in the ribosomal complexes (approximately 20%) (Figure 4.19). RPS19 knockdown resulted in approximately 45% accumulation of the FLAG-tagged RPL11 in the free pool, and a decrease of the FLAG-tagged RPL11 in the ribosomal complexes (55%) (Figure 4.19). This further supports the theory that SSU defects result in an accumulation of the 5S RNP in the nucleoplasm, resulting in its binding on MDM2 and, therefore, p53 activation. However, RPL11 still gets integrated in the ribosomal complexes after RPS19 knockdowns, probably as a part of the 5S RNP. It is worth noting that the gradient analysis was only performed twice and, therefore, another repeat is required to identify whether any differences observed in the localization of the FLAG-tagged RPL11 are significant.

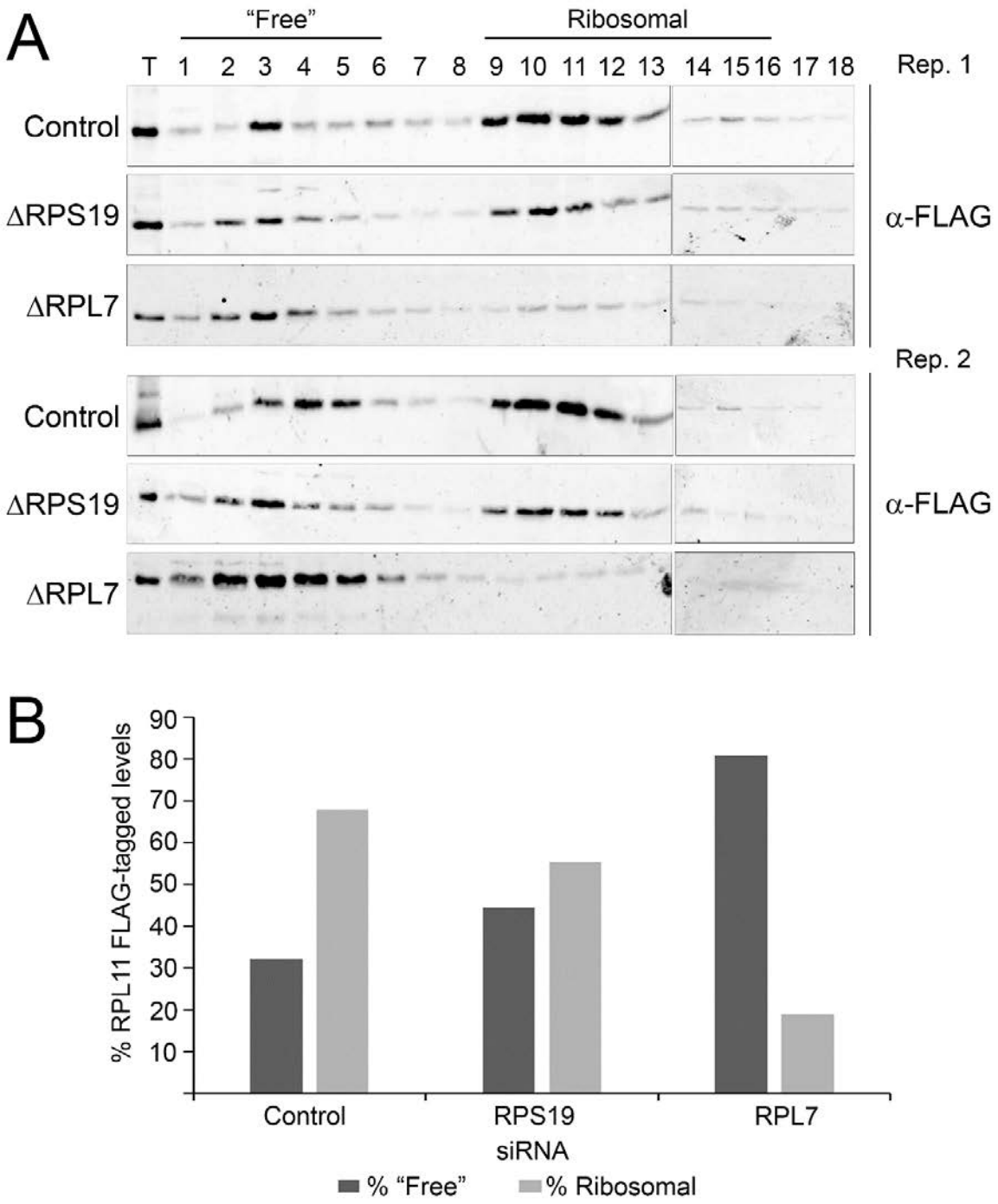

Figure 4.19. RPS19 knockdown results in a decreased integration of RPL11 in the ribosomal complexes. (A) siRNA treatment using Control, RPS19 or RPL7 siRNAs was performed for 48h in U2OS cells expressing FLAG-tagged RPL11 for 48h using 1000ng/µl tetracycline. The whole cell extract was fractionated after 10-40% glycerol gradient analysis. Fractions were loaded on an SDS-PAGE gel, before being analysed by Western Blotting using an α-FLAG antibody. The image was generated using the LICOR system. "T" represents the 10% total sample before gradient analysis. The first experimental repeat is shown at the top (Rep.1) and the second at the bottom (Rep.2). **(B)** The ImageQuant software was used for quantitation of the Western Blots. The graph represents the average percentage of the two experimental repeats shown of the free complexes (dark grey), which is shown as the sum of fractions 1-6, and the ribosomal complexes (light grey), which is shown as the sum of fractions 9-16.

4.2.8 Defects in SSU production result in a decreased export of the LSU in the cytoplasm

Since there was an accumulation of the free 5S RNP after a block in SSU production, I wanted to see whether this resulted in an accumulation of the free 5S RNP in the nucleoplasm or whether the 5S RNP was still integrated in the pre-LSU, but the export of the pre-LSU into the cytoplasm was retarded. For this, I have used immunofluorescence to identify the levels of the FLAG-tagged RPL11 in the nucleoplasm or cytoplasm.

Firstly, the localization of RPL11 FLAG-tagged protein was assessed, to ensure that the FLAG-tagged protein were expressed and localized as expected. The U2OS cells expressing FLAG-tagged RPL11 were treated with Actinomycin D (ActD), which blocks ribosome biogenesis by inhibition of RNA polymerase I and it was previously shown to cause the nuclear accumulation of RPL11 in HEK293T cells (Sloan et al., 2013a). The cells were fixed using 4% paraformaldehyde and immunofluorescence was performed using α-FLAG antibody for the localization of the FLAG-tagged protein RPL11. Fibrillarin was used for nucleolar staining and DAPI was used for DNA staining. U2OS cells containing the empty pcDNA5 vector were used as a control (Figure 4.20).

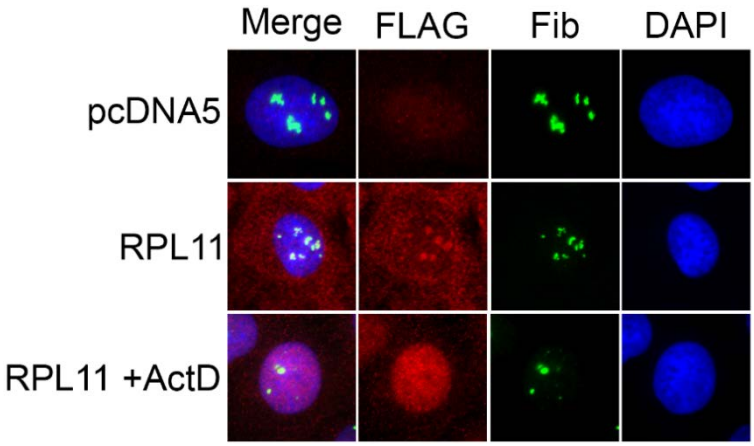

Figure 4.20. Defects in ribosome biogenesis result in nuclear accumulation of RPL5 and RPL11. U2OS cells stably expressing FLAG-tagged RPL11 were treated with 1000ng/μl tetracycline for 18h. ActD treatment was also performed for 18h and the U2OS cells containing the empty vector (pcDNA5) were used as a control. The cells were fixed using 4% paraformaldehyde and α-FLAG antibody was used to stain the FLAG-tagged RPL11 (red). α-Fibrillarin (Fib) was used to stain the nucleolus (green) and DAPI was used to stain DNA (blue). The merge image shows the three channels merged together. Visualization of the images was performed using the Zeiss Axiovision inverted microscope and software.

Very little background signal was observed using the α-FLAG antibody in U2OS cells containing the empty pcDNA5 vector, and the nucleolar staining as seen by the α-Fibrillarin antibody was as expected (Figure 4.20). The FLAG-tagged RPL11 localized mainly in the nucleolus and in the cytoplasm (Figure 4.20), whereas treatment with ActD caused its accumulation in the nucleoplasm (Figure 4.20). These results agreed with previously published results where the localization of the FLAG-tagged RPL11 was investigated in HEK293T cell line (Sloan et al., 2013a).

I next tested the localization of the FLAG-tagged RPL11 after a block in SSU production. For this, knockdowns using RPS19, RIO2 and RPS6 siRNAs in order to inhibit SSU biogenesis, and RPL7 siRNA for LSU biogenesis block as a positive control were performed for 48h in U2OS cells expressing the FLAG-tagged RPL11 for 48h. Therefore, the FLAG-tagged RPL11 was produced after the knockdowns. Knockdown of RPL7 was expected to show a nuclear accumulation of the FLAG-tagged RPL11, similarly to the ActD treatment. U2OS cells containing the empty pcDNA5 vector were used as a negative control to monitor background signal of the α-FLAG antibody during immunofluorescence.

No background signal was observed in U2OS cells containing the empty pcDNA5 vector when α-FLAG antibody was used, and staining with α-Fibrillarin and DAPI showed the expected nucleolar and DNA signal (Figure 4.21). The FLAG-tagged RPL11 localized to the nucleolus and cytoplasm in the control-treated cells, as expected (Figure 4.21). Knockdown of RPS6 or RPS19 resulted in the accumulation of the FLAG-tagged RPL11 in the nucleoplasm as compared to the control, with some also presented in the cytoplasm (Figure 4.21). RIO2 knockdown resulted in a slight accumulation of the FLAG-tagged RPL11 in the nucleoplasm as compared to the control but it was mainly found in the cytoplasm (Figure 4.21). Finally, RPL7 knockdown resulted in a major accumulation of the FLAG-tagged RPL11 in the nucleoplasm (Figure 4.21), as expected.

Taken together, these data suggested that the FLAG-tagged RPL11 accumulated in the nucleus after a block in SSU production, even though the 5S RNP was still integrated in the LSU (Figure 4.19), suggesting a retardation of export of the pre-LSU complexes in the cytoplasm.

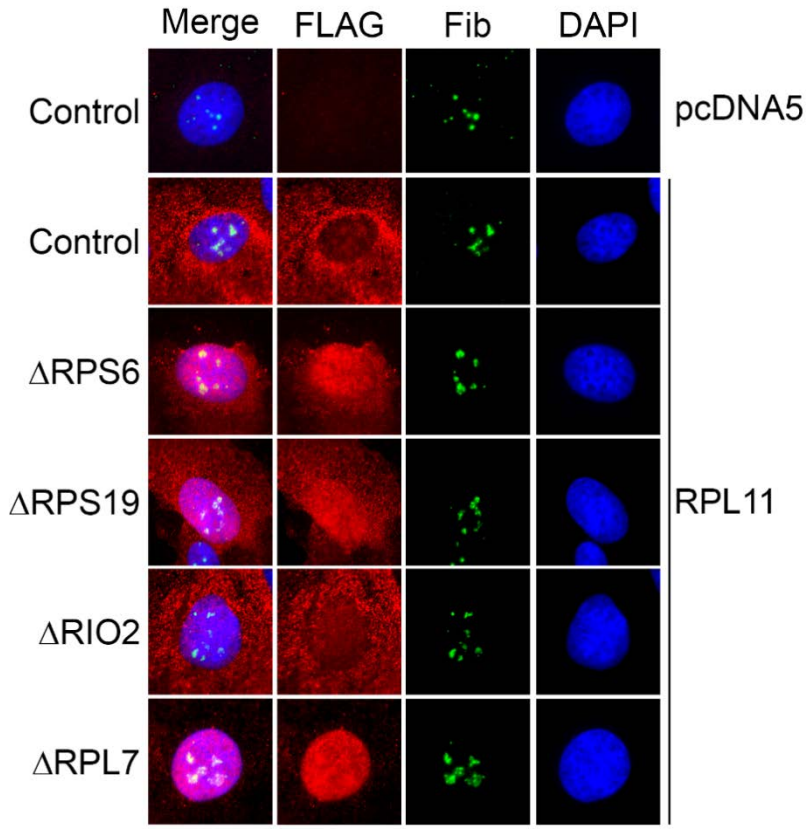

Figure 4.21. SSU defects result in an increased accumulation of RPL11 in the nucleoplasm. siRNA treatment using control, RPS6, RPS19, RIO2 or RPL7 siRNAs was performed for 48h in U2OS cells expressing RPL11 for 48h. The cells were treated with 1000ng/µl tetracycline for expression of the FLAG-tagged protein for 18h and U2OS cells containing the empty vector (pcDNA5) were used as a control. The cells were fixed using 4% paraformaldehyde and immunofluorescence followed. α-FLAG antibody was used for visualization of the FLAG-tagged RPL11 (red) and α-Fibrillarin (Fib) was used for nucleolar staining (green). DAPI was used for DNA staining (blue). The merge image shows the three channels merged together. Visualization of the images was performed using the Zeiss Axiovision inverted microscope and software.

4.2.9 Inhibition of LSU export after SSU production defects lead to the accumulation of the pre-5.8S rRNA precursor

In yeast, the last stages of 5.8S maturation take place in the cytoplasm (Thomson and Tollervey, 2010). Since I have shown that SSU production defects are likely to result in an accumulation of the LSU in the nucleus, I decided to investigate whether this causes defects in late stages of LSU rRNA processing. For this, knockdowns of RPS19 or RPL7a were performed in U2OS cells for 48h, RNA was extracted and loaded on an 8% acrylamide/7M Urea gel. The RNA was transferred on a Hybond N membrane which was incubated with a radiolabelled (^{32}P) probe recognizing the 5' end of ITS2 (Figure 4.22A) (Sloan et al., 2013c). The U1 snRNA was used as a loading control

(Figure 4.22B). RPL7a knockdown resulted in a decrease in both bands of the pre-5.8S rRNA precursor as compared to the control (Figure 4.22 B, C), as expected, since it is involved in LSU production. RPS19 knockdown resulted in a decrease of the levels of the early pre-5.8S rRNA precursor (T), but an increase in the levels of the late pre-5.8S rRNA precursor (B) as compared to the control (Figure 4.22B, C). This suggests that SSU production defects may result in a delay of the 5.8S rRNA maturation in the cytoplasm. This experiment was performed twice and the results were very similar and consistent both times. This is the first evidence that cytoplasmic export is required for the late stages of LSU rRNA processing in humans. Furthermore, this indicates that SSU production defects might cause defects in late stages of LSU production because of inhibition of export of the LSU in the cytoplasm.

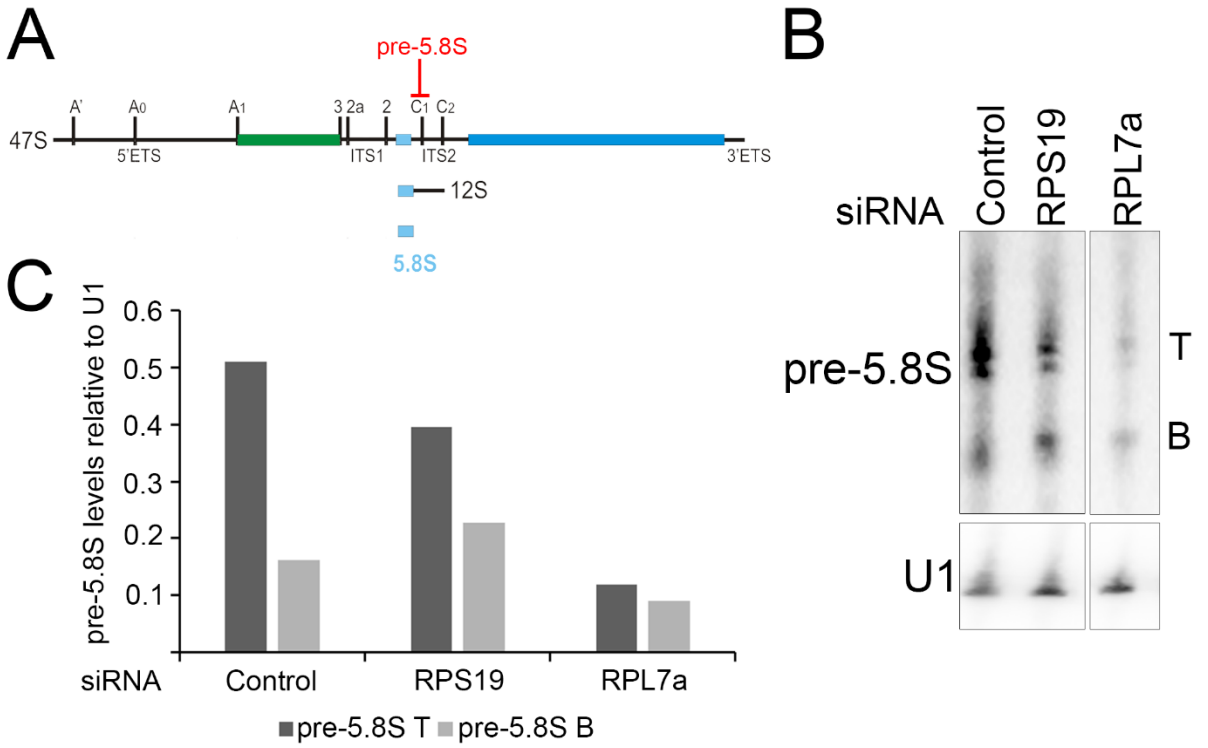

Figure 4.22. Defects in SSU production lead to the accumulation of the pre-5.8S rRNA precursor. (A) Schematic representation of the rRNA precursors of the small (SSU, green) and large (LSU, blue) ribosomal subunits. The site recognized by the radiolabelled (^{32}P) pre-5.8S (5'-ITS2) probe is indicated in red (Adapted from: (Sloan et al., 2013c)).**(B)** Knockdowns using control, RPS19 or RPL7a were performed in U2OS cells for 48h. RNA was extracted and loaded on an 8% Acrylamide/7M Urea gel, and transferred on a Hybond N membrane. The membrane was incubated with a radiolabelled (^{32}P) probe recognizing the pre-5.8S rRNA precursor and U1 snRNA was used as a loading control. Visualization of the RNAs was performed using a Typhoon Phosphorimager. The different bands seen with the pre-5.8S probe (T, B) are shown on the right. **(C)** ImageQuant software was used for quantitation of the RNAs. The levels of the pre-5.8S rRNA were normalized against the U1 RNA levels. The graph represents the average levels of the pre-5.8S T (dark grey) and B (light grey) of two experimental repeats.

4.3 Discussion

Ribosome biogenesis is a complex and energy-consuming process, which is linked with the levels of the tumour suppressor p53 (Pelava et al., 2016). Mutations in genes encoding for ribosomal proteins or ribosome biogenesis factors lead to the development of ribosomopathies (Yelick and Trainor, 2015), a set of rare genetic diseases, such as Diamond-Blackfan Anaemia (DBA), characterized by craniofacial abnormalities, anaemia and increased cancer development, especially Acute Myeloid Leukaemia (AML) (Narla and Ebert, 2010). Even though it was originally thought that the LSU and SSU biogenesis were two independent processes, recent evidence suggests that this may not be the case (Lebaron et al., 2012, Lamanna and Karbstein, 2011). Defects in SSU biogenesis were previously shown to cause p53 accumulation via the 5S RNP-MDM2 pathway MDM2 (Fumagalli et al., 2009, Fumagalli et al., 2012, Golomb et al., 2014), which was proposed to be due to the translation up-regulation of RPL5 and RPL11 (Fumagalli et al., 2012). Here, I have shown that defects in early or late stages of either SSU or LSU biogenesis result in p53 induction via the 5S RNP-MDM2 pathway. The kinetics of p53 accumulation after defects in either LSU or SSU production are very similar, as p53 induction occurs very rapidly, in less than 12h, suggesting that there is only one pathway leading to the accumulation of the free 5S RNP in the nucleoplasm. Furthermore, p53 induction is independent of the levels of the mature 18S rRNA, indicating that it is more likely to be due to ribosome production defects rather than the lack of ribosomes. Finally, I have shown that defects in SSU result in a retardation of export of the LSU in the cytoplasm, which is likely to lead to defects in late stages of LSU production.

Firstly, I have shown that defects in either early or late stage of LSU or SSU biogenesis lead to p53 induction via the 5S RNP-MDM2 pathway (Figure 4.5). A number of previously published studies have shown that defects in LSU rRNA processing result in a significant p53 accumulation via the 5S RNP-MDM2 pathway (Donati et al., 2013, Marechal et al., 1994, Sloan et al., 2013a, Dai and Lu, 2004, Horn and Vousden, 2008, Nishimura et al., 2015). Furthermore, knockdowns of several LSU ribosome biogenesis factors involved in the recruitment of the 5S RNP in the LSU, such as PICT1, have also resulted in p53 induction via the 5S RNP-MDM2 pathway (Donati et al., 2013). I further confirmed these results, by showing that knockdowns of the LSU ribosomal proteins RPL7 and RPL18, or the LSU ribosome biogenesis factor PICT1, resulted in a 5S RNP-

dependent p53 induction. This was expected, since disruptions in the LSU rRNA processing would not affect the production of the 5S RNP, but would affect its integration in the mature LSU complex. Interestingly, I found that defects in either early or late stages of SSU rRNA processing also result in a 5S RNP-dependent p53 induction. It was previously shown that RPS19 knockdown results in a 5S RNP-dependent p53 induction in mouse (Jaako et al., 2015), zebrafish (Danilova et al., 2008, Jia et al., 2013) or cell culture (Dutt et al., 2011) models. RPS6 knockdown was also shown to result in in p53 accumulation via the 5S RNP-MDM2 pathway in human cells (Fumagalli et al., 2009, Fumagalli et al., 2012). This was further confirmed here, where RPS19 knockdown indeed resulted in p53 induction via the 5S RNP-MDM2 pathway and RPS6 knockdown resulted in a p53 induction, presumably also dependent on the 5S RNP. It was surprising to find that defects in late SSU rRNA processing defects, caused by RIO2 knockdown, also resulted in p53 induction via the 5S RNP-MDM2 pathway. These results indicated that defects in SSU production feedback to the recruitment of the 5S RNP in the LSU.

A recent publication has suggested that p53 is significantly induced only after depletion of ribosomal proteins that are involved in the late LSU assembly, and depletion of only one SSU ribosomal protein results in a significant p53 induction. All of these proteins appear to be structurally important around the active site of the ribosome (Nicolas et al., 2016). Knockdowns of some ribosomal proteins presented on this paper were previously shown to also result in a significant p53 induction, such as knockdown of RPL6 (Bai et al., 2014), knockdown of RPL7, which was shown here, or knockdown of RPS27a (Sun et al., 2011). In this study, the authors have used a 5-fold p53 induction as their significance threshold and a lot of the ribosomal proteins that did not appear to significantly induce p53 after depletion have been previously shown to be important for p53 accumulation. For example, knockdown of the ribosomal protein RPL23, which was suggested to not significantly induce p53 in this study (Nicolas et al., 2016), was previously found to be important for p53 stabilisation due to MDM2 inhibition after ribosome biogenesis defects (Dai et al., 2004, Jin et al., 2004). Furthermore, knockdown of the ribosomal protein RPL18 was also below the chosen significance threshold (Nicolas et al., 2016), whereas I have shown here that RPL18 knockdown results in a significant 5S RNP-dependent p53 induction. Moreover, they have suggested that knockdowns of the majority of SSU ribosomal proteins did not result in a significant p53 induction (Nicolas et al., 2016). However, I have shown here that

knockdowns of the SSU ribosomal protein RPS19 or the SSU ribosome biogenesis factor RIO2 resulted in a significant p53 induction, via the 5S RNP-MDM2 pathway. In addition, a number of previous studies have shown that knockdowns of SSU ribosomal proteins, such as RPS19 (Dutt et al., 2011), RPS6 (Fumagalli et al., 2009, Fumagalli et al., 2012) or RPS3 (Yadavilli et al., 2009), result in a significant p53 induction.

I then investigated how defects in SSU lead to p53 accumulation via the 5S RNP-MDM2 pathway. It was previously suggested that the induction of p53 after SSU defects is dependent on the levels of the mature 18S rRNA, since depletion of the SSU is necessary for the proposed mechanism of p53 accumulation (Fumagalli et al., 2012). However, I have shown here that defects in early or late stages of rRNA processing result in p53 accumulation independently of the steady state levels of 18S rRNA (Figures 4.10, 4.11, 4.12). Furthermore, I have shown that p53 was induced as early as 12h (Figures 4.10, 4.11), before the newly-synthesized ribosomes were produced, indicating that p53 accumulation occurs due to SSU rRNA processing defects. Moreover, it was suggested that defects in SSU production result in the translational up-regulation of ribosomal proteins, such as RPL11, so that the 5S RNP is produced in excess, in order to compete binding on both the LSU and MDM2 (Fumagalli et al., 2012). This would suggest that there would be different kinetic rates for p53 induction after LSU or SSU defects. I have found no evidence of this, since p53 is significantly induced 12h after SSU or LSU production defects (Figure 4.10). Therefore, these evidence suggest that there is only one pathway that results in the accumulation of the free 5S RNP in the nucleoplasm leading to p53 induction after SSU or LSU defects, rather than two pathways as previously suggested (Fumagalli et al., 2012).

Here, I have shown that RPS19 knockdown caused a small increase in the accumulation of the FLAG-tagged RPL11 in the free complexes, but most of it was integrated in the ribosomal complexes (Figure 4.19). Furthermore, I have shown that RPS19 knockdown resulted in a nuclear accumulation of the FLAG-tagged RPL11 (Figure 4.21), which was much more than the accumulation of the free 5S RNP shown after gradient analysis. These results indicate that the 5S RNP gets integrated in the LSU, but there is an inhibition of export of the LSU in the cytoplasm. Furthermore, knockdown of RPS6 or RIO2 also resulted in a nuclear accumulation of the FLAG-tagged RPL11 (Figure 4.21), indicating that defects in early or late stages of SSU production are likely to be causing a retardation of export of the LSU complexes in the

cytoplasm. Even though I cannot exclude the possibility of an increase in 5S RNP production, it is presumed that the 5S RNP is produced as normal or in slightly higher amounts, so that it still gets integrated in the ribosome, but there is some accumulation of the free 5S RNP complex in the nucleoplasm. This would result in its binding on MDM2, leading to p53 accumulation. Future work is required for identification of the rate of accumulation of the 5S RNP after LSU or SSU defects, perhaps by investigating the levels of the newly-synthesized 5S rRNA as part of the 5S RNP over time. Furthermore, it is necessary to investigate the localization of other LSU ribosomal proteins after SSU production defects, since RPL11 is a part of the 5S RNP.

Combined defects in LSU and SSU were previously suggested to result in p53 supra-induction because of two separate pathways (Fumagalli et al., 2012), for which, I have very little evidence. In the published paper, the SSU ribosomal protein RPS6 and the LSU ribosomal protein RPL7a were knocked down in lung cancer A549 cells. Furthermore, the authors have stated that the same result was observed in osteosarcoma U2OS cells, but no evidence was presented (Fumagalli et al., 2012). Here, I have shown that only co-depletion of the SSU ribosomal protein RPS19 and the LSU ribosomal protein RPL18 resulted in a p53 supra-induction in U2OS cells (Figure 4.13), but not the combined knockdowns of other SSU and LSU ribosomal proteins in U2OS, MCF7 or LNCaP cells (Figures 4.13, 4.16, 4.17), as previously suggested (Fumagalli et al., 2012). It is worth noting that the authors gave no evidence of statistical analysis, suggesting that the p53 supra-induction seen might have been a result of experimental variation. Interestingly, LNCaP cells were found to have mutations in a number of genes encoding for either ribosomal proteins, such as RPL22, or ribosome biogenesis factors, such as BMS1, whereas MCF7 have a mutation in only the gene encoding for RPL10L and no mutations in the genes encoding for known ribosome biogenesis factors (Iorio et al., 2016). In contrast, U2OS cells have no mutations in genes encoding for ribosomal proteins or known ribosome biogenesis factors (Iorio et al., 2016). These data suggest that LNCaP cells may behave differently when ribosome biogenesis is blocked, as they may be more prone to ribosome biogenesis defects. In the same study, it was suggested that defects on either LSU or SSU lead to a G1 cell cycle arrest, which is further supported by my data, but combined defects on both LSU and SSU result in G1 and G2/M cell cycle arrest (Fumagalli et al., 2012). Here, I have found that RPS6, RPL7a (Figure 4.18) or RPL18 (Figure 4.6) single knockdowns resulted in both G1 and a G2/M cell cycle arrest, but knockdowns of

RPS19 or RPL7 results in a G1 and only a slight G2/M cell cycle arrest (Figure 4.6). Furthermore, the double RPS6 and RPL7a knockdown resulted in a higher G1 cell cycle arrest as compared to any of the single RPS6 or RPL7a knockdowns, but not to a G2/M cell cycle arrest in U2OS cells (Figure 4.18), as opposed to previously published data (Fumagalli et al., 2012). It is likely that ribosomal protein knockdowns result in a significant G1 cell cycle arrest, but the G2/M cell cycle arrest varies depending on the ribosomal protein that is knocked down. This could be because some ribosomal proteins might be more important for ribosome biogenesis and assembly than some others, resulting in a rapid increase in p53 levels and activity, which, in turn, results in more profound defects in the cell cycle (Thapa et al., 2013). It is also possible that some ribosomal proteins have other functions in the cell apart from ribosome biogenesis, such as RPS6 (Magnuson et al., 2012) and RPL7a (Ziemiecki et al., 1990, Kozma et al., 1988), which might contribute for the increased G1 and G2/M cell cycle arrest after their knockdowns due to combined defects of ribosome biogenesis and other cellular processes.

In addition, knockdown of PICT1 or RIO2 did not result in any change in the cell cycle, even though p53 levels were significantly induced (Figure 4.7). This could indicate that p53 might be induced slower after defects in late stages of ribosome biogenesis, so that its effects on cell cycle are not visible after 48h. Indeed, p53 levels after PICT1 or RIO2 knockdowns were not as high as after the ribosomal protein knockdowns (Figure 4.5). Another possibility would be that defects in late stages of ribosome biogenesis activate p53, which is involved in other downstream processes, such as metabolic changes. If this is the case, future work is needed, identifying whether p53 regulates downstream targets involved in glycolysis, such as the glucose transporters GLUT1 and GLUT4 (Schwartzenberg-Bar-Yoseph et al., 2004), or oxidative phosphorylation, such as TIGAR and reactive oxygen species (ROS) (Bensaad et al., 2006).

It was previously shown in yeast that processing of the late stages of LSU biogenesis take place in the cytoplasm (Thomson and Tollervey, 2010). However, not much is known about the late processing stages of LSU production in humans. My data here suggest that SSU production defects lead to the accumulation of the pre-5.8S rRNA precursor (Figure 4.22), which is indicative of the lack of export of the LSU in the cytoplasm (Figure 4.21). This suggests that the last steps of LSU rRNA precursor processing in humans take place in the cytoplasm, as in yeast. These data, and

previous studies (Lebaron et al., 2012, Lamanna and Karbstein, 2011), suggest that a cross-talk between the LSU and SSU rRNA biogenesis is highly likely, possibly by the involvement of a single ribosome biogenesis factor, or even a group of proteins, required for both LSU and SSU rRNA production (Figure 4.23).

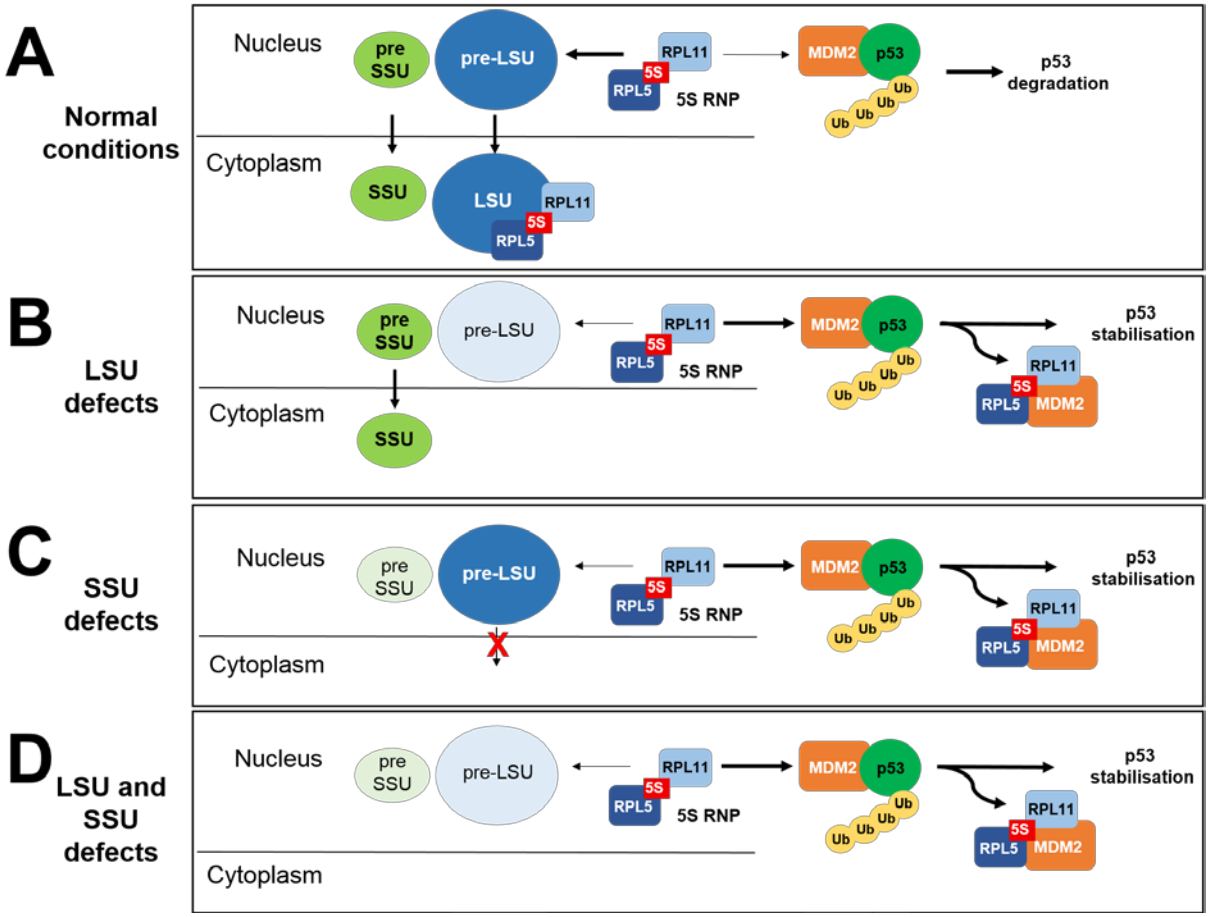

Figure 4.23. The proposed model for p53 induction via the 5S RNP-MDM2 pathway after defects in LSU or SSU production.

It is proposed here that under normal conditions, the 5S RNP gets integrated in the LSU and both SSU and LSU are exported to the cytoplasm. My data suggest that a factor or a group of proteins, which is still uncharacterized, link the SSU production with the LSU export and late LSU rRNA maturation stages (Figure 4.23). Defects in LSU production result in the accumulation of the free 5S RNP in the nucleoplasm, which binds and inhibits MDM2, leading to p53 induction (Figure 4.23), as previously shown (Donati et al., 2013, Sloan et al., 2013a). Defects in SSU production lead to the integration of the 5S RNP in the LSU but the pre-LSU is not exported to the cytoplasm, resulting in the accumulation of the 5S RNP in the nucleoplasm. Thus, the free 5S RNP binds and inhibits MDM2, resulting in p53 induction (Figure 4.23). Furthermore, SSU biogenesis defects may lead to defects in the late stages of LSU rRNA processing.

Finally, defects in both LSU and SSU production lead to the accumulation of the free 5S RNP, resulting in p53 induction but not supra-induction (Figure 4.23).

In conclusion, my data support the fact that the processes of LSU and SSU production during ribosome biogenesis are highly likely to be linked, and that the interaction of the 5S RNP with MDM2 is important for p53 induction after defects in either LSU or SSU production. I have further shown that SSU rRNA processing defects, but not lack of ribosomes, are more likely to cause p53 accumulation, independently of the levels of the mature rRNAs. Given the high importance of ribosome biogenesis in ribosomopathy patients and in cancer development in general, it is essential to further investigate and understand how the biogenesis of LSU and SSU are linked. In addition, the interaction of the 5S RNP with MDM2 is a promising target for the development of future targeted therapeutic treatments for ribosomopathy patients. Finally, the nucleolus is increasingly targeted for anti-cancer therapies and it is becoming clear that it is, indeed, an important player in tumour development.

5. Chapter Five. The role of RPS27a- and RPL40-Ubiquitin proteins in human ribosome biogenesis and p53 induction

5.1 Introduction

Ubiquitin is a small, highly conserved protein which is highly abundant in the cell, that constitutes approximately 0.5-1% of the total cellular protein in the cell (Ryu et al., 2007). Ubiquitination is a post-translational modification important for multiple cell functions. Mono-ubiquitination, which involves the addition of a single ubiquitin molecule on the substrates, is important for several cellular processes such as endocytosis and membrane trafficking (Ikeda and Dikic, 2008), DNA damage repair pathways (Ikura et al., 2007), gene regulation (Hammond-Martel et al., 2012) and cell-cycle regulation (Mukhopadhyay and Riezman, 2007). In contrast, poly-ubiquitination, which involves the addition of several ubiquitin molecules on the substrates, targets the protein substrate for proteosomal degradation (Lecker et al., 2006) and is also involved in cellular processes, such as inflammation (Nathan et al., 2013).

The ubiquitination process involves ATP hydrolysis and three different enzymes (Figure 5.1) (Kimura and Tanaka, 2010). Firstly, the E1 ubiquitin-activating enzyme forms a bond with the ubiquitin molecule (Figure 5.1) (Pickart and Eddins, 2004). The ubiquitin is then transferred to the E2 ubiquitin-conjugating enzyme and, finally, to the E3 ubiquitin ligase, which is responsible for its attachment on the protein substrate (Figure 5.1) (Pickart and Eddins, 2004). Ubiquitination is a reversible modification, where de-ubiquitinases, a group of proteases, cleave the ubiquitin bond between the ubiquitin and the substrate (Reyes-Turcu et al., 2009). Ubiquitin homeostasis is a tightly regulated process, involving more than 600 E3 ubiquitin ligases and approximately 100 de-ubiquitinases in mammals (Li et al., 2008).

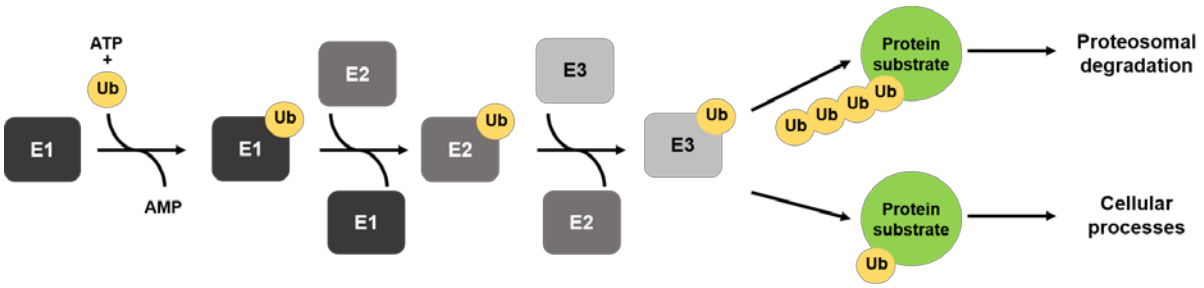

Figure 5.1. Schematic representation of the ubiquitin transfer process. Ubiquitin is bound on E1 ubiquitin-activating enzyme (dark grey) by ATP hydrolysis. The ubiquitin is then transferred on E2 ubiquitin-conjugating enzyme (grey) and, subsequently, on E3 ubiquitin-ligase (light grey). Poly-ubiquitination of the protein substrate (green) leads to proteosomal degradation and mono-ubiquitination is important for other cellular processes (Adapted from (Ardley and Robinson, 2005)).

In yeast, ubiquitin is encoded by four genes: *UBI1* and *UBI2*, which encode for RPL40-ubiquitin protein, *UBI3*, which encodes for RPS27a-ubiquitin protein, and *UBI4*, which encodes for a five-ubiquitin chain (Figure 5.2). In mammals, *Ubb* and *Ubc* encode for a four- or nine-ubiquitin chain, *RPS27a* (*Uba80* in mouse) encodes for the RPS27a-ubiquitin protein and *RPL40* (*Uba52* in mouse) encodes for the RPL40-ubiquitin protein (Figure 5.2) (Kimura and Tanaka, 2010). RPS27a and RPL40 are highly conserved amongst species, especially amongst eukaryotes (Kimura and Tanaka, 2010). RPS27a was identified as a part of the small ribosomal subunit (40S; SSU) in yeast (Finley et al., 1989) and rat (Redman and Rechsteiner, 1989), whereas RPL40 was identified as a part of the large ribosomal subunit (60S; LSU) in yeast (Finley et al., 1989). RPS27a and RPL40 are the only ribosomal proteins that are expressed as ubiquitin-fusion proteins and their transcriptional regulation is highly controlled, since both ribosome production and ubiquitin homeostasis are tightly regulated processes (Kimura and Tanaka, 2010).

	Gene		
	Yeast (*S. cerevisiae*)	**Humans**	**Mouse**
Ub Ub Ub	*UBI4* (5-Ub)	*Ubb* (4-Ub) *Ubc* (9-Ub)	*Ubb* (4-Ub) *Ubc* (9-Ub)
Ub RPS27a	*UBI3*	*RPS27a*	*Uba80*
Ub RPL40	*UBI1* *UBI2*	*RPL40*	*Uba52*

Figure 5.2. Graphical representation of the ubiquitin-encoding genes in yeast *Saccharomyces cerevisiae*, humans and mice (Adapted from: (Kimura and Tanaka, 2010).

The ribosome is a ribonucleoprotein particle essential for protein synthesis in the cell. Ribosomes consist of two subunits: the small ribosomal subunit (40S; SSU), containing the 18S rRNA and approximately 30 ribosomal proteins, and the large ribosomal subunit (60S; LSU), containing the 28S, 5.8S and 5S rRNAs and approximately 46 ribosomal proteins (Granneman and Baserga, 2004). The 28S, 18S and 5.8S rRNAs are transcribed in the nucleolus by RNA polymerase I as a single transcript (47S), whereas the 5S rRNA is transcribed in the nucleolus by RNA polymerase III (Gamalinda and Woolford, 2015). The 5S rRNA is bound by the ribosomal proteins RPL5 and RPL11, forming the 5S RNP, which is integrated in the large ribosomal subunit in the nucleolus (Gamalinda and Woolford, 2015). Ribosome biogenesis, a high energy-consuming process and tightly regulated in the cell, is linked with the levels of the tumour suppressor p53 in humans (Figure 5.3). Under normal conditions, the 5S RNP gets integrated in the LSU. At the same time, the E3 ubiquitin ligase MDM2 targets p53 for proteosomal degradation. Upon stress, defects in ribosome biogenesis lead to the accumulation of the free 5S RNP in the nucleoplasm which binds and inhibits MDM2, resulting in p53 stabilisation (Figure 5.3) (Pelava et al., 2016). Interestingly, all three components of the 5S RNP are essential for p53 activation after ribosome biogenesis defects (Sloan et al., 2013a, Donati et al., 2013, Nishimura et al., 2015). The importance of ribosome biogenesis is highlighted in ribosomopathies, a set of genetic diseases that arise due to mutations in genes encoding for ribosomal proteins or ribosome biogenesis factors (Narla and Ebert, 2010). Ribosomopathy patients appear with anaemia and increased cancer risk, especially for acute myeloid leukaemia (AML), and the levels of p53 have been found to be de-regulated in animal and cell culture models (Pelava et al., 2016).

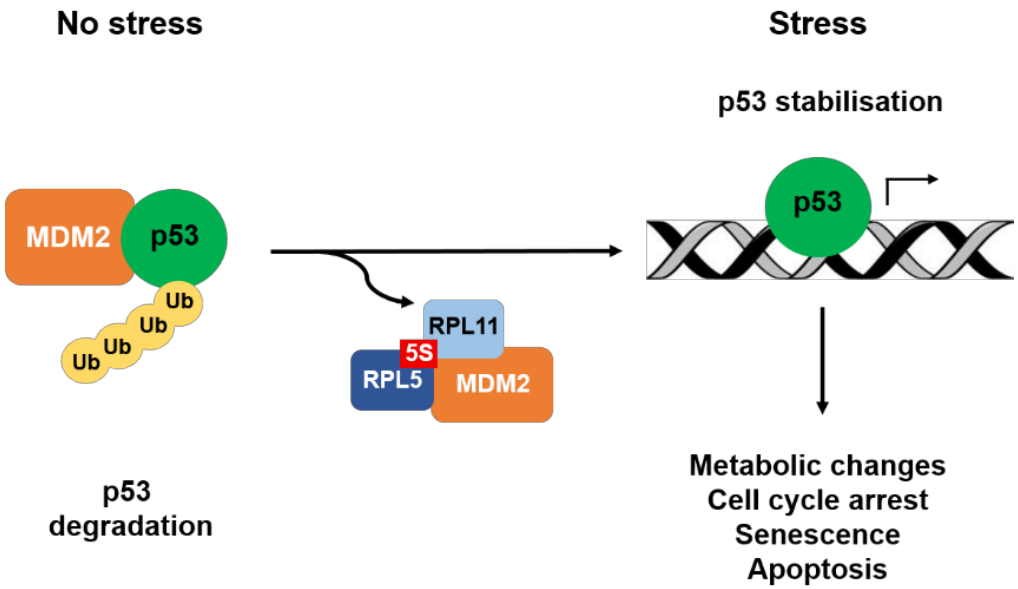

Figure 5.3. Schematic representation of the stabilization of p53 after 5S RNP binding on MDM2. MDM2 is shown in orange, p53 is shown in green and the ubiquitin molecules are shown in yellow. The 5S RNP consists of the 5S rRNA (red), RPL5 (blue) and RPL11 (light blue).

Despite the high conservation and importance of the ubiquitin-ribosomal proteins RPS27a and RPL40, not much is known about their processing or cellular functions in humans. It was recently found that RPS27a is highly expressed in solid tumours and up-regulated in chronic myeloid leukaemia (CML) and acute myeloid leukaemia (AML) patients (Wang et al., 2014). Furthermore, it was found that expression of RPS27a was also elevated in K562 CML cell line, promoting proliferation and inhibiting apoptosis (Wang et al., 2014). This is of particular importance knowing that ribosomopathy patients are highly susceptible in developing leukaemia, especially AML. In addition, RPS27a was shown to be another potential regulator of the p53 inhibition by MDM2. It was found that knockdown of RPS27a reduced the induction of p53 levels after ribosome biogenesis defects and over-expression of RPS27a resulted in p53 activation by inhibition of p53 ubiquitination by MDM2. Finally, RPS27a was shown to bind and inhibit MDM2 when over-expressed, thus resulting in p53 activation (Sun et al., 2011). Yet, it is not clear whether RPS27a interacts with MDM2 as the ubiquitin-ribosomal protein precursor or as the cleaved ribosomal protein.

These studies indicate that the two ubiquitin fusion ribosomal proteins, especially RPS27a, might be key players in the regulation of the p53-MDM2 pathway. However, not much is known about the processing of the ubiquitin-ribosomal protein precursors

or their functions in ribosome biogenesis and cellular signalling. Therefore, the third part of this PhD project aimed to investigate:

- When the ubiquitin-RPS27a or RPL40 precursors are processed for the release of the ubiquitin molecule and ribosomal proteins from the precursor
- The functions of RPS27a and RPL40 in human ribosome biogenesis
- The roles of RPS27a and RPL40 in p53 regulation

5.2 Results

5.2.1 RPS27a- and RPL40-ubiquitin precursors are likely to be processed at very early stages

RPS27a and RPL40 are expressed as ubiquitin-fusion ribosomal proteins (Kimura and Tanaka, 2010), but not much is known about how the precursor is processed to release the ubiquitin molecule and ribosomal proteins. Therefore, I firstly investigated the processing of RPS27a- and RPL40-ubiquitin precursors in human cells. For this, stable U2OS cells lines were created, where the tagged RPS27- or RPL40-ubiquitin proteins were found under a tetracycline promoter to control their expression. A FLAG tag was found at the C-terminus of the protein and an HA tag was added to the N-terminus of the expressed protein, so that the FLAG tag was bound on the ubiquitin and the HA tag was bound on the ribosomal protein (Figure 5.4A).

U2OS cells were treated with different concentrations of tetracycline (0-1000 ng/µl) overnight for expression of the tagged ubiquitin-ribosomal protein RPS27a or RPL40. The whole cell extract was loaded on an SDS-PAGE gel and analysed by Western Blotting. α-HA antibody was used to detect the expressed ribosomal protein and α-FLAG antibody was used to detect the expressed ubiquitin (Figure 5.4B, C). Due to the unavailability of commercial antibodies, the endogenous ribosomal proteins could not be detected.

The RPS27a- or RPL40-ubiquitin proteins were optimally expressed in U2OS cells using 1000ng/µl tetracycline, since both the ribosomal protein and ubiquitin component was expressed in higher levels at this concentration (Figure 5.4B, C). Interestingly, the α-HA antibody revealed the expected cleaved HA-tagged RPS27a (Figure 5.4B) and RPL40 (Figure 5.4C), but there was no indication of the ubiquitin-ribosomal protein precursor. Furthermore, the α-FLAG antibody showed the expected ubiquitin-like phenotype, revealing the conjugated-ubiquitin and histone-ubiquitin (Figure 5.4B, C). However, there was no indication of the ubiquitin-ribosomal protein precursor using the α-FLAG antibody either (Figure 5.4B, C).

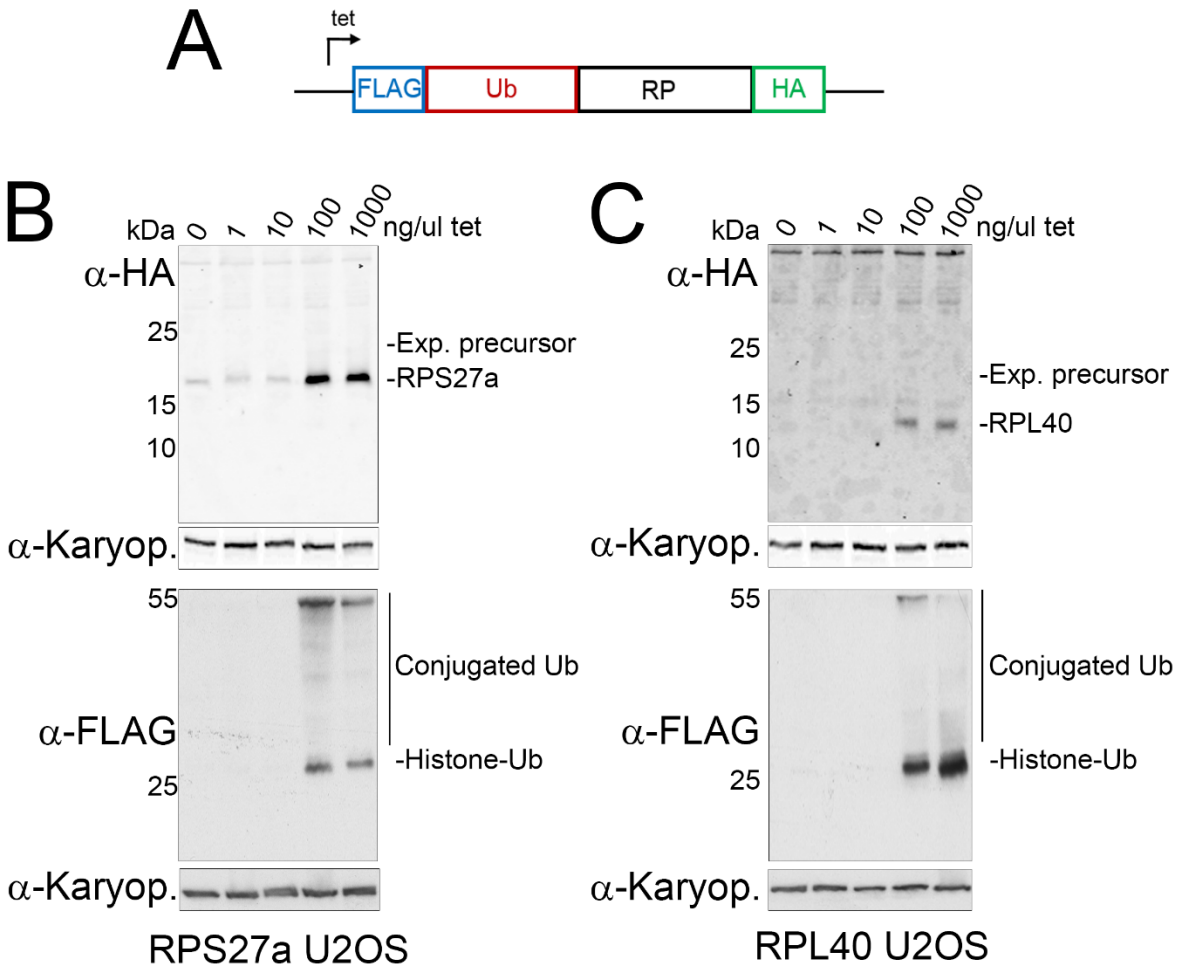

Figure 5.4. The expression of RPS27a and RPL40 in U2OS stable cell lines after tetracycline treatment. (A) Schematic representation of the open reading frame of the ubiquitin-ribosomal proteins as expressed in U2OS cell lines. The FLAG tag (blue) is found at the C-terminus bound on the ubiquitin (red) and the HA tag (green) is found at the N-terminus bound by the ribosomal protein RPS27a or RPL40. **(B-C)** U2OS cells were treated with different concentrations of tetracycline (0-1000ng/µl) (shown on top) overnight (18h) for expression of the ubiquitin fusion RPS27a **(B)** or RPL40 **(C)** proteins (shown at the bottom). The whole cell extract was loaded on an SDS-PAGE gel and analysed by Western blotting using the antibodies shown on the left. The membranes were visualised using the LICOR system (top) or ECL (bottom). Karyopherin (Karyop.) was used as a loading control. The molecular weight (kDa) is shown on the left and the expected precursor, the cleaved RP, the conjugated ubiquitin (Ub) and histone-ubiquitin are shown on the right.

Since the ubiquitin-ribosomal protein precursor could not be seen after tetracycline-inducible expression of the tagged proteins, it was speculated that the precursor is likely to be processed efficiently and, therefore, found in low levels in the cell. I hypothesized that the ubiquitin component might be cleaved when the two ribosomal proteins are integrated in the ribosomal complexes. To test this hypothesis, Actinomycin D (ActD) was used, which blocks RNA polymerase I, inhibiting ribosome biogenesis (Andersen et al., 2005). The tagged proteins were expressed overnight and treatment with ActD was also performed overnight, so that the tagged proteins were expressed after ribosome biogenesis block. The whole cell extract was loaded on an SDS-PAGE gel and analysed by Western Blotting (Figure 5.5).

ActD treatment resulted in a significant decrease of the HA-tagged RPS27a or RPL40 levels (Figure 5.5). This was somewhat expected, since ActD treatment blocks ribosome biogenesis and ribosomal proteins that are not integrated into the ribosome and are known to be unstable (Lam et al., 2007). The levels of ubiquitin did not significantly change after ActD treatment in either case (Figure 5.5), indicating that the production of ubiquitin was as normal and only the ribosomal protein production was affected. Surprisingly, the ubiquitin-fusion RPS27a or RPL40 precursor could not be detected after ActD treatment (Figure 5.5), indicating that the ubiquitin is more likely to be cleaved at very early stages after or during translation.

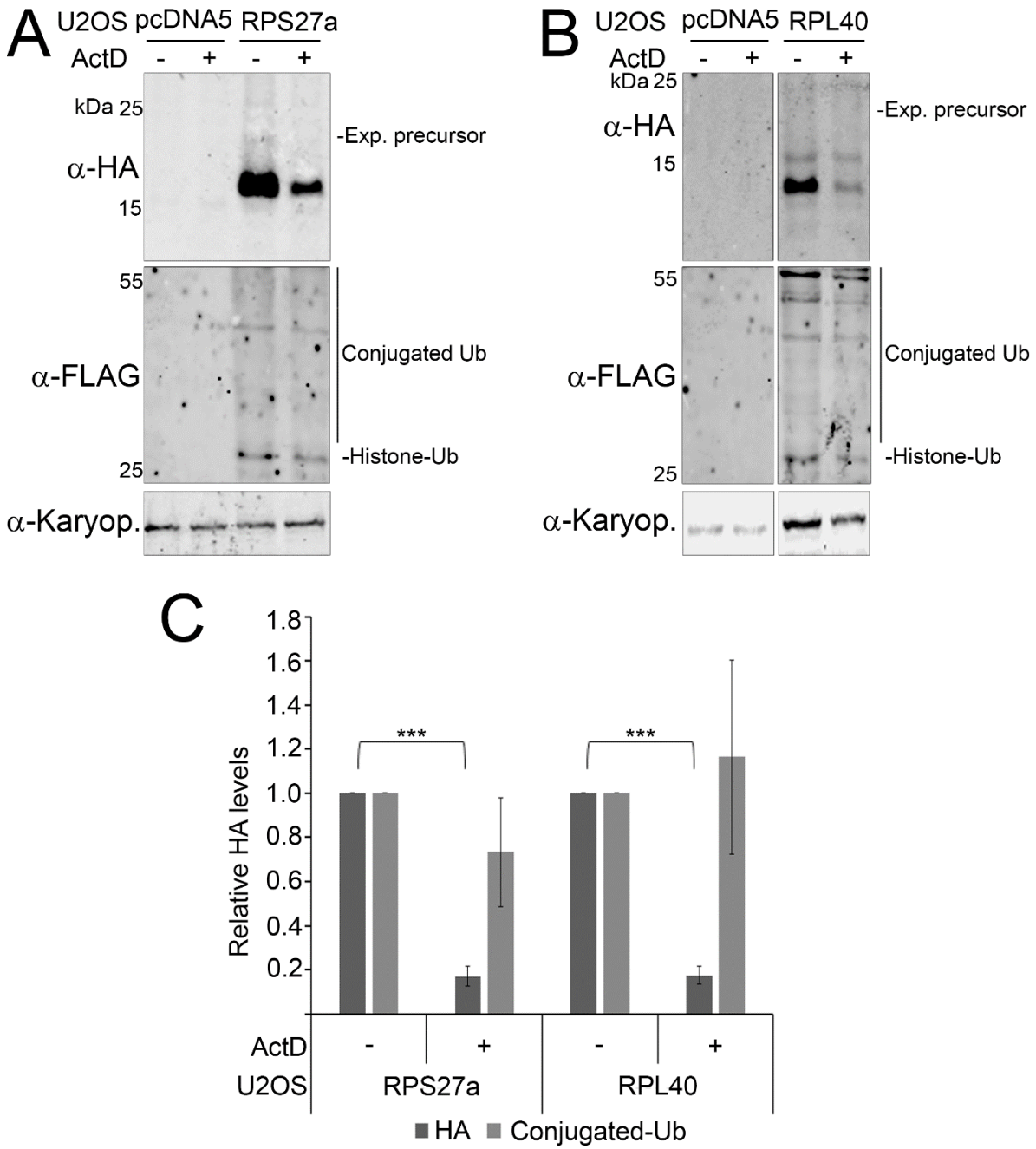

Figure 5.5. Inhibition of ribosome biogenesis resulted in a decrease of the expressed RPS27a and RPL40. (A-B) ActD treatment was performed overnight in U2OS cells expressing the RPS27a **(A)** or RPL40 **(B)** ubiquitin fusion proteins using 1000ng/µl tetracycline. U2OS cells containing the empty pcDNA5 vector, treated with 1000ng/µl tetracycline, were used as a control. In both cases, the whole cell extract was loaded on an SDS-PAGE gel and analysed by Western Blotting using the LICOR system. The antibodies used are shown on the left and Karyopherin (Karyop.) was used as a loading control (shown on the left). The molecular weight (kDa) is shown on the left, and the conjugated ubiquitin and the histone ubiquitin are shown on the right. **(C)** Quantitation of three independent experimental repeats was performed using ImageQuant and the averages of the relative levels of the HA-tagged ribosomal proteins (dark grey) and conjugated ubiquitin (light grey) are represented on the graph. Normalization to the levels of the loading control (α-Karyopherin) was performed for each experiment. The standard error (+/-SEM) is shown by the error bars. Statistical analysis was performed using unpaired t-test and lack of significance values indicates no significant differences as compared to the control. ***p value<0.001.

I then investigated whether specific inhibition of either the small or large ribosomal subunits resulted in a decrease in the levels of the HA-tagged RPS27a or RPL40, but not a change in the ubiquitin levels, as seen by ActD treatment. In order to test this, siRNAs against RPS19 (SSU block) and RPL7 (LSU block) were used, as they are known to affect the SSU and LSU biogenesis respectively (see Chapter 4). Knockdowns of RPS19 or RPL7 were performed for 48h in U2OS cells expressing the tagged ubiquitin-RPS27a or RPL40, where tetracycline was added for 48h as well. Simultaneous treatment of tetracycline and knockdowns allowed for the knockdown to affect the expressed protein as well and not only the endogenous one. The whole cell extract was loaded on an SDS-PAGE gel and analysed by Western blotting, using α-HA antibody to detect the levels of the expressed ribosomal proteins and α-FLAG antibody to detect the levels of the expressed ubiquitin (Figure 5.6).

No signal was detected using the α-HA antibody in U2OS cells containing the empty pcDNA5 vector (Figure 5.6A, B). Knockdown of RPS19 resulted in the significant decrease of the HA-tagged RPS27a as compared to the control (Figure 5.6A, C). However, knockdown of RPL7 did not result in a significant change in the levels of the HA-tagged RPS27a (Figure 5.6A, C). In contrast, knockdown of RPS19 did not result in a significant change on the levels of the HA-tagged RPL40 (Figure 5.6B, C). However, RPL7 knockdown resulted in a significant decrease in the levels of the HA-tagged RPL40 (Figure 5.6B, C). The levels of ubiquitin did not significantly change by knockdown of RPS19 or RPL7 in either case (Figure 5.6), further confirming that the ubiquitin is produced as normal after specific block in either SSU or LSU production.

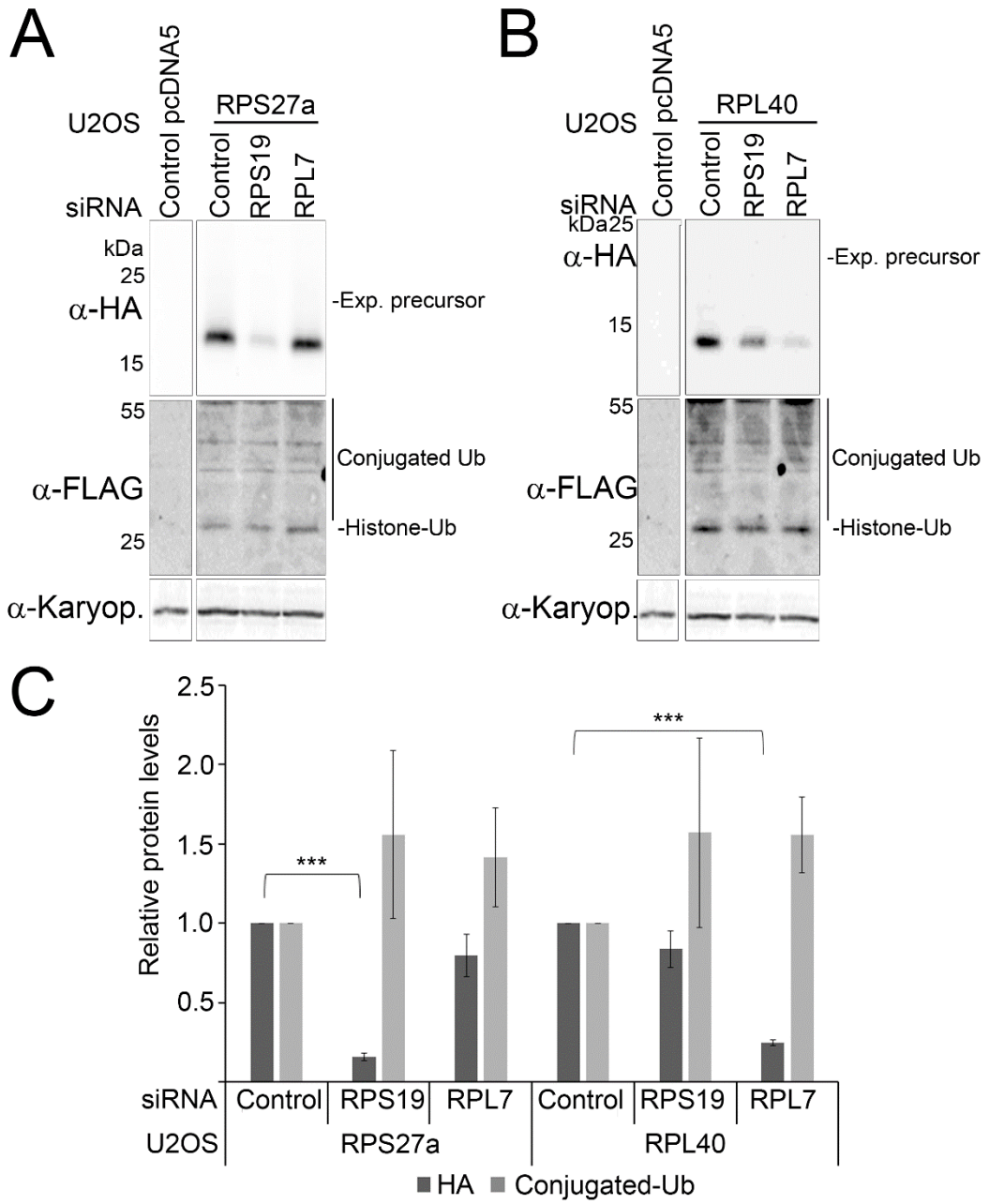

Figure 5.6. SSU and LSU defects affect the levels of RPS27a and RPL40 respectively. (A-B) Knockdowns of RPS19 and RPL7 were performed for 48h in U2OS cells expressing the HA-tagged RPS27a or RPL40, which were treated with 1000ng/µl tetracycline for 48h. U2OS cells containing the empty pcDNA5 vector, treated with 1000ng/µl tetracycline for 48h, were used as a negative control. The whole cell extract was loaded on an SDS-PAGE gel and analysed by Western Blotting using the LICOR system. The antibodies used are shown on the left and Karyopherin (Karyop.) was used as a loading control. The molecular weight (kDa) is shown on the left, the conjugated ubiquitin, histone-ubiquitin and the expected precursor are indicated on the right. **(C)** ImageQuant software was used for quantitation of Western blots. Normalization to the levels of the loading control (α-Karyopherin) was performed for each sample. The graph represents the averages of the relative HA-tagged ribosomal protein levels of three experimental repeats and the error bars show the standard error (+/-SEM). Statistical analysis was performed using an unpaired t-test and absence of significance values indicates no significant differences as compared to the control. ***p value<0.0001.

It is known that ribosomal proteins are produced in excess and the free proteins are quickly degraded by the proteasome (Lam et al., 2007). Since there was no evidence of the ubiquitin-ribosomal protein precursor when ribosome biogenesis was blocked and the ubiquitin was produced as normal (Figures 5.5, 5.6), it was hypothesized that the ubiquitin component might be cleaved before the possible proteosomal degradation of any excess ribosomal proteins, so that the ubiquitin can still be integrated in the ubiquitin pool. In order to test this, U2OS cells expressing the tagged ubiquitin-RPS27a or RPL40 were treated overnight with MG132, a proteosomal inhibitor (Oh et al., 2013). Tetracycline was added to the cells overnight, so that MG132 affected the expressed proteins. The whole cell extract was loaded on an SDS-PAGE gel and analysed by Western Blotting (Figure 5.7).

The levels of the expressed HA-tagged RPS27a did not significantly change when the proteasome was blocked by treatment with MG132 (Figure 5.7A, C). In contrast, the levels of the expressed HA-tagged RPL40 were significantly increased after inhibition of the proteasome by MG132 (Figure 5.7B, C). These results indicate that RPL40 is probably produced in excess and rapidly turned-over by the proteasome. The levels of ubiquitin were not significantly affected by treatment with MG132 in either case, indicating that the ubiquitin is produced as normal. No accumulation of the expected ubiquitin-fusion ribosomal protein precursor was detected after inhibition of the proteasome by MG132 (Figure 5.7).

Taken together, these data indicated that the processing of the ubiquitin-fusion RPS27a and RPL40 is more likely to occur at very early stages after translation, before their integration in the ribosome or the proteosomal degradation of RPL40.

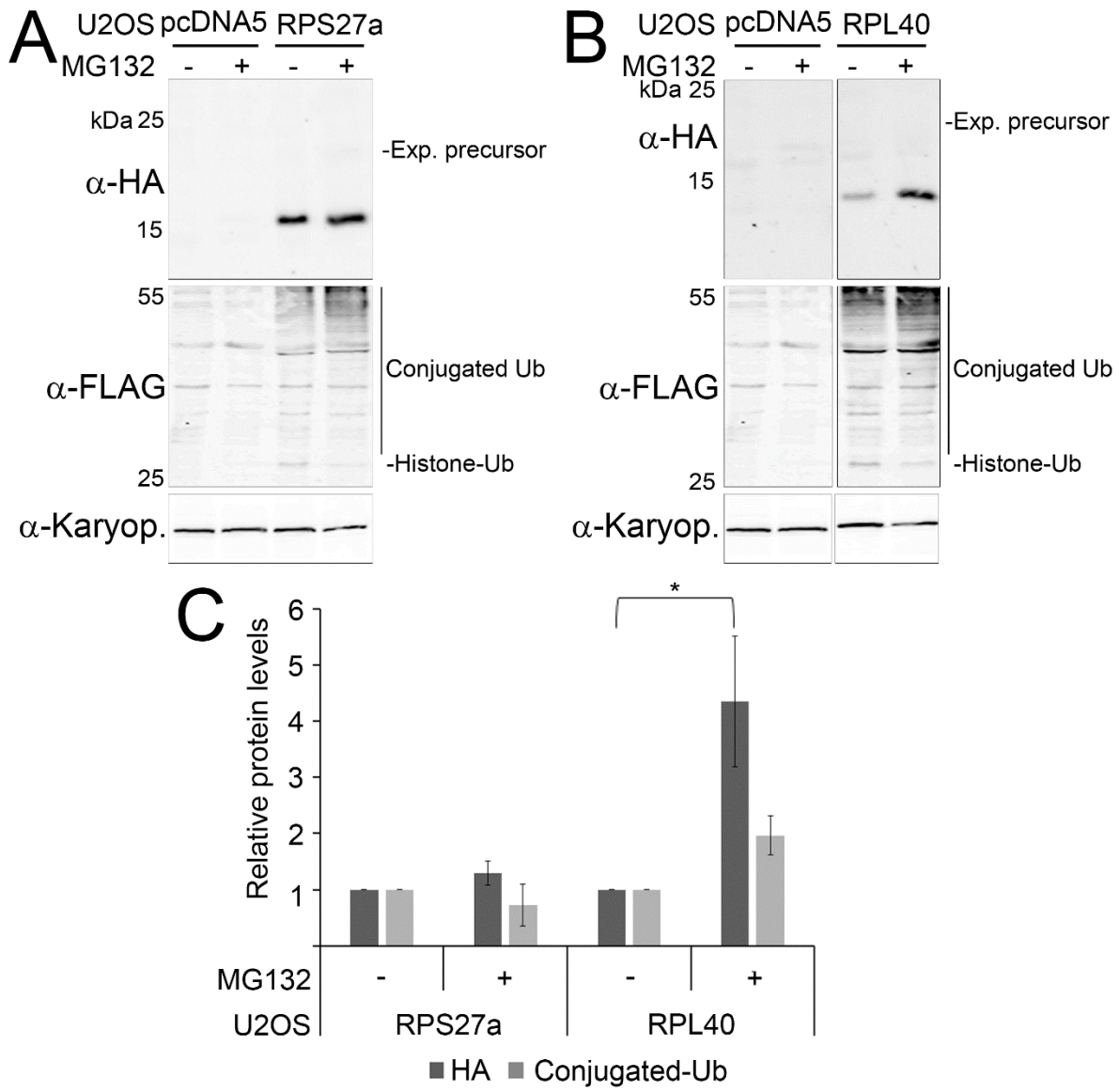

Figure 5.7. Inhibition of the proteasome resulted in stabilization of RPL40 but not RPS27a. (A-B) MG132 treatment was performed overnight in U2OS cells expressing the ubiquitin fusion RPS27a **(A)** or RPL40 **(B)**. 1000ng/µl tetracycline was added to the cells overnight. U2OS cells containing the pcDNA5 empty vector, treated with 1000ng/µl tetracycline overnight, were used as a control. The whole cell extract was loaded on an SDS-PAGE gel and analysed by Western Blotting using the LICOR system. The antibodies used are shown on the left and Karyopherin (Karyop.) was used as a loading control (shown on the left). The molecular weight (kDa) is shown on the left, the expected precursor, conjugated ubiquitin and histone-ubiquitin are shown on the right of each panel. **(C)** ImageQuant software was used for quantitation of the Western Blots. The average relative levels of the expressed RPS27a or RPL40 of three independent experimental repeats is represented on the graph, and the error bars show the standard error (+/-SEM). The values of each sample were normalized to the loading control values (α-Karyopherin). Statistical analysis was performed using unpaired t-test and absence of significance values indicates no significant differences as compared to the untreated cells. *p value<0.05.

5.2.2 RPS27a and RPL40 are found in the small and large ribosomal subunit complexes respectively

I next investigated where the HA-tagged RPS27a and RPL40 localize in the cell. In order to do this, immunofluorescence was performed using U2OS cells containing the pcDNA5 empty vector or U2OS cells expressing the HA-tagged RPS27a or RPL40 proteins. An α-FLAG antibody was used to stain the cleaved FLAG-tagged ubiquitin and an α-HA antibody was used to detect the cleaved HA-tagged ribosomal protein. DAPI was used for DNA staining (Figure 5.8).

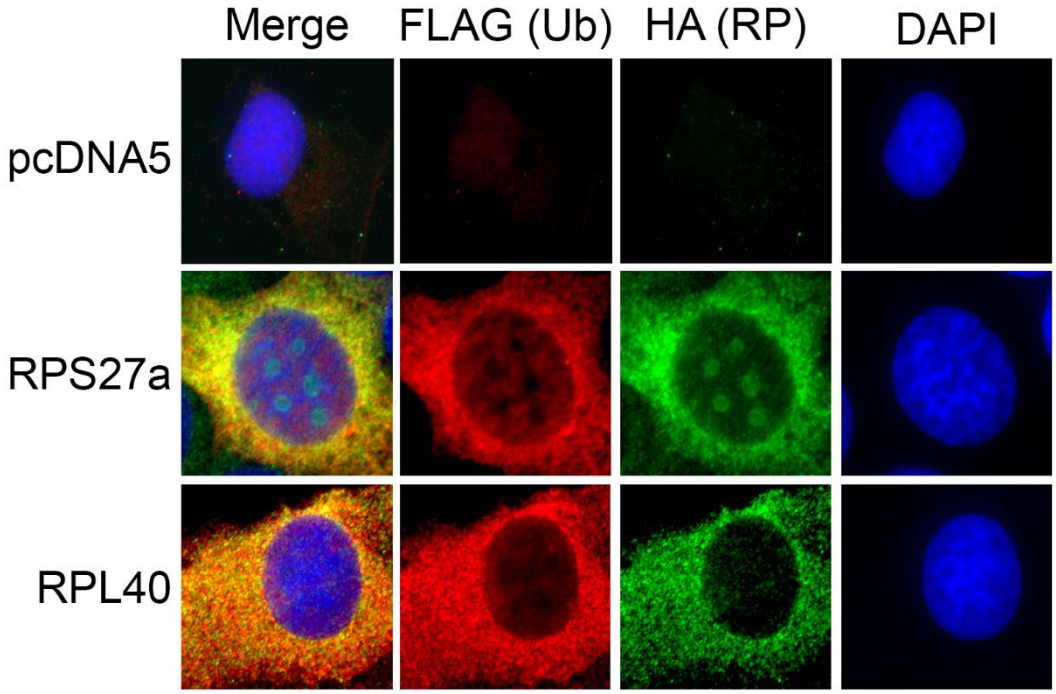

Figure 5.8. The HA-tagged RPS27a or RPL40 show different localization patterns in U2OS cells. U2OS cells containing the empty pcDNA5 vector were used as a control. 1000ng/µl tetracycline was added overnight to U2OS cells expressing the tagged ubiquitin-RPS27a or RPL40, or containing the pcDNA5 vector. Immunofluorescence followed, using an α-FLAG antibody to detect the levels of the FLAG-tagged ubiquitin (red), whereas an α-HA antibody was used to detect the levels of the HA-tagged ribosomal protein (green). DAPI was used for DNA staining (blue). The cells were visualized using the Zeiss Axiovision inverted microscope and software.

U2OS cells containing the pcDNA5 empty vector showed a clear DAPI staining but only background signal was seen when either the α-HA or the α-FLAG antibodies were used (Figure 5.8). HA-tagged RPS27a was localized in both the nucleolus and the cytoplasm (Figure 5.8), which resembled the localization pattern of other ribosomal proteins, such as RPL11 (Chapter 4). In contrast, HA-tagged RPL40 was found mainly in the cytoplasm and almost not at all in the nucleus (Figure 5.8). The FLAG-tagged

ubiquitin was found mainly in the cytoplasm, with some traces in the nucleus but not in the nucleolus (Figure 5.8). This agrees with previous data showing that the FLAG-tagged ubiquitin was found in higher levels as conjugated ubiquitin (Figure 5.4), which is found in the cytoplasm, and histone ubiquitin (Figure 5.4), which is found in the nucleus.

I next wanted to identify which complexes these proteins are found in. To do this, I used glycerol gradient analysis to separate the free and the ribosomal complexes. U2OS cells were expressing the HA-tagged RPS27a or RPL40 after addition of tetracycline overnight. The whole cell extract was fractionated using a 10-40% glycerol gradient. Each fraction was loaded on an SDS-PAGE gel and analysed by Western blotting (Figure 5.9). An α-HA antibody was used to identify the HA-tagged ribosomal proteins expressed, and an α-RPL7 antibody was used as a control to identify the endogenous ribosomal protein RPL7 (Figure 5.9).

The HA-tagged RPS27a was found in the small ribosomal subunit complexes (Figure 5.9, fractions 6-9) and no HA-tagged RPS27a was found in the non-ribosomal complexes (Figure 5.9, fractions 1-5). The HA-tagged RPL40 was also found in the large ribosomal subunit complexes (Figure 5.9, fractions 10-15) and at the same place where the SSU complexes accumulate (Figure 5.9, fractions 6-9). In contrast with RPS27a, the HA-tagged RPL40 was also found in the non-ribosomal complexes (Figure 5.9, fractions 1-5).

The accumulation of the HA-tagged RPS27a in the SSU complexes was expected, as it is a part of the SSU, as was the accumulation of the HA-tagged RPL40 in the LSU complexes, as it is a part of the LSU. Interestingly, the HA-tagged RPL40 accumulated in the non-ribosomal complexes, but no nuclear accumulation was seen during immunofluorescence (Figure 5.8). It is possible that RPL40 is more unstable because it is found as a free ribosomal protein and gets degraded quickly by the proteasome.

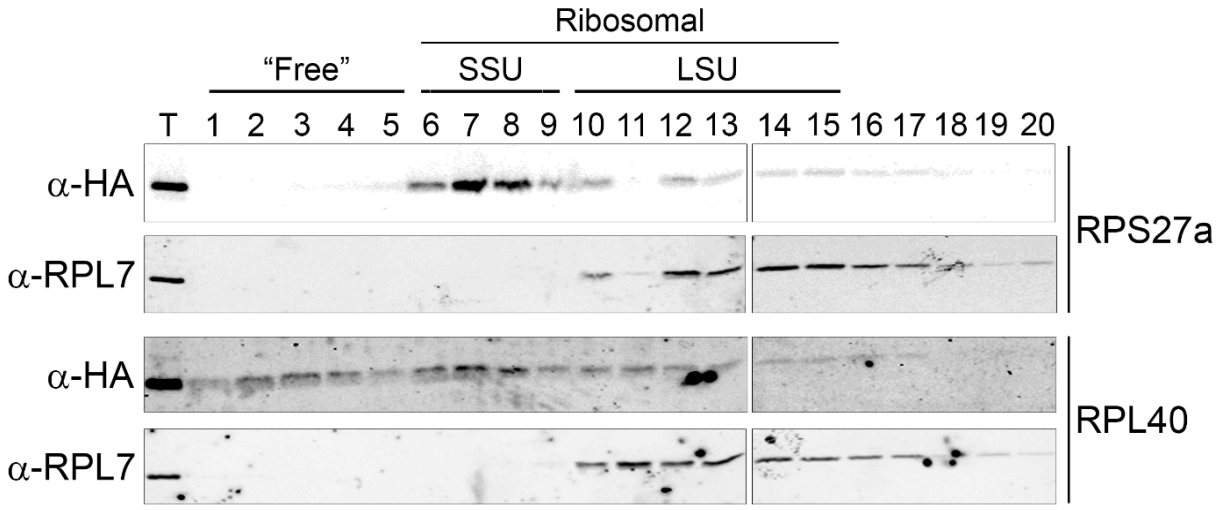

Figure 5.9. Gradient analysis of RPS27a and RPL40 expressing U2OS cells. U2OS expressing the HA-tagged RPS27a or RPL40 (shown on the right) were targeted for glycerol gradient analysis. The whole cell extract (approximately $8x10^6$ cells) was loaded on a 10-40% glycerol gradient and fractionated by centrifugation. The fractions were loaded on an SDS-PAGE gel and analysed by Western Blotting using the LICOR system. The antibodies used are shown on the left. "T" represents 10% of the total sample before fractionation. Fractions 1-5 represent the free complexes, fractions 6-9 represent the small ribosomal subunit complexes (SSU) and fractions 10-15 represent the large ribosomal subunit complexes (LSU) (shown at the top).

5.2.3 RPS27a and RPL40 are required for SSU and LSU production respectively

It is known that RPS27a and RPL40 are ribosomal proteins (Kimura and Tanaka, 2010). I, therefore, investigated their role in the accumulation of the small or large ribosomal subunits. Knockdown efficiency was tested by RT-PCR due to the lack of commercially available antibodies. Knockdowns were performed for 48h in U2OS cells and RNA was extracted, followed by reverse transcription and PCR using primers specific for the human RPS27a or RPL40 open reading frame (ORF). Primers specific the levels of the house-keeping mRNA GAPDH were used as a loading control (Figure 5.10). As compared to the control, knockdown of either RPS27a or RPL40 resulted in a major decrease in the mRNA levels of the ribosomal proteins (Figure 5.10), showing that the knockdowns were efficient.

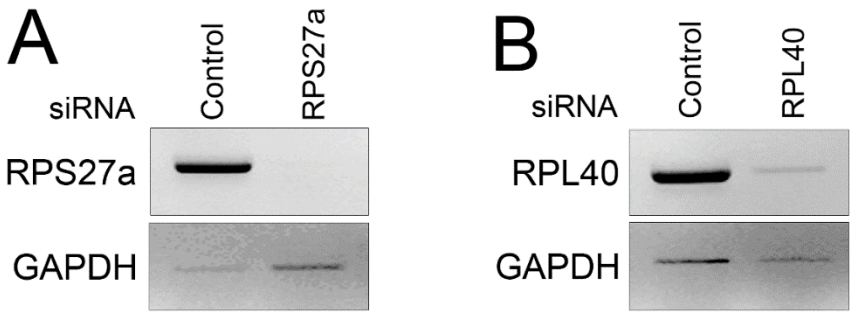

Figure 5.10. The efficiency of RPS27a and RPL40 knockdowns in U2OS cells. Knockdowns of RPS27a **(A)** or RPL40 **(B)** were performed for 48h in U2OS cells. RNA was extracted and RT-PCR was performed using primers specific for RPS27a **(A)** or RPL40 **(B)**. Primers recognizing GAPDH were used as a loading control. The samples were loaded on a 2% agarose/1x TBE DNA gel and visualized using the Typhoon Phosphorimager.

Next, I investigated the importance of these proteins to human ribosome biogenesis. Knockdowns were performed in U2OS cells for 48h and pulse-chase labelling followed, where the phosphate was depleted for 1h using phosphate-free media. Next, radiolabelled (^{32}P) phosphate was added to the cells for 1h and the cells were then left to grow in normal media for 3h (chase). RNA was extracted from the cells, loaded on a glyoxal-agarose gel, and transferred on a Hybond N membrane, which was visualized by the Typhoon Phosphorimager (Figure 5.11A).

Pulse-chase labelling revealed that the levels of the newly-synthesized 18S rRNA after RPS27a knockdown were barely visible as compared to the control (Figure 5.11A). Furthermore, the levels of the mature 18S rRNA were also reduced, as seen by the ethidium bromide staining (UV) (Figure 5.11A). The levels of the other newly-synthesized rRNAs (47/45S, 32S and 28S) were also lower after RPS27a knockdown as compared to the control, whereas the loading was approximately the same as seen by the 28S UV levels (Figure 5.11A). After RPL40 knockdown the levels of the newly synthesized 28S rRNA were lower by approximately 30% as compared to the control (Figure 5.11A). The ratio of the mature 28S to 18S rRNA, as seen by the ethidium bromide staining (UV) was decreased by approximately 30% after knockdown of RPL40 as compared to the control (Figure 5.11A), showing a reduction in the levels of the mature 28S rRNA as well. Furthermore, no major change was observed in the levels of the newly-synthesized 47/45S, 32S or 18S rRNAs after RPL40 as compared to the control (Figure 5.11A). These data indicated that RPS27a is required for SSU biogenesis, whereas RPL40 is required for LSU biogenesis, as expected. Furthermore,

since knockdown of RPS27a affected the levels of the newly-synthesized 47/45S, 32S and 28S rRNAs as well (Figure 5.11A), it is possible that it is an important protein for transcription.

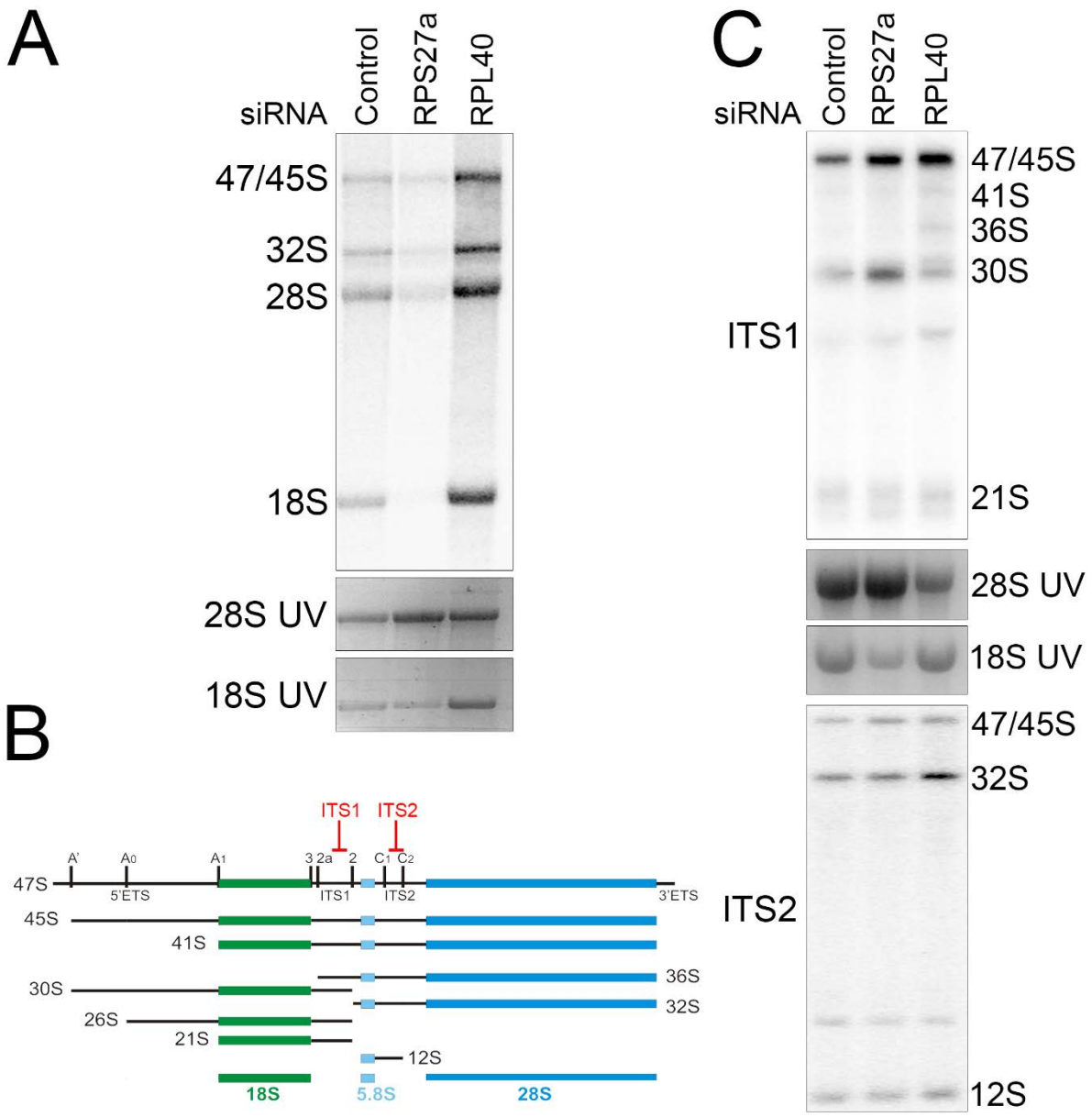

Figure legend on the next page.

Figure 5.11. RPS27a and RPL40 knockdowns affect the SSU and LSU biogenesis respectively. (A) Knockdowns of RPS27a or RPL40 were performed for 48h in U2OS cells, followed by pulse-chase labelling, where the phosphate was depleted for 1h. Radiolabelled (^{32}P) phosphate was added for 1h and the cells were left to grow in normal media for 3h (chase). The RNA was extracted, loaded on a 1.2% agarose/glyoxal gel and transferred on a Hybond N membrane. The RNA was visualized using a Typhoon Phosphorimager. The 28S and 18S rRNA ethidium bromide staining (UV) was used as a loading control. **(B)** Schematic representation of the human LSU (blue) and SSU (green) precursor and mature rRNAs. ITS1 and ITS2, recognized by the radiolabelled (^{32}P) probes, are marked in red (Adapted from (Sloan et al., 2013c)). **(C)** RNA was extracted after knockdowns of RPS27a or RPL40 in U2OS cells for 48h, and loaded on a 1.2% agarose/glyoxal gel. The RNA was transferred on a Hybond N membrane, which was incubated with radiolabelled (^{32}P) probes recognizing ITS1 or ITS2 (indicated on the left) for identification of the precursor rRNAs (shown on the right) whereas 28S and 18S rRNA ethidium bromide staining (UV) was used as a loading control.

In order to identify when these proteins act during ribosome biogenesis in humans, knockdowns were performed for 48h in U2OS cells and RNA was extracted and loaded on a glyoxal-agarose gel, which was analysed by Northern blotting using radiolabelled (^{32}P) probes recognizing ITS1 and ITS2 (Figure 5.11B) (Sloan et al., 2013c). The levels of the 28S or 18S rRNA visualized by ethidium bromide staining (UV) were used as a loading control for RPS27a or RPL40 knockdowns respectively (Figure 5.11C).

RPS27a knockdown resulted in an accumulation of the 30S SSU rRNA precursor as compared to the control (Figure 5.11C) and a slight decrease in 21S rRNA levels was observed, demonstrating that RPS27a is needed for the processing of the 30S SSU rRNA precursor. No major change in the levels of the 47/45S, 41S, 32S, or 12S rRNA precursors after RPS27a knockdown (Figure 5.11C). In contrast, RPL40 knockdown resulted in the accumulation of the 36S and 32S LSU rRNA precursors as compared to the control (Figure 5.11C). Furthermore, a slight accumulation of the 41S rRNA precursor was observed (Figure 5.11C) but no other major change was observed in the levels of the 47/45S, 30S, 26S, 21S or 12S rRNA precursors after RPL40 was knocked down (Figure 5.11C). These data showed that RPS27a is required for the SSU biogenesis for cleavage of the 5' ETS, whereas RPL40 is required for the LSU biogenesis for cleavage at site 2 of ITS1.

5.2.4 Knockdowns of RPS27a and RPL40 in U2OS cells do not affect the levels or activity of p53

Defects in ribosome biogenesis cause p53 accumulation via the 5S RNP-MDM2 pathway (Chapter 4, Sloan et al., 2013a). Since RPS27a and RPL40 knockdowns resulted in SSU and LSU biogenesis defects respectively, I wanted to investigate whether they also affected p53 levels. For this, siRNA-mediated knockdowns of RPS27a or RPL40 were performed in U2OS cells for 48h, and the whole cell extract was loaded on an SDS-PAGE gel and analysed by Western Blotting to detect p53 and p21 levels. Furthermore, in order to investigate the activity of p53, knockdowns were performed for 48h in U2OS cells expressing p53-driven luciferase. However, there was no investigation of p21 mRNA levels or other p53 downstream targets for measuring p53 activity. The whole cell extract was treated according to the manufacturer's instructions (Promega Luciferase Kit) and the luciferase levels were analysed using a Luminometer (Figure 5.12).

ActD treatment was used as a positive control, and resulted in a 6-fold significant increase in p53-driven luciferase levels as compared to the plain, untreated cells (Figure 5.12C). The knockdown of RPS27a or RPL40 did not result in a significant change in p53 protein levels (Figure 5.12A, B). Furthermore, neither knockdown resulted in a change of p21 levels, and the slight decrease seen here was due to experimental variation (Figure 5.12A). In order to confirm that p53 activity was not induced, the levels of p53-driven luciferase were measured (Figure 5.12C), since p53 can be induced in these cells without changing p53 levels. Knockdowns of RPS19, which affects SSU production (Chapter 4), or RPL7 or RPL18, which affect LSU production (Chapter 4), resulted in a significant increase in p53-driven luciferase levels (Figure 5.12C). In contrast, knockdowns of RPS27a or RPL40 did not result in a significant change in the p53-driven luciferase levels (Figure 5.12C). These data indicated that RPS27a or RPL40 do not affect p53 levels or activity in U2OS cells, despite the fact that they result in ribosome biogenesis defects.

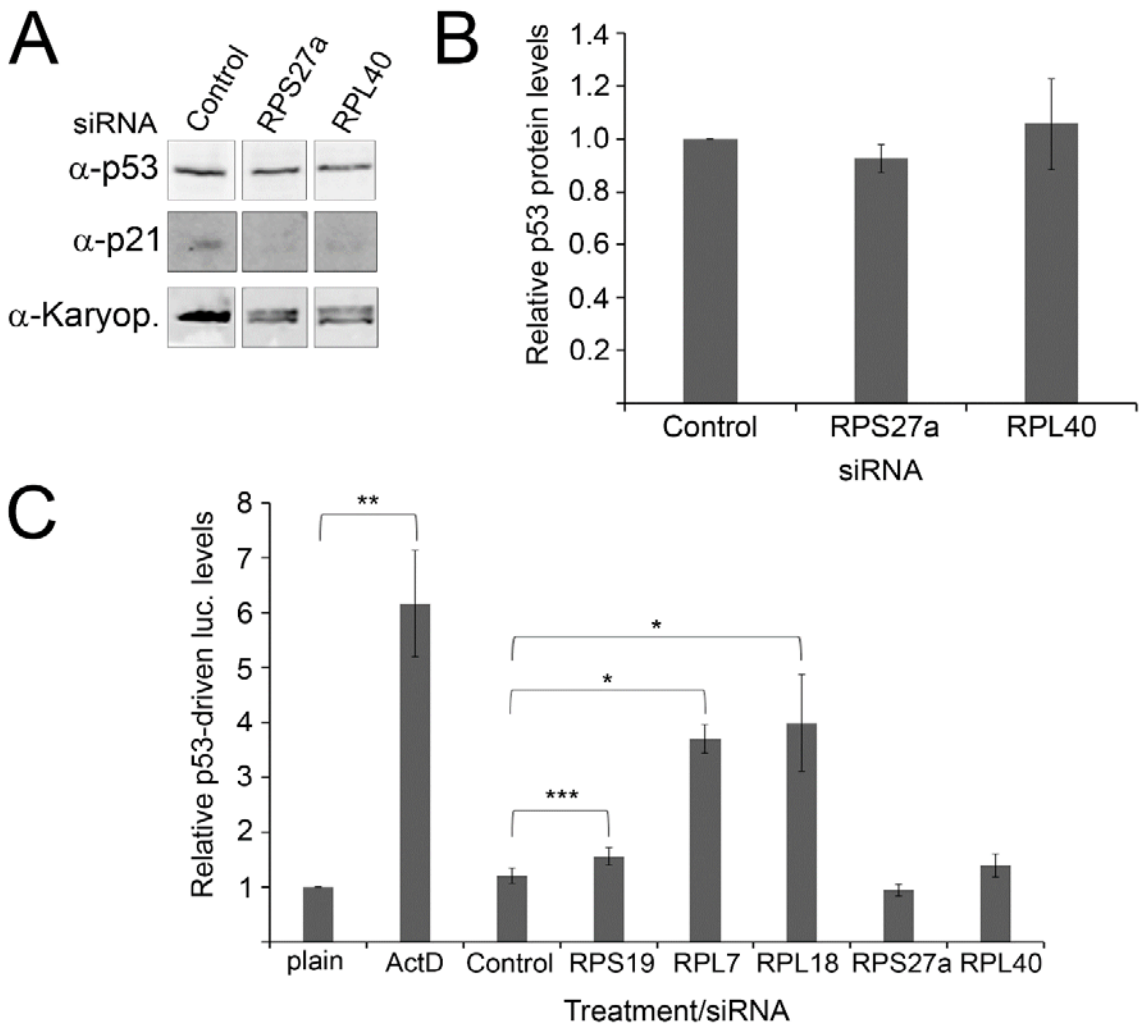

Figure 5.12. RPS27a or RPL40 knockdowns do not affect the levels or activity of p53 in U2OS cells. (A) siRNA treatment of U2OS cells was performed for 48h. Whole cell extract for knockdown cells was loaded on an SDS-PAGE gel and analysed by Western Blotting using the LICOR system. The antibodies used are shown on the left and Karyopherin (Karyop.) was used as a loading control. **(B)** ImageQuant software was used for quantitation of the western blots. The graph represents the averages of p53 protein relative levels of three experimental repeats and the error bars show standard error (+/-SEM). Normalization of the value of each sample to the loading control values (α-Karyopherin) was performed. Statistical analysis was performed using an unpaired t-test and absence of significance values indicates no significant differences compared to the control. **(C)** U2OS cells expressing p53-driven luciferase were treated with ActD overnight or the respective siRNAs for 48h. Non-treated U2OS cells are shown as “plain” (see Chapter 4). The graph represents the average p53-driven luciferase levels of three experimental repeats and the error bars represent the standard error (+/-SEM). Normalization to the cell numbers measured by Bradford assay in each sample was performed. Statistical analysis was performed using an unpaired t-test and absence of significance values indicates no significant differences compared to the control. *p value<0.05, **p value<0.01, ***p value<0.0001.

Since p53 levels or activity were not changed after RPS27a or RPL40 knockdowns, I hypothesized that the knockdowns would have no change in the cell cycle. To confirm this, knockdowns of RPS27a or RPL40 were performed in U2OS cells for 48h, and overnight treatment with ActD was used as a positive control. The cells were then fixed in 70% ethanol and the DNA was stained with propidium iodide, before analysed using the FACS Canto II flow cytometer and software for cell cycle analysis.

As previously (Chapter 4), there was a G1 and G2/M cell cycle arrest after ActD treatment as expected as compared with the non-treated cells (Figure 5.13A, B, F). After knockdown of RPS27a or RPL40, there was no significant difference between G1, S or G2/M phase as compared to the control (Figure 5.13C-F). These results showed that RPS27a or RPL40 knockdowns did not affect the regulation of the cell cycle in U2OS cells, consistent with the lack of p53 induction. These results indicated that, while RPS27a and RPL40 knockdowns induced ribosome biogenesis defects, they did not induce p53, which is consistent with previous data showing that RPS27a knockdown did not result in p53 activation in U2OS cells (Sun et al., 2011).

So far I have shown that knockdowns of the ribosomal proteins RPS27a or RPL40 do not change the levels or activity of p53. The only other two ribosomal proteins showing this phenotype is RPL5 and RPL11, which are components of the signalling pathway connecting ribosome biogenesis and p53 signalling (Pelava et al., 2016). Therefore, I wanted to investigate whether knockdowns of RPS27a or RPL40 prevent the activation of p53 after ribosome biogenesis defects, similarly to RPL5 and RPL11. Knockdowns of RPS27a or RPL40 were performed in U2OS cells for 48h and ActD was added to the cells overnight, for inhibition of ribosome production. The whole cell extract was loaded on an SDS-PAGE gel and analysed by Western blotting for detection of p53 and p21 (Figure 5.14).

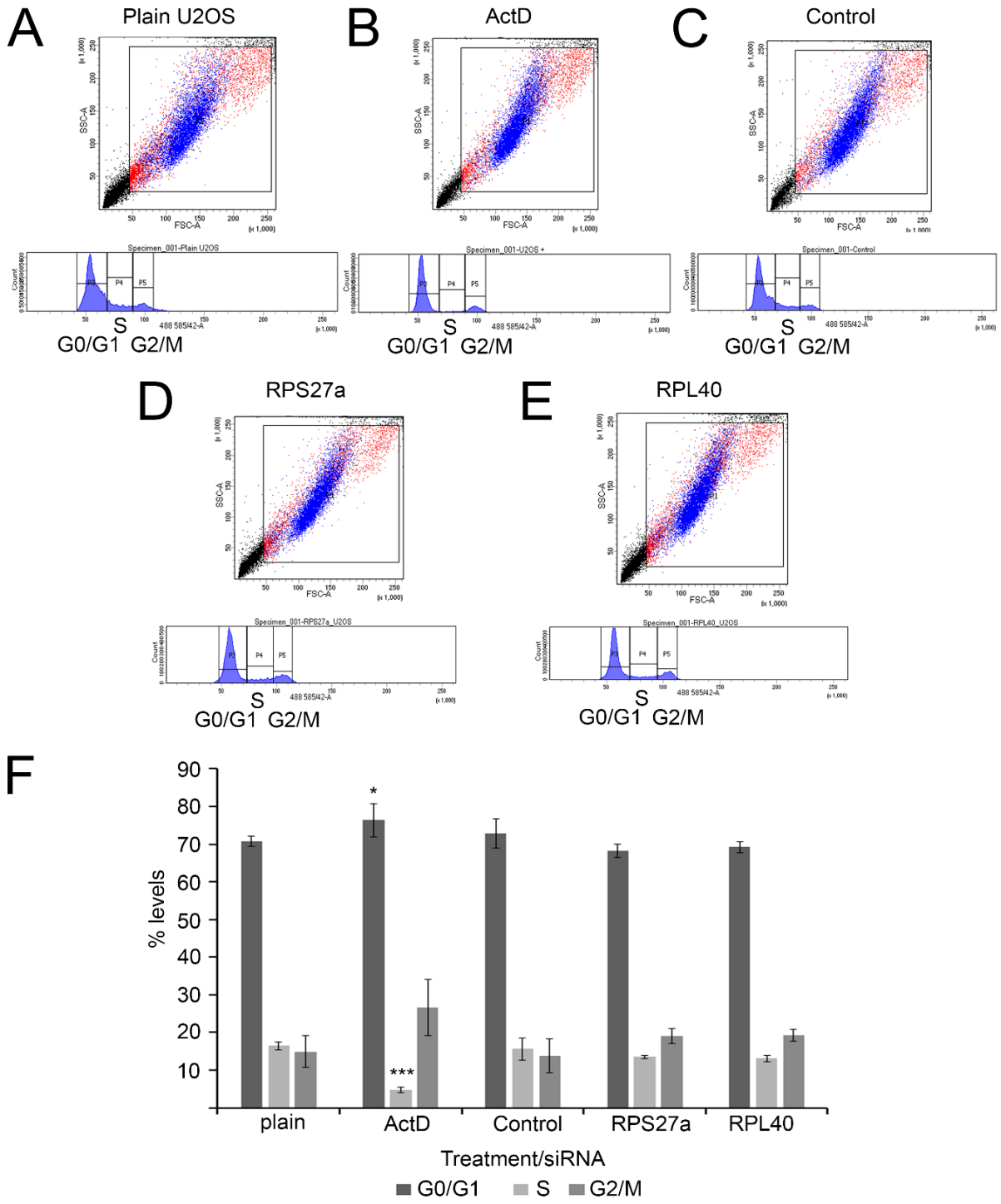

Figure 5.13. RPS27a or RPL40 knockdowns have no effect on cell cycle in U2OS cells. (A-E) ActD treatment was performed overnight, siRNA treatment was performed for 48h in U2OS cells and non-treated U2OS cells are shown as “plain U2OS”. The cells were fixed in 70% ethanol and the DNA was stained with propidium iodide. Cell cycle analysis was performed using the FACS Canto II flow cytometer. The first two samples are the same as the ones presented in Chapter 4. **(F)** The graph represents the averages of three independent experimental repeats of the percentage levels of G0/G1 (dark grey), S (light grey) or G2/M (grey) phases. The error bars show the standard error (+/-SEM). Statistical analysis was performed using an unpaired t-test and absence of significance values indicates no significant difference as compared to the control. *p value<0.05, ***p value<0.001.

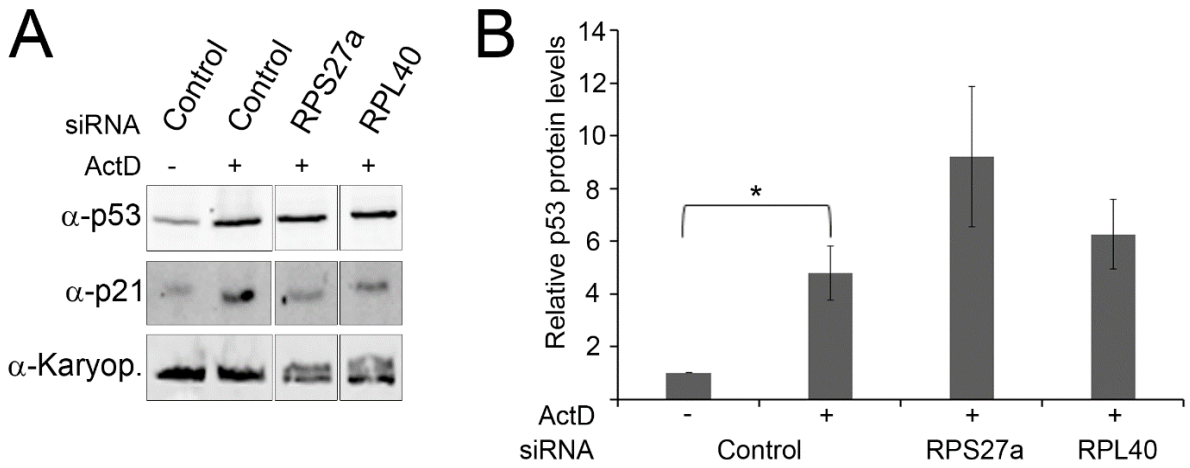

Figure 5.14. Knockdown of RPS27a or RPL40 does not diminish the p53 induction caused by ribosome biogenesis defects. (A) Knockdowns of RPS27a or RPL40 were performed in U2OS cells for 48h, which were treated with ActD overnight (18h). The whole cell extract was loaded on an SDS-PAGE gel and analysed by Western blotting using the antibodies shown on the left. The membranes were visualised using the LICOR system and Karyopherin (Karyop.) was used as a loading control. **(B)** ImageQuant software was used for quantitation of the western blots. The graph represents the relative p53 levels of three experimental repeats after normalisation to the loading control (Karyop.) and the control. The error bars indicate standard error (+/-SEM) and statistical analysis was performed using an unpaired t-test. Absence of significance values indicates no significant differences as compared to the ActD-treated control. *p value<0.05.

Treatment with ActD in control cells resulted in a 4-fold increase in p53 levels (Figure 5.14A, B) and in an increase in p21 levels (Figure 5.12A), indicating an increase in p53 activity, even though p21 mRNA levels or other p53 downstream targets were not assessed. Knockdowns of either RPS27a or RPL40 in U2OS cells treated with ActD did not significantly change the levels of p53 as compared to the ActD-treated control cells (Figure 5.14A, B). Furthermore, the levels of p21 after knockdowns of RPS27a or RPL40 in ActD-treated cells remained mostly unaffected as compared to the ActD-treated control cells, and the slight decrease seen here is due to experimental variation (Figure 5.14A). These results indicate that RPS27a or RPL40 do not induce p53, but they also do not prevent its activation after ribosome production defects. This is not the case with knockdown of RPL5 and RPL11. This is different from previously published data showing that RPS27a knockdown diminished the induction of p53 after ribosome biogenesis defects with ActD in U2OS cells (Sun et al., 2011).

5.2.5 Over-expression of RPS27a or RPL40 results in an increase in p53 levels with reduced activity

Surprisingly, I have shown that knockdown of either RPS27a or RPL40 did not result in a change in p53 levels or activity in U2OS cells. A recent study has shown that RPS27a overexpression resulted in a p53 increase due to inhibition of MDM2 in U2OS cells (Sun et al., 2011). I, therefore, wanted to investigate whether overexpression of RPS27a or RPL40 affected p53 levels or activity. For this, tetracycline was added to U2OS cells expressing the tagged RPS27a or RPL40 proteins overnight. The whole cell extract was loaded on an SDS-PAGE gel and analysed by Western Blotting to monitor p53 and p21 levels (Figure 5.15). Over-expression of RPS27a or RPL40 resulted in a significant 5-fold p53 increase as compared to the U2OS cells containing the empty pcDNA5 vector (Figure 5.15). Surprisingly, even though the p53 levels were elevated, no significant difference was observed in the levels of p21 after expression of the HA-tagged RPS27a or RPL40 (Figure 5.15). These results indicate that overexpression of the HA-tagged RPS27a or RPL40 results in an increase in p53 levels with reduced activity, even though p21 mRNA levels or other p53 downstream targets were not assessed for p53 activity.

I next wanted to see whether over-expression of RPS27a or RPL40 can affect p53 levels when ribosome biogenesis is blocked. To test this, I used overnight treatment with ActD to block rRNA transcription. Tetracycline was added to the cells overnight, as previously. Treatment with ActD in U2OS containing the empty pcDNA5 vector resulted in a significant 2-fold p53 increase and a significant 5-fold increase in p21 levels as compared to the non-treated cells, indicating an increase in p53 levels and activity as expected (Figure 5.15). ActD treatment in U2OS cells expressing the HA-tagged RPS27a or RPL40 did not result in a significant change in p53 levels as compared to the non-ActD treated U2OS cells expressing the HA-tagged ribosomal proteins (Figure 5.15). However, ActD treatment resulted in a significant p21 increase in U2OS cells expressing either HA-tagged RPS27a or RPL40 as compared to the non-treated U2OS cells expressing the HA-tagged ribosomal proteins (Figure 5.15). Interestingly, the levels of p21 after ActD treatment in U2OS cells expressing the HA-tagged RPS27a or RPL40 were significantly lower than the levels of p21 in the ActD-treated U2OS cells containing the empty pcDNA5 vector (Figure 5.15).

These results indicated that expression of the HA-tagged RPS27a and RPL40 resulted in a stabilisation of p53 levels but not activity, which is different from previously published data showing that over-expression of RPS27a leads to an increase in both p53 levels and activity (Sun et al., 2011). Furthermore, these results show that over-expression of RPS27a or RPL40 results in a decreased p53 activity after ribosome biogenesis defects.

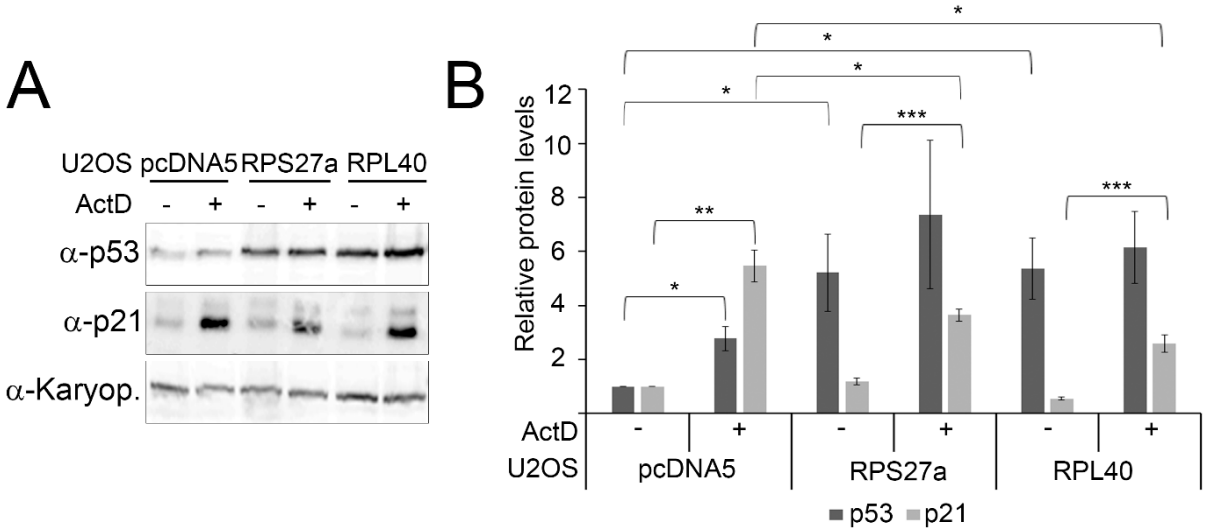

Figure 5.15. RPS27a and RPL40 over-expression results in a stabilisation in p53 levels, but not activity, even after ribosome biogenesis defects. (A) ActD treatment was performed overnight in U2OS cells containing the empty pcDNA5 vector or expressing the HA-tagged RPS27a or RPL40. Tetracycline was added to the cells overnight and the whole cell extract was loaded on an SDS-PAGE gel. Western blotting analysis was performed using the antibodies shown on the left and the membranes were visualized using the LICOR system. Karyopherin (Karyop.) was used as a loading control. **(B)** ImageQuant software was used for quantitation of western blots. Normalization of each sample to the levels of the loading control (α-Karyopherin) was performed and the averages of the relative p53 and p21 levels of three independent experimental repeats are represented on the graph. The error bars show standard error (+/-SEM) and statistical analysis was performed using an unpaired t-test. Absence of significance values indicates no significant difference. *p value<0.05, **p value<0.01, ***p value<0.001.

5.2.6 RPS27a and RPL40 knockdowns result in an increase of p53 levels in both MCF7 and LNCaP cells

Since RPS27a and RPL40 knockdowns resulted in no change in p53 levels in U2OS cells, I wanted to investigate whether these effects were cell-type specific. I, therefore, repeated the knockdowns in breast cancer MCF7 cells and prostate cancer LNCaP cells. The knockdown efficiency was investigated with RT-PCR using primers specific for RPS27a or RPL40. Primers targeting the house-keeping GAPDH mRNA were used

as a loading control (Figure 5.16). Knockdown of either RPS27a or RPL40 in MCF7 or LNCaP cells resulted in a major decrease in the mRNA levels of the ribosomal proteins (Figure 5.16), indicating that the knockdowns were efficient in both cell lines.

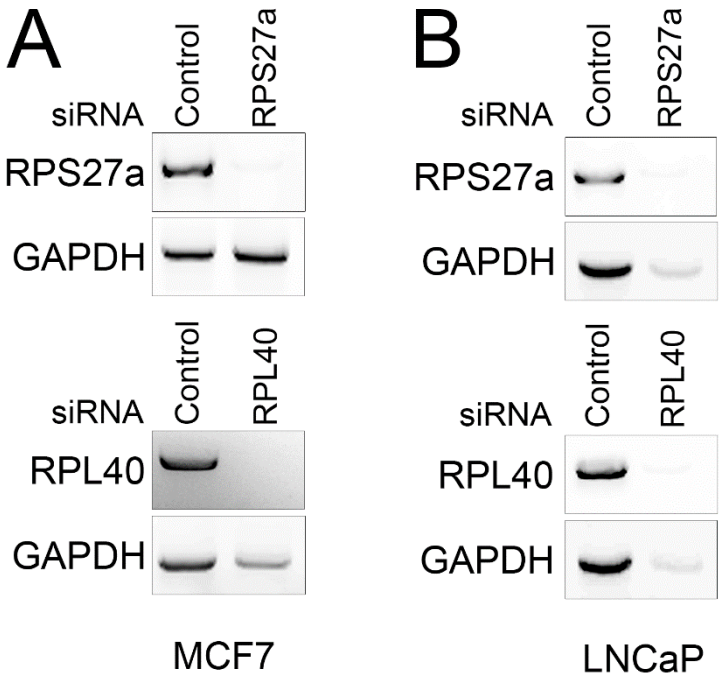

Figure 5.16. Knockdown efficiency of siRNA treatment in MCF7 and LNCaP cells tested by RT-PCR. siRNA-mediated knockdowns of control, RPS27a (top) or RPL40 (bottom) was performed in MCF7 **(A)** or LNCaP **(B)** cells. RNA was extracted from the cells and reverse transcription was performed. PCR followed using primers targeting RPS27a or RPL40 were used, whereas primers recognizing GAPDH were used as a loading control. The samples were loaded on a 2% agarose/1x TBE DNA gel and visualized using the Typhoon Phosphorimager.

Next, I investigated the effects of RPS27a and RPL40 knockdowns on p53 levels in MCF7 and LNCaP cells. The whole cell extract produced from knockdown cells was loaded on an SDS-PAGE gel followed by Western Blotting analysis for detection of p53 or p21 (Figure 5.17). Knockdown of RPS27a resulted in an approximately 3.5-fold and 5-fold increase in p53 levels in MCF7 and LNCaP cells respectively, as compared to the control (Figure 5.17). Furthermore, p21 levels were also increased after knockdown of RPS27a in both MCF7 and LNCaP cells (Figure 5.17A), indicating that p53 activity was also induced. Knockdown of RPL40 resulted in a 2.5-fold and 4-fold increase in p53 levels in MCF7 and LNCaP cells respectively, as compared to the control (Figure 5.17), and in an increase in the levels of p21 (Figure 5.17A), indicating an increase in p53 activity. These results show that RPS27a or RPL40 knockdowns in MCF7 or LNCaP cells result in an increase in p53 levels and activity, as opposed to U2OS cells. Note that p21 can be regulated post-translationally (Jung et al., 2010), but there was

no assessment of p21 mRNA levels or other p53 downstream targets for p53 activity measure.

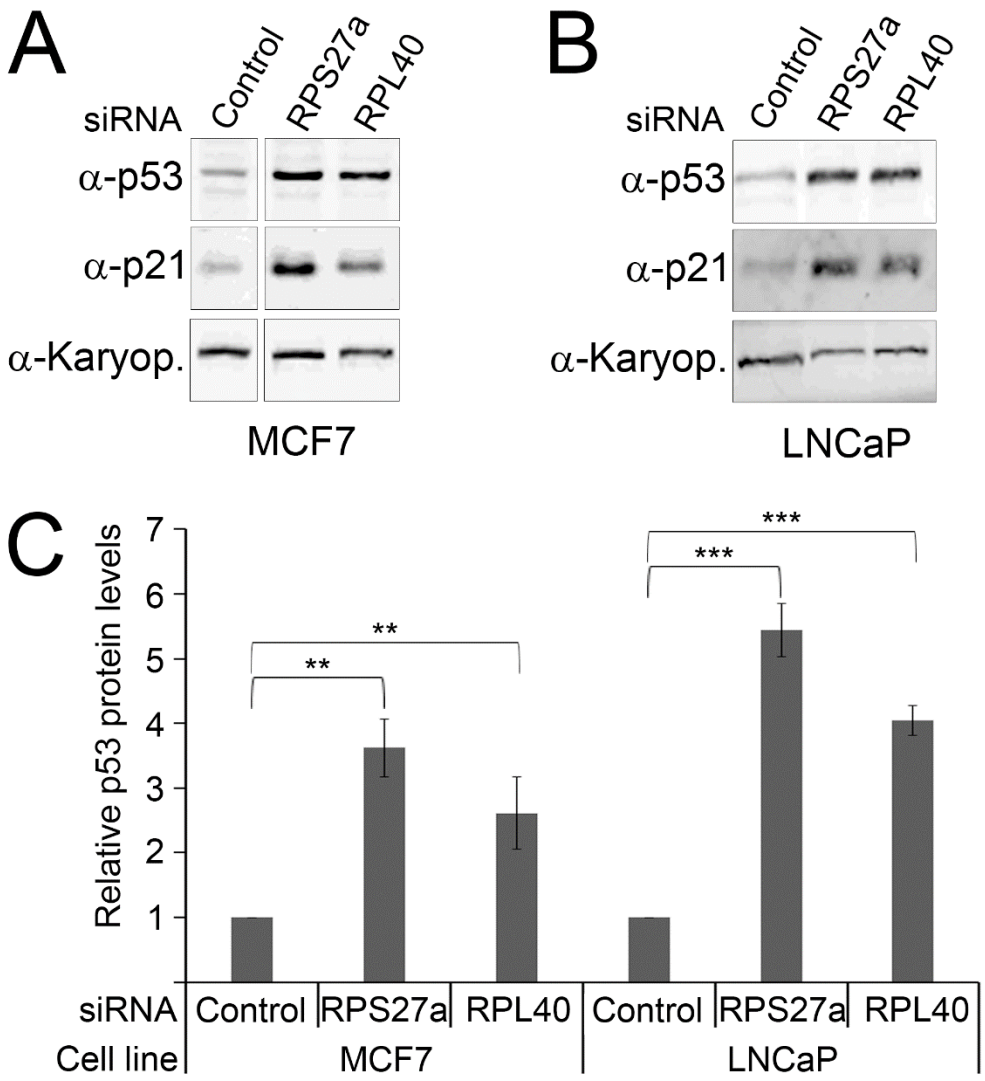

Figure 5.17. RPS27a or RPL40 knockdowns result in p53 induction in MCF7 and LNCaP cells. (A-B) siRNA-mediated knockdowns for control, RPS27a or RPL40 were performed for 48h in MCF7 **(A)** or LNCaP **(B)** cells and the whole cell extract was loaded on an SDS-PAGE gel. Western blot analysis was performed using the LICOR system. The antibodies used are shown on the left and Karyopherin (Karyop.) was used as a loading control. **(C)** ImageQuant software was used for quantitation of the western blots and normalization of the p53 values was performed against the loading control values (Karyopherin). The graph represents the average relative p53 levels of three independent experimental repeats and the error bars represent the standard error (+/-SEM). Statistical analysis was performed using an unpaired t-test. **p value<0.01, ***p value<0.0001.

5.3 Discussion

The *RPS27a* and *RPL40* genes encode for the ubiquitin-ribosomal protein precursors RPS27a and RPL40 in humans, (Redman and Rechsteiner, 1989) and are highly conserved amongst eukaryotes (Kimura and Tanaka, 2010). Ubiquitin is an important and highly conserved molecule, involved in protein degradation and signal transduction pathways (Pickart and Eddins, 2004). Despite the high conservation of these proteins and the importance of both ubiquitination and ribosome biogenesis to the cell, not much is known about their production or function in humans. In this chapter, I have shown that the ubiquitin-ribosomal protein precursor is likely to be processed at very early stages after or during translation. Furthermore, I have shown that RPS27a is important for SSU production and RPL40 is important for LSU production. Since ribosome biogenesis defects result in the stabilisation of p53 via the 5S RNP-MDM2 pathway (Sloan et al., 2013a, Donati et al., 2013, Nishimura et al., 2015), it was of a surprise to find that p53 was not induced after depletion of either RPS27a or RPL40 in U2OS cells.

I firstly investigated when the ubiquitin-ribosomal protein precursor is processed in the cell using U2OS stable cell lines expressing tagged RPS27a or RPL40, under the control of a tetracycline promoter. I found that no precursor was detected when the HA-tagged ubiquitin-fusion RPS27a or RPL40 were expressed in U2OS cells (Figure 5.4), indicating that the de-ubiquitination of these proteins occurs early or the precursor is not stable in the cell. The ubiquitin-fusion precursor was also not visible after block of ribosome biogenesis by ActD (Figure 5.5). These results agree with previously published data where they showed that cleavage of the ubiquitin monomer occurs very rapidly in the cell from the Ubiquitin-RPS27a precursor (Sun et al., 2011). It is, therefore, likely that the ubiquitin molecule is cleaved extremely quickly after or during translation of these proteins, which agrees with a recent study showing that the processing of the ubiquitin-ribosomal protein precursors is most likely to occur post-translationally in mice and human cells (Grou et al., 2015). In future studies, it would be interesting to identify possible de-ubiquitinases that are important for the processing of these proteins. Two likely candidates are the ubiquitin C-terminal hydrolase (UCH) L3 and the ubiquitin-specific protease (USP) 7, which were shown to be involved in the maturation of the ubiquitin-ribosomal protein precursors in mice and human cells (Grou et al., 2015). Furthermore, UCHL3 is mainly found in the cytosol and USP7 is found in both the nucleus and the cytosol (Grou et al., 2015), further supporting the theory that

the processing of the ubiquitin-ribosomal protein precursors takes place during or immediately after translation.

It is known that some ribosomal proteins are produced in excess and rapidly degraded by the proteasome (Lam et al., 2007). Indeed, I showed that the HA-tagged RPL40, but not RPS27a, was stabilised when the proteasome was inhibited using MG132 (Figure 5.7), indicating that RPL40 is likely to be very unstable when it is found free and quickly degraded by the proteasome, whereas RPS27a is probably produced in normal levels. Furthermore, the levels of the FLAG-tagged ubiquitin did not change by treatment with MG132, showing that inhibition of the proteasome only affects the free RPL40 but not the ubiquitin-ribosomal protein precursor. Further supporting these data, I showed that the HA-tagged RPL40, but not RPS27a, is found in the non-ribosomal complexes (Figure 5.9) and that the HA-tagged RPS27a is found in both the nucleolus and the cytoplasm, whereas the HA-tagged RPL40 is mainly found in the cytoplasm (Figure 5.8). It is likely that the RPL40 detected in the free complexes is unstable and it is quickly integrated in the ribosome or degraded by the proteasome if produced in excess. Since I am inclined to assume that the ubiquitin-ribosomal protein precursor is cleaved in the cytoplasm, the mature RPS27a and RPL40 are probably then transported to the nucleus where ribosome biogenesis takes place. In addition, I showed that the HA-tagged RPS27a accumulated in the SSU complexes and the HA-tagged RPL40 accumulated in the LSU complexes, as expected (Figure 5.9). Surprisingly, the HA-tagged RPL40 accumulated in the same place as the SSU complexes, but I have no evidence that it accumulates in the SSU. It is still unclear why this was observed.

Inhibition of rRNA transcription after ActD treatment (Figure 5.5) or specific block of SSU or LSU production (Figure 5.6) resulted in a significant decrease in the levels of the HA-tagged RPS27a or RPL40, but no change was observed in the levels of the FLAG-tagged ubiquitin. These results indicate that ribosome biogenesis defects result in a decrease in the ribosomal protein production but not in a decrease in the ubiquitin-ribosomal protein precursor. Interestingly, depletion of RPS27a and RPL40 affected the small and large ribosomal subunit biogenesis respectively (Figure 5.11). My data indicated that RPS27a is likely to be involved in 30S SSU rRNA precursor processing in humans (Figure 5.11), by cleavage at 5’ ETS and ITS1, for the production of the mature 18S rRNA (Sloan et al., 2014). RPL40 is likely to be important for site 2

endonucleolytic cleavage of ITS1 (Figure 5.11), which separates the SSU and LSU rRNA precursors in humans. A cleavage block at this site results in cleavage of site 2a, leading to the accumulation of the 36S LSU rRNA precursor (Sloan et al., 2013c). It is possible that RPS27a and RPL40 interact with ribosome biogenesis factors important for these cleavage steps. For example, RPL40 could interact or be involved with RRP5 and NOL12 ribosome biogenesis factors, which were found to play an important role in ITS1 site 2 cleavage in humans (Sloan et al., 2013c). This is the first evidence for the direct involvement of both RPS27a and RPL40 in human ribosome biogenesis, and future work is necessary to identify how these proteins may function.

Defects in ribosome biogenesis are directly linked with the levels of the tumour suppressor p53 via the 5S RNP-MDM2 pathway (Pelava et al., 2016). Surprisingly, p53 levels or activity were not significantly changed after RPS27a or RPL40 knockdowns in U2OS cells (Figure 5.12), even though they resulted in ribosome biogenesis defects. My data agree with previously published data where RPS27a knockdown had no major effect on p53 levels in U2OS cells (Sun et al., 2011). Furthermore, I showed that the induction of p53 levels and activity after ribosome biogenesis defects by ActD treatment were not changed after knockdown of RPS27a or RPL40 (Figure 5.14), as opposed to knockdowns of RPL5 or RPL11, which prevent the activation of p53 after ribosome biogenesis defects (Dai and Lu, 2004, Lohrum et al., 2003, Sun et al., 2010, Zhang et al., 2003). In a previous study, it was shown that knockdown of RPS27a resulted in the significant decrease of p53 levels caused by inhibition of rRNA transcription after treatment with ActD in U2OS cells (Sun et al., 2011), as opposed to my data. Why this difference is observed is not clear.

In addition, I show here that the lack of p53 induction seems to be cell-type specific since p53 levels and activity were induced by knockdowns of RPS27a and RPL40 in breast cancer MCF7 cells and prostate cancer LNCaP cells (Figure 5.17). A recent publication has shown that knockdown of RPS27a resulted in a significant increase in p53 levels in HCT116 colorectal carcinoma cells (Nicolas et al., 2016), further confirming that the p53 response is cell-type specific. Interestingly, LNCaP cells have been shown to have mutations in a number of genes encoding for ribosomal proteins, such as RPL22, or ribosome biogenesis factors, such as NOB1. In addition, a mutation in the gene encoding for RPL10L was found in MCF7 and a mutation in RPL22 gene in HCT-116 cells, but no ribosomal protein genes are mutated in U2OS cells (Iorio et

al., 2016). Furthermore, LNCaP cells have a variety of mutations in six genes encoding for ubiquitin-like modifiers, such as UBE3A, but only a few genes were found mutated in MCF7 and HCT-116 cells, and only one in U2OS cells.(Iorio et al., 2016). Moreover, LNCaP cells have mutations in more than 10 genes encoding for USP de-ubiquitinases and HCT-116 have mutations in 9 USP genes, but only one or two USP de-ubiquitinases are mutated in U2OS or MCF7 cells respectively (Iorio et al., 2016). These data suggest that LNCaP, HCT-116 and, probably, MCF7 cells may be more prone in p53 activation after ribosome biogenesis defects by RPS27a or RPL40 depletion than U2OS cells, since a number of genes involved in the ubiquitin homeostasis are mutated in these cells. Another explanation for the cell-line specific phenotype might be that the protein levels of RPS27a vary in different cell lines, since MCF7 cells express RPS27a in medium levels, whereas U2OS cells contain high levels of RPS27a protein. Even though there is no information for LNCaP cells, RPS27a protein is found in medium levels in another prostate cancer cell line, PC-3, similarly to MCF7 cells (Ponten et al., 2008). It was previously suggested that RPS27a binds MDM2, leading to p53 activation when over-expressed, providing a novel regulation of p53 levels (Sun et al., 2011). It may be that, in U2OS, RPS27a or RPL40 are needed for the binding of the 5S RNP to MDM2, but not in MCF7 or LNCaP cells. Why this is the case is unclear and future work is needed to determine this.

I have shown here that over-expression of either RPS27a or RPL40 in U2OS cells resulted in an increase in p53 levels, but not activity (Figure 5.15). Since knockdown of RPS27a or RPL40 had contrasting effects on p53 levels in different cell lines, it would be interesting to see whether over-expression of these proteins in other cell lines affect p53 levels and activity differently. My results are somewhat different from a previous publication where over-expression of RPS27a in U2OS cells resulted in an induction in both p53 levels and activity (Sun et al., 2011), but it is not clear why this is the case. Even though the authors have also used U2OS cells, there are still variations between cells, which might be the main cause of this difference. Furthermore, in the published study, the authors have used transient DNA transfections for over-expression of RPS27a, whereas I have created a U2OS cell line which stably expressed the tetracycline-inducible tagged protein. It is unlikely that this would cause such a difference, but I cannot exclude this possibility. Another explanation would be the use of different tags on the ubiquitin-RPS27a open reading frame, since they have used V5 and FLAG tags (Sun et al., 2011), whereas I have used FLAG and HA tags.

Again, it is not clear whether the different tags would interfere with the function of the expressed protein, but it is a possibility we cannot exclude. Furthermore, I have shown that p53 activity in U2OS cells expressing the HA-tagged RPS27a or RPL40 is reduced, even after ribosome biogenesis defects by ActD treatment (Figure 5.15). These data indicate that RPS27a and RPL40 regulate p53 levels and activity differently than other ribosomal proteins and future work is needed to identify their exact functions in p53 homeostasis.

Inhibition of p53 by MDM2 is achieved by binding of the p53-binding domain of MDM2 on the transactivation (TAD) domain of p53 (Poyurovsky et al., 2010) and of the central domain of MDM2, including the acidic domain and zinc finger domain, on the transactivation domain of p53 (Cross et al., 2011, Ma et al., 2006) (Figure 5.18). Ribosome biogenesis defects lead to the binding of the 5S RNP on MDM2, resulting in a conformational change on MDM2-p53 complex. RPL5 binds the acidic and ring domain of MDM2 whereas RPL11 was shown to only bind the zinc finger domain (Figure 5.18) (Lindstrom et al., 2007, Zheng et al., 2015). This leads to changes in MDM2 arrangement, resulting in an active conformation of the DNA binding domain of p53, which leads to p53 stabilisation and transcriptional activation of downstream targets (Figure 5.18) (Zheng et al., 2015). Sun et al. (2011) have shown that both the expressed and the endogenous RPS27a bind to the acidic domain of MDM2 (Sun et al., 2011). It is possible that RPL40, as RPS27a, can also bind MDM2 when over-expressed, leading to an induction of the p53 levels, by preventing its ubiquitination by MDM2. However, this binding might not be sufficient to activate p53, as it may not be able to bind DNA for transcriptional activation of downstream targets. Furthermore, binding of the 5S RNP on MDM2 after ribosome biogenesis defects might still occur when RPS27a or RPL40 are over-expressed, leading to a collaborative inhibition of MDM2. It is proposed here that binding of either RPS27a or RPL40 and the 5S RNP to MDM2 may result in differential conformational changes of the MDM2-p53 complex, leading to the stabilisation of p53 levels, but not activity, as the DNA-binding domain may remain in the inactive conformation (Figure 5.18). This is only one possibility of how RPS27a and RPL40 may be involved in p53 homeostasis in the cell, but there might be other reasons for this, which are currently unknown. Future research is required to identify whether this is indeed the case or whether other mechanisms exist for p53 regulation by the 5S RNP and RPS27a or RPL40.

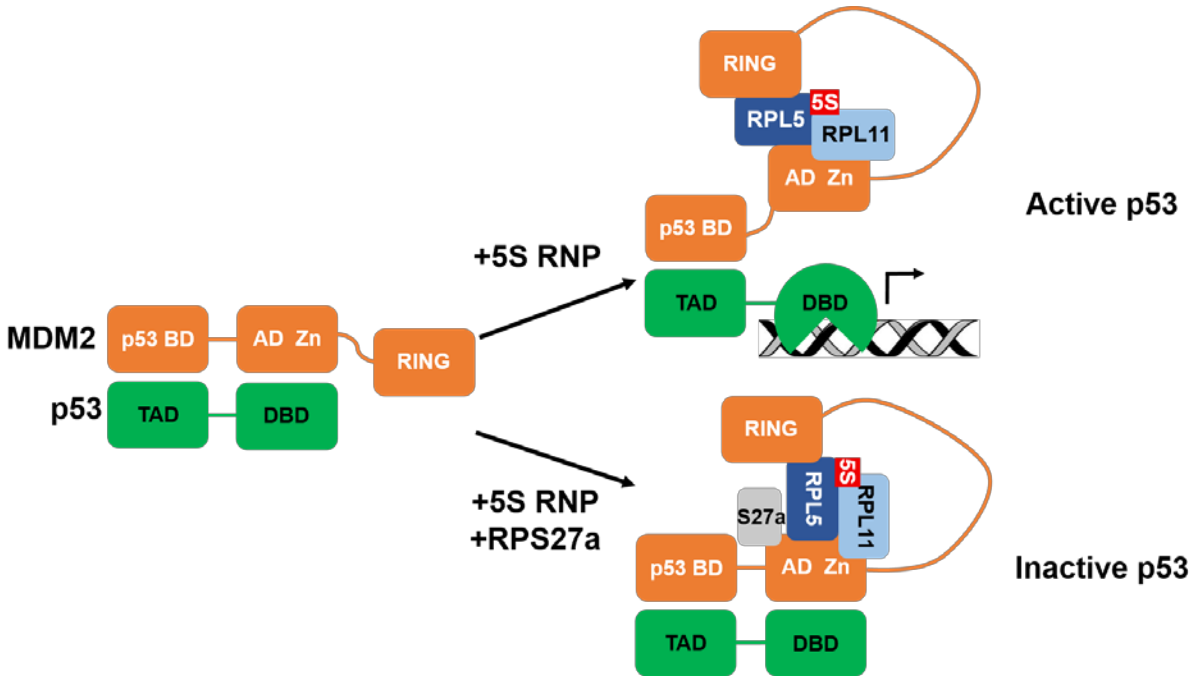

Figure 5.18. Schematic representation of the proposed model of p53 regulation by the 5S RNP and RPS27a or RPL40. The p53-binding domain (p53 BD), acidic domain (AD), zinc finger domain (Zn) and ring domain of MDM2 are shown in orange, and the domain and domain of p53 are shown in green. The 5S RNP is shown by RPL5, RPL11 and the 5S rRNA. RPS27a may also be replaced by RPL40 in this model. The conformational changes on DNA-binding domain of p53 are indicated.

However, one problem with this theory is that it does not explain the fact that p53 levels were not changed after RPS27a or RPL40 depletion in U2OS cells, even though ribosome biogenesis was defective, which would result in an accumulation of the 5S RNP. One possibility would be that the binding of the 5S RNP to MDM2 is dependent on the presence of RPS27a and RPL40 in U2OS cells but not in MCF7 or LNCaP cells, potentially through interactions on MDM2. Further work is needed to identify whether RPS27a and RPL40 are bound on MDM2 at the same time with the 5S RNP or if they interact directly with either RPL5, RPL11 or the 5S rRNA using crosslinking and immunoprecipitation techniques. If this is indeed the case, it would be essential to identify whether this mechanism is different in a number of cell types, since knockdowns of RPS27a or RPL40 resulted in a differential response in p53 levels or activity in the cell lines tested here.

In conclusion, I have shown that the ubiquitin-RPS27a and RPL40 proteins are likely to be processed very rapidly after translation in humans. Furthermore, they play an important role in ribosome biogenesis in humans, since RPS27a is required for the SSU rRNA processing and RPL40 is required for the LSU rRNA processing. RPS27a

and RPL40 might be novel regulators of p53 induction via the 5S RNP-MDM2 pathway. This seems to be cell-type specific, which still remains a mystery. Future work is necessary to identify the functions of RPS27a and RPL40 in p53 homeostasis.

6. Chapter Six. Discussion

6.1 Overview

Ribosome biogenesis is a complex and energy-consuming process, which is directly linked with the regulation of the tumour suppressor p53 (Pelava et al., 2016). Defects in ribosome biogenesis result in the accumulation of the free 5S RNP in the nucleoplasm, which binds and inhibits MDM2, the main p53 inhibitor (Donati et al., 2013, Sloan et al., 2013a). This results in p53 stabilisation and activation, leading to activation of downstream pathways involved in cell cycle arrest and apoptosis. Ribosome biogenesis is an important process that has been linked to a variety of diseases, including neurodegenerative disorders (Lee et al., 2014, Parlato and Liss, 2014), skeletal diseases (Trainor and Merrill, 2014) and cancer (Gentilella et al., 2015). Furthermore, defects in ribosome biogenesis result in the development of ribosomopathies, a number of genetic diseases that arise due to mutations in ribosomal proteins or ribosome biogenesis factors, such as X-linked Dyskeratosis Congenita (DC) and Diamond-Blackfan Anaemia (DBA) (Narla and Ebert, 2010). These diseases present with anaemia and increased cancer risk, especially for AML (Yelick and Trainor, 2015), and the levels of p53 have been found to be de-regulated in cell culture and animal models of ribosomopathies (Pelava et al., 2016).

Despite the high significance of ribosome biogenesis in health and disease, not much is known about the large (LSU) and small (SSU) ribosomal subunit biogenesis in humans. Furthermore, even though the mechanism by which LSU production defects lead to p53 induction via the 5S RNP-MDM2 pathway has been identified, there is minimal and conflicting evidence on how SSU production defects lead to p53 up-regulation. Therefore, this PhD aimed to further explore the processes of LSU and SSU production in humans, and to investigate in more detail how defects in different stages of the human ribosome biogenesis pathway affect p53 regulation. Table 6.1 summarizes the main findings of this project.

Treatment	Cell line	Effects on rRNA processing	Effects on p53 levels
ΔDyskerin	HEK293T	Early SSU and LSU production defects	N/A
Dyskerin D125A	HEK293T	Late SSU and LSU production defects	N/A
ΔDyskerin	U2OS	N/A	p53 induction via 5S RNP
ΔRPS19	U2OS	21S rRNA accumulation	p53 induction via 5S RNP
	MCF7 LNCaP	N/A	p53 induction
ΔRPS6	U2OS MCF7 LNCaP	N/A	p53 induction
ΔRIO2	U2OS	18SE rRNA accumulation	p53 induction via 5S RNP
ΔPNO1	U2OS	26S rRNA accumulation	p53 induction
ΔRPL7	U2OS	N/A	p53 induction via 5S RNP
	MCF7 LNCaP	N/A	p53 induction
ΔRPL18	U2OS	N/A	p53 induction via 5S RNP
	MCF7 LNCaP	N/A	p53 induction
ΔRPL7a	U2OS MCF7	N/A	p53 induction
ΔPICT1	U2OS	N/A	p53 induction via 5S RNP
ΔRPS19+ΔRPL7	U2OS MCF7 LNCaP	N/A	p53 induction
ΔRPS19+ΔRPL18	U2OS	N/A	p53 supra-induction
	MCF7 LNCaP	N/A	p53 induction
ΔRPS6+ΔRPL7a	U2OS MCF7 LNCaP	N/A	p53 induction
ΔRPS27a	U2OS	30S rRNA accumulation	No difference
	MCF7 LNCaP	N/A	p53 induction
ΔRPL40	U2OS	32S, 36S rRNA accumulation	No difference
	MCF7 LNCaP	N/A	p53 induction

Table 6.1. Summary of the main findings of this PhD project.

Firstly, my data indicate that the SSU production is linked to LSU maturation in humans, similarly to yeast, where it was shown that the LSU is needed for the last stages of SSU maturation (Lebaron et al., 2012). I provide evidence that defects in SSU production in humans lead to inhibition of export of the pre-LSU complexes in the

cytoplasm, resulting in defects in the last stages of LSU rRNA processing. This is the first data indicating that the last stages of LSU maturation in humans are likely to take place in the cytoplasm, which agrees with previous yeast data showing that the last maturation steps of LSU production occur in the cytoplasm (Thomson and Tollervey, 2010). Therefore, it is likely that a, yet uncharacterized, factor or group of proteins is involved in the cross-talk between LSU and SSU production. Moreover, my data support previous studies showing that defects in LSU production after ribosomal protein depletion result in a 5S RNP-dependent p53 accumulation (Donati et al., 2013, Sloan et al., 2013a, Golomb et al., 2014, Fumagalli et al., 2009, Fumagalli et al., 2012). In addition, I have shown that p53 is induced via the 5S RNP-MDM2 pathway after depletion of, not only LSU ribosomal proteins, but also of SSU ribosomal proteins or ribosome biogenesis factors, probably by leading to LSU defects, resulting in the accumulation of the free 5S RNP in the cytoplasm. Surprisingly, knockdowns of RPS27a or RPL40, which are transcribed as ubiquitin-ribosomal protein precursors, only induced p53 in specific cell lines, even though they resulted in ribosome biogenesis defects. These data suggest that RPS27a and RPL40 might be novel regulators of the 5S RNP-MDM2 loop.

In this study, I have shown that the H/ACA snoRNP, which is involved in the pseudouridylation of the rRNA, is important for both LSU and SSU production in humans, in contrast with yeast, where it is required for SSU biogenesis (Atzorn et al., 2004, Henras et al., 2004, Lafontaine et al., 1998). This suggests that there are some, yet uncharacterized, H/ACA snoRNAs in humans involved in LSU rRNA processing, similarly to the box C/D U8 snoRNA, which was previously shown to be involved in this pathway (Sloan et al., 2014, Srivastava et al., 2010). Furthermore, depletion of Dyskerin, the pseudouridine synthase of the H/ACA snoRNP which is mutated in X-linked DC, resulted in a 5S RNP-dependent p53 stabilisation. My data suggest that the X-linked DC symptoms might be due to the 5S RNP-MDM2 interaction (Jaako et al., 2015) or due to desensitization of p53-dependent downstream pathways (Pelava et al., 2016), as previously shown in other ribosomopathy models.

Taken together, my data indicate that defects in any stage of ribosome biogenesis, nuclear or cytoplasmic, result in p53 induction via the 5S RNP-MDM2 pathway. I propose that defects in SSU production feedback to LSU production by inhibition of export of the pre-LSU in the cytoplasm, leading to an accumulation of the free 5S RNP in the nucleoplasm, which binds MDM2, resulting in p53 stabilisation (Figure 6.1).

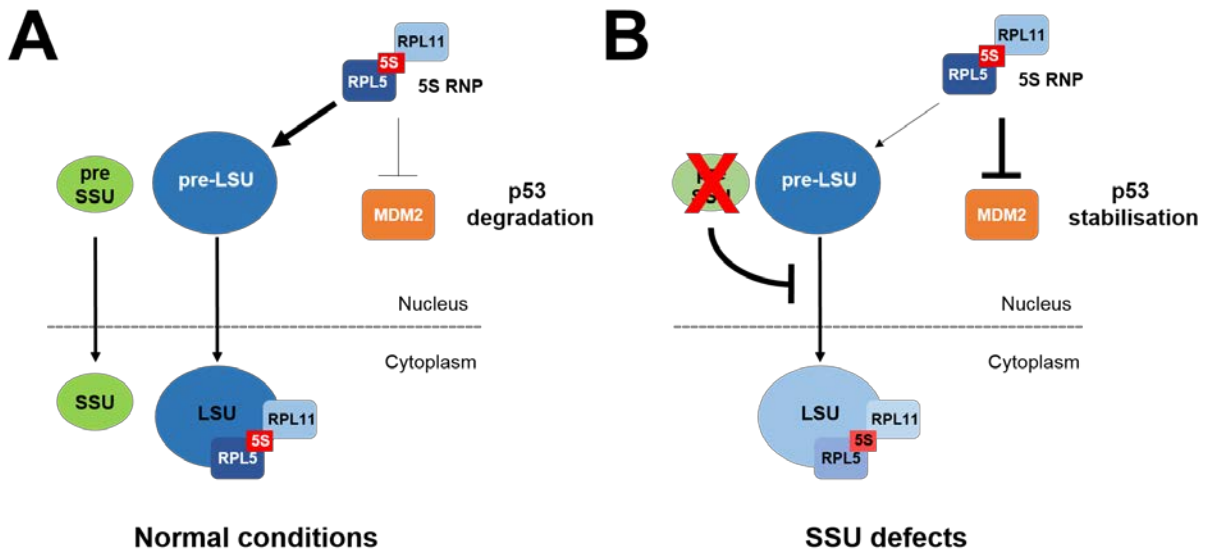

Figure 6.1. Defects on SSU lead to inhibition of export of the pre-LSU in the cytoplasm, resulting in p53 activation via the 5S RNP-MDM2 pathway. The p53 homeostasis under normal conditions **(A)** or after SSU production defects **(B)**. The small ribosomal subunit (SSU) is shown in light green and the large ribosomal subunit (LSU) is shown in blue. The 5S RNP consists of RPL5 (blue), RPL11 (light blue) and the 5S rRNA (red). The MDM2 ubiquitin ligase is shown in orange and p53 is shown in green. The nucleus and the cytoplasm are separated by a light grey dotted line.

6.2 Human ribosome biogenesis and disease

6.2.1 Human ribosome biogenesis

The 18S, 28S and 5.8S rRNAs are transcribed as a single 47S rRNA precursor, which is further cleaved and modified for the production of the mature rRNAs (Gamalinda and Woolford, 2015). The rRNA processing pathway in humans is highly conserved from yeast and involves more than 200 proteins, most of which remain unknown (Henras et al., 2008). In this study, I have shown that RPS27a is involved in SSU production, as it is important for the processing of 30S SSU rRNA precursor, and RPL40 is required for LSU production for cleavage at ITS1. Furthermore, I have identified that PNO1 ribosome biogenesis factor is important for cleavage at site 3 of the 26S SSU rRNA precursor in humans, as previously shown in yeast (Vanrobays et al., 2004).

In addition, I have shown that Dyskerin, the pseudouridine synthase of the H/ACA snoRNP, is required for the production of both LSU and SSU in humans, as opposed to yeast, where Cbf5 (yeast Dyskerin) was shown to be important for SSU biogenesis (Atzorn et al., 2004, Henras et al., 2004, Lafontaine et al., 1998). This further supports the theory that the processes of LSU and SSU biogenesis are linked. Furthermore, I have shown that inactivation of the catalytic activity of Dyskerin resulted in defects in late stages of rRNA maturation, whilst the H/ACA snoRNP still accumulated. During rRNA processing, a number of snoRNAs were shown to be essential for processing rather than modification. The most well-known H/ACA snoRNAs are U17 (snR30 in yeast) (Atzorn et al., 2004, Fayet-Lebaron et al., 2009, Enright et al., 1996) and snR10 (Tollervey, 1987), which are both involved in 18S rRNA processing. To date, no H/ACA snoRNAs were found in eukaryotes to be involved in LSU processing, that resemble the mode of action of either U17/snR30 or snR10. It was previously shown that the box C/D components Fibrillarin, NOP56 and NOP58 are important for the production of both LSU and SSU in humans (Sloan et al., 2014), similarly to Dyskerin, and the U8 box C/D snoRNA was found to be involved in LSU rRNA processing (Sloan et al., 2014, Srivastava et al., 2010). My data indicate that there are some H/ACA snoRNAs in humans that are involved in LSU rRNA processing.

In humans, it is not clear where and how the last stages of LSU rRNA processing occur. In yeast, it was shown that the mature LSU is required for the final processing steps of the SSU rRNAs in the cytoplasm (Lebaron et al., 2012). I show here that the mature SSU is required for the export of the pre-LSU in the cytoplasm in humans, since defects in either early or late stages of SSU production resulted in an accumulation of the pre-LSU complexes in the nucleus. This is similar to the previous data from yeast (Lebaron et al., 2012, Lamanna and Karbstein, 2011), showing that the LSU and SSU production are linked. In addition, it was shown in yeast that the last stages of LSU rRNA processing occur in the cytoplasm (Thomson and Tollervey, 2010). My data indicate that this is likely to be the case in humans as well, since defects in SSU production were shown to cause the accumulation of the pre-5.8S rRNA precursor, presumably due to inhibition of export of the pre-LSU complexes in the cytoplasm.

6.2.2 The importance of human ribosome biogenesis in ribosomopathies

Ribosomopathies are a set of rare genetic diseases caused by mutations in genes encoding ribosomal proteins or ribosome biogenesis factors (Narla and Ebert, 2010). Examples include Diamond-Blackfan Anaemia (DBA), 5q syndrome, Treacher-Collins (TC) syndrome and Dyskeratosis Congenita (DC). Mutations in genes encoding for SSU ribosomal proteins are found in DBA (Lipton and Ellis, 2010) or 5q syndrome patients (Ebert et al., 2008b), mutations in genes encoding for LSU ribosomal proteins are found in DBA patients (Cmejla et al., 2009) and mutations in genes encoding for ribosome biogenesis factors, such as *TCOF1* (Gonzales et al., 2005, Weiner et al., 2012) and *DKC1* (Heiss et al., 1998, Knight et al., 2001, Angrisani et al., 2014), are found in TC and X-linked DC patients respectively. Interestingly, only a few LSU ribosomal proteins have been found to be mutated in ribosomopathies, since most diseases arise due to mutations in SSU ribosomal proteins or ribosome biogenesis factors (Narla and Ebert, 2010). I have shown that block in LSU production results in a rapid and strong p53 activation and that SSU defects result in p53 activation via the 5S RNP-MDM2 after blocking LSU export in the cytoplasm (Figure 6.1). It is likely that most mutations in genes encoding for LSU ribosomal proteins are lethal, as they may not be tolerated for embryonic development. Therefore, haploinsuffiency of some or most LSU ribosomal proteins may result in p53 activation, leading to apoptosis *in utero*, so that the embryos are not viable. It is worth noting that, to date, there is no evidence of inactivation of both alleles encoding for a ribosomal protein in humans (Narla and Ebert, 2010), as it is most likely lethal, resulting in embryonic death.

Ribosomopathy patients present with developmental and erythropoeitic defects, such as craniofacial abnormalities and anaemia (Nakhoul et al., 2014, Narla and Ebert, 2010). It is still unclear, however, how defects in ribosome biogenesis affect the development and maturation of blood cells but no other tissues, even though ribosomes are important in all cells. It is possible that ribosome biogenesis is increased during erythropoiesis, since blood cells require more ribosomes than normal cells (Shenoy et al., 2012). Therefore, defects in ribosome production in normal cells would result in the slower accumulation of ribosomes, but defects in ribosome production in erythroid cells would result in the possible production of dysfunctional ribosomes (Yelick and Trainor, 2015). Alternatively, normal cells might be able to cope with defects in ribosome biogenesis, but the need of a high production of ribosomal proteins

in erythroid cells could result in a major imbalance. It would be interesting to identify whether LSU or SSU ribosome biogenesis defects result in an unusual erythropoiesis, using erythroid precursor cells, such as CD34+, or, perhaps, stem cells, where knockdowns or expression of mutant genes involved in ribosomopathies are used, such as RPS19. Another remaining question is how ribosome dysfunction leads to a variety of clinical manifestations in ribosomopathy patients, even though they are all blood disorders. For example, DBA patients present with erythropoiesis defects, whereas SDS patients present with neutropenia, where neutrophils, a type of white blood cell, are found in low numbers (Khanna-Gupta, 2013). It is therefore clear that identifying the molecular mechanisms underlying ribosomopathies might be a complicated, but essential task, in order to further understand the development of these diseases for the development of future treatments.

A number of studies have shown that p53 and the 5S RNP interaction with MDM2 are important for the clinical symptoms observed in ribosomopathy patients, and my data indicates that SSU defects result in p53 activation via the 5S RNP-MDM2 pathway after defects in LSU export (Figure 6.1). Some of the Diamond-Blackfan Anaemia (DBA) symptoms are dependent on p53 in mouse models, whereas the development of anaemia is dependent on the 5S RNP binding on MDM2 (Jaako et al., 2015). Furthermore, haploinsufficiency of RPS14 in a mouse model of 5q syndrome resulted in a p53-dependent anaemia (Schneider et al., 2016), and mice harbouring a mutation in *TCOF1*, the gene mutated in Treacher-Collins (TC) syndrome, developed p53-dependent craniofacial defects (Jones et al., 2008). I have shown here that p53 induction after RPS19 depletion, which is mutated in DBA, is dependent on the 5S RNP-MDM2 pathway, due to ribosome biogenesis defects, which further supports previous studies. In addition, I have shown that knockdown of Dyskerin, which is mutated in X-linked DC, also leads to p53 induction via the 5S RNP-MDM2 pathway. It is, therefore, surprising and counter-intuitive that ribosomopathy patients have an increased risk in developing cancers (Narla and Ebert, 2010), since p53 levels are increased. It is hypothesized that ribosomopathy patients become desensitized to p53-dependent tumour suppressor pathways in the cells, leading to an increased oncogenic susceptibility (Pelava et al., 2016). Future research is required to identify whether this is indeed the case.

6.2.3 The importance of human ribosome biogenesis in cancer

The nucleolus and ribosome biogenesis play a key role during cancer development. First, the nucleolar structure is altered in cancer cells (Nicolas et al., 2016), since the size and the shape of the nucleolus are increased (Derenzini et al., 2009, Orsolic et al., 2015). Furthermore, ribosome biogenesis is up-regulated during cancer development, since tumour cells require a larger number of ribosomes (Orsolic et al., 2015). A number of ribosomal proteins are mutated in cancers, especially leukaemia, including RPL5 (Iorio et al., 2016), RPL10 (De Keersmaecker et al., 2013), RPL22 (Rao et al., 2012, Iorio et al., 2016), RPS15 (Ljungstrom et al., 2016) and RPS20 (Nieminen et al., 2014). For example, mutations in RPS15 are mostly found in association with mutations in p53 and they result in an aggressive form of chronic lymphocytic leukaemia (CLL) (Ljungstrom et al., 2016). Furthermore, RPL5 was found to be commonly mutated in acute lymphocytic leukaemia (ALL), but also in a variety of solid tumours, such as invasive breast cancer, lung squamous cell carcinoma (LUSC), cutaneous melanoma (SKCM) and uterine corpus endometrial carcinoma (UCEC) (Iorio et al., 2016). In addition, the nucleolar protein nucleophosmin (NPM1) is mutated in a number of cancers and especially leukaemia. Up to 60% of AML cases present with a mutant *NPM1* gene (Grummitt et al., 2008) and it is mutated in almost 30% of all leukaemia and myelodysplastic syndromes (MDS) (Naoe et al., 2006).

Consequently, a number of anti-cancer drugs have been developed, targeting the nucleolus. For example 5-Fluouracil (5-FU) blocks rRNA processing (Burger et al., 2010, Ghoshal and Jacob, 1994, Longley et al., 2003) and data from my lab show that treatment with 5-FU induces p53 in a 5S RNP-dependent manner (Loren Gibson, Nick Watkins, personal communication). Several anti-cancer drugs inhibit ribosome biogenesis by inhibition of RNA polymerase I. Actinomycin D (ActD) intercalates with rDNA in low doses and prevents RNA polymerase I elongation (Ginell et al., 1988), as does the small molecule BMH-21 (Peltonen et al., 2014). CX-3543 also prevents the RNA polymerase I elongation by inhibition of the stabilization between the complexes on the rDNA gene (Drygin et al., 2009). Cisplatin cross-links with the rDNA and prevents the association of the transcription factor UBF at the promoter region, thus preventing the elongation of RNA polymerase I (Jordan and Carmo-Fonseca, 1998). CX-5461 targets the association of SL1 complex with RNA polymerase I, preventing initiation of rDNA transcription (Bywater et al., 2012).

Other drugs are also used for chemotherapeutic treatments of cancer, which target a number of ribosome biogenesis stages. Firstly, the mTOR pathway is targeted by a variety of drugs, leading to a decreased rDNA transcription. MK-2206 inhibits the activation of the mTORC1 complex by Akt pathway (Chan et al., 2011), whereas Rapamycin inhibits the mTORC1 complex directly (Mahajan, 1994). A few drugs target the cyclin-dependent kinase CDK2, including roscovitine, olomoucine (David-Pfeuty et al., 2001) and DRB (CK2 inhibitor 5,6-dichloro-1-beta-ribofuranosylbenzimidazole) (te Poele et al., 1999), or CDK9, such as Flavopiridol (Sedlacek, 2001), leading to cell cycle arrest and inhibition of rDNA transcription initiation.

Apart from targeting ribosome biogenesis pathway, a number of drugs targeting the interaction between MDM2 and p53 are at the stage of pre-clinical development or clinical trials. These drugs are commonly used in cancers expressing a wild-type p53 and they block the binding of MDM2 to p53 by competing for MDM2 binding (Shangary and Wang, 2008), leading to apoptosis of the cancer cells. Nutlin 3a is one example of a drug that inhibits the interaction between MDM2 and p53, leading to cell cycle arrest and senescence of the cancer cells (Shangary and Wang, 2008). Cancer cells that do not harbour a functional p53 were shown to be resistant to treatment with nutlin 3a (Manfe et al., 2012). Nevertheless, combined treatment with nutlin 3a and other chemotherapeutic drugs, such as doxorubicin or cisplatin, was more effective in inducing cytotoxicity as compared to treatment with single chemotherapeutic agents (Ohnstad et al., 2011). Other drugs that bind and inhibit MDM2 are MI-219 (Zheng et al., 2010) and MI-63 (Ding et al., 2006), leading to p53 activation.

The high number of ribosomal proteins or ribosome biogenesis factors that are mutated in cancers and the existing chemotherapeutic drugs highlight the importance of ribosome biogenesis in cancer development. It is, therefore, essential to further explore the mechanisms by which ribosome production occurs in humans, in order to develop more targeted and efficient treatments for cancer.

6.3 Future Directions

In this project, I provide new and exciting information on ribosome biogenesis in humans. Firstly, my data suggest that there are some H/ACA snoRNAs that are involved in LSU rRNA processing in humans, as U17/snR30 and snR10 are involved

in SSU rRNA processing (Fayet-Lebaron et al., 2009, Atzorn et al., 2004, Tollervey, 1987). My data show that there are H/ACA snoRNAs involved in LSU processing in higher eukaryotes. It was previously shown that the U8 box C/D snoRNA is involved in LSU rRNA processing in humans (Sloan et al., 2014, Srivastava et al., 2010) and some H/ACA snoRNAs were identified in protozoan parasites *T. brucei* (Gupta et al., 2010) and *L. major* (Eliaz et al., 2015) that might be involved in LSU rRNA processing. It is not clear which H/ACA snoRNAs might be involved in this pathway in humans and, therefore, future research is required. It is possible that these H/ACA snoRNAs present with base complementarity to the 28S rRNA, similarly to the mechanism of U17/snR30 (Atzorn et al., 2004, Fayet-Lebaron et al., 2009) and snR10 (Tollervey, 1987). There is a number of snoRNAs with unknown functions, called orphan snoRNAs (Bachellerie et al., 2002). It might be that some of these orphan snoRNAs are required for LSU rRNA processing in higher eukaryotes and further research is required to identify which ones are involved in this and their exact mechanism of action.

Secondly, my results, in addition to previous yeast data (Lebaron et al., 2012, Lamanna and Karbstein, 2011), indicate that the SSU and LSU processing pathways are linked by a single factor or a group of proteins, in contrast to previous theories suggesting that the two processes are separate. One likely candidate linking the two processes is the ribosome biogenesis factor ATP-binding-cassette F2 (ABCF2), a member of the ABC protein family of transporters which shuttle between the nucleus and the cytoplasm (Jones and George, 2004). The yeast homologue of ABCF2, ARB1, was shown to be important for both LSU and SSU ribosome biogenesis in yeast (Dong et al., 2005). Depletion of ARB1 in *S. cerevisiae* resulted in the accumulation of the 20S SSU rRNA precursor and a defect in the export of the pre-SSU complex in the cytoplasm, as well as a delayed LSU rRNA processing (Dong et al., 2005). Furthermore, ARB1 was found to be associated with pre-40S, pre-60S and 80S ribosomal complexes, and with proteins involved in either 60S maturation, such as LSG1, 40S maturation, such as SCP160, or both 60S and 40S maturation, such as DED1 (Dong et al., 2005). It was also demonstrated by various publications that ABCF2 is highly associated with different types of cancer (Nishimura et al., 2007, Ogawa et al., 2006, Hlavata et al., 2012, Nishimura et al., 2008). These studies indicate that ABCF2 might be an important ribosome biogenesis factor which links the LSU and SSU production, and it is possible that it is involved in tumour development due to ribosome biogenesis defects. It would, therefore, be interesting to identify whether the

biogenesis of LSU or SSU is affected after ABCF2 knockdown in human cells, and whether this effect is global or specific to certain stages of ribosome biogenesis. If so, it would be important to identify whether ABCF2 depletion affects p53 levels via the 5S RNP-MDM2 pathway, which would explain how SSU processing defects feedback to the 5S RNP integration in the ribosome.

In this study, I have shown that depletion of either ribosomal proteins or ribosome biogenesis factors acting in different stages of ribosome biogenesis lead to p53 activation via the 5S RNP-MDM2 pathway, and not just depletion of LSU ribosomal proteins. This is of particular importance for ribosomopathies, which arise due to mutations in genes encoding for either ribosomal proteins or ribosome biogenesis factors (Narla and Ebert, 2010). Since ribosomopathy patients present with an increased cancer risk and de-regulated p53 levels in cell culture and animal models (Pelava et al., 2016), the interaction between the 5S RNP and MDM2 is an important target for the development of future therapies for ribosomopathy patients. The existing treatments for ribosomopathy patients result in the relief of the symptoms and include steroids for the anaemia or surgery for the craniofacial defects (Narla and Ebert, 2010). Since it was shown that the anaemia phenotype, at least for DBA, is dependent on the interaction between the 5S RNP-MDM2 in mouse models (Jaako et al., 2015), targeting this interaction would potentially replace the need for blood transfusions in ribosomopathy patients. Furthermore, the de-regulation of p53 in ribosomopathy models *in vivo* and the increased cancer incidence in these patients suggest that the interaction between the 5S RNP and MDM2 could result in a reduction of tumourigenesis in ribosomopathy patients.

In addition, the 5S RNP-MDM2 interaction can be targeted for future cancer treatments. Most of the existing chemotherapeutic treatments for cancer target the nucleolus, by inhibition of rDNA transcription by blocking RNA polymerase I (Quin et al., 2014), and are genotoxic. Some of the drugs also target the mTORC1 activation, which controls the protein production by activation downstream pathways for ribosome biogenesis and mRNA translation (Laplante and Sabatini, 2009a). Inhibiting the interaction between the 5S RNP and MDM2 could provide a more targeted approach in cancer therapeutics, since it would mainly be active in cancer cells with an increased or defective ribosome production, leading to less side effects with no genotoxic stress. In addition, I have shown here that block in LSU production leads to a very quick and

high p53 induction. Therefore, blocking the biogenesis of LSU in cancer cells, where the ribosome production is increased, would be an interesting target, since it would lead to a quick p53 activation, leading to cell cycle arrest and apoptosis. This could also be a more targeted approach in developing drugs that would only target an up-regulated LSU production, excluding somatic cells, where ribosome biogenesis takes place as normal.

6.4 Conclusions

In summary, this PhD project has shown that ribosome biogenesis in humans is a more complex process than originally thought, highlighting the importance of Dyskerin in the production of both LSU and SSU, and providing evidence of a link between the LSU and SSU biogenesis. Furthermore, it was shown here that defects in ribosome biogenesis lead to p53 activation, not only due to depletion of ribosomal proteins, but also because of depletion of ribosome biogenesis factors involved rRNA modification or early or late stages of rRNA processing, which is of particular importance in ribosomopathy patients. This information, in addition to ongoing research on the 5S RNP-MDM2 interaction, is important for the development of more targeted and efficient therapies for both ribosomopathy patients and cancer in general, especially for leukaemia. To conclude, ribosome biogenesis is an important process in human health and disease, and an important regulator of p53 homeostasis via the 5S RNP-MDM2 interaction, which is an emerging target for future cancer treatments.

References

- ADIMOOLAM, S. & FORD, J. M. 2002. p53 and DNA damage-inducible expression of the xeroderma pigmentosum group C gene. *Proc Natl Acad Sci U S A,* 99**,** 12985-90.
- AGRIS, P. F. 1996. The importance of being modified: roles of modified nucleosides and Mg2+ in RNA structure and function. *Prog Nucleic Acid Res Mol Biol,* 53**,** 79-129.
- AITTALEB, M., RASHID, R., CHEN, Q., PALMER, J. R., DANIELS, C. J. & LI, H. 2003. Structure and function of archaeal box C/D sRNP core proteins. *Nat Struct Biol,* 10**,** 256-63.
- ALTER, B. P., GIRI, N., SAVAGE, S. A. & ROSENBERG, P. S. 2009. Cancer in dyskeratosis congenita. *Blood,* 113**,** 6549-57.
- AMSTERDAM, A., SADLER, K. C., LAI, K., FARRINGTON, S., BRONSON, R. T., LEES, J. A. & HOPKINS, N. 2004. Many ribosomal protein genes are cancer genes in zebrafish. *PLoS Biol,* 2**,** E139.
- ANDERSEN, J. S., LAM, Y. W., LEUNG, A. K., ONG, S. E., LYON, C. E., LAMOND, A. I. & MANN, M. 2005. Nucleolar proteome dynamics. *Nature,* 433**,** 77-83.
- ANGRISANI, A., VICIDOMINI, R., TURANO, M. & FURIA, M. 2014. Human dyskerin: beyond telomeres. *Biol Chem*.
- ANSEL, K. M., PASTOR, W. A., RATH, N., LAPAN, A. D., GLASMACHER, E., WOLF, C., SMITH, L. C., PAPADOPOULOU, N., LAMPERTI, E. D., TAHILIANI, M., ELLWART, J. W., SHI, Y., KREMMER, E., RAO, A. & HEISSMEYER, V. 2008. Mouse Eri1 interacts with the ribosome and catalyzes 5.8S rRNA processing. *Nat Struct Mol Biol,* 15**,** 523-30.
- ARDLEY, H. C. & ROBINSON, P. A. 2005. E3 ubiquitin ligases. *Essays Biochem,* 41**,** 15-30.
- ARMANIOS, M., CHEN, J. L., CHANG, Y. P., BRODSKY, R. A., HAWKINS, A., GRIFFIN, C. A., ESHLEMAN, J. R., COHEN, A. R., CHAKRAVARTI, A., HAMOSH, A. & GREIDER, C. W. 2005. Haploinsufficiency of telomerase reverse transcriptase leads to anticipation in autosomal dominant dyskeratosis congenita. *Proc Natl Acad Sci U S A,* 102**,** 15960-4.

- ATZORN, V., FRAGAPANE, P. & KISS, T. 2004. U17/snR30 is a ubiquitous snoRNA with two conserved sequence motifs essential for 18S rRNA production. *Mol Cell Biol,* 24**,** 1769-78.
- BABIANO, R. & DE LA CRUZ, J. 2010. Ribosomal protein L35 is required for 27SB pre-rRNA processing in Saccharomyces cerevisiae. *Nucleic Acids Res,* 38**,** 5177-92.
- BACHELLERIE, J. P., CAVAILLE, J. & HUTTENHOFER, A. 2002. The expanding snoRNA world. *Biochimie,* 84**,** 775-90.
- BAI, D., ZHANG, J., XIAO, W. & ZHENG, X. 2014. Regulation of the HDM2-p53 pathway by ribosomal protein L6 in response to ribosomal stress. *Nucleic Acids Res,* 42**,** 1799-811.
- BAKALKIN, G., SELIVANOVA, G., YAKOVLEVA, T., KISELEVA, E., KASHUBA, E., MAGNUSSON, K. P., SZEKELY, L., KLEIN, G., TERENIUS, L. & WIMAN, K. G. 1995. p53 binds single-stranded DNA ends through the C-terminal domain and internal DNA segments via the middle domain. *Nucleic Acids Res,* 23**,** 362-9.
- BAKER, D., YOUSSEF, O., CHASTKOFSKY, M., DY, D., TERNS, R. & TERNS, M. 2005. RNA-guided RNA modification: functional organization of the archaeal H/ACA RNP. *Genes and Development,* 19**,** 1238–1248.
- BALAKIN, A., SMITH, L. & FOURNIER, M. 1996. The RNA world of the nucleolus: two major families of small RNAs defined by different box elements with related functions. *Cell,* 86**,** 823-834.
- BALAKIN, A. G., SCHNEIDER, G. S., CORBETT, M. S., NI, J. & FOURNIER, M. J. 1993. SnR31, snR32, and snR33: three novel, non-essential snRNAs from Saccharomyces cerevisiae. *Nucleic Acids Res,* 21**,** 5391-7.
- BATES, S., BONETTA, L., MACALLAN, D., PARRY, D., HOLDER, A., DICKSON, C. & PETERS, G. 1994. CDK6 (PLSTIRE) and CDK4 (PSK-J3) are a distinct subset of the cyclin-dependent kinases that associate with cyclin D1. *Oncogene,* 9**,** 71-9.
- BEHRENS, K., TRIVIAI, I., SCHWIEGER, M., TEKIN, N., ALAWI, M., SPOHN, M., INDENBIRKEN, D., ZIEGLER, M., MULLER, U., ALEXANDER, W. S. & STOCKING, C. 2016. Runx1 downregulates stem cell/megakaryocytic transcription programs that support niche interactions. *Blood*.

- BENSAAD, K., TSURUTA, A., SELAK, M. A., VIDAL, M. N., NAKANO, K., BARTRONS, R., GOTTLIEB, E. & VOUSDEN, K. H. 2006. TIGAR, a p53-inducible regulator of glycolysis and apoptosis. *Cell,* 126**,** 107-20.
- BERGES, T., PETFALSKI, E., TOLLERVEY, D. & HURT, E. C. 1994. Synthetic lethality with fibrillarin identifies NOP77p, a nucleolar protein required for pre-rRNA processing and modification. *EMBO J,* 13**,** 3136-48.
- BERTRAND, E., HOUSER-SCOTT, F., KENDALL, A., SINGER, R. H. & ENGELKE, D. R. 1998. Nucleolar localization of early tRNA processing. *Genes Dev,* 12**,** 2463-8.
- BIEGING, K. T., MELLO, S. S. & ATTARDI, L. D. 2014. Unravelling mechanisms of p53-mediated tumour suppression. *Nat Rev Cancer,* 14**,** 359-70.
- BLAZQUEZ-DOMINGO, M., GRECH, G. & VON LINDERN, M. 2005. Translation initiation factor 4E inhibits differentiation of erythroid progenitors. *Mol Cell Biol,* 25**,** 8496-506.
- BLEICHERT, F., GAGNON, K. T., BROWN, B. A., 2ND, MAXWELL, E. S., LESCHZINER, A. E., UNGER, V. M. & BASERGA, S. J. 2009. A dimeric structure for archaeal box C/D small ribonucleoproteins. *Science,* 325**,** 1384-7.
- BOISVERT, F. M., VAN KONINGSBRUGGEN, S., NAVASCUES, J. & LAMOND, A. I. 2007. The multifunctional nucleolus. *Nat Rev Mol Cell Biol,* 8**,** 574-85.
- BOOCOCK, G. R., MORRISON, J. A., POPOVIC, M., RICHARDS, N., ELLIS, L., DURIE, P. R. & ROMMENS, J. M. 2003. Mutations in SBDS are associated with Shwachman-Diamond syndrome. *Nat Genet,* 33**,** 97-101.
- BOSCHI-MULLER, S. & MOTORIN, Y. 2013. Chemistry enters nucleic acids biology: enzymatic mechanisms of RNA modification. *Biochemistry (Mosc),* 78**,** 1392-404.
- BRANDT, T., PETROVICH, M., JOERGER, A. C. & VEPRINTSEV, D. B. 2009. Conservation of DNA-binding specificity and oligomerisation properties within the p53 family. *BMC Genomics,* 10**,** 628.
- BRAULT, M. E., LAUZON, C. & AUTEXIER, C. 2013. Dyskeratosis congenita mutations in dyskerin SUMOylation consensus sites lead to impaired telomerase RNA accumulation and telomere defects. *Hum Mol Genet*.

- BRIGGS, M. W., BURKARD, K. T. & BUTLER, J. S. 1998. Rrp6p, the yeast homologue of the human PM-Scl 100-kDa autoantigen, is essential for efficient 5.8 S rRNA 3' end formation. *J Biol Chem,* 273**,** 13255-63.
- BROWN, C. J., LAIN, S., VERMA, C. S., FERSHT, A. R. & LANE, D. P. 2009. Awakening guardian angels: drugging the p53 pathway. *Nat Rev Cancer,* 9**,** 862-73.
- BROWNE, G., TAIPALEENMAKI, H., BISHOP, N. M., MADASU, S. C., SHAW, L. M., VAN WIJNEN, A. J., STEIN, J. L., STEIN, G. S. & LIAN, J. B. 2015. Runx1 is associated with breast cancer progression in MMTV-PyMT transgenic mice and its depletion in vitro inhibits migration and invasion. *J Cell Physiol,* 230**,** 2522-32.
- BURGER, K., MUHL, B., HARASIM, T., ROHRMOSER, M., MALAMOUSSI, A., ORBAN, M., KELLNER, M., GRUBER-EBER, A., KREMMER, E., HOLZEL, M. & EICK, D. 2010. Chemotherapeutic drugs inhibit ribosome biogenesis at various levels. *J Biol Chem,* 285**,** 12416-25.
- BYWATER, M. J., POORTINGA, G., SANIJ, E., HEIN, N., PECK, A., CULLINANE, C., WALL, M., CLUSE, L., DRYGIN, D., ANDERES, K., HUSER, N., PROFFITT, C., BLIESATH, J., HADDACH, M., SCHWAEBE, M. K., RYCKMAN, D. M., RICE, W. G., SCHMITT, C., LOWE, S. W., JOHNSTONE, R. W., PEARSON, R. B., MCARTHUR, G. A. & HANNAN, R. D. 2012. Inhibition of RNA polymerase I as a therapeutic strategy to promote cancer-specific activation of p53. *Cancer Cell,* 22**,** 51-65.
- CADWELL, C., YOON, H. J., ZEBARJADIAN, Y. & CARBON, J. 1997. The yeast nucleolar protein Cbf5p is involved in rRNA biosynthesis and interacts genetically with the RNA polymerase I transcription factor RRN3. *Mol Cell Biol,* 17**,** 6175-83.
- CAHILL, N. M., FRIEND, K., SPECKMANN, W., LI, Z. H., TERNS, R. M., TERNS, M. P. & STEITZ, J. A. 2002. Site-specific cross-linking analyses reveal an asymmetric protein distribution for a box C/D snoRNP. *EMBO J,* 21**,** 3816-28.
- CAI, X., GAO, L., TENG, L., GE, J., OO, Z. M., KUMAR, A. R., GILLILAND, D. G., MASON, P. J., TAN, K. & SPECK, N. A. 2015. Runx1 Deficiency Decreases Ribosome Biogenesis and Confers Stress Resistance to Hematopoietic Stem and Progenitor Cells. *Cell Stem Cell,* 17**,** 165-77.

- CALVINO, F. R., KHARDE, S., ORI, A., HENDRICKS, A., WILD, K., KRESSLER, D., BANGE, G., HURT, E., BECK, M. & SINNING, I. 2015. Symportin 1 chaperones 5S RNP assembly during ribosome biogenesis by occupying an essential rRNA-binding site. *Nat Commun,* 6**,** 6510.
- CARRIER, F., GEORGEL, P. T., POURQUIER, P., BLAKE, M., KONTNY, H. U., ANTINORE, M. J., GARIBOLDI, M., MYERS, T. G., WEINSTEIN, J. N., POMMIER, Y. & FORNACE, A. J., JR. 1999. Gadd45, a p53-responsive stress protein, modifies DNA accessibility on damaged chromatin. *Mol Cell Biol,* 19**,** 1673-85.
- CARRON, C., O'DONOHUE, M. F., CHOESMEL, V., FAUBLADIER, M. & GLEIZES, P. E. 2011. Analysis of two human pre-ribosomal factors, bystin and hTsr1, highlights differences in evolution of ribosome biogenesis between yeast and mammals. *Nucleic Acids Res,* 39**,** 280-91.
- CASSE, C., GIANNONI, F., NGUYEN, V. T., DUBOIS, M. F. & BENSAUDE, O. 1999. The transcriptional inhibitors, actinomycin D and alpha-amanitin, activate the HIV-1 promoter and favor phosphorylation of the RNA polymerase II C-terminal domain. *J Biol Chem,* 274**,** 16097-106.
- CAVAILLÉ, J., BUITING, K., KIEFMANN, M., LALANDE, M., BRANNAN, C., HORSTHEMKE, B., BACHELLERIE, J., BROSIUS, J. & HÜTTENHOFER, A. 2000. Identification of brain-specific and imprinted small nucleolar RNA genes exhibiting an unusual genomic organization. *Proc Natl Acad Sci U S A,* 97**,** 14311-14316.
- CERRUDO, C. S., GHIRINGHELLI, P. D. & GOMEZ, D. E. 2014. Protein universe containing a PUA RNA-binding domain. *FEBS J,* 281**,** 74-87.
- CHALAH, A. & KHOSRAVI-FAR, R. 2008. The mitochondrial death pathway. *Adv Exp Med Biol,* 615**,** 25-45.
- CHAN, J. C., HANNAN, K. M., RIDDELL, K., NG, P. Y., PECK, A., LEE, R. S., HUNG, S., ASTLE, M. V., BYWATER, M., WALL, M., POORTINGA, G., JASTRZEBSKI, K., SHEPPARD, K. E., HEMMINGS, B. A., HALL, M. N., JOHNSTONE, R. W., MCARTHUR, G. A., HANNAN, R. D. & PEARSON, R. B. 2011. AKT promotes rRNA synthesis and cooperates with c-MYC to stimulate ribosome biogenesis in cancer. *Sci Signal,* 4**,** ra56.
- CHARETTE, M. & GRAY, M. W. 2000. Pseudouridine in RNA: what, where, how, and why. *IUBMB Life,* 49**,** 341-51.

- CHEN, S. S. & WILLIAMSON, J. R. 2013. Characterization of the ribosome biogenesis landscape in E. coli using quantitative mass spectrometry. *J Mol Biol,* 425**,** 767-79.
- CHEUTIN, T., O'DONOHUE, M. F., BEORCHIA, A., VANDELAER, M., KAPLAN, H., DEFEVER, B., PLOTON, D. & THIRY, M. 2002. Three-dimensional organization of active rRNA genes within the nucleolus. *J Cell Sci,* 115**,** 3297-307.
- CHOESMEL, V., BACQUEVILLE, D., ROUQUETTE, J., NOAILLAC-DEPEYRE, J., FRIBOURG, S., CRETIEN, A., LEBLANC, T., TCHERNIA, G., DA COSTA, L. & GLEIZES, P. E. 2007. Impaired ribosome biogenesis in Diamond-Blackfan anemia. *Blood,* 109**,** 1275-83.
- CIGANDA, M. & WILLIAMS, N. 2011. Eukaryotic 5S rRNA biogenesis. *Wiley Interdiscip Rev RNA,* 2**,** 523-33.
- CLOIX, C., YUKAWA, Y., TUTOIS, S., SUGIURA, M. & TOURMENTE, S. 2003. In vitro analysis of the sequences required for transcription of the Arabidopsis thaliana 5S rRNA genes. *Plant J,* 35**,** 251-61.
- CMEJLA, R., CMEJLOVA, J., HANDRKOVA, H., PETRAK, J., PETRTYLOVA, K., MIHAL, V., STARY, J., CERNA, Z., JABALI, Y. & POSPISILOVA, D. 2009. Identification of mutations in the ribosomal protein L5 (RPL5) and ribosomal protein L11 (RPL11) genes in Czech patients with Diamond-Blackfan anemia. *Hum Mutat,* 30**,** 321-7.
- COHEN, S. B., GRAHAM, M. E., LOVRECZ, G. O., BACHE, N., ROBINSON, P. J. & REDDEL, R. R. 2007. Protein composition of catalytically active human telomerase from immortal cells. *Science,* 315**,** 1850-3.
- COUTE, Y., KINDBEITER, K., BELIN, S., DIECKMANN, R., DURET, L., BEZIN, L., SANCHEZ, J. C. & DIAZ, J. J. 2008. ISG20L2, a novel vertebrate nucleolar exoribonuclease involved in ribosome biogenesis. *Mol Cell Proteomics,* 7**,** 546-59.
- CROSS, B., CHEN, L., CHENG, Q., LI, B., YUAN, Z. M. & CHEN, J. 2011. Inhibition of p53 DNA binding function by the MDM2 protein acidic domain. *J Biol Chem,* 286**,** 16018-29.
- DAI, M. S., CHALLAGUNDLA, K. B., SUN, X. X., PALAM, L. R., ZENG, S. X., WEK, R. C. & LU, H. 2012. Physical and functional interaction between

ribosomal protein L11 and the tumor suppressor ARF. *J Biol Chem,* 287**,** 17120-9.

- DAI, M. S. & LU, H. 2004. Inhibition of MDM2-mediated p53 ubiquitination and degradation by ribosomal protein L5. *J Biol Chem,* 279**,** 44475-82.
- DAI, M. S., SUN, X. X. & LU, H. 2008. Aberrant expression of nucleostemin activates p53 and induces cell cycle arrest via inhibition of MDM2. *Mol Cell Biol,* 28**,** 4365-76.
- DAI, M. S., ZENG, S. X., JIN, Y., SUN, X. X., DAVID, L. & LU, H. 2004. Ribosomal protein L23 activates p53 by inhibiting MDM2 function in response to ribosomal perturbation but not to translation inhibition. *Mol Cell Biol,* 24**,** 7654-68.
- DANILOVA, N. & GAZDA, H. T. 2015. Ribosomopathies: how a common root can cause a tree of pathologies. *Dis Model Mech,* 8**,** 1013-26.
- DANILOVA, N., SAKAMOTO, K. M. & LIN, S. 2008. Ribosomal protein S19 deficiency in zebrafish leads to developmental abnormalities and defective erythropoiesis through activation of p53 protein family. *Blood,* 112**,** 5228-37.
- DARZACQ, X., JADY, B. E., VERHEGGEN, C., KISS, A. M., BERTRAND, E. & KISS, T. 2002. Cajal body-specific small nuclear RNAs: a novel class of 2'-O-methylation and pseudouridylation guide RNAs. *EMBO J,* 21**,** 2746-56.
- DAVID-PFEUTY, T., NOUVIAN-DOOGHE, Y., SIRRI, V., ROUSSEL, P. & HERNANDEZ-VERDUN, D. 2001. Common and reversible regulation of wild-type p53 function and of ribosomal biogenesis by protein kinases in human cells. *Oncogene,* 20**,** 5951-63.
- DE KEERSMAECKER, K., ATAK, Z. K., LI, N., VICENTE, C., PATCHETT, S., GIRARDI, T., GIANFELICI, V., GEERDENS, E., CLAPPIER, E., PORCU, M., LAHORTIGA, I., LUCA, R., YAN, J., HULSELMANS, G., VRANCKX, H., VANDEPOEL, R., SWERON, B., JACOBS, K., MENTENS, N., WLODARSKA, I., CAUWELIER, B., CLOOS, J., SOULIER, J., UYTTEBROECK, A., BAGNI, C., HASSAN, B. A., VANDENBERGHE, P., JOHNSON, A. W., AERTS, S. & COOLS, J. 2013. Exome sequencing identifies mutation in CNOT3 and ribosomal genes RPL5 and RPL10 in T-cell acute lymphoblastic leukemia. *Nat Genet,* 45**,** 186-90.
- DECATUR, W. A. & FOURNIER, M. J. 2002. rRNA modifications and ribosome function. *TRENDS in Biochemical Sciences,* 27.

- DELAPORTA, P., SOFOCLEOUS, C., STIAKAKI, E., POLYCHRONOPOULOU, S., ECONOMOU, M., KOSSIVA, L., KOSTARIDOU, S. & KATTAMIS, A. 2014. Clinical phenotype and genetic analysis of RPS19, RPL5, and RPL11 genes in Greek patients with Diamond Blackfan Anemia. *Pediatr Blood Cancer,* 61**,** 2249-55.
- DELEO, A. B., JAY, G., APPELLA, E., DUBOIS, G. C., LAW, L. W. & OLD, L. J. 1979. Detection of a transformation-related antigen in chemically induced sarcomas and other transformed cells of the mouse. *Proc Natl Acad Sci U S A,* 76**,** 2420-4.
- DERENZINI, M., MONTANARO, L. & TRERE, D. 2009. What the nucleolus says to a tumour pathologist. *Histopathology,* 54**,** 753-62.
- DERENZINI, M., THIRY, M. & GOESSENS, G. 1990. Ultrastructural cytochemistry of the mammalian cell nucleolus. *J Histochem Cytochem,* 38**,** 1237-56.
- DESHMUKH, M., TSAY, Y. F., PAULOVICH, A. G. & WOOLFORD, J. L., JR. 1993. Yeast ribosomal protein L1 is required for the stability of newly synthesized 5S rRNA and the assembly of 60S ribosomal subunits. *Mol Cell Biol,* 13**,** 2835-45.
- DEVERAUX, Q. L. & REED, J. C. 1999. IAP family proteins--suppressors of apoptosis. *Genes Dev,* 13**,** 239-52.
- DING, K., LU, Y., NIKOLOVSKA-COLESKA, Z., WANG, G., QIU, S., SHANGARY, S., GAO, W., QIN, D., STUCKEY, J., KRAJEWSKI, K., ROLLER, P. P. & WANG, S. 2006. Structure-based design of spiro-oxindoles as potent, specific small-molecule inhibitors of the MDM2-p53 interaction. *J Med Chem,* 49**,** 3432-5.
- DINMAN, J. D. 2005. 5S rRNA: Structure and Function from Head to Toe. *Int J Biomed Sci,* 1**,** 2-7.
- DIXON, J., JONES, N. C., SANDELL, L. L., JAYASINGHE, S. M., CRANE, J., REY, J. P., DIXON, M. J. & TRAINOR, P. A. 2006. Tcof1/Treacle is required for neural crest cell formation and proliferation deficiencies that cause craniofacial abnormalities. *Proc Natl Acad Sci U S A,* 103**,** 13403-8.
- DOBBYN, H. C. & O'KEEFE, R. T. 2004. Analysis of Snu13p mutations reveals differential interactions with the U4 snRNA and U3 snoRNA. *RNA,* 10**,** 308-20.

- DONADIEU, J., LEBLANC, T., BADER MEUNIER, B., BARKAOUI, M., FENNETEAU, O., BERTRAND, Y., MAIER-REDELSPERGER, M., MICHEAU, M., STEPHAN, J. L., PHILLIPE, N., BORDIGONI, P., BABIN-BOILLETOT, A., BENSAID, P., MANEL, A. M., VILMER, E., THURET, I., BLANCHE, S., GLUCKMAN, E., FISCHER, A., MECHINAUD, F., JOLY, B., LAMY, T., HERMINE, O., CASSINAT, B., BELLANNE-CHANTELOT, C., CHOMIENNE, C. & FRENCH SEVERE CHRONIC NEUTROPENIA STUDY, G. 2005. Analysis of risk factors for myelodysplasias, leukemias and death from infection among patients with congenital neutropenia. Experience of the French Severe Chronic Neutropenia Study Group. *Haematologica,* 90**,** 45-53.
- DONATI, G., PEDDIGARI, S., MERCER, C. A. & THOMAS, G. 2013. 5S ribosomal RNA is an essential component of a nascent ribosomal precursor complex that regulates the Hdm2-p53 checkpoint. *Cell Rep,* 4**,** 87-98.
- DONG, J., LAI, R., JENNINGS, J. L., LINK, A. J. & HINNEBUSCH, A. G. 2005. The novel ATP-binding cassette protein ARB1 is a shuttling factor that stimulates 40S and 60S ribosome biogenesis. *Mol Cell Biol,* 25**,** 9859-73.
- DOTSCH, V., BERNASSOLA, F., COUTANDIN, D., CANDI, E. & MELINO, G. 2010. p63 and p73, the ancestors of p53. *Cold Spring Harb Perspect Biol,* 2**,** a004887.
- DRAGON, F., GALLAGHER, J. E., COMPAGNONE-POST, P. A., MITCHELL, B. M., PORWANCHER, K. A., WEHNER, K. A., WORMSLEY, S., SETTLAGE, R. E., SHABANOWITZ, J., OSHEIM, Y., BEYER, A. L., HUNT, D. F. & BASERGA, S. J. 2002. A large nucleolar U3 ribonucleoprotein required for 18S ribosomal RNA biogenesis. *Nature,* 417**,** 967-70.
- DRYGIN, D., O'BRIEN, S. E., HANNAN, R. D., MCARTHUR, G. A. & VON HOFF, D. D. 2014. Targeting the nucleolus for cancer-specific activation of p53. *Drug Discov Today,* 19**,** 259-65.
- DRYGIN, D., SIDDIQUI-JAIN, A., O'BRIEN, S., SCHWAEBE, M., LIN, A., BLIESATH, J., HO, C. B., PROFFITT, C., TRENT, K., WHITTEN, J. P., LIM, J. K., VON HOFF, D., ANDERES, K. & RICE, W. G. 2009. Anticancer activity of CX-3543: a direct inhibitor of rRNA biogenesis. *Cancer Res,* 69**,** 7653-61.
- DUAN, J., LI, L., LU, J., WANG, W. & YE, K. 2009. Structural mechanism of substrate RNA recruitment in H/ACA RNA-guided pseudouridine synthase. *Mol Cell,* 34**,** 427–439.

- DULIC, V., LEES, E. & REED, S. I. 1992. Association of human cyclin E with a periodic G1-S phase protein kinase. *Science,* 257**,** 1958-61.
- DUTT, S., NARLA, A., LIN, K., MULLALLY, A., ABAYASEKARA, N., MEGERDICHIAN, C., WILSON, F. H., CURRIE, T., KHANNA-GUPTA, A., BERLINER, N., KUTOK, J. L. & EBERT, B. L. 2011. Haploinsufficiency for ribosomal protein genes causes selective activation of p53 in human erythroid progenitor cells. *Blood,* 117**,** 2567-76.
- EBERT, B. L., GALILI, N., TAMAYO, P., BOSCO, J., MAK, R., PRETZ, J., TANGUTURI, S., LADD-ACOSTA, C., STONE, R., GOLUB, T. R. & RAZA, A. 2008a. An erythroid differentiation signature predicts response to lenalidomide in myelodysplastic syndrome. *PLoS Med,* 5**,** e35.
- EBERT, B. L., PRETZ, J., BOSCO, J., CHANG, C. Y., TAMAYO, P., GALILI, N., RAZA, A., ROOT, D. E., ATTAR, E., ELLIS, S. R. & GOLUB, T. R. 2008b. Identification of RPS14 as a 5q- syndrome gene by RNA interference screen. *Nature,* 451**,** 335-9.
- EDELMANN, M. J., IPHOFER, A., AKUTSU, M., ALTUN, M., DI GLERIA, K., KRAMER, H. B., FIEBIGER, E., DHE-PAGANON, S. & KESSLER, B. M. 2009. Structural basis and specificity of human otubain 1-mediated deubiquitination. *Biochem J,* 418**,** 379-90.
- EGAN, E. D. & COLLINS, K. 2012. An enhanced H/ACA RNP assembly mechanism for human telomerase RNA. *Mol Cell Biol,* 32**,** 2428-39.
- EL HAGE, A., KOPER, M., KUFEL, J. & TOLLERVEY, D. 2008. Efficient termination of transcription by RNA polymerase I requires the 5' exonuclease Rat1 in yeast. *Genes Dev,* 22**,** 1069-81.
- ELIAZ, D., DONIGER, T., TKACZ, I. D., BISWAS, V. K., GUPTA, S. K., KOLEV, N. G., UNGER, R., ULLU, E., TSCHUDI, C. & MICHAELI, S. 2015. Genome-wide analysis of small nucleolar RNAs of Leishmania major reveals a rich repertoire of RNAs involved in modification and processing of rRNA. *RNA Biol,* 12**,** 1222-55.
- ELLIS, S. R. 2014. Nucleolar stress in Diamond Blackfan anemia pathophysiology. *Biochim Biophys Acta,* 1842**,** 765-8.
- ELMORE, S. 2007. Apoptosis: a review of programmed cell death. *Toxicol Pathol,* 35**,** 495-516.

- ENRIGHT, C. A., MAXWELL, E. S., ELICEIRI, G. L. & SOLLNER-WEBB, B. 1996. 5'ETS rRNA processing facilitated by four small RNAs: U14, E3, U17, and U3. *RNA,* 2**,** 1094-9.
- ESGUERRA, J., WARRINGER, J. & BLOMBERG, A. 2008. Functional importance of individual rRNA 2'-O-ribose methylations revealed by high-resolution phenotyping. *RNA,* 14**,** 649-56.
- FABER, A. W., VOS, H. R., VOS, J. C. & RAUE, H. A. 2006. 5'-end formation of yeast 5.8SL rRNA is an endonucleolytic event. *Biochem Biophys Res Commun,* 345**,** 796-802.
- FANG, F., PHILLIPS, S. & BUTLER, J. S. 2005. Rat1p and Rai1p function with the nuclear exosome in the processing and degradation of rRNA precursors. *RNA,* 11**,** 1571-8.
- FANG, S., JENSEN, J. P., LUDWIG, R. L., VOUSDEN, K. H. & WEISSMAN, A. M. 2000. Mdm2 is a RING finger-dependent ubiquitin protein ligase for itself and p53. *J Biol Chem,* 275**,** 8945-51.
- FAYET-LEBARON, E., ATZORN, V., HENRY, Y. & KISS, T. 2009. 18S rRNA processing requires base pairings of snR30 H/ACA snoRNA to eukaryote-specific 18S sequences. *EMBO J,* 28**,** 1260-70.
- FEDERICI, L. & FALINI, B. 2013. Nucleophosmin mutations in acute myeloid leukemia: a tale of protein unfolding and mislocalization. *Protein Sci,* 22**,** 545-56.
- FENG, J., FUNK, W. D., WANG, S. S., WEINRICH, S. L., AVILION, A. A., CHIU, C. P., ADAMS, R. R., CHANG, E., ALLSOPP, R. C., YU, J. & ET AL. 1995. The RNA component of human telomerase. *Science,* 269**,** 1236-41.
- FERNANDEZ, I. S., NG, C. L., KELLEY, A. C., WU, G., YU, Y. T. & RAMAKRISHNAN, V. 2013. Unusual base pairing during the decoding of a stop codon by the ribosome. *Nature,* 500**,** 107-10.
- FERREIRA-CERCA, S., POLL, G., GLEIZES, P. E., TSCHOCHNER, H. & MILKEREIT, P. 2005. Roles of eukaryotic ribosomal proteins in maturation and transport of pre-18S rRNA and ribosome function. *Mol Cell,* 20**,** 263-75.
- FERREIRA-CERCA, S., POLL, G., KUHN, H., NEUEDER, A., JAKOB, S., TSCHOCHNER, H. & MILKEREIT, P. 2007. Analysis of the in vivo assembly pathway of eukaryotic 40S ribosomal proteins. *Mol Cell,* 28**,** 446-57.

- FINCH, A. J., HILCENKO, C., BASSE, N., DRYNAN, L. F., GOYENECHEA, B., MENNE, T. F., GONZALEZ FERNANDEZ, A., SIMPSON, P., D'SANTOS, C. S., ARENDS, M. J., DONADIEU, J., BELLANNE-CHANTELOT, C., COSTANZO, M., BOONE, C., MCKENZIE, A. N., FREUND, S. M. & WARREN, A. J. 2011. Uncoupling of GTP hydrolysis from eIF6 release on the ribosome causes Shwachman-Diamond syndrome. *Genes Dev,* 25**,** 917-29.
- FINLEY, D., BARTEL, B. & VARSHAVSKY, A. 1989. The tails of ubiquitin precursors are ribosomal proteins whose fusion to ubiquitin facilitates ribosome biogenesis. *Nature,* 338**,** 394-401.
- FINLEY, D., OZKAYNAK, E. & VARSHAVSKY, A. 1987. The yeast polyubiquitin gene is essential for resistance to high temperatures, starvation, and other stresses. *Cell,* 48**,** 1035-46.
- FREED, E., BLEICHERT, F., DUTCA, L. & BASERGA, S. 2010a. When ribosomes go bad: diseases of ribosome biogenesis. *Molecular bioSystems,* 6**,** 481-493.
- FREED, E. F., BLEICHERT, F., DUTCA, L. M. & BASERGA, S. J. 2010b. When ribosomes go bad: diseases of ribosome biogenesis. *Molecular bioSystems,* 6**,** 481-493.
- FRIDMAN, J. S. & LOWE, S. W. 2003. Control of apoptosis by p53. *Oncogene,* 22**,** 9030-40.
- FUCHS, Y. & STELLER, H. 2011. Programmed cell death in animal development and disease. *Cell,* 147**,** 742-58.
- FUMAGALLI, S., DI CARA, A., NEB-GULATI, A., NATT, F., SCHWEMBERGER, S., HALL, J., BABCOCK, G. F., BERNARDI, R., PANDOLFI, P. P. & THOMAS, G. 2009. Absence of nucleolar disruption after impairment of 40S ribosome biogenesis reveals an rpL11-translation-dependent mechanism of p53 induction. *Nat Cell Biol,* 11**,** 501-8.
- FUMAGALLI, S., IVANENKOV, V. V., TENG, T. & THOMAS, G. 2012. Suprainduction of p53 by disruption of 40S and 60S ribosome biogenesis leads to the activation of a novel G2/M checkpoint. *Genes Dev,* 26**,** 1028-40.
- GAMALINDA, M. & WOOLFORD, J. L., JR. 2015. Paradigms of ribosome synthesis: Lessons learned from ribosomal proteins. *Translation (Austin),* 3**,** e975018.

- GANOT, P., BORTOLIN, M. & KISS, T. 1997a. Site-specific pseudouridine formation in preribosomal RNA is guided by small nucleolar RNAs. *Cell,* 89**,** 799-809.
- GANOT, P., CAIZERGUES-FERRER, M. & KISS, T. 1997b. The family of box ACA small nucleolar RNAs is defined by an evolutionarily conserved secondary structure and ubiquitous sequence elements essential for RNA accumulation. *Genes Dev,* 11**,** 941-56.
- GASSE, L., FLEMMING, D. & HURT, E. 2015. Coordinated Ribosomal ITS2 RNA Processing by the Las1 Complex Integrating Endonuclease, Polynucleotide Kinase, and Exonuclease Activities. *Mol Cell,* 60**,** 808-15.
- GAZDA, H. T., PRETI, M., SHEEN, M. R., O'DONOHUE, M. F., VLACHOS, A., DAVIES, S. M., KATTAMIS, A., DOHERTY, L., LANDOWSKI, M., BUROS, C., GHAZVINIAN, R., SIEFF, C. A., NEWBURGER, P. E., NIEWIADOMSKA, E., MATYSIAK, M., GLADER, B., ATSIDAFTOS, E., LIPTON, J. M., GLEIZES, P. E. & BEGGS, A. H. 2012. Frameshift mutation in p53 regulator RPL26 is associated with multiple physical abnormalities and a specific pre-ribosomal RNA processing defect in diamond-blackfan anemia. *Hum Mutat,* 33**,** 1037-44.
- GAZDA, H. T., SHEEN, M. R., VLACHOS, A., CHOESMEL, V., O'DONOHUE, M. F., SCHNEIDER, H., DARRAS, N., HASMAN, C., SIEFF, C. A., NEWBURGER, P. E., BALL, S. E., NIEWIADOMSKA, E., MATYSIAK, M., ZAUCHA, J. M., GLADER, B., NIEMEYER, C., MEERPOHL, J. J., ATSIDAFTOS, E., LIPTON, J. M., GLEIZES, P. E. & BEGGS, A. H. 2008. Ribosomal protein L5 and L11 mutations are associated with cleft palate and abnormal thumbs in Diamond-Blackfan anemia patients. *Am J Hum Genet,* 83**,** 769-80.
- GE, J., CROSBY, S. D., HEINZ, M. E., BESSLER, M. & MASON, P. J. 2010a. SnoRNA microarray analysis reveals changes in H/ACA and C/D RNA levels caused by dyskerin ablation in mouse liver. *Biochem J,* 429**,** 33-41.
- GE, J., RUDNICK, D. A., HE, J., CRIMMINS, D. L., LADENSON, J. H., BESSLER, M. & MASON, P. J. 2010b. Dyskerin ablation in mouse liver inhibits rRNA processing and cell division. *Mol Cell Biol,* 30**,** 413-22.
- GEERLINGS, T. H., FABER, A. W., BISTER, M. D., VOS, J. C. & RAUE, H. A. 2003. Rio2p, an evolutionarily conserved, low abundant protein kinase essential

for processing of 20 S Pre-rRNA in Saccharomyces cerevisiae. *J Biol Chem,* 278**,** 22537-45.

- GEERLINGS, T. H., VOS, J. C. & RAUE, H. A. 2000. The final step in the formation of 25S rRNA in Saccharomyces cerevisiae is performed by 5'-->3' exonucleases. *RNA,* 6**,** 1698-703.
- GENTILELLA, A., KOZMA, S. C. & THOMAS, G. 2015. A liaison between mTOR signaling, ribosome biogenesis and cancer. *Biochim Biophys Acta,* 1849**,** 812-20.
- GERBI, S. A. & BOROVJAGIN, A. 1997. U3 snoRNA may recycle through different compartments of the nucleolus. *Chromosoma,* 105**,** 401-6.
- GHOSHAL, K. & JACOB, S. T. 1994. Specific inhibition of pre-ribosomal RNA processing in extracts from the lymphosarcoma cells treated with 5-fluorouracil. *Cancer Res,* 54**,** 632-6.
- GIGOVA, A., DUGGIMPUDI, S., POLLEX, T., SCHAEFER, M. & KOS, M. 2014. A cluster of methylations in the domain IV of 25S rRNA is required for ribosome stability. *RNA,* 20**,** 1632-44.
- GINELL, S., LESSINGER, L. & BERMAN, H. M. 1988. The crystal and molecular structure of the anticancer drug actinomycin D--some explanations for its unusual properties. *Biopolymers,* 27**,** 843-64.
- GIORDANO, E., PELUSO, I., SENGER, S. & FURIA, M. 1999. minifly, a Drosophila gene required for ribosome biogenesis. *J Cell Biol,* 144**,** 1123-33.
- GIRARD, J. P., LEHTONEN, H., CAIZERGUES-FERRER, M., AMALRIC, F., TOLLERVEY, D. & LAPEYRE, B. 1992. GAR1 is an essential small nucleolar RNP protein required for pre-rRNA processing in yeast. *EMBO J,* 11**,** 673-82.
- GOLOMB, L., VOLAREVIC, S. & OREN, M. 2014. p53 and ribosome biogenesis stress: the essentials. *FEBS Lett,* 588**,** 2571-9.
- GONZALES, B., HENNING, D., SO, R. B., DIXON, J., DIXON, M. J. & VALDEZ, B. C. 2005. The Treacher Collins syndrome (TCOF1) gene product is involved in pre-rRNA methylation. *Hum Mol Genet,* 14**,** 2035-43.
- GOODSELL, D. S. 2000. The molecular perspective: caspases. *Stem Cells,* 18**,** 457-8.
- GOTTLIEB, E. & VOUSDEN, K. H. 2010. p53 regulation of metabolic pathways. *Cold Spring Harb Perspect Biol,* 2**,** a001040.

- GRANNEMAN, S. & BASERGA, S. J. 2004. Ribosome biogenesis: of knobs and RNA processing. *Exp Cell Res,* 296**,** 43-50.
- GREBER, B. J., GERHARDY, S., LEITNER, A., LEIBUNDGUT, M., SALEM, M., BOEHRINGER, D., LEULLIOT, N., AEBERSOLD, R., PANSE, V. G. & BAN, N. 2016. Insertion of the Biogenesis Factor Rei1 Probes the Ribosomal Tunnel during 60S Maturation. *Cell,* 164**,** 91-102.
- GREEN, D. R. & KROEMER, G. 2009. Cytoplasmic functions of the tumour suppressor p53. *Nature,* 458**,** 1127-30.
- GROENEWOUD, M. J. & ZWARTKRUIS, F. J. 2013. Rheb and Rags come together at the lysosome to activate mTORC1. *Biochem Soc Trans,* 41**,** 951-5.
- GROSS, A., JOCKEL, J., WEI, M. C. & KORSMEYER, S. J. 1998. Enforced dimerization of BAX results in its translocation, mitochondrial dysfunction and apoptosis. *EMBO J,* 17**,** 3878-85.
- GROU, C. P., PINTO, M. P., MENDES, A. V., DOMINGUES, P. & AZEVEDO, J. E. 2015. The de novo synthesis of ubiquitin: identification of deubiquitinases acting on ubiquitin precursors. *Sci Rep,* 5**,** 12836.
- GRUMMITT, C. G., TOWNSLEY, F. M., JOHNSON, C. M., WARREN, A. J. & BYCROFT, M. 2008. Structural consequences of nucleophosmin mutations in acute myeloid leukemia. *J Biol Chem,* 283**,** 23326-32.
- GRUMMT, I. 1999. Regulation of mammalian ribosomal gene transcription by RNA polymerase I. *Prog Nucleic Acid Res Mol Biol,* 62**,** 109-54.
- GU, B. W., APICELLA, M., MILLS, J., FAN, J. M., REEVES, D. A., FRENCH, D., PODSAKOFF, G. M., BESSLER, M. & MASON, P. J. 2015. Impaired Telomere Maintenance and Decreased Canonical WNT Signaling but Normal Ribosome Biogenesis in Induced Pluripotent Stem Cells from X-Linked Dyskeratosis Congenita Patients. *PLoS One,* 10**,** e0127414.
- GU, B. W., BESSLER, M. & MASON, P. J. 2008. A pathogenic dyskerin mutation impairs proliferation and activates a DNA damage response independent of telomere length in mice. *Proc Natl Acad Sci U S A,* 105**,** 10173-8.
- GU, B. W., GE, J., FAN, J. M., BESSLER, M. & MASON, P. J. 2013. Slow growth and unstable ribosomal RNA lacking pseudouridine in mouse embryonic fibroblast cells expressing catalytically inactive dyskerin. *FEBS Lett,* 587**,** 2112-7.

- GUO, N. & PENG, Z. 2013. MG132, a proteasome inhibitor, induces apoptosis in tumor cells. *Asia Pac J Clin Oncol,* 9**,** 6-11.
- GUPTA, S. K., HURY, A., ZIPOREN, Y., SHI, H., ULLU, E. & MICHAELI, S. 2010. Small nucleolar RNA interference in Trypanosoma brucei: mechanism and utilization for elucidating the function of snoRNAs. *Nucleic Acids Res,* 38**,** 7236-47.
- HAAF, T., HAYMAN, D. L. & SCHMID, M. 1991. Quantitative determination of rDNA transcription units in vertebrate cells. *Exp Cell Res,* 193**,** 78-86.
- HAAF, T. & SCHMID, M. 1991. Chromosome topology in mammalian interphase nuclei. *Exp Cell Res,* 192**,** 325-32.
- HALL, M., BATES, S. & PETERS, G. 1995a. Evidence for different modes of action of cyclin-dependent kinase inhibitors: p15 and p16 bind to kinases, p21 and p27 bind to cyclins. *Oncogene,* 11**,** 1581-8.
- HALL, P. A., KEARSEY, J. M., COATES, P. J., NORMAN, D. G., WARBRICK, E. & COX, L. S. 1995b. Characterisation of the interaction between PCNA and Gadd45. *Oncogene,* 10**,** 2427-33.
- HALLENBERG, C. & FREDERIKSEN, S. 2001. Effect of mutations in the upstream promoter on the transcription of human 5S rRNA genes. *Biochim Biophys Acta,* 1520**,** 169-73.
- HAMMOND-MARTEL, I., YU, H. & AFFAR EL, B. 2012. Roles of ubiquitin signaling in transcription regulation. *Cell Signal,* 24**,** 410-21.
- HARA, K., MARUKI, Y., LONG, X., YOSHINO, K., OSHIRO, N., HIDAYAT, S., TOKUNAGA, C., AVRUCH, J. & YONEZAWA, K. 2002. Raptor, a binding partner of target of rapamycin (TOR), mediates TOR action. *Cell,* 110**,** 177-89.
- HARPER, J. W., ELLEDGE, S. J., KEYOMARSI, K., DYNLACHT, B., TSAI, L. H., ZHANG, P., DOBROWOLSKI, S., BAI, C., CONNELL-CROWLEY, L., SWINDELL, E. & ET AL. 1995. Inhibition of cyclin-dependent kinases by p21. *Mol Biol Cell,* 6**,** 387-400.
- HAY, N. & SONENBERG, N. 2004. Upstream and downstream of mTOR. *Genes Dev,* 18**,** 1926-45.
- HEISS, N. S., GIROD, A., SALOWSKY, R., WIEMANN, S., PEPPERKOK, R. & POUSTKA, A. 1999. Dyskerin localizes to the nucleolus and its mislocalization is unlikely to play a role in the pathogenesis of dyskeratosis congenita. *Hum Mol Genet,* 8**,** 2515-24.

- HEISS, N. S., KNIGHT, S. W., VULLIAMY, T. J., KLAUCK, S. M., WIEMANN, S., MASON, P. J., POUSTKA, A. & DOKAL, I. 1998. X-linked dyskeratosis congenita is caused by mutations in a highly conserved gene with putative nucleolar functions. *Nat Genet,* 19**,** 32-8.
- HELM, M. 2006. Post-transcriptional nucleotide modification and alternative folding of RNA. *Nucleic Acids Res,* 34**,** 721-33.
- HENDERSON, A. S., WARBURTON, D. & ATWOOD, K. C. 1972. Location of ribosomal DNA in the human chromosome complement. *Proc Natl Acad Sci U S A,* 69**,** 3394-8.
- HENRAS, A. K., DEZ, C. & HENRY, Y. 2004. RNA structure and function in C/D and H/ACA s(no)RNPs. *Curr Opin Struct Biol,* 14**,** 335-43.
- HENRAS, A. K., PLISSON-CHASTANG, C., O'DONOHUE, M. F., CHAKRABORTY, A. & GLEIZES, P. E. 2015. An overview of pre-ribosomal RNA processing in eukaryotes. *Wiley Interdiscip Rev RNA,* 6**,** 225-42.
- HENRAS, A. K., SOUDET, J., GERUS, M., LEBARON, S., CAIZERGUES-FERRER, M., MOUGIN, A. & HENRY, Y. 2008. The post-transcriptional steps of eukaryotic ribosome biogenesis. *Cell Mol Life Sci,* 65**,** 2334-59.
- HERSHKO, A. & CIECHANOVER, A. 1998. The ubiquitin system. *Annu Rev Biochem,* 67**,** 425-79.
- HICKE, L. 2001. Protein regulation by monoubiquitin. *Nat Rev Mol Cell Biol,* 2**,** 195-201.
- HIGA-NAKAMINE, S., SUZUKI, T., UECHI, T., CHAKRABORTY, A., NAKAJIMA, Y., NAKAMURA, M., HIRANO, N., SUZUKI, T. & KENMOCHI, N. 2012. Loss of ribosomal RNA modification causes developmental defects in zebrafish. *Nucleic Acids Res,* 40**,** 391-8.
- HIRAO, A., KONG, Y. Y., MATSUOKA, S., WAKEHAM, A., RULAND, J., YOSHIDA, H., LIU, D., ELLEDGE, S. J. & MAK, T. W. 2000. DNA damage-induced activation of p53 by the checkpoint kinase Chk2. *Science,* 287**,** 1824-7.
- HLAVATA, I., MOHELNIKOVA-DUCHONOVA, B., VACLAVIKOVA, R., LISKA, V., PITULE, P., NOVAK, P., BRUHA, J., VYCITAL, O., HOLUBEC, L., TRESKA, V., VODICKA, P. & SOUCEK, P. 2012. The role of ABC transporters in progression and clinical outcome of colorectal cancer. *Mutagenesis,* 27**,** 187-96.

- HORN, D. M., MASON, S. L. & KARBSTEIN, K. 2011. Rcl1 protein, a novel nuclease for 18 S ribosomal RNA production. *J Biol Chem,* 286**,** 34082-7.
- HORN, H. F. & VOUSDEN, K. H. 2008. Cooperation between the ribosomal proteins L5 and L11 in the p53 pathway. *Oncogene,* 27**,** 5774-84.
- HU, M., LI, P., SONG, L., JEFFREY, P. D., CHENOVA, T. A., WILKINSON, K. D., COHEN, R. E. & SHI, Y. 2005. Structure and mechanisms of the proteasome-associated deubiquitinating enzyme USP14. *EMBO J,* 24**,** 3747-56.
- HUANG, H., JOAZEIRO, C. A., BONFOCO, E., KAMADA, S., LEVERSON, J. D. & HUNTER, T. 2000. The inhibitor of apoptosis, cIAP2, functions as a ubiquitin-protein ligase and promotes in vitro monoubiquitination of caspases 3 and 7. *J Biol Chem,* 275**,** 26661-4.
- HUNG, N. J., LO, K. Y., PATEL, S. S., HELMKE, K. & JOHNSON, A. W. 2008. Arx1 is a nuclear export receptor for the 60S ribosomal subunit in yeast. *Mol Biol Cell,* 19**,** 735-44.
- HUTTEN, S. & KEHLENBACH, R. H. 2007. CRM1-mediated nuclear export: to the pore and beyond. *Trends Cell Biol,* 17**,** 193-201.
- IKEDA, F. & DIKIC, I. 2008. Atypical ubiquitin chains: new molecular signals. 'Protein Modifications: Beyond the Usual Suspects' review series. *EMBO Rep,* 9**,** 536-42.
- IKURA, T., TASHIRO, S., KAKINO, A., SHIMA, H., JACOB, N., AMUNUGAMA, R., YODER, K., IZUMI, S., KURAOKA, I., TANAKA, K., KIMURA, H., IKURA, M., NISHIKUBO, S., ITO, T., MUTO, A., MIYAGAWA, K., TAKEDA, S., FISHEL, R., IGARASHI, K. & KAMIYA, K. 2007. DNA damage-dependent acetylation and ubiquitination of H2AX enhances chromatin dynamics. *Mol Cell Biol,* 27**,** 7028-40.
- IORIO, F., KNIJNENBURG, T. A., VIS, D. J., BIGNELL, G. R., MENDEN, M. P., SCHUBERT, M., ABEN, N., GONCALVES, E., BARTHORPE, S., LIGHTFOOT, H., COKELAER, T., GRENINGER, P., VAN DYK, E., CHANG, H., DE SILVA, H., HEYN, H., DENG, X., EGAN, R. K., LIU, Q., MIRONENKO, T., MITROPOULOS, X., RICHARDSON, L., WANG, J., ZHANG, T., MORAN, S., SAYOLS, S., SOLEIMANI, M., TAMBORERO, D., LOPEZ-BIGAS, N., ROSS-MACDONALD, P., ESTELLER, M., GRAY, N. S., HABER, D. A., STRATTON, M. R., BENES, C. H., WESSELS, L. F., SAEZ-RODRIGUEZ, J., MCDERMOTT,

U. & GARNETT, M. J. 2016. A Landscape of Pharmacogenomic Interactions in Cancer. *Cell,* 166**,** 740-54.

- ISHIGURO, A., KASSAVETIS, G. A. & GEIDUSCHEK, E. P. 2002. Essential roles of Bdp1, a subunit of RNA polymerase III initiation factor TFIIIB, in transcription and tRNA processing. *Mol Cell Biol,* 22**,** 3264-75.
- JAAKO, P., DEBNATH, S., OLSSON, K., ZHANG, Y., FLYGARE, J., LINDSTROM, M. S., BRYDER, D. & KARLSSON, S. 2015. Disruption of the 5S RNP-Mdm2 interaction significantly improves the erythroid defect in a mouse model for Diamond-Blackfan anemia. *Leukemia,* 29**,** 2221-9.
- JADY, B. E. & KISS, T. 2001. A small nucleolar guide RNA functions both in 2'-O-ribose methylation and pseudouridylation of the U5 spliceosomal RNA. *EMBO J,* 20**,** 541-51.
- JANSA, P. & GRUMMT, I. 1999. Mechanism of transcription termination: PTRF interacts with the largest subunit of RNA polymerase I and dissociates paused transcription complexes from yeast and mouse. *Mol Gen Genet,* 262**,** 508-14.
- JIA, H., WANG, X., ANDERSON, J. T. & JANKOWSKY, E. 2012. RNA unwinding by the Trf4/Air2/Mtr4 polyadenylation (TRAMP) complex. *Proc Natl Acad Sci U S A,* 109**,** 7292-7.
- JIA, Q., ZHANG, Q., ZHANG, Z., WANG, Y., ZHANG, W., ZHOU, Y., WAN, Y., CHENG, T., ZHU, X., FANG, X., YUAN, W. & JIA, H. 2013. Transcriptome analysis of the zebrafish model of Diamond-Blackfan anemia from RPS19 deficiency via p53-dependent and -independent pathways. *PLoS One,* 8**,** e71782.
- JIN, A., ITAHANA, K., O'KEEFE, K. & ZHANG, Y. 2004. Inhibition of HDM2 and activation of p53 by ribosomal protein L23. *Mol Cell Biol,* 24**,** 7669-80.
- JOERGER, A. C., RAJAGOPALAN, S., NATAN, E., VEPRINTSEV, D. B., ROBINSON, C. V. & FERSHT, A. R. 2009. Structural evolution of p53, p63, and p73: implication for heterotetramer formation. *Proc Natl Acad Sci U S A,* 106**,** 17705-10.
- JOHNSON, A. W., LUND, E. & DAHLBERG, J. 2002. Nuclear export of ribosomal subunits. *Trends Biochem Sci,* 27**,** 580-5.
- JONES, N. C., LYNN, M. L., GAUDENZ, K., SAKAI, D., AOTO, K., REY, J. P., GLYNN, E. F., ELLINGTON, L., DU, C., DIXON, J., DIXON, M. J. & TRAINOR,

P. A. 2008. Prevention of the neurocristopathy Treacher Collins syndrome through inhibition of p53 function. *Nat Med,* 14**,** 125-33.

- JONES, P. M. & GEORGE, A. M. 2004. The ABC transporter structure and mechanism: perspectives on recent research. *Cell Mol Life Sci,* 61**,** 682-99.
- JORDAN, P. & CARMO-FONSECA, M. 1998. Cisplatin inhibits synthesis of ribosomal RNA in vivo. *Nucleic Acids Res,* 26**,** 2831-6.
- JORJANI, H., KEHR, S., JEDLINSKI, D. J., GUMIENNY, R., HERTEL, J., STADLER, P. F., ZAVOLAN, M. & GRUBER, A. R. 2016. An updated human snoRNAome. *Nucleic Acids Res,* 44**,** 5068-82.
- JUNG, Y. S., QIAN, Y. & CHEN, X. 2010. Examination of the expanding pathways for the regulation of p21 expression and activity. *Cell Signal,* 22**,** 1003-12.
- KAMADA, R., TOGUCHI, Y., NOMURA, T., IMAGAWA, T. & SAKAGUCHI, K. 2015. Tetramer formation of tumor suppressor protein p53: Structure, function, and applications. *Biopolymers*.
- KARBSTEIN, K. 2013. Quality control mechanisms during ribosome maturation. *Trends Cell Biol,* 23**,** 242-50.
- KARIJOLICH, J. & YU, Y. T. 2011. Converting nonsense codons into sense codons by targeted pseudouridylation. *Nature,* 474**,** 395-8.
- KARIMIAN, A., AHMADI, Y. & YOUSEFI, B. 2016. Multiple functions of p21 in cell cycle, apoptosis and transcriptional regulation after DNA damage. *DNA Repair (Amst),* 42**,** 63-71.
- KASSAVETIS, G. A., KUMAR, A., LETTS, G. A. & GEIDUSCHEK, E. P. 1998. A post-recruitment function for the RNA polymerase III transcription-initiation factor IIIB. *Proc Natl Acad Sci U S A,* 95**,** 9196-201.
- KEEL, S. B., DOTY, R. T., YANG, Z., QUIGLEY, J. G., CHEN, J., KNOBLAUGH, S., KINGSLEY, P. D., DE DOMENICO, I., VAUGHN, M. B., KAPLAN, J., PALIS, J. & ABKOWITZ, J. L. 2008. A heme export protein is required for red blood cell differentiation and iron homeostasis. *Science,* 319**,** 825-8.
- KENMOCHI, N., KAWAGUCHI, T., ROZEN, S., DAVIS, E., GOODMAN, N., HUDSON, T. J., TANAKA, T. & PAGE, D. C. 1998. A map of 75 human ribosomal protein genes. *Genome Res,* 8**,** 509-23.
- KHANNA-GUPTA, A. 2013. Bone Marrow Failure Syndromes: The Ribosomopathies. *J Bone Marrow Res,* 1.

- KHARDE, S., CALVINO, F. R., GUMIERO, A., WILD, K. & SINNING, I. 2015. The structure of Rpf2-Rrs1 explains its role in ribosome biogenesis. *Nucleic Acids Res,* 43**,** 7083-95.
- KIERZEK, E. & KIERZEK, R. 2003. The thermodynamic stability of RNA duplexes and hairpins containing N6-alkyladenosines and 2-methylthio-N6-alkyladenosines. *Nucleic Acids Res,* 31**,** 4472-80.
- KIM, D. H., SARBASSOV, D. D., ALI, S. M., LATEK, R. R., GUNTUR, K. V., ERDJUMENT-BROMAGE, H., TEMPST, P. & SABATINI, D. M. 2003. GbetaL, a positive regulator of the rapamycin-sensitive pathway required for the nutrient-sensitive interaction between raptor and mTOR. *Mol Cell,* 11**,** 895-904.
- KIMURA, Y. & TANAKA, K. 2010. Regulatory mechanisms involved in the control of ubiquitin homeostasis. *J Biochem,* 147**,** 793-8.
- KISS-LASZLO, Z., HENRY, Y., BACHELLERIE, J. P., CAIZERGUES-FERRER, M. & KISS, T. 1996. Site-specific ribose methylation of preribosomal RNA: a novel function for small nucleolar RNAs. *Cell,* 85**,** 1077-88.
- KISS, A. M., JADY, B. E., DARZACQ, X., VERHEGGEN, C., BERTRAND, E. & KISS, T. 2002. A Cajal body-specific pseudouridylation guide RNA is composed of two box H/ACA snoRNA-like domains. *Nucleic Acids Res,* 30**,** 4643-9.
- KISS, T., FAYET-LEBARON, E. & JADY, B. E. 2010. Box H/ACA small ribonucleoproteins. *Mol Cell,* 37**,** 597-606.
- KISS, T. & JADY, B. E. 2004. Functional characterization of 2'-O-methylation and pseudouridylation guide RNAs. *Methods Mol Biol,* 265**,** 393-408.
- KLINGE, S., VOIGTS-HOFFMANN, F., LEIBUNDGUT, M., ARPAGAUS, S. & BAN, N. 2011. Crystal structure of the eukaryotic 60S ribosomal subunit in complex with initiation factor 6. *Science,* 334**,** 941-8.
- KNIGHT, S. W., HEISS, N. S., VULLIAMY, T. J., AALFS, C. M., MCMAHON, C., RICHMOND, P., JONES, A., HENNEKAM, R. C., POUSTKA, A., MASON, P. J. & DOKAL, I. 1999. Unexplained aplastic anaemia, immunodeficiency, and cerebellar hypoplasia (Hoyeraal-Hreidarsson syndrome) due to mutations in the dyskeratosis congenita gene, DKC1. *Br J Haematol,* 107**,** 335-9.
- KNIGHT, S. W., VULLIAMY, T. J., HEISS, N. S., MATTHIJS, G., DEVRIENDT, K., CONNOR, J. M., D'URSO, M., POUSTKA, A., MASON, P. J. & DOKAL, I. 1998. 1.4 Mb candidate gene region for X linked dyskeratosis congenita defined

by combined haplotype and X chromosome inactivation analysis. *J Med Genet,* 35**,** 993-6.

- KNIGHT, S. W., VULLIAMY, T. J., MORGAN, B., DEVRIENDT, K., MASON, P. J. & DOKAL, I. 2001. Identification of novel DKC1 mutations in patients with dyskeratosis congenita: implications for pathophysiology and diagnosis. *Hum Genet,* 108**,** 299-303.
- KOMANDER, D., CLAGUE, M. J. & URBE, S. 2009. Breaking the chains: structure and function of the deubiquitinases. *Nat Rev Mol Cell Biol,* 10**,** 550-63.
- KOMANDER, D. & RAPE, M. 2012. The ubiquitin code. *Annu Rev Biochem,* 81**,** 203-29.
- KORNPROBST, M., TURK, M., KELLNER, N., CHENG, J., FLEMMING, D., KOS-BRAUN, I., KOS, M., THOMS, M., BERNINGHAUSEN, O., BECKMANN, R. & HURT, E. 2016. Architecture of the 90S Pre-ribosome: A Structural View on the Birth of the Eukaryotic Ribosome. *Cell,* 166**,** 380-93.
- KOZMA, S. C., REDMOND, S. M., FU, X. C., SAURER, S. M., GRONER, B. & HYNES, N. E. 1988. Activation of the receptor kinase domain of the trk oncogene by recombination with two different cellular sequences. *EMBO J,* 7**,** 147-54.
- KRESSLER, D., HURT, E. & BASSLER, J. 2010. Driving ribosome assembly. *Biochim Biophys Acta,* 1803**,** 673-83.
- KRESSLER, D., LINDER, P. & DE LA CRUZ, J. 1999. Protein trans-acting factors involved in ribosome biogenesis in Saccharomyces cerevisiae. *Mol Cell Biol,* 19**,** 7897-912.
- KRZESNIAK, M., ZAJKOWICZ, A., MATUSZCZYK, I. & RUSIN, M. 2014. Rapamycin prevents strong phosphorylation of p53 on serine 46 and attenuates activation of the p53 pathway in A549 lung cancer cells exposed to actinomycin D. *Mech Ageing Dev*.
- KUAI, L., FANG, F., BUTLER, J. S. & SHERMAN, F. 2004. Polyadenylation of rRNA in Saccharomyces cerevisiae. *Proc Natl Acad Sci U S A,* 101**,** 8581-6.
- KUHN, J. F., TRAN, E. J. & MAXWELL, E. S. 2002. Archaeal ribosomal protein L7 is a functional homolog of the eukaryotic 15.5kD/Snu13p snoRNP core protein. *Nucleic Acids Res,* 30**,** 931-41.
- KUMAR, A., GROVE, A., KASSAVETIS, G. A. & GEIDUSCHEK, E. P. 1998. Transcription factor IIIB: the architecture of its DNA complex, and its roles in

initiation of transcription by RNA polymerase III. *Cold Spring Harb Symp Quant Biol,* 63**,** 121-9.

- KURANDA, K., BERTHON, C., LEPRETRE, F., POLAKOWSKA, R., JOUY, N. & QUESNEL, B. 2011. Expression of CD34 in hematopoietic cancer cell lines reflects tightly regulated stem/progenitor-like state. *J Cell Biochem,* 112**,** 1277-85.
- LAFONTAINE, D. L., BOUSQUET-ANTONELLI, C., HENRY, Y., CAIZERGUES-FERRER, M. & TOLLERVEY, D. 1998. The box H + ACA snoRNAs carry Cbf5p, the putative rRNA pseudouridine synthase. *Genes Dev,* 12**,** 527-37.
- LAM, Y. W., LAMOND, A. I., MANN, M. & ANDERSEN, J. S. 2007. Analysis of nucleolar protein dynamics reveals the nuclear degradation of ribosomal proteins. *Curr Biol,* 17**,** 749-60.
- LAMANNA, A. C. & KARBSTEIN, K. 2011. An RNA conformational switch regulates pre-18S rRNA cleavage. *J Mol Biol,* 405**,** 3-17.
- LANE, D. P. & CRAWFORD, L. V. 1979. T antigen is bound to a host protein in SV40-transformed cells. *Nature,* 278**,** 261-3.
- LAPLANTE, M. & SABATINI, D. M. 2009a. An emerging role of mTOR in lipid biosynthesis. *Curr Biol,* 19**,** R1046-52.
- LAPLANTE, M. & SABATINI, D. M. 2009b. mTOR signaling at a glance. *J Cell Sci,* 122**,** 3589-94.
- LARONGA, C., YANG, H. Y., NEAL, C. & LEE, M. H. 2000. Association of the cyclin-dependent kinases and 14-3-3 sigma negatively regulates cell cycle progression. *J Biol Chem,* 275**,** 23106-12.
- LAYAT, E., PROBST, A. V. & TOURMENTE, S. 2013. Structure, function and regulation of Transcription Factor IIIA: From Xenopus to Arabidopsis. *Biochim Biophys Acta,* 1829**,** 274-82.
- LEBARON, S., SCHNEIDER, C., VAN NUES, R. W., SWIATKOWSKA, A., WALSH, D., BOTTCHER, B., GRANNEMAN, S., WATKINS, N. J. & TOLLERVEY, D. 2012. Proofreading of pre-40S ribosome maturation by a translation initiation factor and 60S subunits. *Nat Struct Mol Biol,* 19**,** 744-53.
- LECKER, S. H., GOLDBERG, A. L. & MITCH, W. E. 2006. Protein degradation by the ubiquitin-proteasome pathway in normal and disease states. *J Am Soc Nephrol,* 17**,** 1807-19.

- LEE, J., HWANG, Y. J., RYU, H., KOWALL, N. W. & RYU, H. 2014. Nucleolar dysfunction in Huntington's disease. *Biochim Biophys Acta,* 1842**,** 785-90.
- LEE, J. C. & PETER, M. E. 2003. Regulation of apoptosis by ubiquitination. *Immunol Rev,* 193**,** 39-47.
- LEE, Y., ERKINE, A. M., VAN RYK, D. I. & NAZAR, R. N. 1995. In vivo analyses of the internal control region in the 5S rRNA gene from Saccharomyces cerevisiae. *Nucleic Acids Res,* 23**,** 634-40.
- LESTRADE, L. & WEBER, M. J. 2006. snoRNA-LBME-db, a comprehensive database of human H/ACA and C/D box snoRNAs. *Nucleic Acids Res,* 34**,** D158-62.
- LEVINE, A. J. 1989. The p53 tumor suppressor gene and gene product. *Princess Takamatsu Symp,* 20**,** 221-30.
- LEVY, S., AVNI, D., HARIHARAN, N., PERRY, R. P. & MEYUHAS, O. 1991. Oligopyrimidine tract at the 5' end of mammalian ribosomal protein mRNAs is required for their translational control. *Proc Natl Acad Sci U S A,* 88**,** 3319-23.
- LI, H. D., ZAGORSKI, J. & FOURNIER, M. J. 1990. Depletion of U14 small nuclear RNA (snR128) disrupts production of 18S rRNA in Saccharomyces cerevisiae. *Mol Cell Biol,* 10**,** 1145-52.
- LI, L. & YE, K. 2006. Crystal structure of an H/ACA box ribonucleoprotein particle. *Nature,* 443**,** 302-7.
- LI, M. & GU, W. 2011. A critical role for noncoding 5S rRNA in regulating Mdmx stability. *Mol Cell,* 43**,** 1023-32.
- LI, S., DUAN, J., LI, D., YANG, B., DONG, M. & YE, K. 2011. Reconstitution and structural analysis of the yeast box H/ACA RNA-guided pseudouridine synthase. *Genes Dev,* 25**,** 2409-21.
- LI, W., BENGTSON, M. H., ULBRICH, A., MATSUDA, A., REDDY, V. A., ORTH, A., CHANDA, S. K., BATALOV, S. & JOAZEIRO, C. A. 2008. Genome-wide and functional annotation of human E3 ubiquitin ligases identifies MULAN, a mitochondrial E3 that regulates the organelle's dynamics and signaling. *PLoS One,* 3**,** e1487.
- LI, W. & YE, Y. 2008. Polyubiquitin chains: functions, structures, and mechanisms. *Cell Mol Life Sci,* 65**,** 2397-406.

- LIANG, B., ZHOU, J., KAHEN, E., TERNS, R. M., TERNS, M. P. & LI, H. 2009. Structure of a functional ribonucleoprotein pseudouridine synthase bound to a substrate RNA. *Nat Struct Mol Biol,* 16**,** 740-6.
- LIANG, X. H., LIU, Q., LIU, Q., KING, T. H. & FOURNIER, M. J. 2010. Strong dependence between functional domains in a dual-function snoRNA infers coupling of rRNA processing and modification events. *Nucleic Acids Res,* 38**,** 3376-87.
- LIAO, J. M., ZHOU, X., GATIGNOL, A. & LU, H. 2014. Ribosomal proteins L5 and L11 co-operatively inactivate c-Myc via RNA-induced silencing complex. *Oncogene,* 33**,** 4916-23.
- LIN, J., LAI, S., JIA, R., XU, A., ZHANG, L., LU, J. & YE, K. 2011. Structural basis for site-specific ribose methylation by box C/D RNA protein complexes. *Nature,* 469**,** 559-63.
- LIN, Y., MA, W. & BENCHIMOL, S. 2000. Pidd, a new death-domain-containing protein, is induced by p53 and promotes apoptosis. *Nat Genet,* 26**,** 122-7.
- LIN, Y. C., BOONE, M., MEURIS, L., LEMMENS, I., VAN ROY, N., SOETE, A., REUMERS, J., MOISSE, M., PLAISANCE, S., DRMANAC, R., CHEN, J., SPELEMAN, F., LAMBRECHTS, D., VAN DE PEER, Y., TAVERNIER, J. & CALLEWAERT, N. 2014. Genome dynamics of the human embryonic kidney 293 lineage in response to cell biology manipulations. *Nat Commun,* 5**,** 4767.
- LINARES, L. K., HENGSTERMANN, A., CIECHANOVER, A., MULLER, S. & SCHEFFNER, M. 2003. HdmX stimulates Hdm2-mediated ubiquitination and degradation of p53. *Proc Natl Acad Sci U S A,* 100**,** 12009-14.
- LINDSTROM, M. S. 2011. NPM1/B23: A Multifunctional Chaperone in Ribosome Biogenesis and Chromatin Remodeling. *Biochem Res Int,* 2011**,** 195209.
- LINDSTROM, M. S., JIN, A., DEISENROTH, C., WHITE WOLF, G. & ZHANG, Y. 2007. Cancer-associated mutations in the MDM2 zinc finger domain disrupt ribosomal protein interaction and attenuate MDM2-induced p53 degradation. *Mol Cell Biol,* 27**,** 1056-68.
- LINZER, D. I. & LEVINE, A. J. 1979. Characterization of a 54K dalton cellular SV40 tumor antigen present in SV40-transformed cells and uninfected embryonal carcinoma cells. *Cell,* 17**,** 43-52.

- LIPFORD, J. R., SMITH, G. T., CHI, Y. & DESHAIES, R. J. 2005. A putative stimulatory role for activator turnover in gene expression. *Nature,* 438**,** 113-6.
- LIPTON, J. M. & ELLIS, S. R. 2010. Diamond Blackfan anemia 2008-2009: broadening the scope of ribosome biogenesis disorders. *Curr Opin Pediatr,* 22**,** 12-9.
- LIST, A., DEWALD, G., BENNETT, J., GIAGOUNIDIS, A., RAZA, A., FELDMAN, E., POWELL, B., GREENBERG, P., THOMAS, D., STONE, R., REEDER, C., WRIDE, K., PATIN, J., SCHMIDT, M., ZELDIS, J., KNIGHT, R. & MYELODYSPLASTIC SYNDROME-003 STUDY, I. 2006. Lenalidomide in the myelodysplastic syndrome with chromosome 5q deletion. *N Engl J Med,* 355**,** 1456-65.
- LJUNGSTROM, V., CORTESE, D., YOUNG, E., PANDZIC, T., MANSOURI, L., PLEVOVA, K., NTOUFA, S., BALIAKAS, P., CLIFFORD, R., SUTTON, L. A., BLAKEMORE, S. J., STAVROYIANNI, N., AGATHANGELIDIS, A., ROSSI, D., HOGLUND, M., KOTASKOVA, J., JULIUSSON, G., BELESSI, C., CHIORAZZI, N., PANAGIOTIDIS, P., LANGERAK, A. W., SMEDBY, K. E., OSCIER, D., GAIDANO, G., SCHUH, A., DAVI, F., POTT, C., STREFFORD, J. C., TRENTIN, L., POSPISILOVA, S., GHIA, P., STAMATOPOULOS, K., SJOBLOM, T. & ROSENQUIST, R. 2016. Whole-exome sequencing in relapsing chronic lymphocytic leukemia: clinical impact of recurrent RPS15 mutations. *Blood,* 127**,** 1007-16.
- LOCKSLEY, R. M., KILLEEN, N. & LENARDO, M. J. 2001. The TNF and TNF receptor superfamilies: integrating mammalian biology. *Cell,* 104**,** 487-501.
- LOHRUM, M. A., LUDWIG, R. L., KUBBUTAT, M. H., HANLON, M. & VOUSDEN, K. H. 2003. Regulation of HDM2 activity by the ribosomal protein L11. *Cancer Cell,* 3**,** 577-87.
- LONGLEY, D. B., HARKIN, D. P. & JOHNSTON, P. G. 2003. 5-fluorouracil: mechanisms of action and clinical strategies. *Nat Rev Cancer,* 3**,** 330-8.
- LU, Y. Z. A. H. 2006. Signaling to p53: Ribosomal Proteins Find Their Way. *Cancer Cell,* 16**,** 169-377.
- LUKOWIAK, A. A., NARAYANAN, A., LI, Z. H., TERNS, R. M. & TERNS, M. P. 2001. The snoRNA domain of vertebrate telomerase RNA functions to localize the RNA within the nucleus. *RNA,* 7**,** 1833-44.

- LYGEROU, Z., ALLMANG, C., TOLLERVEY, D. & SERAPHIN, B. 1996. Accurate processing of a eukaryotic precursor ribosomal RNA by ribonuclease MRP in vitro. *Science,* 272**,** 268-70.
- MA, J., MARTIN, J. D., ZHANG, H., AUGER, K. R., HO, T. F., KIRKPATRICK, R. B., GROOMS, M. H., JOHANSON, K. O., TUMMINO, P. J., COPELAND, R. A. & LAI, Z. 2006. A second p53 binding site in the central domain of Mdm2 is essential for p53 ubiquitination. *Biochemistry,* 45**,** 9238-45.
- MACHADO-PINILLA, R., CARRILLO, J., MANGUAN-GARCIA, C., SASTRE, L., MENTZER, A., GU, B. W., MASON, P. J. & PERONA, R. 2012. Defects in mTR stability and telomerase activity produced by the Dkc1 A353V mutation in dyskeratosis congenita are rescued by a peptide from the dyskerin TruB domain. *Clin Transl Oncol,* 14**,** 755-63.
- MADEN, B. E. 1990. The numerous modified nucleotides in eukaryotic ribosomal RNA. *Prog Nucleic Acid Res Mol Biol,* 39**,** 241-303.
- MADHUMALAR, A., LEE, H. J., BROWN, C. J., LANE, D. & VERMA, C. 2009. Design of a novel MDM2 binding peptide based on the p53 family. *Cell Cycle,* 8**,** 2828-36.
- MADRU, C., LEBARON, S., BLAUD, M., DELBOS, L., PIPOLI, J., PASMANT, E., RETY, S. & LEULLIOT, N. 2015. Chaperoning 5S RNA assembly. *Genes Dev,* 29**,** 1432-46.
- MAGALHAES, P. J., ANDREU, A. L. & SCHON, E. A. 1998. Evidence for the presence of 5S rRNA in mammalian mitochondria. *Mol Biol Cell,* 9**,** 2375-82.
- MAGNUSON, B., EKIM, B. & FINGAR, D. C. 2012. Regulation and function of ribosomal protein S6 kinase (S6K) within mTOR signalling networks. *Biochem J,* 441**,** 1-21.
- MAHAJAN, P. B. 1994. Modulation of transcription of rRNA genes by rapamycin. *Int J Immunopharmacol,* 16**,** 711-21.
- MANFE, V., BISKUP, E., JOHANSEN, P., KAMSTRUP, M. R., KREJSGAARD, T. F., MORLING, N., WULF, H. C. & GNIADECKI, R. 2012. MDM2 inhibitor nutlin-3a induces apoptosis and senescence in cutaneous T-cell lymphoma: role of p53. *J Invest Dermatol,* 132**,** 1487-96.
- MARECHAL, V., ELENBAAS, B., PIETTE, J., NICOLAS, J. C. & LEVINE, A. J. 1994. The ribosomal L5 protein is associated with mdm-2 and mdm-2-p53 complexes. *Mol Cell Biol,* 14**,** 7414-20.

- MASON, P. J. & BESSLER, M. 2011. The genetics of dyskeratosis congenita. *Cancer Genet,* 204**,** 635-45.
- MCCAUGHAN, U. M., JAYACHANDRAN, U., SHCHEPACHEV, V., CHEN, Z. A., RAPPSILBER, J., TOLLERVEY, D. & COOK, A. G. 2016. Pre-40S ribosome biogenesis factor Tsr1 is an inactive structural mimic of translational GTPases. *Nat Commun,* 7**,** 11789.
- MCGOWAN, K. A., LI, J. Z., PARK, C. Y., BEAUDRY, V., TABOR, H. K., SABNIS, A. J., ZHANG, W., FUCHS, H., DE ANGELIS, M. H., MYERS, R. M., ATTARDI, L. D. & BARSH, G. S. 2008. Ribosomal mutations cause p53-mediated dark skin and pleiotropic effects. *Nat Genet,* 40**,** 963-70.
- MCGOWAN, K. A., PANG, W. W., BHARDWAJ, R., PEREZ, M. G., PLUVINAGE, J. V., GLADER, B. E., MALEK, R., MENDRYSA, S. M., WEISSMAN, I. L., PARK, C. Y. & BARSH, G. S. 2011. Reduced ribosomal protein gene dosage and p53 activation in low-risk myelodysplastic syndrome. *Blood,* 118**,** 3622-33.
- MCLURE, K. G. & LEE, P. W. 1998. How p53 binds DNA as a tetramer. *EMBO J,* 17**,** 3342-50.
- MCSTAY, B. & GRUMMT, I. 2008. The epigenetics of rRNA genes: from molecular to chromosome biology. *Annu Rev Cell Dev Biol,* 24**,** 131-57.
- MEEK, D. W. 2015. Regulation of the p53 response and its relationship to cancer. *Biochem J,* 469**,** 325-46.
- MEEK, D. W. & ANDERSON, C. W. 2009. Posttranslational modification of p53: cooperative integrators of function. *Cold Spring Harb Perspect Biol,* 1**,** a000950.
- MEIER, U. T. 2005. The many facets of H/ACA ribonucleoproteins. *Chromosoma,* 114**,** 1-14.
- MENNE, T. F., GOYENECHEA, B., SANCHEZ-PUIG, N., WONG, C. C., TONKIN, L. M., ANCLIFF, P. J., BROST, R. L., COSTANZO, M., BOONE, C. & WARREN, A. J. 2007. The Shwachman-Bodian-Diamond syndrome protein mediates translational activation of ribosomes in yeast. *Nat Genet,* 39**,** 486-95.
- MIHARA, M., ERSTER, S., ZAIKA, A., PETRENKO, O., CHITTENDEN, T., PANCOSKA, P. & MOLL, U. M. 2003. p53 has a direct apoptogenic role at the mitochondria. *Mol Cell,* 11**,** 577-90.

- MIRANDA, M. & SORKIN, A. 2007. Regulation of receptors and transporters by ubiquitination: new insights into surprisingly similar mechanisms. *Mol Interv,* 7**,** 157-67.
- MISHRA, R. K. & ELICEIRI, G. L. 1997. Three small nucleolar RNAs that are involved in ribosomal RNA precursor processing. *Proc Natl Acad Sci U S A,* 94**,** 4972-7.
- MITCHELL, J., CHENG, J. & COLLINS, K. 1999. A box H/ACA small nucleolar RNA-like domain at the human telomerase RNA 3' end. *Molecular Cell Biology,* 19**,** 567-576.
- MIYASHITA, T., KRAJEWSKI, S., KRAJEWSKA, M., WANG, H. G., LIN, H. K., LIEBERMANN, D. A., HOFFMAN, B. & REED, J. C. 1994. Tumor suppressor p53 is a regulator of bcl-2 and bax gene expression in vitro and in vivo. *Oncogene,* 9**,** 1799-805.
- MIYOSHI, K., TSUJII, R., YOSHIDA, H., MAKI, Y., WADA, A., MATSUI, Y., TOH, E. A. & MIZUTA, K. 2002. Normal assembly of 60 S ribosomal subunits is required for the signaling in response to a secretory defect in Saccharomyces cerevisiae. *J Biol Chem,* 277**,** 18334-9.
- MOMAND, J., WU, H. H. & DASGUPTA, G. 2000. MDM2--master regulator of the p53 tumor suppressor protein. *Gene,* 242**,** 15-29.
- MOMAND, J., ZAMBETTI, G. P., OLSON, D. C., GEORGE, D. & LEVINE, A. J. 1992. The mdm-2 oncogene product forms a complex with the p53 protein and inhibits p53-mediated transactivation. *Cell,* 69**,** 1237-45.
- MOORE, P. B. & STEITZ, T. A. 2002. The involvement of RNA in ribosome function. *Nature,* 418**,** 229-35.
- MORITA, D., MIYOSHI, K., MATSUI, Y., TOH, E. A., SHINKAWA, H., MIYAKAWA, T. & MIZUTA, K. 2002. Rpf2p, an evolutionarily conserved protein, interacts with ribosomal protein L11 and is essential for the processing of 27 SB Pre-rRNA to 25 S rRNA and the 60 S ribosomal subunit assembly in Saccharomyces cerevisiae. *J Biol Chem,* 277**,** 28780-6.
- MORRISSEY, J. & D.TOLLERVEY 1993. Yeast snR30 is a small nucleolar RNA required for 18S rRNA synthesis. *Molecular Cell Biology,* 13**,** 2469-2477.
- MUKHOPADHYAY, D. & RIEZMAN, H. 2007. Proteasome-independent functions of ubiquitin in endocytosis and signaling. *Science,* 315**,** 201-5.

- MULLINEUX, S. T. & LAFONTAINE, D. L. 2012. Mapping the cleavage sites on mammalian pre-rRNAs: where do we stand? *Biochimie,* 94**,** 1521-32.
- NAKANO, K. & VOUSDEN, K. H. 2001. PUMA, a novel proapoptotic gene, is induced by p53. *Mol Cell,* 7**,** 683-94.
- NAKHOUL, H., KE, J., ZHOU, X., LIAO, W., ZENG, S. X. & LU, H. 2014. Ribosomopathies: mechanisms of disease. *Clin Med Insights Blood Disord,* 7**,** 7-16.
- NAOE, T., SUZUKI, T., KIYOI, H. & URANO, T. 2006. Nucleophosmin: a versatile molecule associated with hematological malignancies. *Cancer Sci,* 97**,** 963-9.
- NARLA, A. & EBERT, B. L. 2010. Ribosomopathies: human disorders of ribosome dysfunction. *Blood,* 115**,** 3196-205.
- NATHAN, J. A., KIM, H. T., TING, L., GYGI, S. P. & GOLDBERG, A. L. 2013. Why do cellular proteins linked to K63-polyubiquitin chains not associate with proteasomes? *EMBO J,* 32**,** 552-65.
- NI, J., TIEN, A. L. & FOURNIER, M. J. 1997. Small nucleolar RNAs direct site-specific synthesis of pseudouridine in ribosomal RNA. *Cell,* 89**,** 565-73.
- NICOLAS, E., PARISOT, P., PINTO-MONTEIRO, C., DE WALQUE, R., DE VLEESCHOUWER, C. & LAFONTAINE, D. L. 2016. Involvement of human ribosomal proteins in nucleolar structure and p53-dependent nucleolar stress. *Nat Commun,* 7**,** 11390.
- NIEMINEN, T. T., O'DONOHUE, M. F., WU, Y., LOHI, H., SCHERER, S. W., PATERSON, A. D., ELLONEN, P., ABDEL-RAHMAN, W. M., VALO, S., MECKLIN, J. P., JARVINEN, H. J., GLEIZES, P. E. & PELTOMAKI, P. 2014. Germline mutation of RPS20, encoding a ribosomal protein, causes predisposition to hereditary nonpolyposis colorectal carcinoma without DNA mismatch repair deficiency. *Gastroenterology,* 147**,** 595-598 e5.
- NIGG, E. A. 1995. Cyclin-dependent protein kinases: key regulators of the eukaryotic cell cycle. *Bioessays,* 17**,** 471-80.
- NIJMAN, S. M., LUNA-VARGAS, M. P., VELDS, A., BRUMMELKAMP, T. R., DIRAC, A. M., SIXMA, T. K. & BERNARDS, R. 2005. A genomic and functional inventory of deubiquitinating enzymes. *Cell,* 123**,** 773-86.
- NISHIMURA, K., KUMAZAWA, T., KURODA, T., KATAGIRI, N., TSUCHIYA, M., GOTO, N., FURUMAI, R., MURAYAMA, A., YANAGISAWA, J. & KIMURA,

K. 2015. Perturbation of ribosome biogenesis drives cells into senescence through 5S RNP-mediated p53 activation. *Cell Rep,* 10**,** 1310-23.

- NISHIMURA, S., TSUDA, H., ITO, K., JOBO, T., YAEGASHI, N., INOUE, T., SUDO, T., BERKOWITZ, R. S. & MOK, S. C. 2007. Differential expression of ABCF2 protein among different histologic types of epithelial ovarian cancer and in clear cell adenocarcinomas of different organs. *Hum Pathol,* 38**,** 134-9.
- NISHIMURA, S., TSUDA, H., MIYAGI, Y., HIRASAWA, A., SUZUKI, A., KATAOKA, F., NOMURA, H., CHIYODA, T., BANNO, K., FUJII, T., SUSUMU, N. & AOKI, D. 2008. Can ABCF2 protein expression predict the prognosis of uterine cancer? *Br J Cancer,* 99**,** 1651-5.
- NISSAN, T. A., BASSLER, J., PETFALSKI, E., TOLLERVEY, D. & HURT, E. 2002. 60S pre-ribosome formation viewed from assembly in the nucleolus until export to the cytoplasm. *EMBO J,* 21**,** 5539-47.
- NOMURA, M., GOURSE, R. & BAUGHMAN, G. 1984. Regulation of the synthesis of ribosomes and ribosomal components. *Annu Rev Biochem,* 53**,** 75-117.
- NURSE, P. 1990. Universal control mechanism regulating onset of M-phase. *Nature,* 344**,** 503-8.
- O'BRIEN, R., TRAN, S. L., MARITZ, M., LIU, B., KONG, C. F., PURGATO, S., YANG, C., MURRAY, J., RUSSEL, A. J., FLEMMING, C. L., VON JONQUIERES, G., PICKETT, H. A., LONDON, W. B., HABER, M., GUNARATNE, P. H., NORRIS, M. D., PERRINI, G., FLETCHER, J. I. & MACKENZIE, K. L. 2016a. MYC-driven neuroblastomas are addicted to a telomerase-independent function of dyskerin. *Cancer Res*.
- O'BRIEN, R., TRAN, S. L., MARITZ, M. F., LIU, B., KONG, C. F., PURGATO, S., YANG, C., MURRAY, J., RUSSELL, A. J., FLEMMING, C. L., VON JONQUIERES, G., PICKETT, H. A., LONDON, W. B., HABER, M., GUNARATNE, P. H., NORRIS, M. D., PERINI, G., FLETCHER, J. I. & MACKENZIE, K. L. 2016b. MYC-Driven Neuroblastomas Are Addicted to a Telomerase-Independent Function of Dyskerin. *Cancer Res*.
- O'DONOHUE, M. F., CHOESMEL, V., FAUBLADIER, M., FICHANT, G. & GLEIZES, P. E. 2010. Functional dichotomy of ribosomal proteins during the synthesis of mammalian 40S ribosomal subunits. *J Cell Biol,* 190**,** 853-66.

- ODA, E., OHKI, R., MURASAWA, H., NEMOTO, J., SHIBUE, T., YAMASHITA, T., TOKINO, T., TANIGUCHI, T. & TANAKA, N. 2000. Noxa, a BH3-only member of the Bcl-2 family and candidate mediator of p53-induced apoptosis. *Science,* 288**,** 1053-8.
- OEFFINGER, M., DLAKIC, M. & TOLLERVEY, D. 2004. A pre-ribosome-associated HEAT-repeat protein is required for export of both ribosomal subunits. *Genes Dev,* 18**,** 196-209.
- OEFFINGER, M., ZENKLUSEN, D., FERGUSON, A., WEI, K. E., EL HAGE, A., TOLLERVEY, D., CHAIT, B. T., SINGER, R. H. & ROUT, M. P. 2009. Rrp17p is a eukaryotic exonuclease required for 5' end processing of Pre-60S ribosomal RNA. *Mol Cell,* 36**,** 768-81.
- OGAWA, Y., TSUDA, H., HAI, E., TSUJI, N., YAMAGATA, S., TOKUNAGA, S., NAKAZAWA, K., TAMAMORI, Y., OGAWA, M., SHIMIZU, S., INOUE, T. & NISHIGUCHI, Y. 2006. Clinical role of ABCF2 expression in breast cancer. *Anticancer Res,* 26**,** 1809-14.
- OH, C., PARK, S., LEE, E. K. & YOO, Y. J. 2013. Downregulation of ubiquitin level via knockdown of polyubiquitin gene Ubb as potential cancer therapeutic intervention. *Sci Rep,* 3**,** 2623.
- OHGA, S., KAI, T., HONDA, K., NAKAYAMA, H., INAMITSU, T. & UEDA, K. 1997. What are the essential symptoms in the Hoyeraal-Hreidarsson syndrome? *Eur J Pediatr,* 156**,** 80-1.
- OHMAYER, U., GAMALINDA, M., SAUERT, M., OSSOWSKI, J., POLL, G., LINNEMANN, J., HIERLMEIER, T., PEREZ-FERNANDEZ, J., KUMCUOGLU, B., LEGER-SILVESTRE, I., FAUBLADIER, M., GRIESENBECK, J., WOOLFORD, J., TSCHOCHNER, H. & MILKEREIT, P. 2013. Studies on the assembly characteristics of large subunit ribosomal proteins in S. cerevisae. *PLoS One,* 8**,** e68412.
- OHNSTAD, H. O., PAULSEN, E. B., NOORDHUIS, P., BERG, M., LOTHE, R. A., VASSILEV, L. T. & MYKLEBOST, O. 2011. MDM2 antagonist Nutlin-3a potentiates antitumour activity of cytotoxic drugs in sarcoma cell lines. *BMC Cancer,* 11**,** 211:1-11.
- OMER, A. D., ZIESCHE, S., EBHARDT, H. & DENNIS, P. P. 2002. In vitro reconstitution and activity of a C/D box methylation guide ribonucleoprotein complex. *Proc Natl Acad Sci U S A,* 99**,** 5289-94.

- ORSOLIC, I., JURADA, D., PULLEN, N., OREN, M., ELIOPOULOS, A. G. & VOLAREVIC, S. 2015. The relationship between the nucleolus and cancer: Current evidence and emerging paradigms. *Semin Cancer Biol*.
- OSHEIM, Y. N., FRENCH, S. L., KECK, K. M., CHAMPION, E. A., SPASOV, K., DRAGON, F., BASERGA, S. J. & BEYER, A. L. 2004. Pre-18S ribosomal RNA is structurally compacted into the SSU processome prior to being cleaved from nascent transcripts in Saccharomyces cerevisiae. *Mol Cell,* 16**,** 943-54.
- OSHIRO, N., TAKAHASHI, R., YOSHINO, K., TANIMURA, K., NAKASHIMA, A., EGUCHI, S., MIYAMOTO, T., HARA, K., TAKEHANA, K., AVRUCH, J., KIKKAWA, U. & YONEZAWA, K. 2007. The proline-rich Akt substrate of 40 kDa (PRAS40) is a physiological substrate of mammalian target of rapamycin complex 1. *J Biol Chem,* 282**,** 20329-39.
- PANOV, K. I., FRIEDRICH, J. K. & ZOMERDIJK, J. C. 2001. A step subsequent to preinitiation complex assembly at the ribosomal RNA gene promoter is rate limiting for human RNA polymerase I-dependent transcription. *Mol Cell Biol,* 21**,** 2641-9.
- PANT, V., XIONG, S., IWAKUMA, T., QUINTAS-CARDAMA, A. & LOZANO, G. 2011. Heterodimerization of Mdm2 and Mdm4 is critical for regulating p53 activity during embryogenesis but dispensable for p53 and Mdm2 stability. *Proc Natl Acad Sci U S A,* 108**,** 11995-2000.
- PARLATO, R. & LISS, B. 2014. How Parkinson's disease meets nucleolar stress. *Biochim Biophys Acta,* 1842**,** 791-7.
- PAULE, M. R. & WHITE, R. J. 2000. Survey and summary: transcription by RNA polymerases I and III. *Nucleic Acids Res,* 28**,** 1283-98.
- PECULIS, B. A. & STEITZ, J. A. 1993. Disruption of U8 nucleolar snRNA inhibits 5.8S and 28S rRNA processing in the Xenopus oocyte. *Cell,* 73**,** 1233-45.
- PELAVA, A., SCHNEIDER, C. & WATKINS, N. J. 2016. The importance of ribosome production, and the5S RNP–MDM2 pathway, in health and disease. *Biochemical Society Transactions,* 44**,** 1086-1090.
- PELHAM, H. R. & BROWN, D. D. 1980. A specific transcription factor that can bind either the 5S RNA gene or 5S RNA. *Proc Natl Acad Sci U S A,* 77**,** 4170-4.
- PELLAGATTI, A., MARAFIOTI, T., PATERSON, J. C., BARLOW, J. L., DRYNAN, L. F., GIAGOUNIDIS, A., PILERI, S. A., CAZZOLA, M., MCKENZIE,

A. N., WAINSCOAT, J. S. & BOULTWOOD, J. 2010. Induction of p53 and up-regulation of the p53 pathway in the human 5q- syndrome. *Blood,* 115**,** 2721-3.

- PELTONEN, K., COLIS, L., LIU, H., TRIVEDI, R., MOUBAREK, M. S., MOORE, H. M., BAI, B., RUDEK, M. A., BIEBERICH, C. J. & LAIHO, M. 2014. A targeting modality for destruction of RNA polymerase I that possesses anticancer activity. *Cancer Cell,* 25**,** 77-90.
- PENDE, M., UM, S. H., MIEULET, V., STICKER, M., GOSS, V. L., MESTAN, J., MUELLER, M., FUMAGALLI, S., KOZMA, S. C. & THOMAS, G. 2004. S6K1(-/-)/S6K2(-/-) mice exhibit perinatal lethality and rapamycin-sensitive 5'-terminal oligopyrimidine mRNA translation and reveal a mitogen-activated protein kinase-dependent S6 kinase pathway. *Mol Cell Biol,* 24**,** 3112-24.
- PERTSCHY, B., SCHNEIDER, C., GNADIG, M., SCHAFER, T., TOLLERVEY, D. & HURT, E. 2009. RNA helicase Prp43 and its co-factor Pfa1 promote 20 to 18 S rRNA processing catalyzed by the endonuclease Nob1. *J Biol Chem,* 284**,** 35079-91.
- PETFALSKI, E., DANDEKAR, T., HENRY, Y. & TOLLERVEY, D. 1998. Processing of the precursors to small nucleolar RNAs and rRNAs requires common components. *Mol Cell Biol,* 18**,** 1181-9.
- PFANDER, B., MOLDOVAN, G. L., SACHER, M., HOEGE, C. & JENTSCH, S. 2005. SUMO-modified PCNA recruits Srs2 to prevent recombination during S phase. *Nature,* 436**,** 428-33.
- PFOH, R., LACDAO, I. K. & SARIDAKIS, V. 2015. Deubiquitinases and the new therapeutic opportunities offered to cancer. *Endocr Relat Cancer,* 22**,** T35-54.
- PHILLIPS, B., BILLIN, A. N., CADWELL, C., BUCHHOLZ, R., ERICKSON, C., MERRIAM, J. R., CARBON, J. & POOLE, S. J. 1998. The Nop60B gene of Drosophila encodes an essential nucleolar protein that functions in yeast. *Mol Gen Genet,* 260**,** 20-9.
- PHIPPS, K. R., CHARETTE, J. & BASERGA, S. J. 2011. The small subunit processome in ribosome biogenesis-progress and prospects. *Wiley Interdiscip Rev RNA,* 2**,** 1-21.
- PICKART, C. M. 2001. Mechanisms underlying ubiquitination. *Annu Rev Biochem,* 70**,** 503-33.
- PICKART, C. M. & EDDINS, M. J. 2004. Ubiquitin: structures, functions, mechanisms. *Biochim Biophys Acta,* 1695**,** 55-72.

- PIELER, T., HAMM, J. & ROEDER, R. G. 1987. The 5S gene internal control region is composed of three distinct sequence elements, organized as two functional domains with variable spacing. *Cell,* 48**,** 91-100.
- PLAS, D. R. & THOMAS, G. 2009. Tubers and tumors: rapamycin therapy for benign and malignant tumors. *Curr Opin Cell Biol,* 21**,** 230-6.
- PODLEVSKY, J. D., BLEY, C. J., OMANA, R. V., QI, X. & CHEN, J. J. 2008. The telomerase database. *Nucleic Acids Res,* 36**,** D339-43.
- POMBO, A., JACKSON, D. A., HOLLINSHEAD, M., WANG, Z., ROEDER, R. G. & COOK, P. R. 1999. Regional specialization in human nuclei: visualization of discrete sites of transcription by RNA polymerase III. *EMBO J,* 18**,** 2241-53.
- PONTEN, F., JIRSTROM, K. & UHLEN, M. 2008. The Human Protein Atlas--a tool for pathology. *J Pathol,* 216**,** 387-93.
- POSNICK, J. C. & RUIZ, R. L. 2000. Treacher Collins syndrome: current evaluation, treatment, and future directions. *Cleft Palate Craniofac J,* 37**,** 434.
- POYUROVSKY, M. V., KATZ, C., LAPTENKO, O., BECKERMAN, R., LOKSHIN, M., AHN, J., BYEON, I. J., GABIZON, R., MATTIA, M., ZUPNICK, A., BROWN, L. M., FRIEDLER, A. & PRIVES, C. 2010. The C terminus of p53 binds the N-terminal domain of MDM2. *Nat Struct Mol Biol,* 17**,** 982-9.
- PRETI, M., O'DONOHUE, M. F., MONTEL-LEHRY, N., BORTOLIN-CAVAILLE, M. L., CHOESMEL, V. & GLEIZES, P. E. 2013. Gradual processing of the ITS1 from the nucleolus to the cytoplasm during synthesis of the human 18S rRNA. *Nucleic Acids Res,* 41**,** 4709-23.
- QU, G., VAN NUES, R. W., WATKINS, N. J. & MAXWELL, E. S. 2011. The spatial-functional coupling of box C/D and C'/D' RNPs is an evolutionarily conserved feature of the eukaryotic box C/D snoRNP nucleotide modification complex. *Mol Cell Biol,* 31**,** 365-74.
- QUIN, J. E., DEVLIN, J. R., CAMERON, D., HANNAN, K. M., PEARSON, R. B. & HANNAN, R. D. 2014. Targeting the nucleolus for cancer intervention. *Biochim Biophys Acta,* 1842**,** 802-16.
- RAMAMURTHY, V., SWANN, S. L., PAULSON, J. L., SPEDALIERE, C. J. & MUELLER, E. G. 1999. Critical aspartic acid residues in pseudouridine synthases. *J Biol Chem,* 274**,** 22225-30.
- RAO, S., LEE, S. Y., GUTIERREZ, A., PERRIGOUE, J., THAPA, R. J., TU, Z., JEFFERS, J. R., RHODES, M., ANDERSON, S., ORAVECZ, T., HUNGER, S.

P., TIMAKHOV, R. A., ZHANG, R., BALACHANDRAN, S., ZAMBETTI, G. P., TESTA, J. R., LOOK, A. T. & WIEST, D. L. 2012. Inactivation of ribosomal protein L22 promotes transformation by induction of the stemness factor, Lin28B. *Blood,* 120**,** 3764-73.

- REDMAN, K. L. & RECHSTEINER, M. 1989. Identification of the long ubiquitin extension as ribosomal protein S27a. *Nature,* 338**,** 438-40.
- REICHOW, S. L., HAMMA, T., FERRE-D'AMARE, A. R. & VARANI, G. 2007. The structure and function of small nucleolar ribonucleoproteins. *Nucleic Acids Res,* 35**,** 1452-64.
- REYES-TURCU, F. E., VENTII, K. H. & WILKINSON, K. D. 2009. Regulation and cellular roles of ubiquitin-specific deubiquitinating enzymes. *Annu Rev Biochem,* 78**,** 363-97.
- RICHARD, P., DARZACQ, X., BERTRAND, E., JADY, B. E., VERHEGGEN, C. & KISS, T. 2003. A common sequence motif determines the Cajal body-specific localization of box H/ACA scaRNAs. *EMBO J,* 22**,** 4283-93.
- RIMOLDI, O. J., RAGHU, B., NAG, M. K. & ELICEIRI, G. L. 1993. Three new small nucleolar RNAs that are psoralen cross-linked in vivo to unique regions of pre-rRNA. *Mol Cell Biol,* 13**,** 4382-90.
- ROTHE, B., BACK, R., QUINTERNET, M., BIZARRO, J., ROBERT, M. C., BLAUD, M., ROMIER, C., MANIVAL, X., CHARPENTIER, B., BERTRAND, E. & BRANLANT, C. 2014. Characterization of the interaction between protein Snu13p/15.5K and the Rsa1p/NUFIP factor and demonstration of its functional importance for snoRNP assembly. *Nucleic Acids Res,* 42**,** 2015-36.
- ROUQUETTE, J., CHOESMEL, V. & GLEIZES, P. E. 2005. Nuclear export and cytoplasmic processing of precursors to the 40S ribosomal subunits in mammalian cells. *EMBO J,* 24**,** 2862-72.
- ROZHDESTVENSKY, T., TANG, T., TCHIRKOVA, I., BROSIUS, J., BACHELLERIE, J. & HUTTENHOFER, A. 2003. Binding of L7Ae protein to the K-turn of archaeal snoRNAs: a shared RNA binding motif for C/D and H/ACA box snoRNAs in Archaea. *Nucleic acid research,* 31**,** 869–877.
- RUGGERO, D., GRISENDI, S., PIAZZA, F., REGO, E., MARI, F., RAO, P. H., CORDON-CARDO, C. & PANDOLFI, P. P. 2003. Dyskeratosis congenita and cancer in mice deficient in ribosomal RNA modification. *Science,* 299**,** 259-62.

- RUGGERO, D. & PANDOLFI, P. P. 2003. Does the ribosome translate cancer? *Nat Rev Cancer,* 3**,** 179-92.
- RUSSELL, J. & ZOMERDIJK, J. C. 2005. RNA-polymerase-I-directed rDNA transcription, life and works. *Trends Biochem Sci,* 30**,** 87-96.
- RYU, K. Y., MAEHR, R., GILCHRIST, C. A., LONG, M. A., BOULEY, D. M., MUELLER, B., PLOEGH, H. L. & KOPITO, R. R. 2007. The mouse polyubiquitin gene UbC is essential for fetal liver development, cell-cycle progression and stress tolerance. *EMBO J,* 26**,** 2693-706.
- SAKAI, D. & TRAINOR, P. A. 2009. Treacher Collins syndrome: unmasking the role of Tcof1/treacle. *Int J Biochem Cell Biol,* 41**,** 1229-32.
- SANCAR, A., LINDSEY-BOLTZ, L. A., UNSAL-KACMAZ, K. & LINN, S. 2004. Molecular mechanisms of mammalian DNA repair and the DNA damage checkpoints. *Annu Rev Biochem,* 73**,** 39-85.
- SATO, Y., YOSHIKAWA, A., YAMAGATA, A., MIMURA, H., YAMASHITA, M., OOKATA, K., NUREKI, O., IWAI, K., KOMADA, M. & FUKAI, S. 2008. Structural basis for specific cleavage of Lys 63-linked polyubiquitin chains. *Nature,* 455**,** 358-62.
- SAUER, B. 1994. Site-specific recombination: developments and applications. *Curr Opin Biotechnol,* 5**,** 521-7.
- SAVAGE, S. A. 2009. *Dyskeratosis Congenita* [Online]. Seattle WA. Available: http://www.ncbi.nlm.nih.gov/books/NBK22301/ [Accessed 25 February 2013].
- SCHAFER, K. A. 1998. The cell cycle: a review. *Vet Pathol,* 35**,** 461-78.
- SCHAFER, T., STRAUSS, D., PETFALSKI, E., TOLLERVEY, D. & HURT, E. 2003. The path from nucleolar 90S to cytoplasmic 40S pre-ribosomes. *EMBO J,* 22**,** 1370-80.
- SCHATTNER, P., BARBERAN-SOLER, S. & LOWE, T. M. 2006. A computational screen for mammalian pseudouridylation guide H/ACA RNAs. *RNA,* 12**,** 15-25.
- SCHILDERS, G., VAN DIJK, E. & PRUIJN, G. J. 2007. C1D and hMtr4p associate with the human exosome subunit PM/Scl-100 and are involved in pre-rRNA processing. *Nucleic Acids Res,* 35**,** 2564-72.
- SCHNEIDER, R. K., SCHENONE, M., FERREIRA, M. V., KRAMANN, R., JOYCE, C. E., HARTIGAN, C., BEIER, F., BRUMMENDORF, T. H., GERMING, U., PLATZBECKER, U., BUSCHE, G., KNUCHEL, R., CHEN, M. C., WATERS,

C. S., CHEN, E., CHU, L. P., NOVINA, C. D., LINDSLEY, R. C., CARR, S. A. & EBERT, B. L. 2016. Rps14 haploinsufficiency causes a block in erythroid differentiation mediated by S100A8 and S100A9. *Nat Med,* 22**,** 288-97.

- SCHWARTZENBERG-BAR-YOSEPH, F., ARMONI, M. & KARNIELI, E. 2004. The tumor suppressor p53 down-regulates glucose transporters GLUT1 and GLUT4 gene expression. *Cancer Res,* 64**,** 2627-33.
- SEDLACEK, H. H. 2001. Mechanisms of action of flavopiridol. *Crit Rev Oncol Hematol,* 38**,** 139-70.
- SEISER, R. M., SUNDBERG, A. E., WOLLAM, B. J., ZOBEL-THROPP, P., BALDWIN, K., SPECTOR, M. D. & LYCAN, D. E. 2006. Ltv1 is required for efficient nuclear export of the ribosomal small subunit in Saccharomyces cerevisiae. *Genetics,* 174**,** 679-91.
- SENGER, B., LAFONTAINE, D. L., GRAINDORGE, J. S., GADAL, O., CAMASSES, A., SANNI, A., GARNIER, J. M., BREITENBACH, M., HURT, E. & FASIOLO, F. 2001. The nucle(ol)ar Tif6p and Efl1p are required for a late cytoplasmic step of ribosome synthesis. *Mol Cell,* 8**,** 1363-73.
- SENGUPTA, J., BUSSIERE, C., PALLESEN, J., WEST, M., JOHNSON, A. W. & FRANK, J. 2010. Characterization of the nuclear export adaptor protein Nmd3 in association with the 60S ribosomal subunit. *J Cell Biol,* 189**,** 1079-86.
- SHANGARY, S. & WANG, S. 2008. Targeting the MDM2-p53 interaction for cancer therapy. *Clin Cancer Res,* 14**,** 5318-24.
- SHARP, S. J. & GARCIA, A. D. 1988. Transcription of the Drosophila melanogaster 5S RNA gene requires an upstream promoter and four intragenic sequence elements. *Mol Cell Biol,* 8**,** 1266-74.
- SHENOY, N., KESSEL, R., BHAGAT, T. D., BHATTACHARYYA, S., YU, Y., MCMAHON, C. & VERMA, A. 2012. Alterations in the ribosomal machinery in cancer and hematologic disorders. *J Hematol Oncol,* 5**,** 32.
- SHENOY, S. K., MCDONALD, P. H., KOHOUT, T. A. & LEFKOWITZ, R. J. 2001. Regulation of receptor fate by ubiquitination of activated beta 2-adrenergic receptor and beta-arrestin. *Science,* 294**,** 1307-13.
- SHERR, C. J. & WEBER, J. D. 2000. The ARF/p53 pathway. *Curr Opin Genet Dev,* 10**,** 94-9.
- SHIVJI, K. K., KENNY, M. K. & WOOD, R. D. 1992. Proliferating cell nuclear antigen is required for DNA excision repair. *Cell,* 69**,** 367-74.

- SLOAN, K. E., BOHNSACK, M. T., SCHNEIDER, C. & WATKINS, N. J. 2014. The roles of SSU processome components and surveillance factors in the initial processing of human ribosomal RNA. *RNA,* 20**,** 540-50.
- SLOAN, K. E., BOHNSACK, M. T. & WATKINS, N. J. 2013a. The 5S RNP couples p53 homeostasis to ribosome biogenesis and nucleolar stress. *Cell Rep,* 5**,** 237-47.
- SLOAN, K. E., MATTIJSSEN, S., LEBARON, S., TOLLERVEY, D., PRUIJN, G. J. & WATKINS, N. J. 2013b. Both endonucleolytic and exonucleolytic cleavage mediate ITS1 removal during human ribosomal RNA processing. *J Cell Biol,* 200**,** 577-88.
- SLOAN, K. E., MATTIJSSEN, S., LEBARON, S., TOLLERVEY, D., PRUIJN, G. J. M. & WATKINS, N. J. 2013c. Both endonucleolytic and exonucleolytic cleavage mediate ITS1 removal during human ribosomal RNA processing. *Journal of Cell Biology,* 200**,** 577-588.
- SMIRNOV, E., CMARKO, D., MAZEL, T., HORNACEK, M. & RASKA, I. 2016. Nucleolar DNA: the host and the guests. *Histochem Cell Biol*.
- SORENSEN, P. D. & FREDERIKSEN, S. 1991. Characterization of human 5S rRNA genes. *Nucleic Acids Res,* 19**,** 4147-51.
- SRIVASTAVA, L., LAPIK, Y. R., WANG, M. & PESTOV, D. G. 2010. Mammalian DEAD box protein Ddx51 acts in 3' end maturation of 28S rRNA by promoting the release of U8 snoRNA. *Mol Cell Biol,* 30**,** 2947-56.
- STEEGENGA, W. T., VAN LAAR, T., RITECO, N., MANDARINO, A., SHVARTS, A., VAN DER EB, A. J. & JOCHEMSEN, A. G. 1996. Adenovirus E1A proteins inhibit activation of transcription by p53. *Mol Cell Biol,* 16**,** 2101-9.
- STERN, J. L., ZYNER, K. G., PICKETT, H. A., COHEN, S. B. & BRYAN, T. M. 2012. Telomerase recruitment requires both TCAB1 and Cajal bodies independently. *Mol Cell Biol,* 32**,** 2384-95.
- STORER, A. C. & MENARD, R. 1994. Catalytic mechanism in papain family of cysteine peptidases. *Methods Enzymol,* 244**,** 486-500.
- STOTT, F. J., BATES, S., JAMES, M. C., MCCONNELL, B. B., STARBORG, M., BROOKES, S., PALMERO, I., RYAN, K., HARA, E., VOUSDEN, K. H. & PETERS, G. 1998. The alternative product from the human CDKN2A locus, p14(ARF), participates in a regulatory feedback loop with p53 and MDM2. *EMBO J,* 17**,** 5001-14.

- STRUNK, B. S., LOUCKS, C. R., SU, M., VASHISTH, H., CHENG, S., SCHILLING, J., BROOKS, C. L., 3RD, KARBSTEIN, K. & SKINIOTIS, G. 2011. Ribosome assembly factors prevent premature translation initiation by 40S assembly intermediates. *Science,* 333**,** 1449-53.
- SULIC, S., PANIC, L., DIKIC, I. & VOLAREVIC, S. 2005. Deregulation of cell growth and malignant transformation. *Croat Med J,* 46**,** 622-38.
- SUN, C. & WOOLFORD, J. L., JR. 1994. The yeast NOP4 gene product is an essential nucleolar protein required for pre-rRNA processing and accumulation of 60S ribosomal subunits. *EMBO J,* 13**,** 3127-35.
- SUN, X. X., DEVINE, T., CHALLAGUNDLA, K. B. & DAI, M. S. 2011. Interplay between ribosomal protein S27a and MDM2 protein in p53 activation in response to ribosomal stress. *J Biol Chem,* 286**,** 22730-41.
- SUN, X. X., WANG, Y. G., XIRODIMAS, D. P. & DAI, M. S. 2010. Perturbation of 60 S ribosomal biogenesis results in ribosomal protein L5- and L11-dependent p53 activation. *J Biol Chem,* 285**,** 25812-21.
- SZEWCZAK, L. B., GABRIELSEN, J. S., DEGREGORIO, S. J., STROBEL, S. A. & STEITZ, J. A. 2005. Molecular basis for RNA kink-turn recognition by the h15.5K small RNP protein. *RNA,* 11**,** 1407-19.
- SZYMANSKI, M., BARCISZEWSKA, M. Z., ERDMANN, V. A. & BARCISZEWSKI, J. 2002. 5S Ribosomal RNA Database. *Nucleic Acids Res,* 30**,** 176-8.
- TAFFOREAU, L., ZORBAS, C., LANGHENDRIES, J. L., MULLINEUX, S. T., STAMATOPOULOU, V., MULLIER, R., WACHEUL, L. & LAFONTAINE, D. L. 2013. The complexity of human ribosome biogenesis revealed by systematic nucleolar screening of Pre-rRNA processing factors. *Mol Cell,* 51**,** 539-51.
- TANOWITZ, M. & VON ZASTROW, M. 2002. Ubiquitination-independent trafficking of G protein-coupled receptors to lysosomes. *J Biol Chem,* 277**,** 50219-22.
- TE POELE, R. H., OKOROKOV, A. L. & JOEL, S. P. 1999. RNA synthesis block by 5, 6-dichloro-1-beta-D-ribofuranosylbenzimidazole (DRB) triggers p53-dependent apoptosis in human colon carcinoma cells. *Oncogene,* 18**,** 5765-72.
- TEIXEIRA, L. K. & REED, S. I. 2013. Ubiquitin ligases and cell cycle control. *Annu Rev Biochem,* 82**,** 387-414.

- THAPA, M., BOMMAKANTI, A., SHAMSUZZAMAN, M., GREGORY, B., SAMSEL, L., ZENGEL, J. M. & LINDAHL, L. 2013. Repressed synthesis of ribosomal proteins generates protein-specific cell cycle and morphological phenotypes. *Mol Biol Cell,* 24**,** 3620-33.
- THOMSON, E. & TOLLERVEY, D. 2010. The final step in 5.8S rRNA processing is cytoplasmic in Saccharomyces cerevisiae. *Mol Cell Biol,* 30**,** 976-84.
- TOLLERVEY, D. 1987. A yeast small nuclear RNA is required for normal processing of pre-ribosomal RNA. *EMBO J,* 6**,** 4169-75.
- TORCHET, C., BADIS, G., DEVAUX, F., COSTANZO, G., WERNER, M. & JACQUIER, A. 2005. The complete set of H/ACA snoRNAs that guide rRNA pseudouridylations in Saccharomyces cerevisiae. *RNA,* 11**,** 928-38.
- TRAINOR, P. A. & MERRILL, A. E. 2014. Ribosome biogenesis in skeletal development and the pathogenesis of skeletal disorders. *Biochim Biophys Acta,* 1842**,** 769-78.
- TSAI, L. H., HARLOW, E. & MEYERSON, M. 1991. Isolation of the human cdk2 gene that encodes the cyclin A- and adenovirus E1A-associated p33 kinase. *Nature,* 353**,** 174-7.
- TYCOWSKI, K. T., SHU, M. D., KUKOYI, A. & STEITZ, J. A. 2009. A conserved WD40 protein binds the Cajal body localization signal of scaRNP particles. *Mol Cell,* 34**,** 47-57.
- TYCOWSKI, K. T., SHU, M. D. & STEITZ, J. A. 1994. Requirement for intron-encoded U22 small nucleolar RNA in 18S ribosomal RNA maturation. *Science,* 266**,** 1558-61.
- ULDRIJAN, S., PANNEKOEK, W. J. & VOUSDEN, K. H. 2007. An essential function of the extreme C-terminus of MDM2 can be provided by MDMX. *EMBO J,* 26**,** 102-12.
- VALDEZ, B. C., HENNING, D., SO, R. B., DIXON, J. & DIXON, M. J. 2004. The Treacher Collins syndrome (TCOF1) gene product is involved in ribosomal DNA gene transcription by interacting with upstream binding factor. *Proc Natl Acad Sci U S A,* 101**,** 10709-14.
- VAN DEN BERGHE, H., CASSIMAN, J. J., DAVID, G., FRYNS, J. P., MICHAUX, J. L. & SOKAL, G. 1974. Distinct haematological disorder with deletion of long arm of no. 5 chromosome. *Nature,* 251**,** 437-8.

- VAN HOOF, A., LENNERTZ, P. & PARKER, R. 2000. Three conserved members of the RNase D family have unique and overlapping functions in the processing of 5S, 5.8S, U4, U5, RNase MRP and RNase P RNAs in yeast. *EMBO J,* 19**,** 1357-65.
- VAN NUES, R. W., GRANNEMAN, S., KUDLA, G., SLOAN, K. E., CHICKEN, M., TOLLERVEY, D. & WATKINS, N. J. 2011. Box C/D snoRNP catalysed methylation is aided by additional pre-rRNA base-pairing. *EMBO J,* 30**,** 2420-30.
- VANROBAYS, E., GELUGNE, J. P., CAIZERGUES-FERRER, M. & LAFONTAINE, D. L. 2004. Dim2p, a KH-domain protein required for small ribosomal subunit synthesis. *RNA,* 10**,** 645-56.
- VANROBAYS, E., GELUGNE, J. P., GLEIZES, P. E. & CAIZERGUES-FERRER, M. 2003. Late cytoplasmic maturation of the small ribosomal subunit requires RIO proteins in Saccharomyces cerevisiae. *Mol Cell Biol,* 23**,** 2083-95.
- VARDIMAN, J. W., HARRIS, N. L. & BRUNNING, R. D. 2002. The World Health Organization (WHO) classification of the myeloid neoplasms. *Blood,* 100**,** 2292-302.
- VENEMA, J. & TOLLERVEY, D. 1995. Processing of pre-ribosomal RNA in Saccharomyces cerevisiae. *Yeast,* 11**,** 1629-50.
- VENEMA, J. & TOLLERVEY, D. 1996. RRP5 is required for formation of both 18S and 5.8S rRNA in yeast. *EMBO J,* 15**,** 5701-14.
- VENTEICHER, A. S., ABREU, E. B., MENG, Z., MCCANN, K. E., TERNS, R. M., VEENSTRA, T. D., TERNS, M. P. & ARTANDI, S. E. 2009. A human telomerase holoenzyme protein required for Cajal body localization and telomere synthesis. *Science,* 323**,** 644-8.
- VENTEICHER, A. S. & ARTANDI, S. E. 2009. TCAB1: driving telomerase to Cajal bodies. *Cell Cycle,* 8**,** 1329-31.
- VLACHOS, A., FEDERMAN, N., REYES-HALEY, C., ABRAMSON, J. & LIPTON, J. M. 2001. Hematopoietic stem cell transplantation for Diamond Blackfan anemia: a report from the Diamond Blackfan Anemia Registry. *Bone Marrow Transplant,* 27**,** 381-6.
- VLACHOS, A., ROSENBERG, P. S., ATSIDAFTOS, E., ALTER, B. P. & LIPTON, J. M. 2012. Incidence of neoplasia in Diamond Blackfan anemia: a report from the Diamond Blackfan Anemia Registry. *Blood,* 119**,** 3815-9.

- VOGELSTEIN, B., LANE, D. & LEVINE, A. J. 2000. Surfing the p53 network. *Nature,* 408**,** 307-10.
- VULLIAMY, T., BESWICK, R., KIRWAN, M., MARRONE, A., DIGWEED, M., WALINE, A. & DOKAL, I. 2008. Mutations in the telomerase component NHP2 cause the premature ageing syndrome dyskeratosis congenita. *Proc Natl Acad Sci U S A,* 105**,** 8073-8.
- VULLIAMY, T., MARRONE, A., GOLDMAN, F., DEARLOVE, A., BESSLER, M., MASON, P. J. & DOKAL, I. 2001. The RNA component of telomerase is mutated in autosomal dominant dyskeratosis congenita. *Nature,* 413**,** 432-5.
- VULLIAMY, T. J., MARRONE, A., KNIGHT, S. W., WALNE, A., MASON, P. J. & DOKAL, I. 2006. Mutations in dyskeratosis congenita: their impact on telomere length and the diversity of clinical presentation. *Blood,* 107**,** 2680-5.
- WADE, M., LI, Y. C. & WAHL, G. M. 2013. MDM2, MDMX and p53 in oncogenesis and cancer therapy. *Nat Rev Cancer,* 13**,** 83-96.
- WALNE, A. J., VULLIAMY, T., MARRONE, A., BESWICK, R., KIRWAN, M., MASUNARI, Y., AL-QURASHI, F. H., ALJURF, M. & DOKAL, I. 2007. Genetic heterogeneity in autosomal recessive dyskeratosis congenita with one subtype due to mutations in the telomerase-associated protein NOP10. *Hum Mol Genet,* 16**,** 1619-29.
- WANG, H., YU, J., ZHANG, L., XIONG, Y., CHEN, S., XING, H., TIAN, Z., TANG, K., WEI, H., RAO, Q., WANG, M. & WANG, J. 2014. RPS27a promotes proliferation, regulates cell cycle progression and inhibits apoptosis of leukemia cells. *Biochem Biophys Res Commun,* 446**,** 1204-10.
- WANG, M. & PESTOV, D. G. 2011. 5'-end surveillance by Xrn2 acts as a shared mechanism for mammalian pre-rRNA maturation and decay. *Nucleic Acids Res,* 39**,** 1811-22.
- WARD, C. L., OMURA, S. & KOPITO, R. R. 1995. Degradation of CFTR by the ubiquitin-proteasome pathway. *Cell,* 83**,** 121-7.
- WARNER, J. R. 1999. The economics of ribosome biosynthesis in yeast. *Trends Biochem Sci,* 24**,** 437-40.
- WATKINS, N. J. & BOHNSACK, M. T. 2011. The box C/D and H/ACA snoRNPs: key players in the modification, processing and the dynamic folding of ribosomal RNA. *WIRES RNA,* 3**,** 397-414.

- WATKINS, N. J., GOTTSCHALK, A., NEUBAUER, G., KASTNER, B., FABRIZIO, P., MANN, M. & LUHRMANN, R. 1998. Cbf5p, a potential pseudouridine synthase, and Nhp2p, a putative RNA-binding protein, are present together with Gar1p in all H BOX/ACA-motif snoRNPs and constitute a common bipartite structure. *RNA,* 4**,** 1549-68.
- WEI, S., CHEN, X., ROCHA, K., EPLING-BURNETTE, P. K., DJEU, J. Y., LIU, Q., BYRD, J., SOKOL, L., LAWRENCE, N., PIREDDU, R., DEWALD, G., WILLIAMS, A., MACIEJEWSKI, J. & LIST, A. 2009. A critical role for phosphatase haplodeficiency in the selective suppression of deletion 5q MDS by lenalidomide. *Proc Natl Acad Sci U S A,* 106**,** 12974-9.
- WEINER, A. M., SCAMPOLI, N. L. & CALCATERRA, N. B. 2012. Fishing the molecular bases of Treacher Collins syndrome. *PLoS One,* 7**,** e29574.
- WELLS, G. R., WEICHMANN, F., COLVIN, D., SLOAN, K. E., KUDLA, G., TOLLERVEY, D., WATKINS, N. J. & SCHNEIDER, C. 2016. The PIN domain endonuclease Utp24 cleaves pre-ribosomal RNA at two coupled sites in yeast and humans. *Nucleic Acids Res*.
- WENG, C., LI, Y., XU, D., SHI, Y. & TANG, H. 2005. Specific cleavage of Mcl-1 by caspase-3 in tumor necrosis factor-related apoptosis-inducing ligand (TRAIL)-induced apoptosis in Jurkat leukemia T cells. *J Biol Chem,* 280**,** 10491-500.
- WEST, M., HEDGES, J. B., CHEN, A. & JOHNSON, A. W. 2005. Defining the order in which Nmd3p and Rpl10p load onto nascent 60S ribosomal subunits. *Mol Cell Biol,* 25**,** 3802-13.
- WILD, T., HORVATH, P., WYLER, E., WIDMANN, B., BADERTSCHER, L., ZEMP, I., KOZAK, K., CSUCS, G., LUND, E. & KUTAY, U. 2010. A protein inventory of human ribosome biogenesis reveals an essential function of exportin 5 in 60S subunit export. *PLoS Biol,* 8**,** e1000522.
- WOOLFORD, J. L., JR. & BASERGA, S. J. 2013. Ribosome biogenesis in the yeast Saccharomyces cerevisiae. *Genetics,* 195**,** 643-81.
- WORTON, R. G., SUTHERLAND, J., SYLVESTER, J. E., WILLARD, H. F., BODRUG, S., DUBE, I., DUFF, C., KEAN, V., RAY, P. N. & SCHMICKEL, R. D. 1988. Human ribosomal RNA genes: orientation of the tandem array and conservation of the 5' end. *Science,* 239**,** 64-8.

- WU, L. & LEVINE, A. J. 1997. Differential regulation of the p21/WAF-1 and mdm2 genes after high-dose UV irradiation: p53-dependent and p53-independent regulation of the mdm2 gene. *Mol Med,* 3**,** 441-51.
- XIN, H., LIU, D. & SONGYANG, Z. 2008. The telosome/shelterin complex and its functions. *Genome Biol,* 9**,** 232.
- XIRODIMAS, D., SAVILLE, M. K., EDLING, C., LANE, D. P. & LAIN, S. 2001. Different effects of p14ARF on the levels of ubiquitinated p53 and Mdm2 in vivo. *Oncogene,* 20**,** 4972-83.
- YADAVILLI, S., MAYO, L. D., HIGGINS, M., LAIN, S., HEGDE, V. & DEUTSCH, W. A. 2009. Ribosomal protein S3: A multi-functional protein that interacts with both p53 and MDM2 through its KH domain. *DNA Repair (Amst),* 8**,** 1215-24.
- YAGHMAI, R., KIMYAI-ASADI, A., ROSTAMIANI, K., HEISS, N. S., POUSTKA, A., EYAID, W., BODURTHA, J., NOUSARI, H. C., HAMOSH, A. & METZENBERG, A. 2000. Overlap of dyskeratosis congenita with the Hoyeraal-Hreidarsson syndrome. *J Pediatr,* 136**,** 390-3.
- YANG, Y., ISAAC, C., WANG, C., DRAGON, F., POGACIC, V. & MEIER, U. T. 2000. Conserved composition of mammalian box H/ACA and box C/D small nucleolar ribonucleoprotein particles and their interaction with the common factor Nopp140. *Mol Biol Cell,* 11**,** 567-77.
- YELICK, P. C. & TRAINOR, P. A. 2015. Ribosomopathies: Global process, tissue specific defects. *Rare Dis,* 3**,** e1025185.
- YING ZHANG, MORIMOTO, K., DANILOVA, N., ZHANG, B. & LIN, S. 2012. Zebrafish Models for Dyskeratosis Congenita Reveal Critical Roles of p53 Activation Contributing to Hematopoietic Defects through RNA Processing. *PLOS One,* 7**,** e30188.
- ZEBARJADIAN, Y., KING, T., FOURNIER, M. J., CLARKE, L. & CARBON, J. 1999. Point mutations in yeast CBF5 can abolish in vivo pseudouridylation of rRNA. *Mol Cell Biol,* 19**,** 7461-72.
- ZEMP, I. & KUTAY, U. 2007. Nuclear export and cytoplasmic maturation of ribosomal subunits. *FEBS Lett,* 581**,** 2783-93.
- ZEMP, I., WILD, T., O'DONOHUE, M. F., WANDREY, F., WIDMANN, B., GLEIZES, P. E. & KUTAY, U. 2009. Distinct cytoplasmic maturation steps of 40S ribosomal subunit precursors require hRio2. *J Cell Biol,* 185**,** 1167-80.

- ZHANG, J., HARNPICHARNCHAI, P., JAKOVLJEVIC, J., TANG, L., GUO, Y., OEFFINGER, M., ROUT, M. P., HILEY, S. L., HUGHES, T. & WOOLFORD, J. L., JR. 2007. Assembly factors Rpf2 and Rrs1 recruit 5S rRNA and ribosomal proteins rpL5 and rpL11 into nascent ribosomes. *Genes Dev,* 21**,** 2580-92.
- ZHANG, Y., WOLF, G. W., BHAT, K., JIN, A., ALLIO, T., BURKHART, W. A. & XIONG, Y. 2003. Ribosomal protein L11 negatively regulates oncoprotein MDM2 and mediates a p53-dependent ribosomal-stress checkpoint pathway. *Mol Cell Biol,* 23**,** 8902-12.
- ZHENG, J., LANG, Y., ZHANG, Q., CUI, D., SUN, H., JIANG, L., CHEN, Z., ZHANG, R., GAO, Y., TIAN, W., WU, W., TANG, J. & CHEN, Z. 2015. Structure of human MDM2 complexed with RPL11 reveals the molecular basis of p53 activation. *Genes Dev,* 29**,** 1524-34.
- ZHENG, M., YANG, J., XU, X., SEBOLT, J. T., WANG, S. & SUN, Y. 2010. Efficacy of MDM2 inhibitor MI-219 against lung cancer cells alone or in combination with MDM2 knockdown, a XIAP inhibitor or etoposide. *Anticancer Res,* 30**,** 3321-31.
- ZHOU, X., HAO, Q., ZHANG, Q., LIAO, J. M., KE, J. W., LIAO, P., CAO, B. & LU, H. 2015. Ribosomal proteins L11 and L5 activate TAp73 by overcoming MDM2 inhibition. *Cell Death Differ,* 22**,** 755-66.
- ZIEMIECKI, A., MULLER, R. G., FU, X. C., HYNES, N. E. & KOZMA, S. 1990. Oncogenic activation of the human trk proto-oncogene by recombination with the ribosomal large subunit protein L7a. *EMBO J,* 9**,** 191-6.